

LATE QUATERNARY WEST ANTARCTIC ICE SHEET DYNAMICS:  
REMOTE SENSING AND SUBSTRATE STUDIES OF PALAEO-ICE SHEET  
BEDS ON THE AMUNDSEN SEA SHELF

Kumulative Dissertation  
zur Erlangung des akademischen Grades eines  
Doktors der Naturwissenschaften  
Dr. rer. nat.

am Fachbereich Geowissenschaften  
der Universität Bremen

vorgelegt von  
Johann Philipp Klages

Bremen, Januar 2014

Gutachter:

Professor Dr. Ralf Tiedemann

Professor Dr. Cornelia Spiegel





This PhD thesis was conducted within the Research Division Marine Geology and Paleontology at the Alfred-Wegener-Institut, Helmholtz-Zentrum für Polar- und Meeresforschung (AWI), Am Alten Hafen 26, 27568 Bremerhaven, Germany, between February 2011 and January 2014. The study was part of the Helmholtz Research Programme “Polar Regions and Coasts in the changing Earth System (PACES I – 2009-2013)” at the Alfred Wegener Institute. It was carried out in collaboration with the British Antarctic Survey, Ice Sheets Programme, High Cross, Madingley Road, Cambridge, United Kingdom, and the University of Exeter, College of Life and Environmental Sciences, Rennes Drive, Exeter, United Kingdom.

**Gutachter der Dissertation:**

Professor Dr. Ralf Tiedemann

Professor Dr. Cornelia Spiegel

**Weitere Mitglieder des Prüfungsausschusses:**

Professor Dr. Tilo von Dobeneck

Dr. Alastair G.C. Graham

Dr. Karl-Heinz Baumann

Florian Riefstahl

**Tag des öffentlichen Kolloquiums:**

1. April 2014



Name: Johann P. Klages

28. Januar 2014

Anschrift: An der Gete 138, 28211 Bremen

## **Erklärung**

Hiermit versichere ich, dass ich

1. die Arbeit ohne unerlaubte fremde Hilfe angefertigt habe,
2. keine anderen als die von mir angegebenen Quellen und Hilfsmittel benutzt habe und
3. die den benutzten Werken wörtlich oder inhaltlich entnommenen Stellen als solche kenntlich gemacht habe.

Bremen, den 28. Januar 2014

---

Johann P. Klages



## Abstract

Extensive parts of the largely marine-based West Antarctic Ice Sheet are currently subject to the most rapid changes in the global cryosphere. In recent decades, ice streams that drain >35% from the ice sheet's interior into the Amundsen Sea have been affected most dramatically. As upwelling, relatively warm Circumpolar Deep Water flows onto the continental shelf towards the deep inner shelf cavities, it melts the ice shelves from below, thins them, and causes ice stream acceleration and grounding line retreat in response to decreased buttressing. Since ice streams are marine-based on slopes that significantly deepen inland, they are susceptible to increased future ice mass loss, directly resulting in a sea-level rise of up to 3.4 meters, assuming that all marine-based West Antarctic ice portions would disintegrate and melt (Fretwell et al. 2013). However, 'state-of-the-art' ice sheet models that aim to elucidate these future scenarios are only initialised with observational data covering the past 30-40 years (e.g. Favier et al. 2014), thus excluding long-term empirical data of ice sheet change spanning the Last Glacial Maximum and the subsequent deglacial period. To test the reliability of predicted future scenarios it is essential that models are validated against past ice sheet configurations confirmed by empirical data from palaeo-ice sheet beds on modern Antarctic continental shelves. Attempts at reproducing the LGM ice sheet (Golledge et al. 2013), have revealed considerable mismatches between model simulations and empirical data. Such disparities have been attributed principally, to a lack of comprehensive palaeoglaciological data particularly from outer continental shelves and regions in between the large palaeo-ice stream troughs, regions known as inter-ice stream ridges, that would reveal the spatial and temporal variations of the West Antarctic Ice Sheet in the Amundsen Sea sector of the Southern Ocean more precisely.

This thesis presents the mapping and detailed analysis of new marine geophysical and geological data from three formerly unstudied regions on the Amundsen Sea shelf that significantly improve our understanding of Antarctic palaeo-ice sheet dynamics. In Chapter 2 I will present the first sea-floor geomorphological record of former basal ice conditions on an inter-ice stream ridge that entirely differ from those commonly investigated in the nearby palaeo-ice stream troughs. From these data, an improved temporal and spatial reconstruction of flow conditions of the former ice sheet in inter-ice stream areas of the eastern Amundsen Sea Embayment is revealed. Age constraints aiming to reveal the minimum grounding line retreat from the ridge broadly correspond with

those from the nearby Pine Island Trough. Palaeo-ice sheet dynamics as inferred from the glacial landform and sediment record on the inter-ice stream ridge are well complemented by a large-scale multibeam bathymetry survey of the middle and outer shelf, north of the inter-ice stream area, presented in Chapter 3. This new dataset compiles bathymetry from 11 separate research cruises to the region, and is supplemented by the analysis of new sedimentological and seismic data. From comprehensive landform mapping, the detailed palaeo-flow pathways of the WAIS in the northern and easternmost Amundsen Sea Embayment is revealed. Furthermore, geomorphological analysis of the bathymetry data allows thermal regimes at the palaeo-ice sheet bed to be defined in unprecedented detail, showing the complex relation of trough geometries and the subglacial geology to palaeo-ice flow behaviour. In combination with findings from Chapter 2, a coherent pattern of episodic post-Last Glacial Maximum retreat between the Pine Island and Abbot glacial troughs across the inter-ice stream ridge is revealed by the landform information, from which uniform retreat across the entire eastern Amundsen Sea Embayment is inferred. The same episodic style of retreat is also evident for a formerly unstudied part of the Amundsen Sea shelf offshore the Hobbs Coast presented in Chapter 4, as here the analysis and interpretation of marine geophysical and geological data reveal a large grounding-zone wedge recording a prolonged grounding line stabilization phase after the West Antarctic Ice Sheet reached the continental shelf edge during the last maximum extent. The initial retreat here is demonstrated to have been initiated at a pre- or early Last Glacial Maximum stage with deglaciation of inner shelf regions completed by ~12.9 cal. ka BP. Set in the context of other studies, a diachronous initial retreat of West Antarctic Ice Sheet grounding lines is indicated, which is discussed as a possible response to different local settings.

This thesis will ultimately help to better understand West Antarctic Ice Sheet dynamics during and since the Last Glacial Maximum. The new information will significantly add to a hitherto sparse database of previous work, helping to test, validate, and improve ice sheet models in the vital region of the Amundsen Sea. Only by enhancing their ability to simulate past ice sheet configurations more accurately will more reliable predictions of the future evolution of these dramatically changing parts of the West Antarctic Ice Sheet be possible.

## Kurzfassung

Beträchtliche Gebiete des größtenteils unter dem Meeresspiegel aufliegenden Westantarktischen Eisschildes unterliegen derzeit den schnellsten Veränderungen der globalen Kryosphäre. Seit einigen Jahrzehnten sind besonders die großen Eisströme, die mehr als 35% des Westantarktischen Inlandeises in das Amundsenmeer abfließen lassen, betroffen. Als Hauptverursacher dafür gilt der Tiefenauftrieb des relativ warmen Zirkumpolaren Tiefenwassers, welches auf die Kontinentalschelfe gelangt und anschließend in die tiefen Becken der inneren Schelfbereiche fließt. Hier sorgt es für Abschmelzprozesse an der Basis der Schelfeise, welche dadurch ausdünnen und in der Folge eine Beschleunigung des kontinentalen Eisabflusses und einen gleichzeitigen Rückzug der Aufsetzlinie der Eisströme hervorrufen, da der Stabilisierungs- und Rückhalteeffekt, den Schelfeise auf kontinentale Eismassen ausüben, immer stärker abnimmt. Da die schnellfließenden Eisströme auf einem Gletscherbett aufsitzen, das unter dem Meeresspiegel liegt und sich zusätzlich signifikant in Richtung des Inlandes abteuft, sind sie sehr anfällig für einen zunehmenden Verlust ihrer Eismasse. Angenommen, alle unter dem Meeresspiegel aufsitzenen Bereiche des Westantarktischen Eisschildes brächen zusammen und schmelzen anschließend, würde dies den globalen Meeresspiegel um bis zu 3.4 Meter ansteigen lassen (Fretwell et al. 2013). Die meisten aktuellen Modelle, die das zukünftige Verhalten des Westantarktischen Eisschildes besser einzuschätzen versuchen, basieren jedoch auf Beobachtungsdatenreihen, die nur die letzten 30-40 Jahre einschließen (z.B. Favier et al. 2014) und somit wichtige langzeitliche Änderungen des Eisschildes ausklammern, die den Zeitraum des Letzten Glazialen Maximums und der anschließenden Abschmelzphase umfassen. Um aber die Verlässlichkeit möglicher zukünftiger Änderungen des Westantarktischen Eisschildes zu prüfen, ist es unerlässlich, ihre Verlässlichkeit im Bezug auf die Vorhersage ehemaliger Eisschildkonfigurationen zu testen, welche durch empirische Daten von ehemals vom Eisschild bedeckten Gebieten bekannt sind. Erste Bestrebungen, die Eisschildkonfiguration des Letzten Glazialen Maximums zu rekonstruieren (Golledge et al. 2013), zeigten erhebliche Diskrepanzen zwischen Modellsimulationen und empirischen Daten. Ausschlaggebend für diese starken Unterschiede ist ein genereller Mangel an flächendeckenden paläo-glaziologischen Daten von äußeren Kontinentalschelfen und Gebieten zwischen den großen Paläo-Eisstromtrögen, sogenannten Inter-Eisstrom-Rücken. Diese bisher größtenteils unbekannt Gebiete würden räumli-

che und zeitliche Variationen des Westantarktischen Eisschildes im Amundsenmeer-Sektor des Südozeans präziser aufzeigen.

Die vorliegende Arbeit präsentiert Kartierungen und detaillierte Analysen neuer marin-geophysikalischer und –geologischer Daten aus drei bisher unbekanntem Gebieten des Amundsenmeer-Kontinentalschelfes, die maßgeblich zu einem besseren Verständnis ehemaliger Antarktischer Eisschilddynamik beitragen werden. In *Kapitel 2* werde ich erste geomorphologische Daten ehemaliger basaler Eisschildbedingungen auf Inter-Eisstrom-Rücken präsentieren, welche sich grundlegend von bisher bekannten Bedingungen in den benachbarten Paläo-Eisstromtrögen unterscheiden. Basierend auf diesen Daten konnten erstmals zeitliche und räumliche Rekonstruktionen der Eisflussbedingungen des ehemaligen Eisschildes in Gebieten von Inter-Eisstrom-Rücken dargelegt werden. Neue Altersdatierungen, die ein Minimumalter für den Rückzug der Aufsetzlinie des Eisschildes vom Inter-Eisstrom-Rücken liefern, passen zu Abschätzungen des Rückzugs in den benachbarten Eisstromtrögen. In *Kapitel 3* wird die aus Glazialformen und Sedimentkernen abgeleitete Paläo-Eisschilddynamik des Inter-Eisstrom-Rückens sehr gut durch eine großflächige bathymetrische Untersuchung des mittleren und äußeren Kontinentalschelfes ergänzt. Dieser neue Datensatz vereinigt bathymetrische Daten 11 unterschiedlicher Expeditionen in die Region und wird durch neue sedimentologische und seismische Analysen ergänzt. Eine flächendeckende Kartierung der Glazialformen ermöglichte die detaillierte Enthüllung von Paläo-Eisflüssen des Westantarktischen Eisschildes im nördlichen und östlichsten Bereich des Amundsenmeer-Schelfes. Des Weiteren erlaubt die geomorphologische Analyse der bathymetrischen Daten die Definition vorherrschender thermischer Bedingungen am ehemaligen Eisschildbett in beispielloser Genauigkeit. Dies macht deutlich, wie komplex das Verhältnis zwischen Trog-Geometrien und der subglazialen Geologie in Bezug auf das Paläo-Eisflussverhalten ist. In Kombination mit Ergebnissen aus *Kapitel 2* lässt sich ein zusammenhängendes Muster von episodischem Eisrückzug zwischen den Pine Island- und Abbot-Glazialtrögen über den Inter-Eisstrom-Rücken feststellen, von welchem ein einheitlicher Eisrückzug über den gesamten Schelfbereich des östlichen Amundsenmeeres im Anschluss an das Letzte Glaziale Maximum gefolgert werden kann. Das gleiche Rückzugsmuster konnte auch für einen bisher unerforschten Teil des Amundsenmeer-Schelfes vor der Hobbs-Küste gezeigt werden, welcher in *Kapitel 4* näher betrachtet wird. Die Analyse und Interpretation marin-geophysikalischer und –geologischer Daten hat einen massiven Sedimentkeil auf dem inneren Schelf offenbart, der eine lange Stabilisierungsphase der



ehemaligen Aufsetzlinie anzeigt, nachdem in diesem Gebiet der Westantarktische Eisschild während der letzten maximalen Vereisungsphase die Kontinentalschelfkante erreicht hatte. Es wird gezeigt, dass der initiale Eisrückzug von der Schelfkante vor oder während der frühen Phase des Letzten Glazialen Maximums begonnen haben muss und der innere Kontinentalschelf bereits vor ~12.9 cal. ka BP eisfrei war. Im Zusammenhang mit anderen Studien, weisen diese neuen Ergebnisse auf einen diachronen initialen Rückzug der Aufsetzlinien des Westantarktischen Eisschildes hin, welcher im Hinblick unterschiedlicher lokaler Verhältnisse diskutiert wird.

Diese Arbeit wird letztendlich dazu beitragen, die Dynamik des Westantarktischen Eisschildes während und nach dem Letzten Glazialen Maximum besser zu verstehen. Die neuen Informationen werden signifikant zu einer bisher spärlichen Datenlage beitragen, welche wiederum helfen wird, Eisschildmodelle zu testen, zu bestätigen und somit ihre Vorhersagegenauigkeit für die sich schnell ändernde Amundsenmeer-Region weiterzuentwickeln. Nur eine Verbesserung der Fähigkeit ehemalige Eisschildkonfigurationen genauer zu simulieren, wird für verlässlichere Vorhersagen der zukünftigen Entwicklung für diese sich derzeit dramatisch wandelnden Teile des Westantarktischen Eisschildes sorgen.

## Acknowledgements

First of all I would like to thank my four mentors and supervisors Gerhard Kuhn, Claus-Dieter Hillenbrand, Alastair G.C. Graham, and James A. Smith from the Alfred-Wegener-Institut Helmholtz-Zentrum für Polar und Meeresforschung in Bremerhaven, the British Antarctic Survey in Cambridge, and the University of Exeter, respectively. During the past three years you fascinated me for the field of Antarctic Marine Geology, shared your deep knowledge with me, and supported my work and myself in every aspect and at any time. Without you believing in me, the following thesis would not be reality. Thank you!

Secondly, I would like to acknowledge Professor Dr. Ralf Tiedemann for accepting and reviewing this doctoral thesis! The same applies to Professor Dr. Cornelia Spiegel, who additionally reviewed the thesis.

Thirdly, I am deeply grateful for the love and support from my fiancé Laurie and my family, especially my parents. Your never-ending fascination for my studies and research, your support, and your trust in me were and are just amazing! Your unbreakable positive way in looking at life and your ability in turning every situation into a good one, no matter how bad it seems in that moment, constantly influences and inspires me! Es hört sich wahrscheinlich merkwürdig an, aber ihr wart und seid mein Vorbild und meine Inspiration! Dafür bin ich euch sehr dankbar.

And finally, I would like to thank all my colleagues and friends within the Marine Geology and Paleontology group at the AWI as well as the captain and crew of the RV *Polarstern* expedition ANT-XXVI/3 in early 2010. Particularly, I thank all the technicians (Rita, Susi, Ute and Norbert) for their reliable and diligent help in the lab and on board, as well as all the senior scientists, PostDocs, and PhD students for helpful advices, fruitful discussions, and just a funny time...

## Table of contents

ABSTRACT	I
KURZFASSUNG	III
ACKNOWLEDGEMENTS	VI

<b>TABLE OF CONTENTS</b>	<b>1</b>
<b>CHAPTER 1 GENERAL INTRODUCTION AND MOTIVATION</b>	<b>3</b>
<b>CHAPTER 2 FIRST GEOMORPHOLOGICAL RECORD AND GLACIAL HISTORY OF AN INTER-ICE STREAM RIDGE ON THE WEST ANTARCTIC CONTINENTAL SHELF</b> KLAGES, J.P., KUHN, G., HILLENBRAND, C.-D., GRAHAM, A.G.C., SMITH, J.A., LARTER, R.D., GOHL, K.	<b>12</b>
2.1 INTRODUCTION	14
2.2 STUDY AREA	15
2.3 METHODS	16
2.4 RESULTS AND INTERPRETATION	17
2.5 DISCUSSION	29
2.6 CONCLUSIONS	37
<b>CHAPTER 3 DETAILED PALAEO-ICE FLOW PATHWAYS IN THE EASTERN-MOST AMUNDSEN SEA EMBAYMENT, WEST ANTARCTICA</b> KLAGES, J.P., KUHN, G., GRAHAM, A.G.C., SMITH, J.A., HILLENBRAND, C.-D., NITSCHKE, F.O., LARTER, R.D., GOHL, K.	<b>39</b>
3.1 INTRODUCTION	40
3.2 MATERIAL AND METHODS	43
3.3 RESULTS AND INTERPRETATION	44
3.4 DISCUSSION	62
3.5 CONCLUSIONS	70
<b>CHAPTER 4 RETREAT OF THE WEST ANTARCTIC ICE SHEET FROM THE WESTERN AMUNDSEN SEA SHELF AT A PRE- OR EARLY LGM STAGE</b> KLAGES, J.P., KUHN, G., HILLENBRAND, C.-D., GRAHAM, A.G.C., SMITH, J.A., LARTER, R.D., GOHL, K., WACKER, L.	<b>72</b>

	4.1 INTRODUCTION	73
	4.2 STUDY AREA AND METHODS	75
	4.3 RESULTS AND INTERPRETATION	78
	4.4 DISCUSSION	92
	4.5 CONCLUSIONS	99
<b>CHAPTER 5</b>	<b>GENERAL CONCLUSIONS AND FUTURE PERSPECTIVES</b>	<b>101</b>
	5.1 NEW INSIGHTS INTO THE PALAEO-GLACIOLOGY OF THE AMUNDSEN SEA SHELF	101
	5.2 IMPLICATIONS OF THE NEW FINDINGS	103
	5.3 PERSPECTIVES FOR FUTURE WORK ON THE AMUNDSEN SEA SHELF	105
	<b>DATA HANDLING</b>	<b>108</b>
	<b>REFERENCES</b>	<b>109</b>
<hr/>		
APPENDIX 1a	KEY FOR CORE DESCRIPTIONS	i
APPENDIX 1b	CORE DESCRIPTIONS FOR CHAPTER 2	ii
APPENDIX 1c	CORE DESCRIPTIONS FOR CHAPTER 3	iv
APPENDIX 1d	CORE DESCRIPTIONS FOR CHAPTER 4	viii
APPENDIX 2a	SEISMIC PROFILE FOR CHAPTER 2	xiv
APPENDIX 2b	SEISMIC PROFILE FOR CHAPTER 3	xv
APPENDIX 2c	SEISMIC PROFILE FOR CHAPTER 4	xvi
APPENDIX 3a	<b>GROUNDING-LINE RETREAT OF THE WEST ANTARCTIC ICE SHEET FROM INNER PINE ISLAND BAY</b> HILLENBRAND, C.-D. ET AL. 2013. GEOLOGY 41, 35-38.	xvii
APPENDIX 3b	<b>RECONSTRUCTION OF CHANGES IN THE AMUNDSEN SEA AND BELLINGSHAUSEN SEA SECTOR OF THE WEST ANT- ARCTIC ICE SHEET SINCE THE LAST GLACIAL MAXIMUM</b> LARTER, R.D. ET AL. 2013. QUATERNARY SCIENCE REVIEWS, IN PRESS.	xxi
APPENDIX 3c	CO-AUTHOR PUBLICATIONS (SUBMITTED/UNDER REVIEW)	liii

## Chapter 1.

### General introduction and motivation

#### 1.1 The West Antarctic Ice Sheet – a ‘hotspot’ of recent cryospheric changes

The Antarctic Ice Sheet (AIS), as the largest ice mass on earth, is separated into three main components, the East Antarctic Ice Sheet (EAIS), the West Antarctic Ice Sheet (WAIS), and the Antarctic Peninsula Ice Sheet (APIS) that, together accumulate,  $\sim 27 \times 10^6 \text{ km}^3$  of ice (Fretwell et al. 2013). The EAIS accounts for  $\sim 85\%$  of the AIS and has a base largely grounded upon bedrock above sea level, whereas almost 80% of the smaller WAIS grounds on bedrock up to  $\sim 2.5 \text{ km}$  below modern sea level (Fretwell et al. 2013) (Fig. 1-1). The geometry, stability, and mass balance of the ice sheet are steered by its fast-flowing component, referred to as ice streams, as they drain the vast majority of ice from the continent’s interior into ice shelves where it is released to the ocean at the calving front (e.g. Stokes and Clark 2001). Over recent decades, satellite missions that cross the Antarctic continent detected considerable changes mainly affecting large marine-terminating ice streams that drain extensive parts of the WAIS. These changes include increased thinning, ice flow acceleration, and grounding line retreat (Figs. 1-2a+c, 1-3a+b) (e.g. Vaughan 2008; Pritchard et al. 2009, 2012; Jenkins et al. 2010; Joughin and Alley 2011; Rignot et al. 2011; Dutrieux et al. 2013). The causes and potential forcings for these changes were widely debated and, amongst several others (cf. Livingstone et al. 2012), ranged from changes in basal ice hydrology (e.g. Anandakrishnan and Alley 1997; Fricker and Scambos 2009), flow over varying subglacial substrates and bathymetries that steer the ice flow (e.g. Schoof 2007; Golledge et al. 2013), to increasing air temperatures (e.g. Bromwich et al. 2013). However, increasing ocean temperatures by upwelling Circumpolar Deep Water (CDW) onto West Antarctic continental shelves (e.g. Holland et al. 2008; Jacobs et al. 2011; Nakayama et al. 2013) appear to be the main driver for the ice mass loss (Fig. 1-3) (Rignot et al. 2013). Livingstone et al. (2012) pointed out that fully assessing the influence of each of the processes mentioned above remains problematic since comprehensive data is still sparse and modern ice sheet beds are hardly accessible, thus hampering reliable predictions on how the WAIS may develop in the future (IPCC 2013). More precise future projections, however, are urgently needed as the WAIS is thought to be inherently unstable in a warming climate, raising

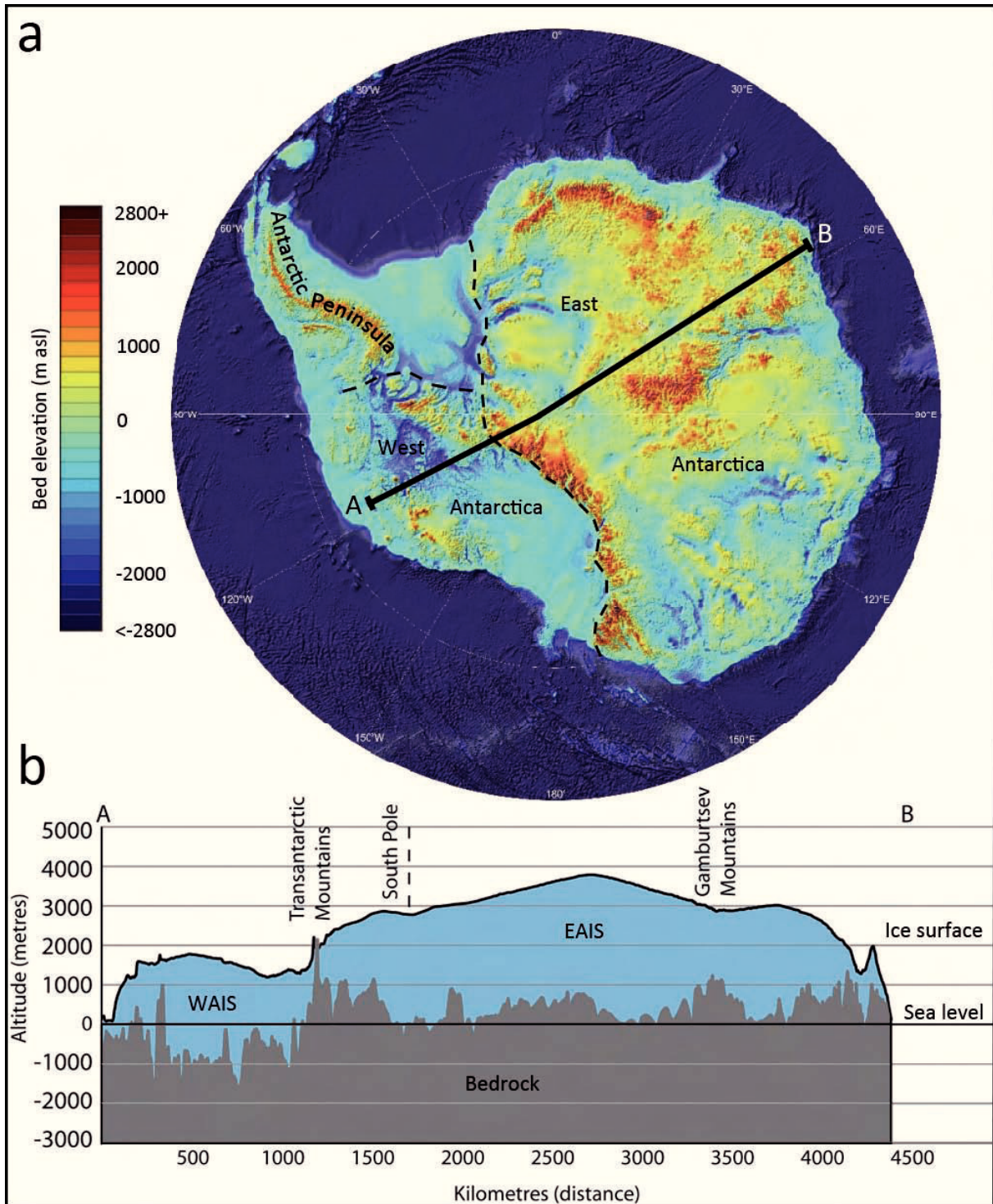


**Figure 1-1.** The Antarctic Ice Sheet (AIS) and its components. a) BEDMAP2 (Fretwell et al. 2013) with dashed lines for boundaries between the East Antarctic Ice Sheet (EAIS), the West Antarctic Ice Sheet (WAIS), and the Antarctic Peninsula Ice Sheet (APIS). Profile A-B is shown in 'b'. ('m asl' = metres above sea level), b) Profile A-B of the Antarctic Ice Sheet (modified from Fretwell et al. 2013).

concern for a partial future disintegration of the most vulnerable marine-based ice portions that would raise the global sea level by 3.4 m (e.g. Bamber et al. 2009; Fretwell et al. 2013). This concern is mainly based on the fact that the WAIS bed largely lies below the sea level and slopes downward significantly inland, enabling relatively warm CDW



to intrude the sub-ice shelf cavity and melt the ice shelf from below (Figs. 1-1, 1-2, 1-3) (e.g. Jacobs et al. 2012; Pritchard et al. 2012; Nakayama et al. 2013; Favier et al. 2014). As the WAIS is assumed to have advanced towards the continental shelf edge during past glacial maxima, its fast flowing portions repeatedly carved into the shelf substrate moulding these deep reverse-sloped cross-shelf bathymetric troughs (e.g. Anderson 1999). The Last Glacial Maximum (LGM; ~23-19 ka BP) represents the most recent phase of a shelf-wide glaciation during which the bathymetric troughs as well as the neighbouring shallower shelf regions were occupied by the WAIS, and thus provide the unique opportunity to study processes and conditions on its palaeo-ice sheet bed that is

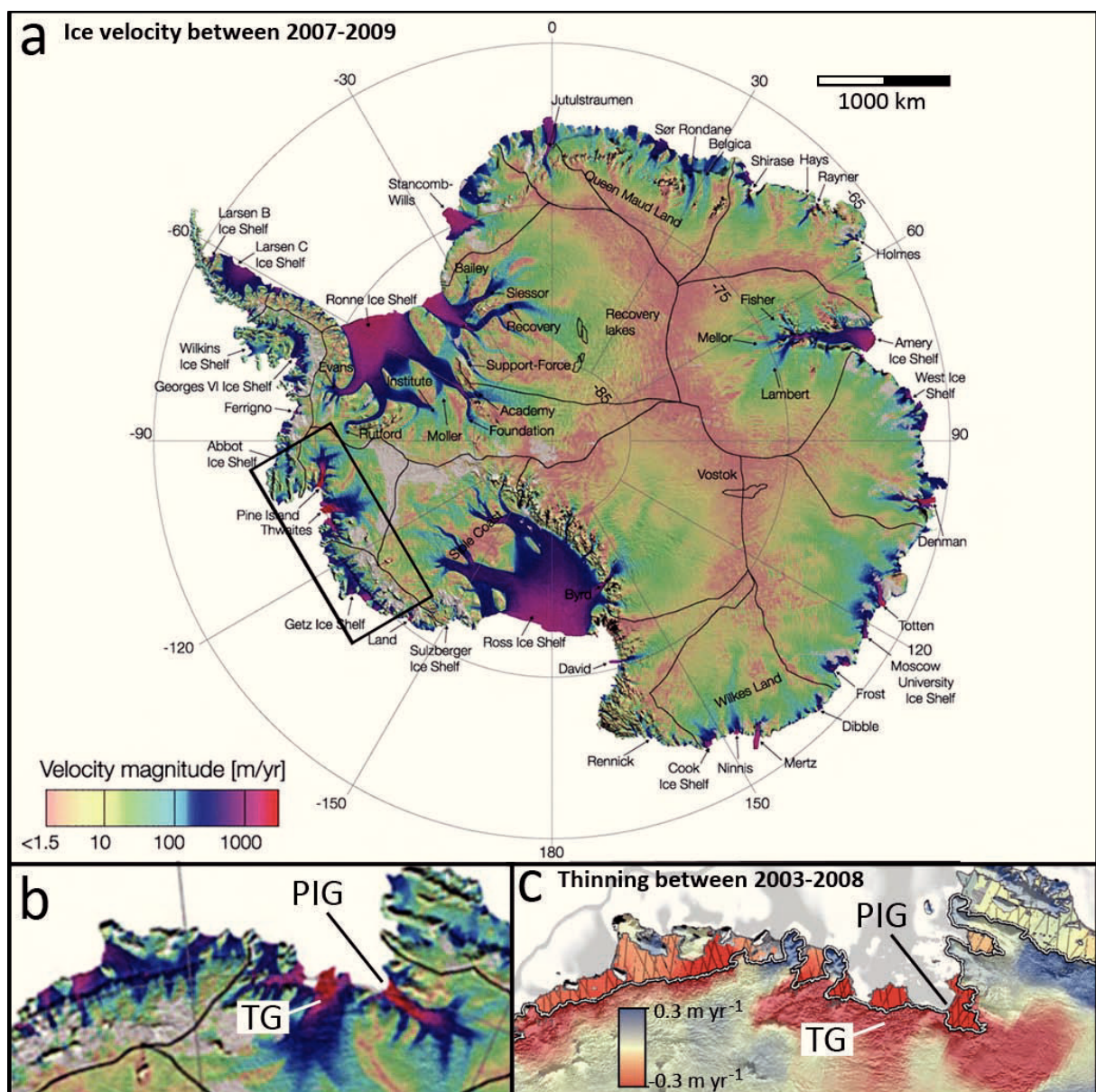


**Figure 1-2.** a) Ice flow velocities of the Antarctic Ice Sheet (AIS) in between 2007 and 2009 (modified from Rignot et al. 2011); Black frame shows location of 'b'. b) Ice flow velocities of ice streams draining the WAIS into the Amundsen Sea; PIG: Pine Island Glacier, TG: Thwaites Glacier; Colour code same as in 'a'. c) Thinning of ice shelves and grounded ice in between 2003 and 2008 (modified from Pritchard et al. 2012).

difficult to access in its modern counterpart. It is a general consensus that also during the LGM grounded ice at least reached outer shelf positions but likely extended all the way to the continental shelf edge (e.g. Larter et al. 2013; Anderson et al. 2013b).

Of all the ice streams draining the WAIS, those discharging into the Amundsen Sea Embayment (ASE) have been subject to the most dramatic changes; accelerating, thinning, and retreating more rapidly than any other polar glaciers over the past two decades (Figs. 1-2, 1-3) (e.g. Rignot and Jacobs 2002; Rignot et al. 2008, 2011, 2013; Jacobs et al. 2011; Pritchard et al. 2012; Favier et al. 2014). Since these ice streams account for >35 % of the total WAIS ice discharge, their potential contribution to global sea level rise is estimated with up to ~1.5 m (Vaughan 2008). Also here, sub-ice shelf melting facilitated by intruding CDW into the deep inner shelf trough has been proposed to be the dominant factor for the rapid changes in the ASE region (e.g. Jacobs et al. 1996, 2011; Pritchard et al. 2011; Rignot et al. 2013), which additionally appear to be controlled by geological properties on the ice sheet bed (Tinto and Bell 2011; Dutrioux et al. 2014). Recently, Nakayama et al. (2013) showed that the inflow of the relatively warm CDW onto the ASE shelf strengthened in recent years and is preferably routed through the eastern (AGT) and central (PITW) bathymetric troughs (Fig. 1-4) towards the deep inner shelf cavities beneath the ice shelves. Furthermore, Tinto and Bell (2011) as well as Favier et al. (2014) have shown that unpinning from ice stream stabilizing seafloor highs at the grounding line of the Pine Island and Thwaites ice streams – the major glaciers feeding the ASE – could result in an accelerated retreat into the deep basins of the WAIS interiors, since the gradual deepening of the bed inland causes a positive feedback

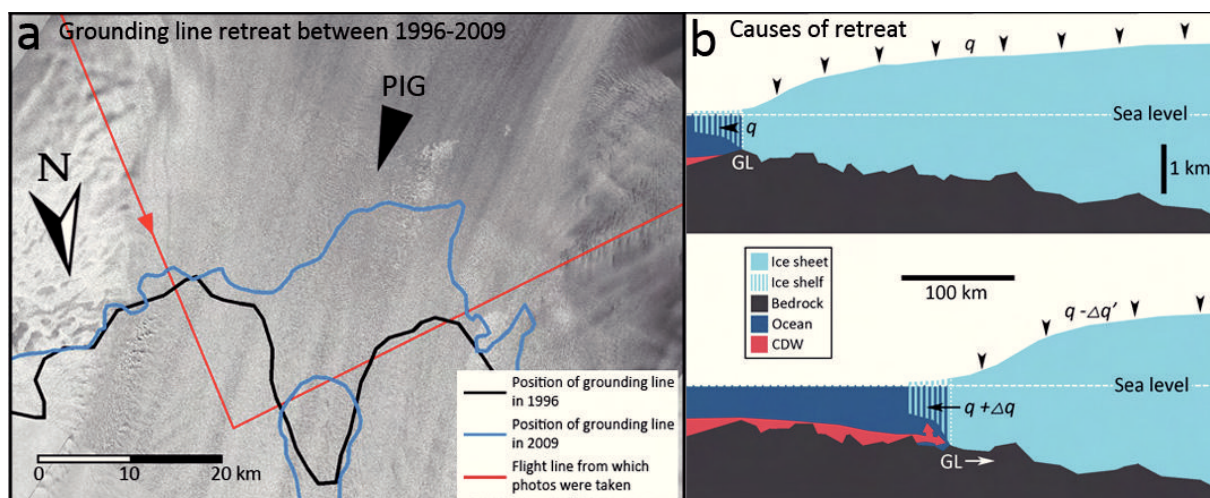


**Figure 1-3.** a) Grounding line retreat of Pine Island Glacier between 1996 and 2009 (modified from Dutrioux et al. 2013); PIG: Pine Island Glacier. b) Causes of a backstepping grounding line on ice sheet stability (modified from Vaughan and Arthern 2007); CDW: Circumpolar Deep Water, GL: Grounding line,  $q$ : Inflow/Outflow.



between grounding line recession and ice flux discharge (i.e. the marine ice sheet instability hypothesis, Fig. 1.3b; e.g. Schoof 2007; Vaughan and Arthern 2007; Joughin et al. 2010). These observations suggest an increasing ice mass loss in this sector of the WAIS for the near future, i.e. a stronger contribution to rising sea levels as ice shelves thin, and thus may disintegrate more quickly, thereby decreasing their ability of buttressing the ice sheet, which may result in ice stream acceleration and grounding line retreat (e.g. Scambos et al. 2004; Dupont and Alley 2005; Hughes 1981; Pritchard et al. 2009). For the near future, new estimates state values of a 7 cm global eustatic sea-level rise by the year 2100 (Gladstone et al. 2012) and 3.5-10 mm over the following 20 years (Favier et al. 2014), solely sourced from Pine Island Glacier.

## **1.2 Modelling challenges and the significance of long-term dynamical ice sheet records**

Ice sheet models that aim to elucidate the future behaviour of the WAIS, i.e. its potential contribution to global eustatic sea-level rise, mainly base on observational data that only cover the past 30-40 years of ice sheet change, and hence largely exclude long-term information on the ice sheet's spatial and temporal variations (Larter et al. 2013; Jamieson et al. in press). This information however is essential to firstly set recent rapid changes in the Amundsen Sea sector into a long-term context spanning the last 10-20,000 years thus covering the last deglacial period, and secondly provide more precise information on the configuration of the ice sheet during that time, i.e. thermal regimes, flow pathways, and style of post-LGM retreat (e.g. Larter et al. 2013; Golledge et al. 2013), since it is widely interpreted that the WAIS reached the Amundsen Sea shelf edge during the LGM (e.g. Evans et al. 2006; Graham et al. 2009, 2010; Smith et al. 2011; Jakobsson et al. 2012; Kirshner et al. 2012; *Chapter 4*, in the following referred to as Klages et al. in review). However, Golledge et al. (2013) recently pointed out that in trying to simulate the LGM configuration of the ice sheet in the ASE region, their model resulted in considerable mismatches when tested against the sparse available empirical data from high-resolution bathymetric surveys on middle and outer shelves (e.g. Evans et al. 2006; Graham et al. 2010; Jakobsson et al. 2012), particularly when trying to evaluate regions of fast palaeo-ice flow at the LGM. This highlights the urgent need for more comprehensive high-resolution bathymetric data, equally supplemented by reliable chronological data

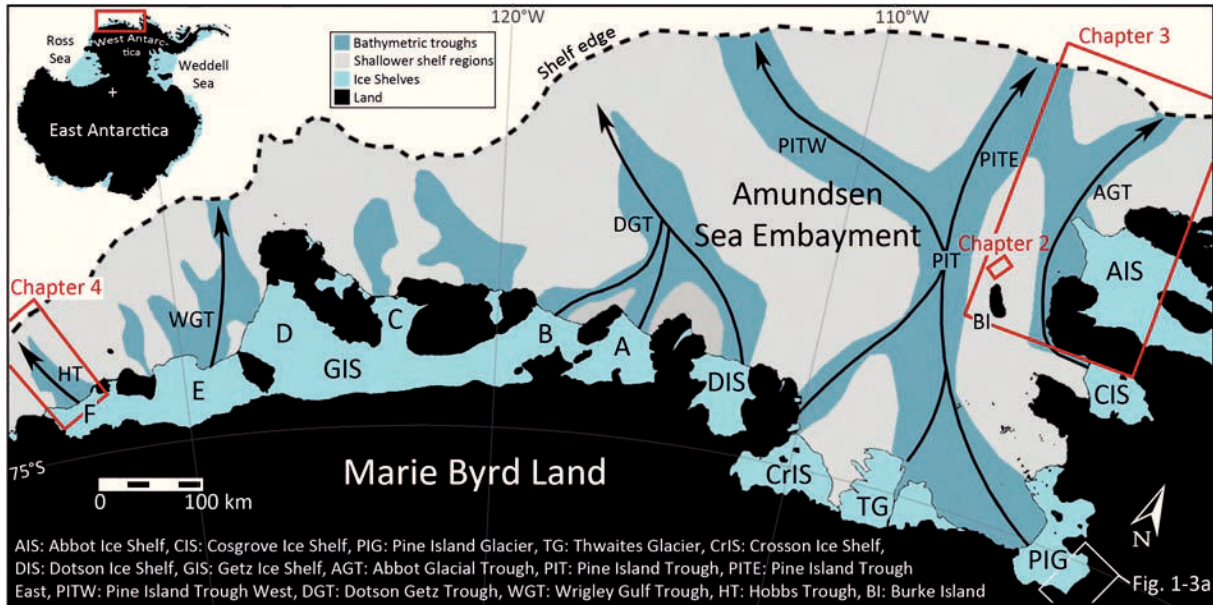


**Figure 1-4.** Overview map of the Amundsen Sea shelf. The locations of the three study areas (Chapters 2-4) are indicated by red frames. General palaeo-ice stream pathways are indicated by black arrows. Location of satellite image in Figure 1-3a is indicated by white frame. Abbreviations for ice shelves and main bathymetric troughs are given in figure. Bathymetric troughs were drawn based on Arndt et al. 2013.

of the post-LGM ice sheet retreat. This would allow an improved definition of regions of fast and slow palaeo-ice flow during and since the LGM, approaching increased confidence in model simulations, and thereby improving their ability in estimating the future development of the WAIS in the Amundsen Sea region more precisely. Larter et al. (2013) stated that the intensity of recent changes is certainly not representative of a “simple continuation” of a progressive deglaciation following the LGM, as a projection of the modern rate of grounding line retreat ( $>1$  km/yr; Rignot et al. 1998; 2008) would require a minimum shelf width of nearly 20,000 km. Additionally, it has been shown that significant parts of the ASE including the inner shelf regions must have already been deglaciated before the onset of the Holocene, thereby highlighting how exceptional the recent changes must be (*Appendix 3a*, in the following referred to as Hillenbrand et al. 2013). These authors conclude that during the Holocene the style of retreat to the modern grounding line must have either been very slow and constant, or, alternatively, episodic and thus characterized by 3-4 phases of rapid retreat. Kirshner et al. (2014) may have found sedimentological evidence for at least 3 events of meltwater-intensive retreat phases during the Holocene that eventually coincide with the episodes of rapid retreat proposed by Hillenbrand et al. (2013). Furthermore, several studies showed that ice streams draining the WAIS onto the Amundsen Sea shelf and adjacent shelf sectors responded diachronously (e.g. Hillenbrand et al. 2010; Smith et al. 2011; Kirshner et al. 2012; Klages et al. in review; Smith et al. submitted for publication) rather than syn-

chronously (Weber et al. 2011) in response to post-LGM sea-level rise, and atmospheric and oceanic warming, although these external forcings are assumed to have affected the region in a similar way (*Appendix 3b*, and references therein; in the following referred to as Larter et al. 2013). This highlights the need in focusing on other significant factors that additionally steer ice sheet dynamics, such as variations of the subglacial geology and ice stream trough constrictions (e.g. Graham et al. 2010; Dowdeswell and Fugelli 2012; Jakobsson et al. 2012). The current knowledge of LGM flow and the style and timing of the subsequent retreat on the Amundsen Sea shelf is hitherto based on well-constrained geological (e.g. Kirshner et al. 2012; Hillenbrand et al. 2013) and geophysical data (e.g. Larter et al. 2009; Graham et al. 2009; Gohl et al. 2013; Nitsche et al. 2013) from the inner shelf, whereas it is rather sparse and sometimes contradictory on middle and outer shelf regions (e.g. Evans et al. 2006; Graham et al. 2010; Kirshner et al. 2012). This emphasizes the need for robust shelf-wide chronologies and comprehensive high-resolution bathymetries from these parts of the ASE in order to fully assess flow pattern, extent, thermal regimes, retreat initiation, and subsequent style and timing of retreat across the Amundsen Sea shelf.

### **1.3 Research aims of this thesis: Help fill significant knowledge gaps by new marine geological and geophysical data from the Amundsen Sea shelf**

The overarching aim of this thesis is to collect, analyse, and interpret new high-resolution marine geological and geophysical data that give insights into previously neglected parts of the Amundsen Sea shelf (Fig. 1-4), at and since the LGM. The results of the thesis revealed new information that turned out to be crucial in terms of understanding past ice sheet dynamics in this sector of the WAIS. The findings of the thesis have already received growing attention from the Antarctic earth science community, demonstrated, for example, by the incorporation of data into a new community-wide ice sheet reconstruction (Larter et al. 2013). The *Chapters 2 & 3* will concentrate on detailed palaeo-ice sheet dynamics in the easternmost ASE (Fig. 1-4), east of the main Pine Island Trough (PIT), whereas *Chapter 4* will focus attention on the previously unknown ice sheet history on the westernmost part of the Amundsen Sea shelf, west of the ASE (Fig. 1-4). Hence, my studies will close geographic gaps on the Amundsen Sea shelf, but will

also close significant gaps of understanding, as I concentrated on three main research foci that are as follows:

- 1) Shallower shelf regions that are situated in between the deep cross-shelf palaeo-ice stream troughs, termed inter-ice stream ridges, cover significant portions of the former ice sheet bed. However, due to strong iceberg scouring that usually eradicate the glacial landform record here, they have rarely been investigated yet. Therefore, palaeo-ice sheet dynamics in these regions are largely unknown leaving a serious gap in understanding and at the same time hampering a complete reconstruction of post-LGM WAIS history. Such a region that separated the Pine Island-Thwaites palaeo-ice stream in the west from the Cosgrove palaeo-ice stream in the east (Fig. 1-4) could be investigated during Austral summer 2009/2010 due to favourable sea ice conditions. In *Chapter 2*, I will present the first systematic geological and geophysical survey on its glacial geomorphology and glacial history, thereby providing a diagnostic tool for future studies that aim to interpret the palaeo-glaciological record on inter-ice stream ridges elsewhere.
  
- 2) Simulating the flow pattern of the past ice sheet requires detailed empirical data about regions of fast and slow palaeo-ice flow, flow directions, and the style of subsequent retreat, as only these data can prove the accuracy and reliability of ice sheet models, and are essential requirements in trying to estimate the future behaviour of the ice sheet more precisely. In *Chapter 3* I present a new compilation of comprehensive bathymetric data that were acquired on 11 research cruises, revealing 1) detailed palaeo-ice flow pathways in the easternmost ASE east of the main PIT for the first time (Fig. 1-4) and 2) the style of retreat following the last glaciation, complementing findings from *Chapter 2*. Particularly for the ASE sector, where modern ice streams change at an alarming rate, precise information on palaeo-ice flow pathways, especially for middle and outer shelf regions, are urgently needed, as only validated models that are tested with these palaeo-data may better estimate possible future changes. Additionally, detailed bathymetric data are needed to fully elucidate the routing of warm CDW across the ASE towards the modern grounding line (e.g. Nakayama et al. 2013).

3) During the past decade, palaeo-glaciological studies mainly focused on palaeo-ice streams that drained the WAIS into the ASE or the Ross Sea Embayment (RSE). The narrower shelf sectors in between these wide embayments, however, remained largely neglected, although they cover extensive areas of the West Antarctic shelf. In order to achieve a better understanding about palaeo-ice sheet flow, LGM extent, and retreat dynamics on these shelf sectors, a formerly unknown palaeo-ice stream trough offshore from the Hobbs Coast (Fig. 1-4) has been detected and closely investigated. These new palaeo-glaciological insights and their implications for LGM ice sheet extent and retreat in the entire region are discussed in *Chapter 4*.

## Chapter 2.

### First geomorphological record and glacial history of an inter-ice stream ridge on the West Antarctic continental shelf

J.P. Klages <sup>a,\*</sup>, G. Kuhn <sup>a</sup>, C.-D. Hillenbrand <sup>b</sup>, A.G.C. Graham <sup>b, c</sup>, J.A. Smith <sup>b</sup>, R.D. Larter <sup>b</sup>, K. Gohl <sup>a</sup>

<sup>a</sup> Alfred Wegener Institute for Polar and Marine Research, Am Alten Hafen 26, 27568 Bremerhaven, Germany

<sup>b</sup> British Antarctic Survey, High Cross, Madingley Road, Cambridge CB3 0ET, United Kingdom

<sup>c</sup> College of Life and Environmental Sciences, University of Exeter, Amory Building, Rennes Drive, Exeter EX4 4RJ, United Kingdom

Published in *Quaternary Science Reviews* 61 (2013), p. 47-61.

#### Abstract

Inter-ice stream areas cover significant portions of Antarctica's formerly glaciated shelves, but have been largely neglected in past geological studies because of overprinting by iceberg scours. Here, we present results of the first detailed survey of an inter-ice stream ridge from the West Antarctic continental shelf. Well-preserved sub- and proglacial bedforms on the sea floor of the ridge in the eastern Amundsen Sea Embayment (ASE) provide new insights into the flow dynamics of this sector of the West Antarctic Ice Sheet (WAIS) during the last glacial cycle. Multibeam swath bathymetry and PARASOUND acoustic sub-bottom profiler data acquired across a mid-shelf bank, between the troughs of the Pine Island-Thwaites (PITPIS) and Cosgrove palaeo-ice streams (COPIS), reveal large-scale ribbed moraines, hill-hole pairs, terminal moraines, and crevasse-squeeze ridges. Together, these features form an assemblage of landforms that is entirely different from that in the adjacent ice-stream troughs, and appears to be unique in the context of previous studies of Antarctic sea floor geomorphology. From this assemblage, the history of ice flow and retreat from the inter-stream ridge is reconstructed. The bedforms indicate that ice flow was significantly slower on the inter-ice stream ridge than in the neighbouring troughs. While terminal moraines record at least two re-advances or stillstands of the ice sheet during deglaciation, an extensive field of crevasse-squeeze ridges indicates ice stagnation subsequent to re-advancing ice, which deposited the field of terminal moraines in the NE. The presented data suggest



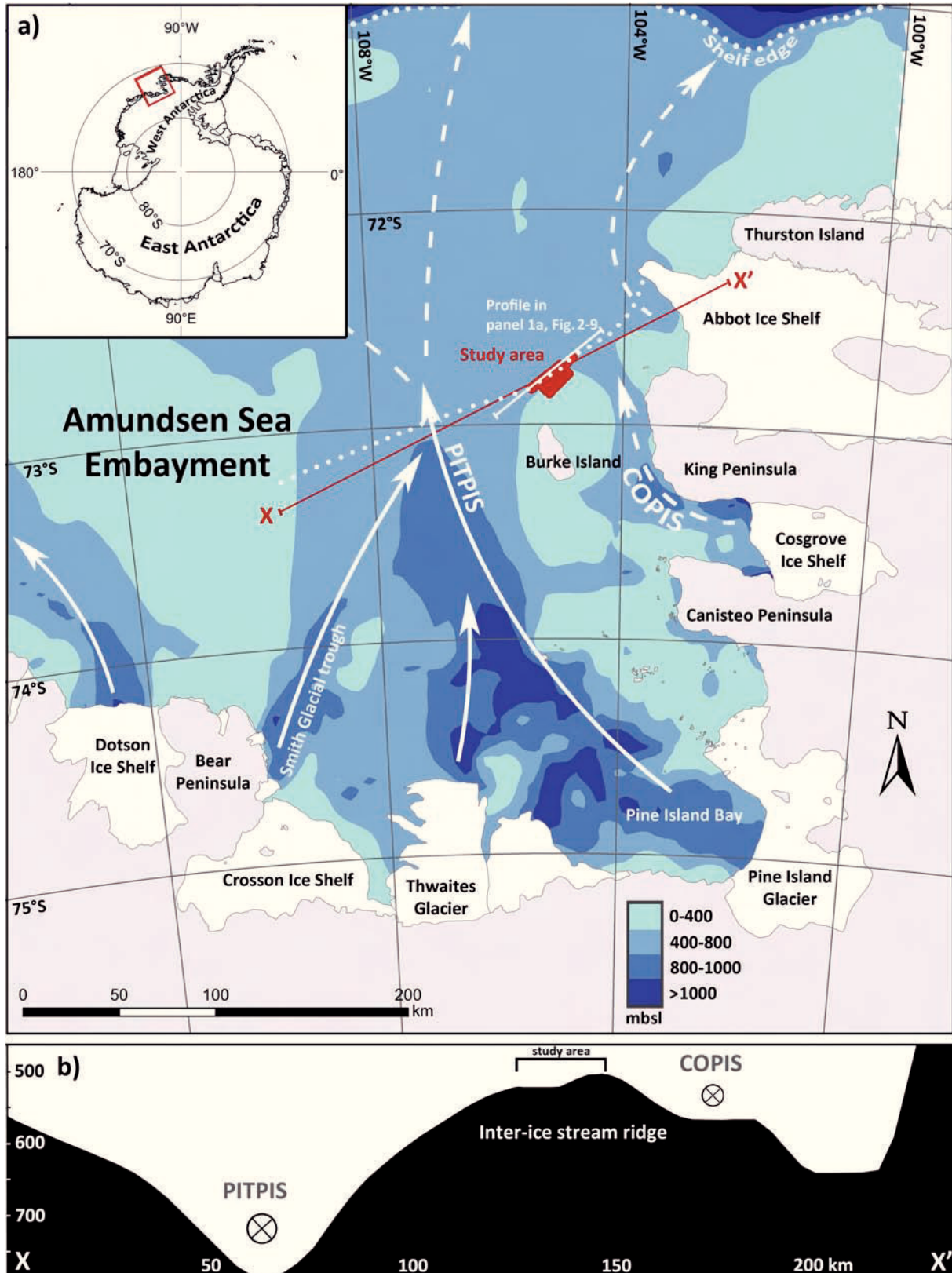


**Figure 2-1.** Overview map (a) showing the study area (in red) and the general bathymetry of the eastern ASE (Nitsche et al. 2007). The location of the cross-section on the bottom of the figure (b) is indicated by the red line (X-X'). The continuous white line indicates the profile of panel 1a in Figure 2-9. The white dotted line refers to the seismic line in Figure 2-6. White arrows mark the main bathymetric troughs eroded by Pine Island, Thwaites and Smith ice streams. Ice shelves are displayed in white. COPIS – Cosgrove Palaeo-Ice Stream; PITPIS – Pine Island-Thwaites Palaeo-Ice Stream. Note that cross-section on the bottom is derived from the general bathymetry of the eastern ASE, thus water depths might differ from the high-resolution bathymetry data of following figures.

that the ice flow behaviour on the inter-ice-stream ridge was substantially different from that in the adjacent troughs. However, newly obtained radiocarbon ages on two sediment cores recovered from the inter-ice stream ridge suggest a similar timing in the deglaciation of both areas. This information closes an important gap in the understanding of past WAIS behaviour in the eastern ASE. Our newly-documented bedforms will also serve as an important diagnostic tool in future studies for interpreting ice-sheet histories in similar inter-ice stream areas.

## 2.1 Introduction

Pine Island, Thwaites and Smith glaciers drain the WAIS into the eastern ASE. Complete ice loss of the catchment of these three major ice streams has the potential to raise global sea level by ~1.5 m (Vaughan 2008). The glaciers of the eastern ASE sector have recently shown rapid thinning, ice flow acceleration and grounding-line retreat (e.g. Vaughan 2008; Pritchard et al. 2009; Jenkins et al. 2010; Joughin and Alley 2011), probably in response to major sub-ice shelf melting by upwelling of warm Circumpolar Deep Water (CDW) (e.g. Rignot and Jacobs 2002; Shepherd 2004; Jacobs et al. 2011; Pritchard et al. 2012). The WAIS is potentially unstable because its bed lies mainly below sea-level and slopes down inland from the coast, giving reason for concern that certain WAIS sectors may collapse in the near future (Bamber et al. 2009; Katz and Worster 2010).

To predict the future behaviour of the WAIS, detailed knowledge about its long-term behaviour is essential. Studies offshore of the Pine Island and Thwaites systems have begun to provide the critical geological context for recent changes. The ice streams of the eastern ASE probably extended near to the shelf edge at the Last Glacial Maximum (LGM; ~19-23 ka BP) and subsequently retreated to their current position (Lowe and Anderson 2002; Graham et al. 2010; Jakobsson et al. 2011; Jakobsson et al. 2012; Kirshner et al. 2012). The dynamics of former ice flow in the eastern ASE have previously been reconstructed from pro- and subglacial landforms preserved on the seafloor, the acoustic properties of sub-seafloor strata and via sediment core information (Kellogg and Kellogg 1987a, b; Lowe and Anderson 2002, 2003; Evans et al. 2006; Graham et al. 2010; Jakobsson et al. 2011; Jakobsson et al. 2012; Kirshner et al. 2012). However, as with other parts of the Antarctic shelf, the majority of these previous



investigations focused on ice sheet behaviour in palaeo-ice stream troughs eroded into the shelf (e.g. Anderson et al. 2002; Livingstone et al. 2012) and thus solely on the reconstruction of the fast-flowing parts of the WAIS.

In contrast, there is a considerable lack of data constraining basal conditions and ice-retreat histories from shallower inter-ice stream areas on the Antarctic shelf, where iceberg scouring often has overprinted or eradicated any pre-existing subglacial landforms on the seabed (e.g. Barnes and Lien 1988; Lien et al. 1989; Dowdeswell and Bamber 2007). This lack of data leaves a serious gap in our understanding of palaeo-ice sheet dynamics. Additional studies in the Antarctic that focus on shallow regions between fast-flowing ice streams (termed “inter-ice stream ridges” after Ottesen and Dowdeswell 2009) are required in order to address this problem and achieve a detailed and complete reconstruction of WAIS history.

Here we present new high-resolution marine geophysical and sedimentological data from an inter-ice stream ridge located between the troughs of the PITPIS and COPIS in the eastern ASE (Fig. 2-1). Some of the observed glacial bedforms are described for the first time from the Antarctic shelf and differ significantly from bedforms imaged in the adjacent and other palaeo-ice stream troughs. The bedforms are largely unaffected by iceberg scouring and are exceptionally well preserved, thus providing new detailed insights into the glacial history of the ASE.

## 2.2 Study area

The study area is located on the mid shelf of the eastern ASE, north of Burke Island, on a ridge between two troughs, one carved out by the PITPIS to the west and the other eroded by a palaeo-ice stream that flowed from the area now occupied by the Cosgrove Ice Shelf to the east (Fig. 2-1a). The study area covers  $\sim 150 \text{ km}^2$  ( $\sim 9 \times 17 \text{ km}$ ) upon the central part of the ridge. Water depths range between 560 and 620 m, whereas maximum water depths in the adjacent NS-striking Pine Island Trough and the NNW-SSE striking Cosgrove Trough are  $\sim 300 \text{ m}$  and  $\sim 60 \text{ m}$  deeper, respectively (Fig. 2-1b).

### 2.3 Methods

The marine geophysical and geological data used in this study were collected on cruise ANT-XXVI/3 of the RV Polarstern in early 2010 (Gohl 2010). The bathymetry data were collected with a hull-mounted Atlas Hydrosweep DS-2 multibeam swath bathymetry system, which emits 59 beams at a frequency of 15.5 kHz. Depth values and beam ray paths were calibrated during the cruise using sound velocity profiles from conductivity-temperature-depth (CTD) measurements of the water column. The raw data from the bathymetric survey were processed in MB-system (Caress and Chayes 2003) to remove data outliers, and subsequently gridded at a 20-m cell size.

An Atlas PARASOUND acoustic sub-bottom profiler was used simultaneously with the multibeam swath bathymetry system to collect information on the properties of the sea floor and sub-seafloor. PARASOUND uses parametric interference between two high frequency primary signals to generate a low frequency secondary signal (frequencies 2.5-5.5 kHz, chirp pulse). In the study area, the system only achieved ~5-15 m of penetration due to a combination of a relatively 'hard' seabed and a highly consolidated homogenous sub-seafloor substrate.

Sediment cores were recovered with a Kiel-type gravity corer. The core locations were identified using sub-bottom and multibeam data. Following recovery, the cores were cut into 1 m long sections and sealed. After logging the sections for P-wave velocity ( $V_p$ ), magnetic susceptibility (MS) and wet-bulk density (WBD) with a GEOTEK Multi Sensor Core Logger (MSCL), the cores were stored at +4°C onboard. The core sections were split at the Alfred Wegener Institute for Polar and Marine Research (AWI) in Bremerhaven, Germany, and photographed and described visually by logging their lithology, sedimentary structures and colour. 1 cm-thick sediment slabs were taken along the core for X-radiographs and shear strength was determined at 5-10 cm intervals with a hand held GEOVANE shear vane. The water content was calculated from the difference between wet and freeze-dried 10 cm<sup>3</sup> bulk samples. For grain-size analyses, discrete sediment samples were taken from the cores every 5–10 cm, disaggregated in deionised H<sub>2</sub>O and then wet-sieved using 63 µm and 2 mm mesh sizes. The proportions of the grain-size fractions (mud: <63 µm, sand: 63 µm–2 mm, gravel: >2 mm) were determined on a weight basis. Total carbon and organic carbon (C<sub>org</sub>) were measured with the element analysers LECO CS-125, CS-400 and CNS-2000 at the AWI. Accelerator Mass

Spectrometry (AMS) radiocarbon dating was carried out at the Beta Analytic Radiocarbon Dating Laboratory in Miami, Florida, USA. Due to a lack of biogenic carbonate, the AMS  $^{14}\text{C}$  ages had to be obtained from the acid insoluble organic (AIO) matter. All downcore AIO ages were corrected by subtracting the uncorrected AIO date from the core top, which is assumed to represent modern deposition. Our down-core correction assumes that (i) the offset of the uncorrected AIO core-top date from the modern Antarctic Marine Reservoir effect (ca. 1300 years, e.g. Anderson et al. 2002; Kirshner et al. 2012) results from contamination with reworked fossil organic matter (e.g. Licht et al. 1996, 1999; Domack et al. 1999), and (ii) the degree of this contamination has not changed since the LGM. We express the AIO dates as uncorrected  $^{14}\text{C}$  years BP and corrected ka BP, respectively. For supplementary information, see doi:10.1594/PANGAEA.779863, *Appendices 1b*, and *2a*.

## 2.4 Results and interpretation

### 2.4.1 Seafloor morphology

In contrast to the seafloor in neighbouring ice-stream troughs, which are glacially scoured and dominated by various types of streamlined bedforms (Lowe and Anderson 2002, 2003; Graham et al. 2010; Jakobsson et al. 2011, 2012), the morphology of the study area shows four distinct types of bedforms on a relatively even, SW-wards dipping seafloor (Fig. 2-2):

#### i) Large-scale hummocks

In the northwestern part of the study area  $\pm$ NW-SE striking large-scale hummocks with a wavelength of  $\sim 4$  km and crest heights between 20 and 25 m are identified (Fig. 2-2). Their length varies from 3.2 to 4.5 km and their width is  $\sim 3.3 \pm 0.1$  km, while their crest-to-crest distances are  $4.2 \pm 0.1$  km. The two northernmost hummocks have a slightly arcuate shape (Figs. 2-2, 2-3). Due to their regular spacing, similar height and close spatial relationship, it is likely that the hummocks are relict moraines that formed beneath an ice sheet (cf. Clark and Meehan 2001). Their dimensions (wavelengths of  $\sim 4$  km) distinguish them from similar but smaller features, which also have a hummocky shape, such as ribbed/rogen moraines and transverse subglacial bedforms (Clark and

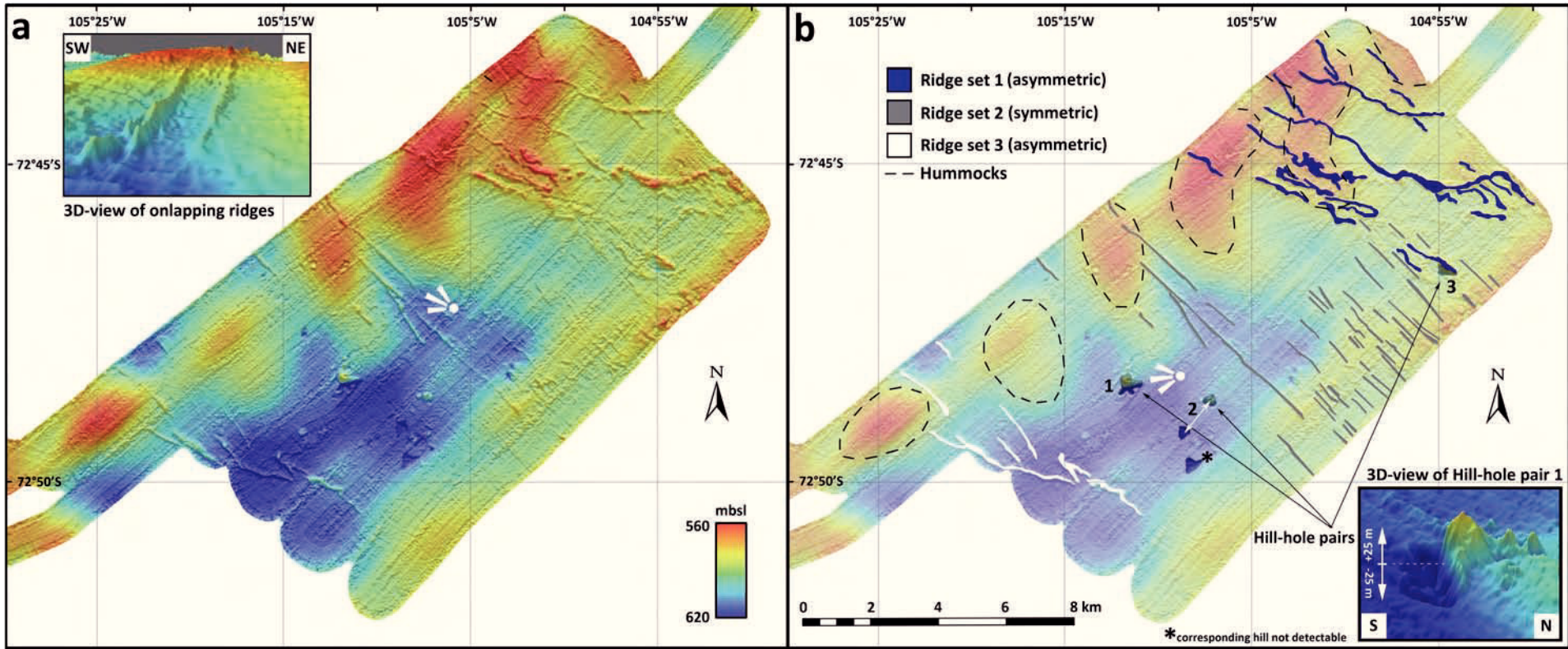


**Figure 2-2.** Close-up of study area. (a) Bathymetry of the study area, (b) Different sets of bedforms (highlighted); Insets show 3D-views of ridges onlapping onto hummock and Hill-hole pair 1, respectively (each point of view is indicated by white perspective symbol). Grid cell size 20 m. Grid illuminated from the NNE.

Meehan 2001; Marich et al. 2005; Dunlop and Clark 2006; Ottesen and Dowdeswell 2009). Glacial bedforms with similar dimensions to those described here have been reported from the relict beds of the former Irish and Laurentide Ice Sheets (Clark and Meehan 2001; Greenwood and Kleman 2010). Greenwood and Kleman (2010) interpret ‘mega-scale’ ridges as subglacial bedforms resulting from the large-scale transverse organisation of till beneath the ice sheet. They are analogous to ribbed/rogen moraines, which have been widely mapped on palaeo-ice sheet beds across northern Europe (e.g. Hättestrand 1997; Lundqvist 1997; Möller 2010) and North America (e.g. Aylsworth and Shilts 1989; Bouchard 1989). Based on this analogy and their size we term these features large-scale ribbed moraines.

#### ii) Hill-hole pairs

Three pairs of hills and holes are observed in the working area (Fig. 2-2). The first hill hole pair (Fig. 2-2b, Hill-hole pair 1) consists of a hill-size (~25 m) that matches the hole-size exactly (inset Fig. 2-2b; Fig. 2-3, panel 10). Its width and length are 650 m and 1000 m, respectively. The two other pairs are smaller with a hill-hole height/depth relationship of 12/12 m (Fig. 2-2b, Hill-hole pair 2) and 10/10 m (Fig. 2-2b, Hill-hole pair 3; Fig. 2-3, panel 9) and widths/lengths of 450/1500 m and 780/500 m, respectively (note the large distance of 1500 m between the hill and hole of Hill-hole pair 2). The dimensions of the hill-hole pairs vary, but individual pairs show the same systematic relationship in size and volume of the hole and the corresponding hill. The hill is consistently located to the NE of the corresponding hole, while the distance between the crest of the hill and the centre of the hole increases from ~400 m for pair 1 to ~1.5 km for pair 2. For the southernmost hole no corresponding hill could be detected (Fig. 2-2b). Following Bluemle and Clayton (1984), who described a hill-hole pair as “a discrete hill of ice-thrust material, situated a short distance down glacier from a depression of similar size and shape” (p. 284), we suggest the hill-hole pairs in the eastern ASE are ice-thrust features, whereby slow flowing, grounded, and cold-based ice ripped up a raft of sediment from its bed, forming a hole, entrained and transported the material at the ice base and subsequently deposited the raft down-stream, to form a hill (cf. Hogan et al. 2010, and references therein).



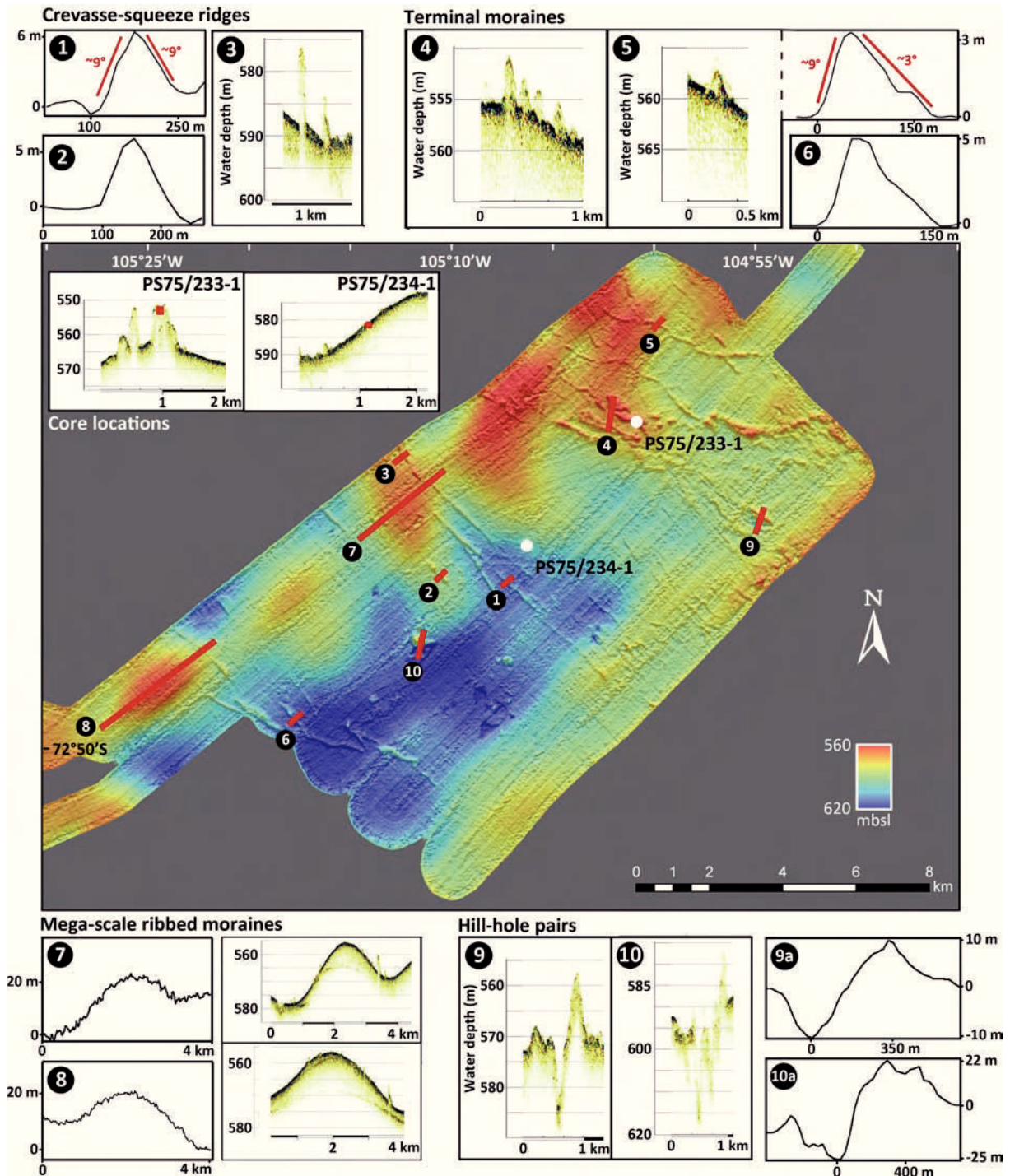


**Figure 2-3.** Profiles of the different types of bedforms derived from sub-bottom (PARASOUND) and multibeam swath bathymetry (Hydrosweep) data. Red lines with corresponding numbers indicate the locations within the study area. The y-axis gives the water depth in the PARASOUND profiles and the height from sea floor in Hydrosweep profiles, respectively. Locations of gravity cores are given in panel 'Core locations' (sub-bottom core penetration is marked in red) and as white dots in the map of the study area. In panel 1 and 5 slope angles of ridges are indicated.

### iii) Asymmetric ridges

Two sets of asymmetric, continuous to discontinuous ridges occur in the eastern and western parts of the study area (Fig. 2-2, Ridge sets 1, 3). The ridges are linear to curvilinear, strike in a WNW-ESE (Ridge set 1) and NW-SE (Ridge set 3) direction. The

steeper ( $\sim 9^\circ$ ) flanks of the ridges usually face SW-wards, while their more gentle ( $\sim 3^\circ$ ) flanks face NE-wards (Fig. 2-3, panel 5). The ridges have heights of 3-15 m, widths of 80-250 m ( $\sim 160$  m on average), and lengths between  $\sim 1$  and  $\sim 6$  km. Stratigraphically, the ridges overlie the large-scale ribbed moraines (Fig. 2-3, panel 4 and 5). Similar asymmetric ridges with almost identical slope angles were recently described from the East Greenland shelf, where they have been interpreted as ‘push moraines’ (Winkelmann et al. 2010). We interpret the asymmetric ridges in the study area as terminal moraines, recording phases of minor ice advance, which either pushed or deposited subglacial debris along a NE-ward facing ice front. The ice-flow direction is inferred from the ridges’ steeper SW flanks and the more gentle NE flanks, with the latter possibly having been formed by proglacial gravity flows or sediment bulldozing (e.g. Winkelmann et al. 2010).

#### iv) Symmetric ridges

Highly linear and parallel symmetric ridges occur in the central part of the study area (Fig. 2-2b, Ridge set 2). The NW-SE striking ridges (strike angle  $\sim 45^\circ$ ) are continuous to discontinuous. Their flanks have steeper slope angles than the asymmetric ridge sets ( $\sim 9^\circ$  on both flanks). The lengths of the symmetric ridges vary between 0.5 and 6 km and their widths between 60 and 140 m. Their crest heights range from 4 to 8 m ( $\sim 6$  m on average). The ridges clearly onlap the large-scale ribbed moraines indicating that the symmetric ridges formed at a later stage (inset Fig. 2-2a) and that they are not constructional features, like the terminal moraines described previously. Because of this geometry, their highly linear and parallel orientation and their symmetric slope angles, we suggest the features are crevasse-squeeze ridges, formed by squeezing of basal till into subglacial crevasses of overlying ice (e.g. Boulton et al. 1996; Evans and Rea 1999).

### 2.4.2 Sub-bottom acoustic stratigraphy

Several undulating and discontinuous sub-bottom reflectors, which define the bases of acoustically transparent sedimentary units, were observed in the study area (Figs. 2-4, 2-5). The previously described and interpreted bedforms (Section 2.1 ‘i-iv’) were either formed on top of the upper transparent unit or at its base, where the shallowest sub-bottom reflector crops out at the seafloor (boxes in Fig. 2-4). The minimum thickness of

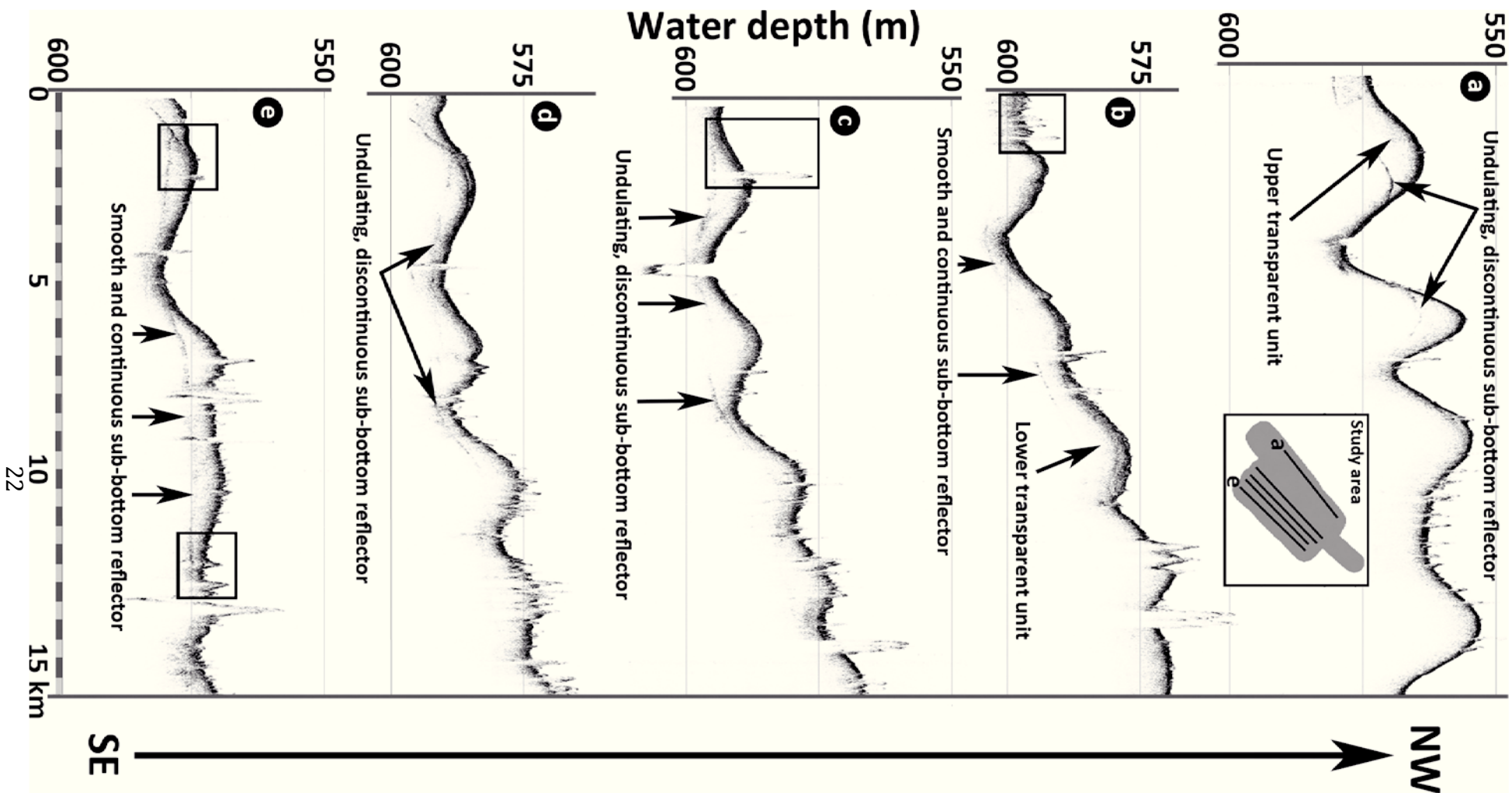


**Figure 2-4.** PARASOUND sub-bottom information of the study area. The PARASOUND profiles are orientated from the southwest (left) to the northeast (right) and are presented in a northwestward succession (upwards; vertical exaggeration is 15x). A clear eastward rise and several distinct sub-bottom reflectors are recognisable. The locations of the profiles within the study area are shown in the small box 'working area'. Locations of outcropping sub-bottom reflectors are indicated by black boxes. The penetration depth is ~10-15 m.



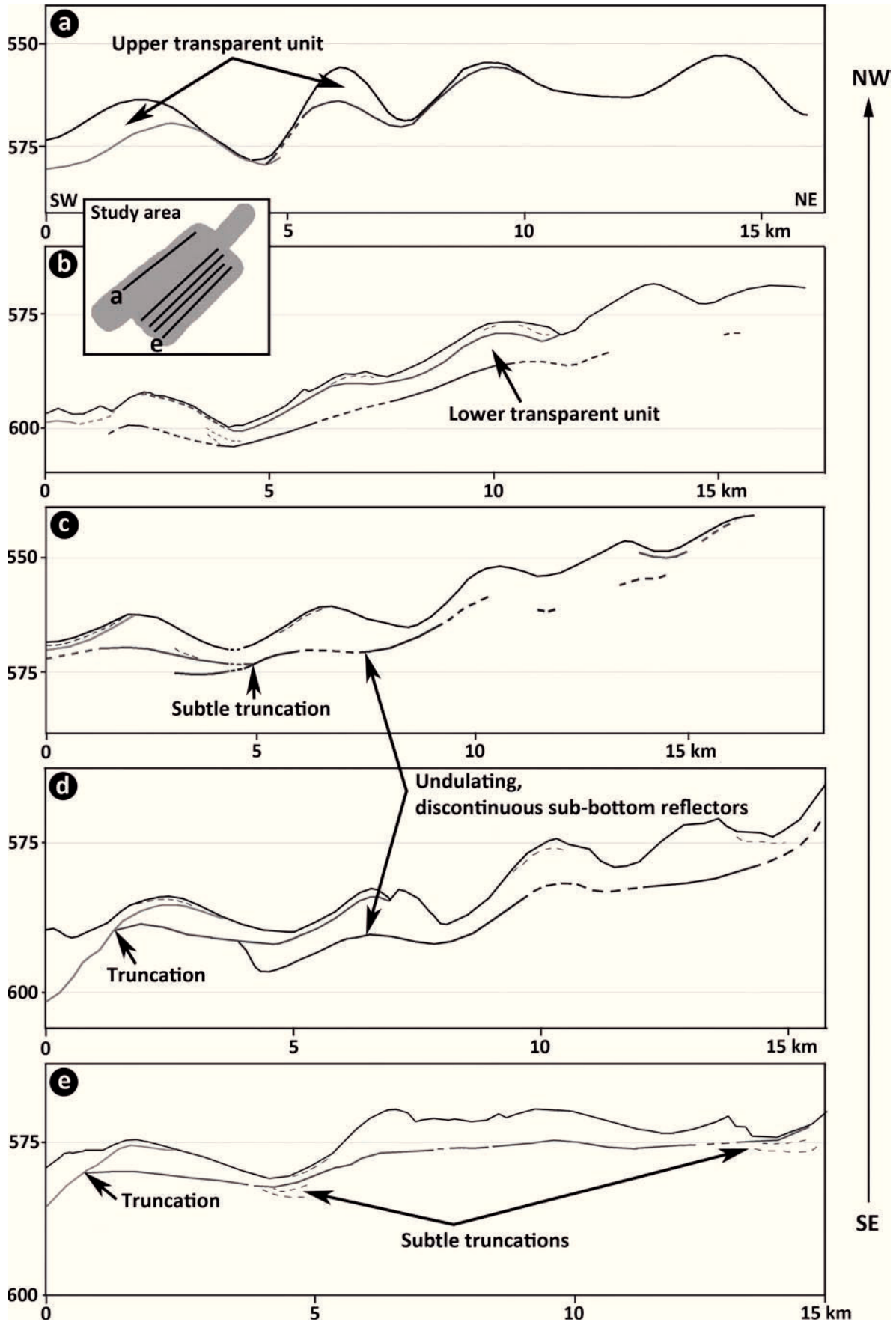
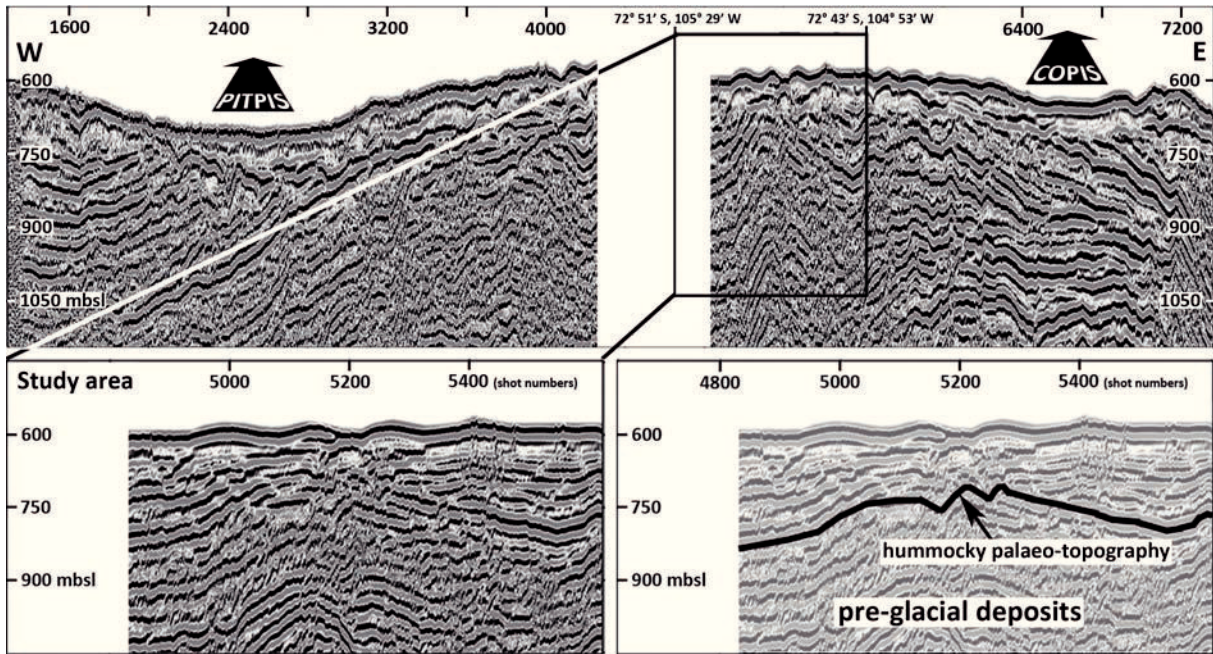


Figure 2-5. Illustration of PARASOUND profiles from figure 6. Dashed lines indicate weak or intrapolated sections of sub-bottom reflectors; minor reflectors are indicated by thin lines. The locations of the profiles within the working area are shown in the small box 'working area'.



**Figure 2-6.** Detail of seismic line AWI-20100126a, crossing the study area (black box) and showing a hummocky topography at ~150 mbsf (black line, lower right panel), representing the onset of subglacial deposition (Hochmuth and Gohl, in review). Locations and flow directions of COPIS and PITPIS troughs are indicated.

the transparent units ranges from no cover up to 12 m. Locally, the transparent units show subtle discontinuous internal reflectors (Fig. 2-5, thin dashed lines). In some places the basal reflector of these units mirrors the undulations of the shallower reflector but with a minor lateral offset (Fig. 2-5). Fewer sub-bottom reflectors occur in the NE part of the study area than in its SW part. Although the undulating sub-bottom reflectors are discontinuous, they seem to be the palaeo-surfaces of older hummocks and to indicate that the modern hummocky seabed topography forms the uppermost, youngest part of a whole succession of large-scale ribbed moraines. This relationship is consistent with a section of seismic line AWI-20100126a (Fig. 2-6), which shows hummocky palaeo-topographies between the surface and a depth of ~150 m below the seafloor (mbsf). According to Hochmuth and Gohl (in review), the basal reflector of this seismic unit marks the onset of subglacial deposition. Occasionally, shallow PARASOUND sub-bottom reflectors are smooth and extend over several kilometres (Figs. 2-4, 2-5, profiles b and e). In some cases a shallower sub-bottom reflector truncates deeper reflectors (Figs. 2-4, 2-5, profiles c, d and e). In the SW part of the study area a distinct sub-bottom reflector crops out at the seafloor and truncates another reflector at a sub-bottom depth of ~1 and ~5 m, respectively (Figs. 2-4, 2-5; profiles d and e). Similar truncations of more subtle sub-bottom reflectors at low angles are also identified (Fig. 2-5, thin dashed lines in profiles b and c). Locally, the seabed outcrop of

the shallowest sub-bottom reflector seems to coincide with the presence of the asymmetric ridges (boxes in Fig. 2-4). Both the asymmetric and the symmetric ridges are recorded in the PARASOUND profiles as several strong hyperbolic reflections with acoustic blanking below them.

### 2.4.3 Sediment cores

To provide geological context to the described bedforms, we recovered two sediment cores from the study area. Gravity core PS75/233-1 recovered 2.34 m of sediment from the top of a terminal moraine in the NE part of the study area, while core PS75/234-1 retrieved 0.85 m from the southern flank of a large-scale ribbed moraine, proximal to the area of crevasse-squeeze ridges (Fig. 2-3, panel 'Core locations').

#### 2.4.3.1 Lithology

Core PS75/233-1 recovered two distinct lithological units (Fig. 2-7). The lower unit contains olive to dark grey, poorly sorted, massive gravelly sandy mud with a high content of pebbles (with diameters  $\leq 7$  cm) and is characterised by uniform MS values, medium shear strength values, and uniformly low water contents. Grain-size distribution is homogenous, and WBD values and  $C_{org}$  contents are also uniform. Discrete peaks and troughs in the MS curve are frequently associated with either pebbles/larger cobbles or voids, respectively. These peaks mostly occur in the lower part of the unit (115-234 cmbsf). Core photos and X-radiographs show that pebbles and clasts of various sizes are dispersed throughout this unit.

The overlying lithological unit contains a structureless sandy mud, which differs from the underlying sediments by higher water contents and very low shear strengths. The MS and WBD values drop to  $\sim 60 \times 10^{-5}$  SI units and  $\sim 1.6$  g/cm<sup>3</sup>, respectively. The mud content increases to very high values near the core surface, while both the sand and gravel contents decrease concurrently. The  $C_{org}$  content rises up to 0.25 wt.%. Photos and radiographs show an up-core decrease in smaller pebbles and a homogenous fine-grained matrix containing infrequent larger clasts.



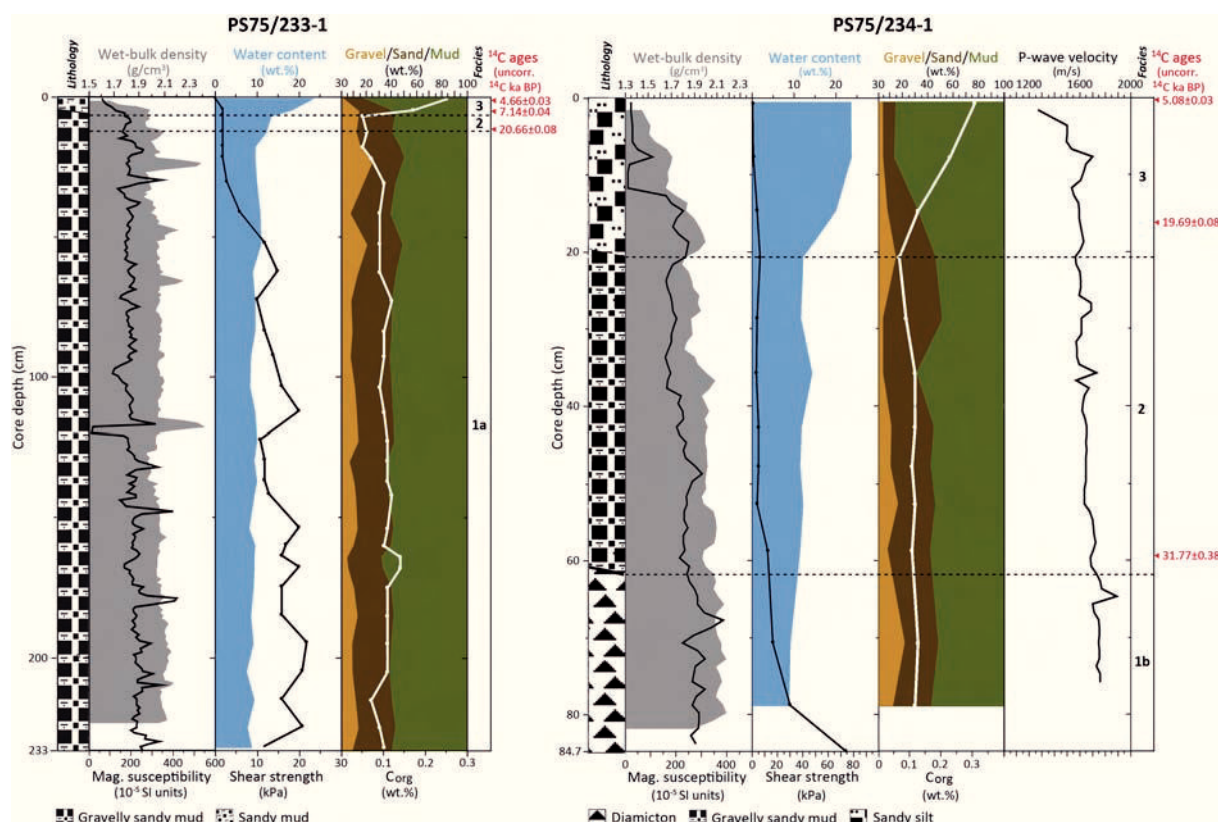


**Figure 2-7.** Core parameters for PS75/233-1 and PS75/234-1 (Lithology, Wet-bulk density (WBD), Magnetic susceptibility, Water content, Shear strength, Grain-size fractions (Gravel, Sand, Mud),  $C_{org}$  content, P-wave velocity (data only available for PS75/234-1). Dashed lines mark the facies boundaries: (1a) Grounding line (1b) Subglacial, (2) Proximal grounding line, (3) Seasonal open-marine. Sampling locations for AMS  $^{14}C$  dating and corresponding (uncorrected) ages are indicated with red arrows.

Core PS75/234-1 is characterised by three distinct lithological units (Fig. 2-7). The lower unit comprises a dark grey diamicton with MS values between 250 and 300  $\times 10^{-5}$  SI units. Within the diamicton, there is a significant drop in shear strength from 74 kPa in the core catcher sample at ~86 cmbsf to 12 kPa at 63 cmbsf. The high shear strength values in the lower part of the diamicton coincide with high  $V_p$ . The water and  $C_{org}$  contents are low, while the WBD is relatively high and constant. The grain-size distribution shows only minor variations with relatively high contents of gravel.

The middle lithological unit comprises a gravelly sandy mud with MS values between 150 and 250  $10^{-5}$  SI units, a low to medium shear strength, medium water and low  $C_{org}$  contents. The  $V_p$  ranges between 1750 and 1560  $ms^{-1}$ . The WBD is relatively constant throughout. The mud content remains at ~60 wt.% with a maximum (~70 wt.%) at 36 cmbsf. The sand content slightly increases towards the upper part of the unit. The photos and radiographs reveal lamination between 22 and 40 cmbsf. The gravel content ranges between 4 and 18 wt.% with lowest values in the middle section of the unit (29-36 cmbsf).

The upper lithological unit is characterised by homogeneous sandy silt, which shows a significant MS drop, a slight decrease in shear strength and a strong increase of the water content. Concurrently, the mud and  $C_{org}$  contents increase, while the WBD decreases towards the top of the unit.

#### 2.4.3.2 Facies interpretation of lithological units

Our facies interpretation of the lithological units in cores PS75/233-1 and PS75/234-1 (Fig. 2-7) follows the interpretation of similar sedimentary sequences reported from the Antarctic shelf (e.g. Licht et al. 1996; Domack et al. 1998, 1999; Licht et al. 1999; Pudsey and Evans 2001; Evans and Pudsey 2002; Evans et al. 2005; Heroy and Anderson 2005; Hillenbrand et al. 2005, 2010; Ó Cofaigh et al. 2005; Mosola and Anderson 2006; Smith et al. 2009, 2011).

Except its uppermost 5 cm, we interpret the gravelly sandy mud section in core PS75/233-1 as a till deposited at the grounding line of a glacier terminus (Facies 1a). This interpretation is based on the absence of both sedimentary structures and biogenic components (expressed by the very low  $C_{org}$  contents), relatively high shear strength, low water content and a lack of down-core variability in grain-size and physical properties within this section. A close inspection of the physical properties and sedimentological parameters of core PS75/233-1 reveals that the uppermost part of the gravelly sandy mud is characterised by higher water and mud contents, but lower shear strength values and  $C_{org}$  contents than the rest of this lithological unit (Fig. 2-7). These sediments were probably deposited in a glaciomarine setting proximal to the grounding line and under perennial sea-ice or ice-shelf cover (Facies 2). The overlying sandy mud is characterised by significantly higher water content, very low MS and shear strength, and high contents of mud and  $C_{org}$ , indicating its deposition under seasonal open-marine conditions distal from the grounding line (Facies 3).

The three lithological units recovered in core PS75/234-1 reflect the transition from subglacial to open-marine conditions (Figs. 2-7, 2-8). We interpret the over-consolidated diamicton at the core base as a subglacial 'stiff till' (Fig. 2-7, Facies 1b) based on its high  $V_p$ , shear strength and low water content. Similar 'stiff tills' have been described elsewhere on the Antarctic continental shelf (e.g. Marguerite Trough: Ó Cofaigh et al. 2005; Robertson Trough: Evans et al. 2005) and were attributed to deposition beneath a

slow-flowing or stagnant cold-based ice sheet (Fig. 2-8a). The overlying gravelly sandy mud unit was probably deposited during initial ice retreat in a glaciomarine setting proximal to the grounding line (Fig. 2-7, Facies 2; Fig. 2-8b), because stratification of sandy and gravelly layers within this unit indicates the influence of currents, i.e. deposition by meltwater flows and/or grain flows. In contrast, the sandy silt near the core top is interpreted as seasonal open-marine sediment deposited distal from the grounding line (Fig. 2-7, Facies 3; Fig. 2-8c), because it has very low shear strength, and high contents of water, mud and  $C_{org}$ .

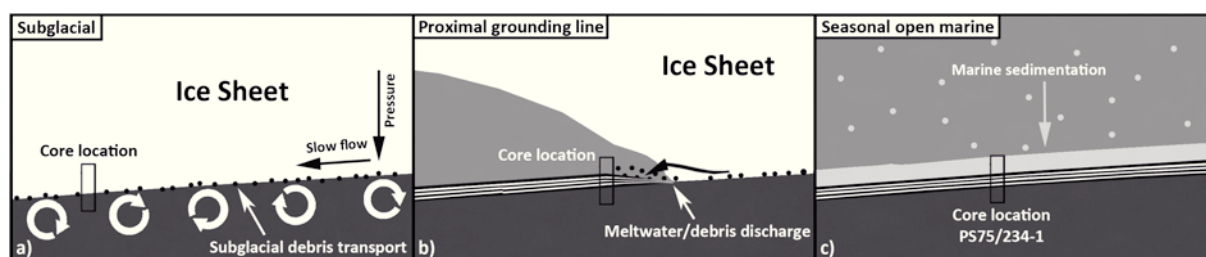


**Figure 2-8.** Description of facies succession in core PS75/234-1. Core location and penetration is illustrated by the black box. Facies: Subglacial (a), Proximal grounding line (b), Seasonal open-marine (c). Illustration is not to scale.

#### 2.4.4 Radiocarbon chronology

All conventional and corrected (corr.) AMS  $^{14}C$  dates obtained from cores PS75/233-1 and PS75/234-1 are given in Table 2-1. The uncorrected core-top AIO dates are  $4660 \pm 30$   $^{14}C$  yrs BP for core PS75/233-1 and  $5080 \pm 30$   $^{14}C$  yrs BP for core PS75/234-1. These dates lie within the range of AIO  $^{14}C$  ages of seabed surface sediments from the middle and inner shelf of the Dotson-Getz Trough in the western ASE (Smith et al. 2011). The uncorrected AIO dates from the glaciomarine sediments at 4-5 cmbsf and 12-13 cmbsf in core PS75/233-1 are  $7140 \pm 40$   $^{14}C$  yrs BP and  $20,660 \pm 80$   $^{14}C$  yrs BP, respectively. The older date was obtained from the very base of Facies 2 and provides a minimum age of 16.0 corr.  $^{14}C$  ka BP for the deposition of the NE terminal moraines and the grounding-line retreat from site PS75/233-1.

The uncorrected AIO dates from the bases of the open marine Facies 3 and the ice sheet proximal Facies 2 in core PS75/234-1 are  $19,690 \pm 80$   $^{14}C$  yrs BP and  $31,770 \pm 380$   $^{14}C$  yrs BP, respectively. In contrast to the younger AIO date, the very old AIO age from the base of Facies 2 probably results from significant contamination with fossil organic matter supplied from the nearby grounding line. Therefore, this old date is unreliable for constraining the time of grounding-line retreat from site PS75/234-1 (cf. Mosola &

Anderson 2006). Consequently, we assume that the grounded WAIS retreated from this site at some time before the onset of seasonal open-marine deposition, i.e. before 14.6 corr.  $^{14}\text{C}$  ka BP.

**Table 2-1.** Uncorrected and corrected AMS  $^{14}\text{C}$  dates from sediment cores PS75/233-1 and PS75/234-1 together with locations, water depth, sample depth and dated material (AIO = Acid Insoluble Organic matter).

Core	Publication code	Lat.	Lon.	Water depth (m)	Core depth (cmbsf)	Material dated	Uncorrected $^{14}\text{C}$ age (yrs BP)	$\pm 1\sigma$	Correction	Corrected $^{14}\text{C}$ age (yrs BP)
PS75/233-1	Beta-315967	-72.754167	-105.0165	560	0.5	AIO	4660	30	N/A	0
PS75/233-1	Beta-315968	-72.754167	-105.0165	560	4.5	AIO	7140	40	4660	2480
PS75/233-1	Beta-315969	-72.754167	-105.0165	560	12.5	AIO	20660	80	4660	16000
PS75/234-1	Beta-318119	-72.784167	-105.1048	584	0.5	AIO	5080	30	N/A	0
PS75/234-1	Beta-318120	-72.784167	-105.1048	584	15.5	AIO	19690	80	5080	14610
PS75/234-1	Beta-318121	-72.784167	-105.1048	584	59.5	AIO	31770	380	5080	26690

## 2.5 Discussion

### 2.5.1 Reconstruction of palaeo-ice flow and basal ice conditions from bedforms

#### i) Large-scale ribbed moraine

The formation processes of ribbed moraines are poorly defined (Dunlop and Clark 2006; Dunlop et al. 2008). Some authors have assigned the transition from hummocky/transverse ribbed terrain to streamlined bedforms to an increase in ice flow velocity (Dunlop and Clark 2006; Ottesen and Dowdeswell 2009). A similar transition from ribbed terrain on the inter-ice stream ridge to streamlined bedforms within the PITPIS and COPIS troughs (e.g. Graham et al. 2010; Jakobsson et al. 2012; Kirshner et al. 2012) characterises our study area. Therefore, we attribute the formation of the large-scale ribbed moraine field in the eastern ASE to slow flow of grounded ice. Dunlop et al. (2008) presented a theoretical model, which predicts the formation of ‘mega-scale ribbed moraines’ with wavelengths of  $\leq 5.8$  km at the ice-bed interface. According to these authors, the mechanism for the formation of hummocky/ribbed terrain is the ‘Bed Ribbing Instability Explanation [BRIE]’. BRIE describes bed ribbing as a wave-like process, which occurs below slowly flowing ice and is caused by ribbing instabilities due to perturbations in the underlying bed. This model provides the first physically based explanation for the genesis of ribbed/hummocky terrain at the ice-bed interface.

The large-scale ribbed moraines in the eastern ASE are observed on an elevated inter-ice stream ridge north of Burke Island. We expect that at the LGM this area was a zone of slow ice flow between the fast-flowing PITPIS and COPIS in analogy to inter-ice stream

ridges in the modern Antarctic ice sheet, where ice flow velocity tends to be low (Hulbe and MacAyeal 1999). The direction of the palaeo-ice flow in our study area can be inferred from (i) the shape of the two arcuate large-scale ribbed moraines (Fig. 2-2b), whose 'horns' point downstream (cf. Dunlop and Clark 2006), and (ii) the long axes of the four northern large-scale ribbed moraines (Figs. 2-2, 2-3), which are orientated transverse to the ice flow (Dunlop and Clark 2006; Dunlop et al. 2008). Thus, the palaeo-ice flow direction on the inter-ice stream ridge was towards ENE. In contrast, mega-scale glacial lineations (MSG L) in nearby PITPIS trough indicate ice flow towards NNE (Graham et al. 2010; Jakobsson et al. 2011). We suggest that the formation of the large-scale ribbed moraine was related to the flow of PITPIS, thus the discrepancy in flow directions might indicate a diachronous formation from the MSG L.

Sediment core PS75/234-1 was recovered from the southern flank of a large-scale ribbed moraine. The corresponding PARASOUND profile reveals a strong reflector at or close to the sea floor (Fig. 2-3, panel 'Core locations'), which most likely corresponds to the top of the subglacial stiff till recovered at site PS75/234-1. The widespread occurrence of a hard sea floor substrate across the large-scale ribbed moraine field is also indicated by the lack of iceberg scours. In contrast, the terminal moraines and crevasse-squeeze ridges show some indication of post-depositional 'cut through' by icebergs. Iceberg scours in the eastern ASE are observed down to ca. 700 m water depth (e.g. Lowe and Anderson 2002, 2003; Dowdeswell and Bamber 2007; Graham et al. 2010; Jakobsson et al. 2011), which is well below the maximum water depth of our study area. Furthermore, Dowdeswell and Bamber (2007) conclude maximum keel depths of up to 633 m for modern icebergs calving from Pine Island Glacier, implying that even today our study area is potentially vulnerable to iceberg scouring. These findings indicate that the large-scale ribbed moraines were formed in hard substrate, such as stiff till, which does not allow penetration of iceberg keels. This conclusion is consistent with results from Evans et al. (2005) and Ó Cofaigh et al. (2005, 2007), who observed an undulating sub-seafloor reflector in acoustic sub-bottom profiles from the Antarctic Peninsula shelf. The sub-bottom reflector indicates a hummocky palaeo-topography with its 2D expression resembling that of the large-scale ribbed moraines in the eastern ASE, although the wavelength of the latter is almost four times larger. In sediment cores recovered from the Antarctic Peninsula shelf, the top of the subbottom hummocks corresponds to the surface of a stiff till (e.g. Reinardy et al. 2011b). Evans et



al. (2005) and Ó Cofaigh et al. (2005, 2007) attributed the genesis of this stiff till to a combination of deformation (cf. Van der Meer et al. 2003) and subglacial traction (cf. Evans et al. 2006) at the base of slowly flowing ice, possibly during periods of ice sheet advance. This hypothesis was also supported by findings of Reinardy et al. (2011a, b), who detected corresponding microscale deformation features within the stiff till and suggested that grounded-ice flow over stiff till substrate was mainly facilitated by basal sliding.

#### ii) Hill-hole pairs

Hill-hole pairs provide reliable information about both the palaeo-flow directions and the basal ice regime. The hill-hole pairs in our study area, which post-date the formation of the large-scale ribbed moraines (Fig. 2-2), document slow flow of cold-based ice, strongly-coupled to its bed, in a NE direction. In contrast, the large-scale ribbed moraines indicate flow to ENE. This change in flow direction suggests that the hill-hole pairs formed after the ribbed moraines, but prior to or synchronous with the terminal moraines in the NE of the study area (see following paragraph 'iii'). The lack of streamlined bedforms on both the hills and the large-scale ribbed moraines suggests that their formation was not related to streaming ice, but probably resulted from slowly flowing ice over a resistant substrate.

#### iii) Terminal moraines

The orientation of both the terminal moraines and the hill-hole pairs (Figs. 2-2, 2-3) provides evidence for a change in flow direction to the NE. The same phase of ice sheet flow (likely a minor advance before ~16.0 corr. <sup>14</sup>C ka BP) that formed the terminal moraines in the NE of the study area, probably also generated the three hill-hole pairs, because Hill-hole pair 3 (Fig. 2-2b) forms part of the NE terminal moraine field. Core PS75/233-1, which was taken on top of one of these moraines, recovered a massive soft till (Facies 1a), which we assume was reworked from underlying stiff till (cf. Reinardy et al. 2011a). We argue that the terminal moraines were deposited at the ice sheet terminus during phases of re-advance or brief pauses during retreat. The SW moraine field may have formed later between c. 14.6 corr. <sup>14</sup>C ka BP, which is the minimum age for grounded ice retreat from site PS75/234-1, and c. 10.5 corr. <sup>14</sup>C ka BP, which is the most reliable minimum age for the final WAIS retreat within nearby Pine Island Trough

(see  $^{14}\text{C}$  -dates at site KC19 in Table 1 of Kirshner et al., 2012). The latter age constraint applies only if the deposition of the terminal moraines in the SW of our study area coincided with the re-advance of ice into the western branch of PITPIS as reported by Jakobsson et al. (2012).

#### iv) Crevasse-squeeze ridges

Fracturing of a glacier terminus during a phase of stagnation that often follows a phase of rapid advance usually results in the opening of supra-, en- and subglacial crevasses. These are often orientated transverse to ice flow and are filled with subglacial sediments by basal squeezing (e.g. Boulton et al. 1996; Ottesen and Dowdeswell 2006; Ottesen et al. 2008; Bennett and Glasser 2009). After ice sheet decay symmetric moraines (identical to the symmetric ridges in the eastern ASE) persist, which can evolve crest-heights of up to  $\sim 12$  m in marine environments (Boulton et al. 1996).

Assuming that the crevasse-squeeze ridges (Fig. 2-2b, Ridge set 2) in our study area were formed transverse to ice flow, their orientation indicates a flow direction towards NE, which complements ice flow direction inferred from both the terminal moraines and hill-hole pairs. They probably formed after the deposition of the NE terminal moraines and before the terminal moraines in the SW. Their geographical position close to PS75/234-1 (Fig. 2-3) suggests that they formed before 14.6 corr.  $^{14}\text{C}$  ka BP, but after c. 16.0 corr.  $^{14}\text{C}$  ka BP (= minimum age of the NE terminal moraines).

The occurrence of the large-scale ribbed moraines, the hill-hole pairs and the crevasse-squeeze ridges on the inter-ice stream ridge of the eastern ASE all give evidence for slow ice flow and stagnant ice. The absence of overprinting bedforms such as MSGL or other streamlined features, especially on top of the terminal moraines and the crevasse-squeeze ridges, suggests that the stationary ice most likely decayed in-situ and decoupled rapidly from the bed, possibly in response to post-LGM sea level rise.

### 2.5.2 Sub-bottom characteristics and seafloor bathymetry

The presence of large-scale hummocky sub-bottom topography visible in PARASOUND and seismic profiles demonstrates that the area was repeatedly influenced by slow-flowing grounded ice, probably during several glacial cycles. We also consider a structural origin for the hummocks (i.e. that they are imprints of the underlying bedrock

topography), but some of the sub-bottom reflectors are truncated either by the seabed surface reflector or by other sub-bottom reflectors. Therefore, we suggest these truncations are the result of glacial erosion. In the SW part of the study area (Fig. 2-4), all five PARASOUND profiles reveal a sub-bottom reflector that crops out at the seabed surface and becomes the seafloor reflector further to the NE. In profiles b, c and e of Figure 2-4, the sub-bottom reflector outcrop coincides with the presence of terminal moraines, suggesting that the advance of ice resulted in the deposition of a basal till sheet in the SW (corresponding to the acoustic transparent unit between the sub-bottom reflector and the seafloor) and of a 'push' moraine at its front.

### 2.5.3 Glacial history of the inter-ice stream ridge

We now present a conceptual model (Fig. 2-9) illustrating the sequence of bedform genesis in the study area, which is based on the spatial relationship of the bedforms, information from sediment cores, and data from previously published studies (Lowe and Anderson 2002; Evans et al. 2006; Graham et al. 2010; Jakobsson et al. 2011, 2012; Kirshner et al. 2012). All ages from our cores and earlier publications are given as corrected  $^{14}\text{C}$  dates.

#### Phase 1 – Maximum ice advance

During the LGM, PITPIS and COPIS flowed in their troughs around the topographical high surrounding Burke Island towards NNE and NNW, respectively (Fig. 2-1; Lowe and Anderson 2002; Graham et al. 2010; Jakobsson et al. 2011, 2012; Kirshner et al. 2012). The observation of a prominent sub-bottom reflector in profiles from PITPIS (Evans et al. 2006; Ó Cofaigh et al. 2007; Graham et al. 2010) may indicate that a stiff till was deposited at the base of the ice as it advanced across the shelf (cf. Reinardy et al. 2011a; Livingstone et al. 2012). The presence of MSGL in a soft deformation till overlying the prominent sub-bottom reflector in PITPIS indicates that ice streaming was active during the LGM and continued during retreat (Lowe and Anderson 2002; Evans et al. 2006; Graham et al. 2010; Jakobsson et al. 2011, 2012; Kirshner et al. 2012). The presence of stiff till near the sea floor in our study area and the apparent absence of a widespread deformation till may demonstrate that ice flow on the inter-ice stream ridge remained slow throughout the last glacial period, possibly even while ice was streaming in the

troughs. Slow ice flow on the ridge certainly resulted in the moulding of the large-scale ribbed moraines, whose transverse orientation indicates an initial ice flow towards ENE (Fig. 2-9, panel 1), perhaps associated the formation of marginal shear zones at the transition from slow to fast flowing ice. However, seismic and sub-bottom information suggests that similar large-scale ribbed moraines may have evolved previously on the ridge (Fig. 2-9, panel 1a). Thus it is possible that the modern surface expression of these ribbed moraines has been shaped by several phases of grounded-ice flow (Figs. 2-4, 2-5, 2-6).

### Phase 2 – Initial ice retreat

The initial ice retreat on the eastern ASE shelf was characterised by stepwise grounding line retreat of PITPIS with deglaciation of the outer shelf occurring sometime before 17.4  $^{14}\text{C}$  ka BP (see  $^{14}\text{C}$ -date at site KC13 in Table 1 of Kirshner et al., 2012) and the mid-shelf in the vicinity of Burke Island between 17.4 and 10.5  $^{14}\text{C}$  ka BP (see  $^{14}\text{C}$ -dates at sites KC13, PC39 and KC19 in Table 1 of Kirshner et al., 2012). Newly obtained  $^{14}\text{C}$ -dates in our study constrain the timing of initial inter-ice stream ridge deglaciation to before  $\sim 16.0$   $^{14}\text{C}$  ka BP. Prior to the initial ice sheet retreat, the ice in the troughs was still flowing rapidly compared to the ice flow on the ridge, which resulted in ice flow speed variations between the troughs and the inter-ice stream ridge (Fig. 2-9, panel 2). Therefore, marginal shear zones probably existed somewhere at the boundaries of the inter-ice stream ridge (cf. Hulbe and MacAyeal 1999), but which we have yet to characterise in terms of their geomorphic expression. Phases of rapid retreat on the middle shelf, possibly in response to ice-shelf collapses, were interrupted by phases of grounding-line stagnation, which lasted several hundred to a few thousand years and caused the formation of grounding-zone wedges (Lowe and Anderson 2002; Evans et al. 2006; Graham et al. 2010; Jakobsson et al. 2011, 2012; Kirshner et al. 2012). During this early retreat period, the grounding line on the inter-ice stream ridge may either have remained stationary or retreated to a position just to the south of the study area, as it was suggested for the PITPIS trough by Jakobsson et al. (2012).

### Phase 3 – Stillstand/Minor re-advance I

The general post-LGM warming was interrupted by several episodes of cooling (e.g. the Antarctic Cold Reversal), which caused re-advances of ice in the southern hemisphere

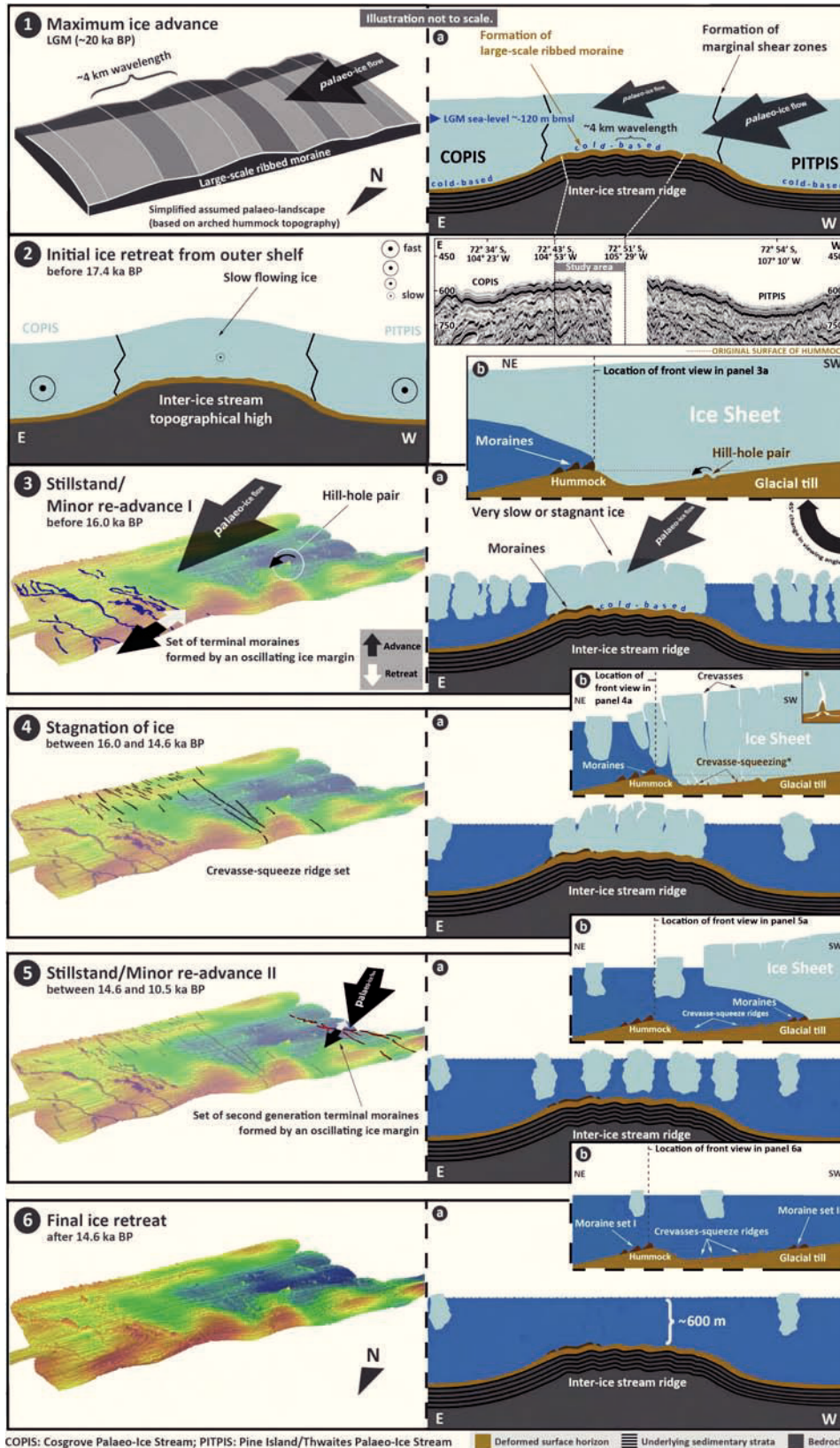


**Figure 2-9.** Relative chronology of inter-ice stream ridge deglaciation in six phases, (1) Maximum ice advance and conditions of full-glacial flow formed large-scale ribbed moraine, (2) Initial ice retreat from outer shelf, (3) Minor re-advance I caused deposition of northeastern set of terminal moraines, (4) Stagnation of ice was characterised by formation of an extensive field of crevasse-squeeze ridges, (5) Minor re-advance II caused deposition of southwestern set of terminal moraines. (6) Final ice retreat, (no disturbance or overprinting of bedforms, except of some indication for post-depositional ‘cut through’ by iceberg keels, north of the southwestern terminal moraines can be detected). For further detailed description see text. Note that profiles in 1a, 2, 3a, 4a, 5a and 6a are E-W orientated (View from N to S).



(Putnam et al. 2010). These re-advances are unlikely to have reached the LGM extent, but it is possible that some of them left moraines on the shelf. We suggest that during phase 3 the ice paused or re-advanced on the inter-ice stream ridge, and as a result terminal moraines were deposited by an oscillating ice margin in the NE of our study area at an early post-LGM stage, i.e. just prior to 16.0  $^{14}\text{C}$  ka BP (Fig. 2-9, panel 3, 3a, 3b). The ice flow switched its direction from ENE (large-scale ribbed moraines) to NNE. Prior to or synchronous with the deposition of the NE set of terminal moraines at  $\sim 16.0$   $^{14}\text{C}$  ka BP, slowly flowing cold-based ice probably eroded plugs of debris from the stiff till substrate, thereby creating the three holes, and re-deposited them as hills further downstream to the NNE (Fig. 2-9, panel 3b).

#### Phase 4 – Stagnation of ice

The ice flow slowed down until stagnation before 14.6  $^{14}\text{C}$  ka BP. The ice was still thick enough for grounding and possibly decayed and melted in-situ (cf. Evans and Rea 1999). As a result, subglacial crevasses formed. Due to the pressure of the overlying ice, till was squeezed into these basal crevasses and formed crevasse-squeeze ridges (Fig. 2-9, panel 4b). According to the radiocarbon constraints presented by Kirshner et al. (2012), the ice on the same latitudinal position in PITPIS trough decoupled from its bed between 17.4 and 10.5  $^{14}\text{C}$  ka BP.

#### Phase 5 – Stillstand/Minor re-advance II

As the ice sheet retreated further landward, a second pause or re-advance occurred in the SW part of the study area, possibly after 14.6  $^{14}\text{C}$  ka BP, and deposited another set of terminal moraines (Fig. 2-9, panel 5b). Their gentle slopes face mainly NNE-wards indicating no change in configuration between this phase and phase 3. This SW terminal moraine field could hint at another ice advance in PITPIS trough related to the westward flow-switch of PITPIS before 10.5  $^{14}\text{C}$  ka BP as reported by Jakobsson et al. (2012).

#### Phase 6 – Final ice retreat

After 14.6  $^{14}\text{C}$  ka BP, no further ice sheet influence is observed in the seabed morphology of the inter-ice stream ridge, because the bedforms are pristine and have not been overridden subsequent to their formation. Only the terminal moraines and crevasse-squeeze ridges show some indication that they have been disturbed ('cut through') by

icebergs after their formation, and even these erosional features may have been created soon after the deposition of the moraines and ridges. One possible explanation is that during the grounding line retreat of PITPIS and COPIS from the middle to the inner shelf the keel depth of most icebergs was too large to ground on the shallow banks outside the ice-stream troughs and/or the substrate was too hard for scouring the sea floor by iceberg keels.

## 2.6 Conclusions

We have presented the first geophysical and sedimentological data on a bedform assemblage preserved on an inter-ice stream ridge in the eastern ASE. This assemblage of bedforms has not been described before from the Antarctic shelf. However, the assemblage is typical for formerly glaciated margins in the Northern Hemisphere, where it is referred to as ‘inter-stream’ (Ottesen and Dowdeswell 2009) or ‘ice-marginal’ (Hogan et al. 2010). Our bedform data suggest that during the LGM the ice on the inter-ice stream ridge between PITPIS and COPIS flowed significantly slower than in the nearby troughs. The dimensions of large-scale ribbed moraines formed at the LGM support the existence of the theoretically predicted ‘mega-scale ribbed moraines’ for the first time (cf. Dunlop et al. 2008) and provide crucial insights into the basal regime of the ice sheet between PITPIS and COPIS, thus filling a significant gap in our understanding of subglacial dynamics for the palaeo-WAIS. Subsequent to the LGM the grounding line on the ridge paused or re-advanced twice, which is recorded by two sets of terminal moraines. The deposition of the NE set may have ended just before 16.0  $^{14}\text{C}$  ka BP, but certainly before 14.6  $^{14}\text{C}$  ka, while that of the SW set possibly occurred after 14.6  $^{14}\text{C}$  ka BP. Three hill-hole pairs confirm NE-ward advance and also indicate a slow, cold-based ice sheet with a strong coupling to its bed. In at least one case, minor advances were followed by a subsequent stagnation of ice, recorded by an extensive field of crevasse-squeeze ridges. This phase of stagnation must have taken place before 14.6  $^{14}\text{C}$  ka BP. The hill-hole pairs and the orientation of terminal moraines, which overlie the large-scale ribbed moraines, indicate that the ice flow direction during the LGM and the following re-advance(s) had switched from ENE to NNE. After 14.6  $^{14}\text{C}$  ka BP and the deposition of the SW terminal moraines no grounded ice has overridden the study area. The WAIS subsequently retreated to a location proximal to its modern position before

~9.8 <sup>14</sup>C ka BP (Hillenbrand et al. 2012). Thus, the deglaciation of the inter-ice stream ridge in the eastern ASE, which was previously poorly understood, may have followed the ice retreat pattern in the PITPIS trough, but shows significantly different basal ice dynamics. Further studies with a larger coverage of these areas and supplementary, more extensive sedimentological sampling and radiocarbon dating are necessary to confirm this conclusion. The new landform assemblage mapped on the eastern ASE shelf can be used as a reference dataset for interpreting other inter-ice stream areas of the Antarctic margin in future studies in order to develop a complete glacial history of the WAIS. Because inter-ice stream ridges are key areas for stabilising ice streams and major components of ice sheets in general, new insights into the flow properties and ice dynamics in these regions may help to improve models of ice-stream flow and behaviour, which ultimately aim to predict the future behaviour of the WAIS.

### **Acknowledgements**

We thank the captain and crew who participated in RV Polarstern cruise ANT-XXVI/3, and N. Lensch, M. Gutjahr, M. Forwick, P. Jernas, D. Baqué, S. Wiers, I. MacNab, M. Seebeck, and R. Fröhlking for their assistance with coring operations and post-cruise analyses, respectively. K. Hochmuth is acknowledged for processing and displaying the seismic data. The work was financially supported by the Alfred Wegener Institute research program Polar Regions and Coasts in a changing Earth System (PACES). Finally we thank Lorna Linch for her constructive, thorough and thoughtful review, which helped to improve the manuscript.



## Chapter 3.

### Detailed palaeo-ice flow pathways in the easternmost Amundsen Sea Embayment, West Antarctica

J.P. Klages <sup>a,\*</sup>, G. Kuhn <sup>a</sup>, A.G.C. Graham <sup>c</sup>, J.A. Smith <sup>b</sup>, C.-D. Hillenbrand <sup>b</sup>, F.O. Nitsche <sup>d</sup>,  
R.D. Larter <sup>b</sup>, K. Gohl <sup>a</sup>

<sup>a</sup> Alfred-Wegener-Institut, Helmholtz-Zentrum für Polar- und Meeresforschung, Marine Geology and Paleontology, Am Alten Hafen 26, 27568 Bremerhaven, Germany

<sup>b</sup> British Antarctic Survey, High Cross, Madingley Road, Cambridge CB3 0ET, United Kingdom

<sup>c</sup> College of Life and Environmental Sciences, University of Exeter, Amory Building, Rennes Drive, Exeter EX4 4RJ, United Kingdom

<sup>d</sup> Lamont-Doherty Earth Observatory of Columbia University, 61 Route 9W, Palisades, NY 10964, USA

To be submitted to *Geomorphology*.

#### Abstract

High-resolution swath bathymetry datasets collected during 11 research cruises over the past two decades have been compiled to identify detailed palaeo-ice stream pathways in the easternmost Amundsen Sea Embayment, east of the main Pine Island-Thwaites palaeo-ice stream trough. We mapped 3010 glacial landforms allowing a precise definition of the ~250 km-long Abbot Glacial Trough that was occupied by a large palaeo-ice stream fed by two tributaries, the Cosgrove and Abbot palaeo-ice streams, and reached the continental shelf edge during the Last Glacial Maximum (LGM). The detailed mapping also allows to precisely distinguish between shelf areas that were characterized by fast and slow palaeo-ice flow, i.e. areas that bear glacial landforms indicative of warm- (mega-scale glacial lineations and drumlins) and cold-based basal ice conditions (hill-hole pairs and rafts) during the last glaciation. Both the regions of fast palaeo-ice flow within the central trough, and the regions of slow palaeo-ice flow on adjacent seafloor highs (referred to as inter-ice stream ridges) additionally record glacial landforms such as grounding-zone wedges and recessional moraines that indicate an episodic retreat of the ice sheet following the LGM. As the palaeo-ice stream flowed along a trough of highly variable geometries and subglacial substrates, it appears that regions characterized by trough constrictions and outcropping resistant substrates that

change the bed gradient, led the ice stream to slow down and subsequently stabilize, resulting in the deposition of grounding-zone wedges. This stepped retreat recorded within the central trough and on the inter-ice stream ridge corresponds well to post-glacial stepped retreat phases within the neighbouring Pine Island-Thwaites Palaeo-Ice Stream trough, thus suggesting a uniform pattern of episodic retreat across the eastern Amundsen Sea Embayment and at the same time emphasizing the significance of subglacial geology in steering ice stream flow. Our new mapping resolves detailed palaeo-ice stream pathways in the easternmost Amundsen Sea Embayment that were active during and since the LGM. We additionally can give insights to the style of the post-LGM retreat. These new information will help to validate the predictability of ice flow models that aim to simulate past WAIS dynamics in the ASE region in order to improve simulations of the ice sheet's future behaviour.

### 3.1 Introduction

Ice streams are key arteries of the Antarctic ice sheet draining large amounts of ice from the continent's interior towards the ocean (e.g. Rignot et al. 2008, 2011). Dramatic changes in West Antarctic ice streams such as increased thinning, ice stream acceleration, and grounding line retreat have been recently observed, leading to concerns over future changes and their contribution to sea level rise (e.g. Vaughan 2008; Pritchard et al. 2009, 2012; Tinto and Bell 2011; Joughin and Alley 2011; Gladstone et al. 2012). The complex and nonlinear behaviour of ice streams suggests that the contemporary observational record spanning the last two to three decades is unlikely to fully elucidate processes controlling long-term ice-stream behaviour (i.e. over centuries to millennia; Jamieson et al. in press). Therefore, numerical simulations of ice sheets over the past 10–20,000 years of ice-sheet change, i.e. the time of large-scale ice-sheet changes throughout the last glacial period and deglaciation, are required to test these models and evaluate their reliability in predicting future change. Reconstructions of ice flow extent, especially ice stream width, and the history of grounded ice retreat from geological and geophysical data form the basis for validating the models. While some studies have already attempted to include geological data in their modelling (e.g. Gollledge et al. 2013), there are still significant gaps in understanding West Antarctic Ice Sheet (WAIS) behaviour (e.g. Larter et al. 2013; Bentley et al. in press).

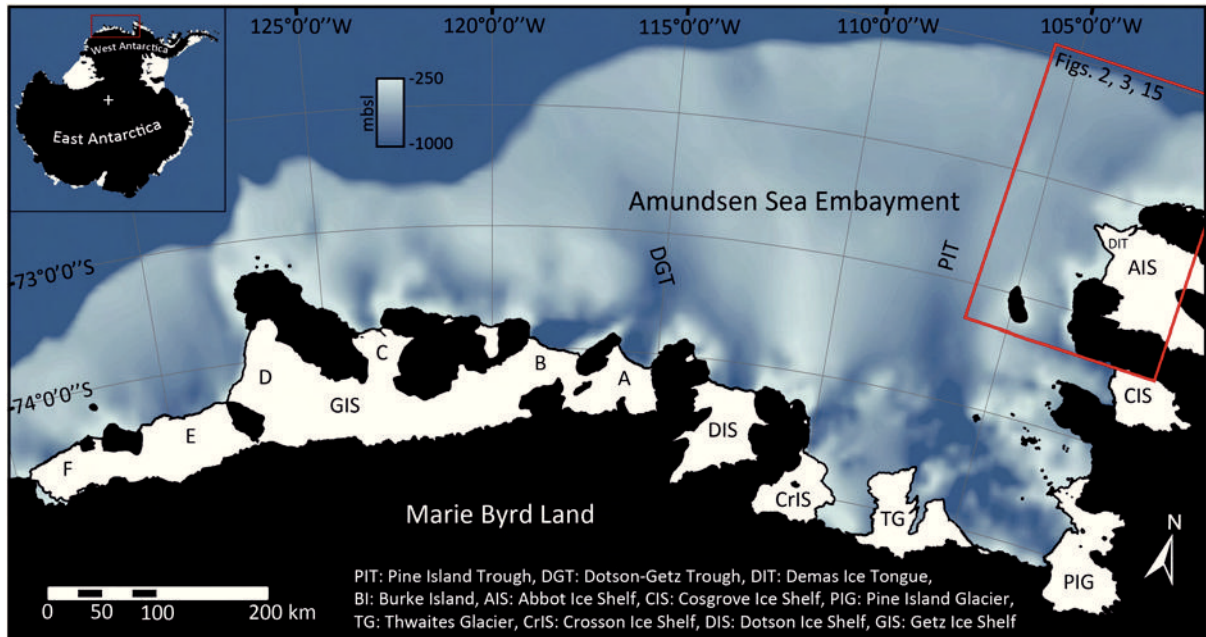


**Figure 3-1.** Map of the Amundsen Sea showing the location of the study area (red frame). The general shelf bathymetry is derived from IBCSO data (Arndt et al. 2013; mbsl = metres below sea level). Ice shelves are displayed in white; the Antarctic continent is displayed in black. Nomenclature ‘Getz Ice Shelf 1-5’ was chosen according to previous studies (Larter et al. 2009; Hillenbrand et al. 2013; Klages et al. in review, Chapter 4). Abbreviations for the main ice shelves and bathymetric troughs are given in the figure.

One area where modern-day changes are most rapid and thus palaeo-reconstructions are most urgently required is the Amundsen Sea drainage sector of the WAIS (Fig. 3-1). Whilst models simulate empirically derived locations and widths of palaeo-ice streams (e.g. Larter et al. 2009; Nitsche et al. 2013) relatively well on the inner and middle shelf of the Amundsen Sea, there are still considerable mismatches on the outer shelf (Golledge et al. 2013). Particularly on the outer shelf of the eastern Amundsen Sea Embayment (ASE) model results deviate significantly from existing empirical data. In addition, the coverage of geological and geophysical data in this area is still sparse (e.g. Evans et al. 2006; Graham et al. 2010; Jakobsson et al. 2012) and thus hampers a full reconstruction of ice-flow dynamics that is essential to validate these models. To date it is assumed that ice flowed at different times within two outer shelf troughs branching off from the Pine Island palaeo-ice stream trough (PIT), which extends seaward from the modern front of Pine Island Glacier (Fig. 3-1) (Evans et al. 2006; Graham et al. 2010; Jakobsson et al. 2012). Graham et al. (2010) concluded that prior to the end of the most recent extensive glaciation, i.e. the Last Glacial Maximum (LGM; ~23-19 ka BP), the eastern rather than the western trough was the major pathway of the palaeo-ice stream, since subglacial landforms indicative of fast ice flow on its bed are more pronounced and better preserved than in the western trough, thus suggesting a younger age for the bed-

forms in the eastern trough. The authors further concluded that the ice stream reached at least to within 68 km of the shelf edge (cf. Kirshner et al. 2012) but probably occupied the trough all the way to the shelf edge.

The middle and outer shelf regions east of the main PIT have hardly been investigated. Kellogg and Kellogg (1987) were the first who described a “narrow, relatively shallow trough” seaward of the Abbot Ice Shelf (Fig. 3-1), but it remained unclear whether or not this trough extended to the shelf edge. Furthermore, these authors proposed the presence of a smaller ice stream that may have occupied Ferrero Bay, offshore from the Cosgrove Ice Shelf (Fig. 3-1). Nitsche et al. (2007) provided the first comprehensive compilation of ASE bathymetry data that confirmed the presence of a small trough extending from Cosgrove Ice Shelf along the southern coast of King Peninsula as well as a shelf break depression NW of Thurston Island (Fig. 3-1). However, due to insufficient coverage of high-resolution bathymetry data, a possible inner to outer shelf connection of these depressions remained unsolved. Based on seismic reflection data from the shelf between Burke Island and King Peninsula (Uenzelmann-Neben et al. 2007) and west of the Abbot Ice Shelf and Thurston Island (Hochmuth and Gohl 2013), the latter authors concluded confluent ice streams emanating from the Cosgrove and Abbot ice shelves, including an additional eastward contribution from the PIT, during past glacial maxima. However, firm evidence for these reconstructions is still pending, primarily due to a lack of high-resolution multibeam bathymetry data that may resolve palaeo-ice stream pathways during the LGM.

In addition to the ice sheet modelling community, accurate regional bathymetries are also needed for oceanographic studies, and specifically, determining the pathways of warm circumpolar deep water (CDW) to the modern ice sheets grounding line (e.g. Jacobs et al. 2011; Nakayama et al. 2013).

Here we present a new comprehensive high-resolution swath-bathymetric dataset from the middle and outer shelf of the easternmost ASE between 106°W and 101°W and ~71°S and 73°22'S (Fig. 3-1), i.e. east of the main PIT and west of King Peninsula, the Abbot Ice Shelf, and Thurston Island. We mapped 3010 glacial landforms in order to reconstruct palaeo-ice stream pathways across this hitherto poorly mapped part of the ASE shelf. In agreement with previous work we presume for the purposes of this study that (i) all the subglacial landforms in the study area are of LGM age or younger, since no older ages have been obtained from the sediment drape covering these landforms and

their till substrate (Kirshner et al. 2012, Later et al. 2013, Smith et al. submitted), and (ii) grounded ice extended to the shelf break at the LGM (Larter et al. 2013).

The new data allow us to resolve a palaeo-ice stream, which flowed through a trough that we refer to as “Abbot glacial trough” (AGT) (cf. Hochmuth and Gohl 2013) and which was mainly fed by the Cosgrove and Abbot palaeo-ice streams, but also several smaller tributaries, and which probably reached the shelf edge. Moreover, our bedform mapping also reveals detailed information about basal processes acting at the ice sheet bed, which we will discuss in relation to subglacial geology and basal thermal regime.

### 3.2 Material and methods

The marine geophysical data used in this study were acquired during 11 scientific cruises between 1994 and 2013. All cruises, including methods used and acquisition systems, are summarized in Table 3-1. All bathymetry datasets were derived from ship-borne multibeam echo sounders. Depth values and beam ray paths of the bathymetric data

**Table 3-1. Bathymetry and sub-bottom profiler datasets (Cruise (year), Vessel, Method, System, Principal investigator / operator, Reference/data access).**

Cruise (year)	Vessel	Method	System	Principal investigator / operator	Reference / data access
ANT-XI/3 (1994)	RV <i>Polarstern</i>	Swath bathymetry	Atlas Hydro-sweep DS-1	Miller, H	Miller and Grobe 1996 / <a href="http://www.pangaea.de">www.pangaea.de</a>
ANT-XXIII/4 (2006)	RV <i>Polarstern</i>	Swath bathymetry	Atlas Hydro-sweep DS-2	Schenke, HW	Gohl 2007 / <a href="http://www.pangaea.de">www.pangaea.de</a>
ANT-XXIII/4 (2006)	RV <i>Polarstern</i>	Sediment echosounding	Atlas PA-RASOUND P70	Kuhn, G	Gohl 2007 / <a href="http://www.pangaea.de">www.pangaea.de</a>
ANT-XXVI/3 (2010)	RV <i>Polarstern</i>	Swath bathymetry	Atlas Hydro-sweep DS-2	Schenke, HW	Gohl 2010 / <a href="http://www.pangaea.de">www.pangaea.de</a>
ANT-XXVI/3 (2010)	RV <i>Polarstern</i>	Sediment echosounding	Atlas PA-RASOUND P70	Kuhn, G	Gohl 2010 / <a href="http://www.pangaea.de">www.pangaea.de</a>
NBP0001 (2000)	RV <i>Nathaniel B. Palmer</i>	Swath bathymetry	SeaBeam 2012	Jacobs, S	Carbotte et al. 2007 / <a href="http://www.marine-geo.org">www.marine-geo.org</a>
NBP0702 (2007)	RV <i>Nathaniel B. Palmer</i>	Swath bathymetry	Kongsberg EM 120	Jacobs, S	- / <a href="http://www.marine-geo.org">www.marine-geo.org</a>
NBP0901 (2009)	RV <i>Nathaniel B. Palmer</i>	Swath bathymetry	Kongsberg EM 120	Jacobs, S	- / <a href="http://www.marine-geo.org">www.marine-geo.org</a>
NBP1210 (2013)	RV <i>Nathaniel B. Palmer</i>	Swath bathymetry	Kongsberg EM 120	United States Antarctic Program (USAP)	- / <a href="http://www.marine-geo.org">www.marine-geo.org</a>
JR84 (2003)	RRS <i>James Clark Ross</i>	Swath bathymetry	Kongsberg EM 120	Jenkins, A	- / <a href="http://geoportal.nerc-bas.ac.uk/GDP/">http://geoportal.nerc-bas.ac.uk/GDP/</a>
JR141 (2006)	RRS <i>James Clark Ross</i>	Swath bathymetry	Kongsberg EM 120	Larter, RD	- / <a href="http://geoportal.nerc-bas.ac.uk/GDP/">http://geoportal.nerc-bas.ac.uk/GDP/</a>
OSO0910 (2010)	IB <i>Oden</i>	Swath bathymetry	Kongsberg EM 122	Jakobsson, M; Anderson, J; Nitsche, FO	Anderson and Jakobsson 2010 / <a href="http://oden.geo.su.se/OSO0910.php">http://oden.geo.su.se/OSO0910.php</a>
OSO0708 (2007)	IB <i>Oden</i>	Swath bathymetry	Kongsberg EM 120	Jakobsson, M	- / <a href="http://oden.geo.su.se/OSO0708.php">http://oden.geo.su.se/OSO0708.php</a>

were calibrated during each individual cruise using sound velocity profiles from conductivity-temperature-depth (CTD) measurements or the systems own cross-fan calibration. Subsequently the data were ping edited, processed, compiled, and gridded as a combined dataset at a 30 x 30 m cell size. The grid was visualized in ArcGIS 10 and glacial landforms were manually identified and mapped using criteria established by other workers (e.g. Graham et al. 2009; Livingstone et al. 2013) and specified in Table 3-2.

In order to provide context to subglacial bedforms mapped on the seabed and to reveal information on the substrate geology, multibeam bathymetry data were supplemented by acoustic sub-bottom profiler data (PARASOUND; Table 3-1) and multichannel reflection seismic data collected on RV *Polarstern* cruises ANT-XXIII/4 and ANT-XXVI/3 (Gohl 2007; Gohl 2010; *App. 2b*). Additionally, we use information from four sediment cores (*App. 1c*) recovered during cruise ANT-XXIII/4 to complement the bathymetric and seismic data sets. The sampling, processing, and analysis of these cores followed standard methods outlined in *Chapter 2* (in the following referred to as Klages et al. 2013).

### 3.3 Results and interpretation

#### 3.3.1 Large-scale bathymetry of the study area

The study area is characterized by the ~250 km-long AGT that extends from SW of King Peninsula in a northward direction along ca. 104°W (Fig. 3-2). NW of the Demas Ice Tongue of the Abbot Ice Shelf (Fig. 3-1) it deflects NE-ward and reaches the shelf edge between 102°W and 103°W (Fig. 3-2, inset 'i'). The trough deepens inland on the outer shelf, reveals shallower sections W and NW of King Peninsula, as well as WNW of the Demas Ice Tongue, and is characterized by considerable changes in its width along the flow path (~5-~35 km). Shallow shelf regions (400-500 metres below sea level (mbsl)) that flank the AGT to the east probably correspond to eastward subsea extensions of the King Peninsula and Thurston Island, respectively. In the west the trough is flanked by a seafloor high (~500-600 mbsl) that emanates from Burke Island in a northward direction and separates the trough from PIT. AGT reaches its greatest water depths south of 73°S (~900 mbsl) and north of 72°S (~760 mbsl). The seafloor of AGT at its mouth at the shelf edge has a water depth of 560 mbsl and thus is ~60 m deeper than the surrounding seafloor (Fig. 3-2, inset 'i').



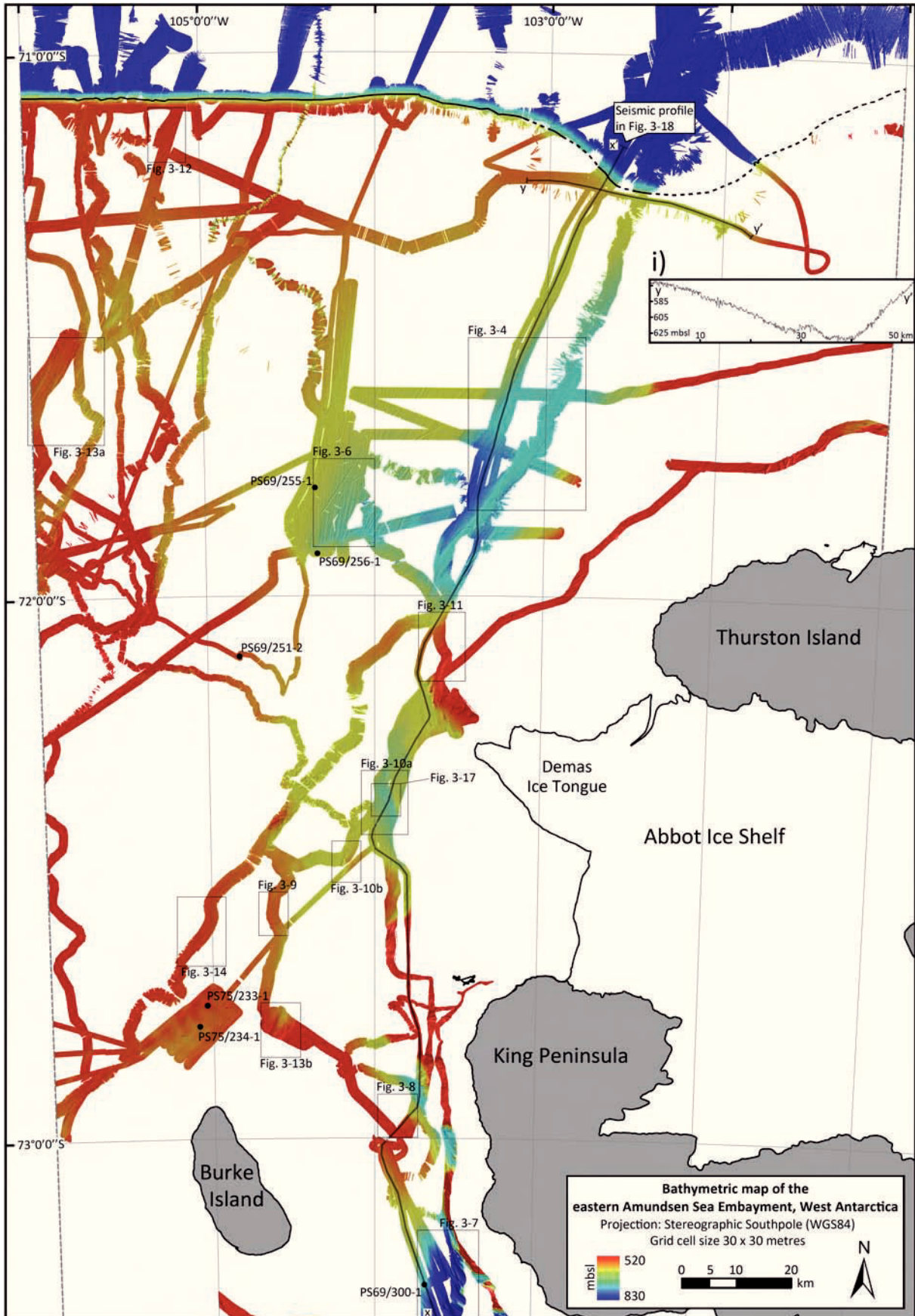


**Figure 3-2.** Detailed bathymetric map of the study area in the eastern Amundsen Sea Embayment. Black frames indicate the locations of detailed bedform figures 3-4, 3-6 – 3-14, and 3-17. Inset ‘i’ displays the bathymetric profile y-y’ across the mouth of Abbot Glacial Trough near the shelf edge. Continuous dark grey line x-x’ marks the location of the interpreted seismic profile shown in Figure 3-18. Core locations are marked with black circles. Continuous black line indicates the location of the continental shelf edge, and dotted sections illustrate its inferred location. Ice shelves are displayed in white, land in black. Grid cell size 30 m. Grid illuminated from NW.



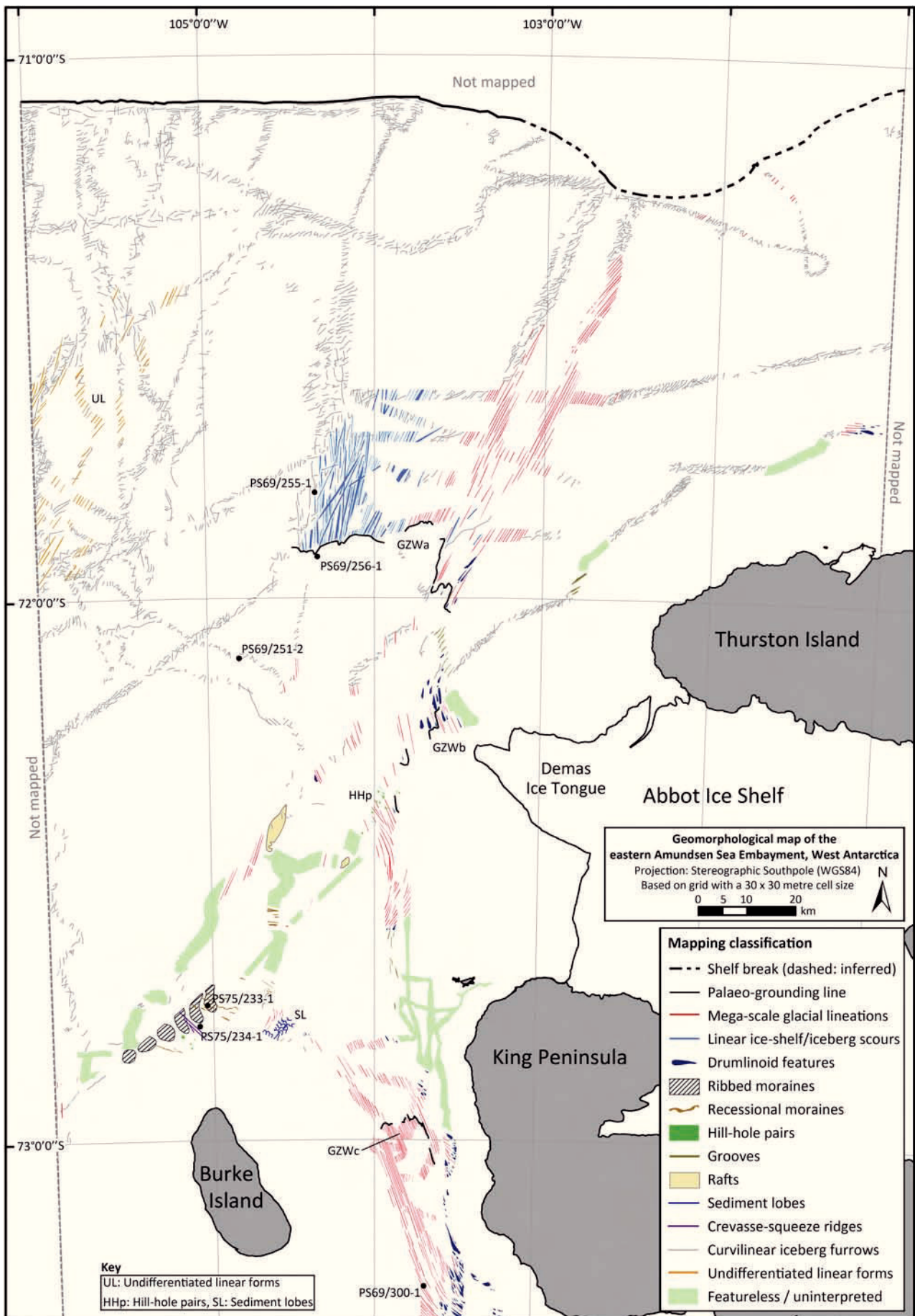


Figure 3-3. Geomorphological map of the study area. Features digitized from the 30 m swath bathymetric grid shown in Figure 3-2.

### 3.3.2 Glacial landforms

Both AGT and the shallower regions on either side bear a wide range of glacial landforms indicating the presence of a grounded ice sheet in the recent geological past. The palaeo-ice stream flowing through AGT apparently originates from the confluence of two tributaries emanating from the Cosgrove Ice Shelf to the south of the study area and the Abbot Ice Shelf in the east of the study area (Figs. 3-1, 3-2). Based on the bathymetric map (Fig. 3-2) and the criteria listed in Table 3-2, we identified, differentiated, and mapped the individual glacial landforms within the central AGT and on the shallow trough flanks, and combined them in a geomorphological landform map (Fig. 3-3). The shallow shelf area north of Burke Island has earlier been interpreted as an ‘inter-ice stream ridge’ by Klages et al. (2013), and here we apply this interpretation also to the other seafloor highs flanking AGT. In the following, we give information on the distribution, abundance, and morphologic characteristics (e.g. orientation, depth distribution, etc.) for each feature/mapping class listed in Table 3-2, and propose possible formation processes. Figure examples for each feature is supplemented by bathymetric profiles and, if available, by sedimentological data from cores.

#### 3.3.2.1 Mega-scale glacial lineations (MSGSLs)

In total 592 mega-scale glacial lineations (MSGSLs) were mapped in the study area. They are characterised by (i) high elongation, (ii) ridge-grooved topography, (iii) parallel alignment, (iv) close proximity, and (v) occurrence in sets typical of other MSGSL bedform assemblages (e.g. Clark, 1993, 1999; Clark et al. 2003; Table 3-2). The most prominent and complete sets of MSGSLs are situated in the south of AGT between Burke Island and King Peninsula (Figs. 3-2, 3-3), where they are SSE-NNW-oriented, and NNW of Abbot Ice Shelf where they are oriented SSW to NNE. This northern set reveals elongation ratios of up to  $\sim 70/1$  and amplitudes of 1-6 m (Fig. 3-4). The southern set bears the longest mapped MSGSLs with maximum elongation ratios of up to  $\sim 100/1$  and amplitudes of 4-15 m. Directly WSW of the Demas Ice Tongue, a third set of shorter MSGSLs is mapped (elongation ratios up to  $\sim 40/1$ ). These MSGSLs are sinuous and parallel, and record SSW-NNE to SSE-NNW flow through a curvilinear trough. Small clusters and individual MSGSLs with a northerly orientation are observed north of Burke Island, on the

**Table 3-2. Criteria for differentiating landforms (Interpreted feature name/GIS mapping class., Description (non-genetic), Dimensions min. (max.), Genetic interpretation, Figure reference, Literature reference).**

Interpreted feature name / GIS mapping classification (Fig. 3-3)	Description (non-genetic)	Dimensions min. (max.) L-W-H	Genetic Interpretation	Figure reference	Literature reference
Mega-scale glacial lineations (MSGSL)	Highly linear and parallel ridge-groove sets with elongation ratios (L:W) of >10:1, usually formed in soft till	3 km-100 m-1 m (27.5 km-360 m-15 m)	Combined erosional/depositional origin through grooving and ploughing of a fast-flowing ice stream base on deformable substrate (soft till)	Fig. 3-4	Marguerite Trough (Ó Cofaigh et al. 2002, Fig. 2e)
Linear ice-shelf/iceberg scours	Parallel to sub-parallel highly linear v-shaped scours with parallel ridges on either side, often cross-cutting of other scours	4.5 km-60 m-5 m (22 km-900 m-18 m)	Linear scouring of the seabed through the keels of an ice shelf or large tabular icebergs (restricted in motion), scoured material re-deposited as berms on either side of scour	Fig. 3-6	Filchner Trough (Larter et al. 2012, Fig. 4a)
Drumlinoid features	Streamlined, attenuated, oval-shaped hills with tear-drop shaped heads	650 m-230 m-15 m (6.2 km-1.1 km-200 m)	Flow across and erosion of resistant subglacial material with sediment deposition and formation of a tail that is attenuated and points in the direction of palaeo-ice flow	Fig. 3-7	Western Amundsen Sea Embayment (Graham et al. 2009, Fig. 7)
Grounding-zone wedges (GZW) – only crest-line of GZWs mapped as ‘Palaeo-grounding line’	Wedges with gently rising stoss-sides and steeply dipping, sinuously-shaped lee-sides that point in direction of former ice flow, lineations on top terminate at the wedge crest	≥25 km-≥11 km-14 m (~28 km-≥35 km-100 m)	Sediment deposition at a palaeo-ice stream terminus during extended stabilization phases, subglacial till deposition – proglacial debris flow deposition on lee-side (foresets)	Fig. 3-8	Eastern Ross Sea (Bart and Owolana, 2012, Fig. 5)
Ribbed moraines	Large-scale hummocks with regular spacing (λ~4 km), similar heights and close spatial relationships	3.2 km-~3.3 km-20 m (4.5 km-~3.3 km-25 m)	Relict moraines deposited beneath a slow-flowing ice sheet through the organisation of till transverse to flow	see Fig. 3 in Klages et al. (2013)	Former Irish Ice Sheet (Clark and Meehan, 2001, Fig. 4)
Recessional moraines	Linear to curvilinear ridges with steep stoss-flanks (~9°) and gentle lee-flanks (~3°)	~1 km-80 m-3 m (~6 km-250 m-15 m)	Proglacial deposition of pushed or deposited subglacial debris along the grounding line during minor halts or re-advances of the ice sheet, stoss-flank points upstream	Fig. 3-9; see also Fig. 3 in Klages et al. (2013)	NE Greenland shelf (Winkelmann et al. 2010, Fig. 2)
Hill-hole pairs and rafts (mapped as discrete features ‘Hill-hole pairs’ and ‘Rafts’)	Discrete holes/depressions in the sea floor with corresponding hills/bumps of similar size or volume in downstream direction	370 m-200 m-12 m (2 km-1.5 km-50 m)	Ice-thrust raft of sediment ripped up from its bed by slow-flowing, cold-based ice that transported it further downstream to form a similar-sized hill	Figs. 3-10a, b; see also Fig. 3 in Klages et al. (2013)	Eastern Svalbard, Norway (Hogan et al. 2010, Fig. 3b)
Crevasse-squeeze ridges	Highly linear and parallel ridges with identical slope angles on both flanks (~9°), similar heights but varying lengths	500 m-60 m-4 m (6 km-140 m-8 m)	Squeezing of basal till into subglacial crevasses of overlying ice likely during ice sheet stillstands	see Fig. 3 in Klages et al. (2013)	North of Burke Island (Klages et al. 2013, Fig. 3)
Grooves	Linear to curvilinear erosional features of varying lengths formed parallel to palaeo-ice flow direction	920 m-120 m-3 m (3.2 km-240 m-8 m)	Formed by subglacial abrasion and/or erosion by subglacial meltwater into resistant substrate	Fig. 3-11	NE Antarctic Peninsula shelf (Reinardy et al. 2011, Figs. 2, 9)
Curvilinear iceberg furrows	Randomly oriented furrows of varying depth that often cross-cut one another	520 m-30 m-5 m (8 km-450 m-15 m)	Result of icebergs that plough into the sea floor with their keels	Fig. 3-12	NE Greenland shelf (Evans et al. 2009, Figs. 3b-d)
Undifferentiated features i) Undifferentiated linear bedforms ii) Sediment lobes	i) Set of crudely-aligned linear ridges and furrows, linear furrows sometimes have berms on either side  ii) Fan-shaped stacked sediment lobes	i) 2 km-135 m-3 m (≥8.2 km-760 m-25 m)  ii) ≥1.8 km-470 m-3.5 m (≥2.6 km-1 km-8 m)	i) Linear scouring of seabed by ice-shelf/iceberg keels and/or subglacial grooving/ploughing by a grounded ice sheet  ii) Deposition of glaciogenic debris flow deposits in front of a palaeo-glacier terminus	i) Fig. 3-13a  ii) Fig. 3-13b	i) Pine Island trough (Graham et al. 2010, Fig. 2a)  ii) Spitsbergen, Norway (Ottesen et al. 2008, Fig. 8a)
Featureless / uninterpreted seafloor	Seafloor showing (i) no notable bathymetric features or (ii) features that were not interpreted for this study	-	i) Slow flow of cold-based ice over resistant substrate, not forming glaciotectonic features ii) -	Fig. 3-14	-

outer shelf and between the three prominent MSGL sets (Fig. 3-3). A small single cluster of EW-oriented MSGLs is identified north of Thurston Island, directly west of  $101^{\circ}\text{W}$ . The majority of MSGLs are situated within the deepest part of AGT along its central axis (Figs. 3-2, 3-3). The MSGLs extend to within  $\sim 10$  km landward of the shelf edge where they become increasingly overprinted by curvilinear iceberg furrows. MSGLs with high elongations are a reliable indicator for ice-sheet grounding, specifically fast ice flow, usually facilitated by several meter thick, water saturated deformable sediments, or basal sliding on a thin deformable upper layer on top of harder substrate (e.g. Smith and Murray 2009, and references therein). These bed conditions are confirmed by sediment core PS69/300-1 from the southern set of MSGLs (Fig. 3-3) that recovered a homogeneous soft diamicton with medium shear strength (8-10 kPa) at its base (Fig. 3-5d; Appendix 1), which has been interpreted as a deformation till deposited beneath a fast-flowing ice stream (Ehrmann et al. 2011; Smith et al. submitted). The three sets of MSGLs in our study area likely represent a combined time-transgressive footprint of palaeo-ice flow across the study area at and since the LGM, indicated by several more minor sets and individual MSGLs along the flow path.

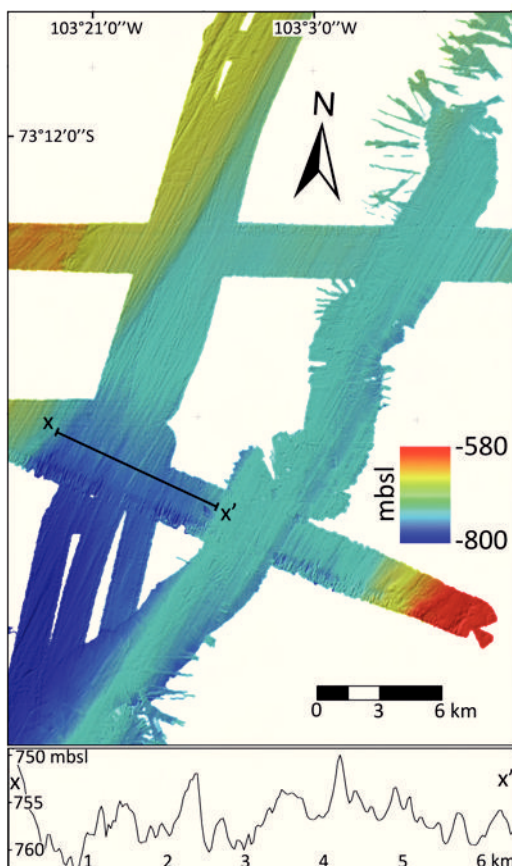


**Figure 3-4. Mega-scale glacial lineations (MSGLs).** Continuous black line x-x' indicates location of bathymetric profile shown as inset in same figure. Grid cell size 30 m. Illuminated from NW.



### 3.3.2.2 Linear ice-shelf/iceberg scours

We mapped 117 S-N to SSW-NNE-oriented linear scours that are restricted to the southward-dipping outer shelf section of AGT north of 72°S and that occur at water depths between ~640 and 720 mbsl in its western part (Figs. 3-2, 3-3, 3-6). The scours are distinct from nearby MSGs because they are v-shaped and flanked by prominent berms on either side (Fig. 3-6, inset 'a'; Table 3-2) and because they have slightly different strike orientations. The longest scour is ~22 km long and ~750 m wide. Sediment core PS69/255-1, which was recovered from within a smaller linear scour (Fig. 3-3), comprises a massive diamicton that is directly overlain by well laminated to stratified seasonal-open marine sediments (Fig. 3-5b; Appendix 1). As the massive diamicton is characterized by medium water contents (~20 wt.%), low to medium shear strength (5-

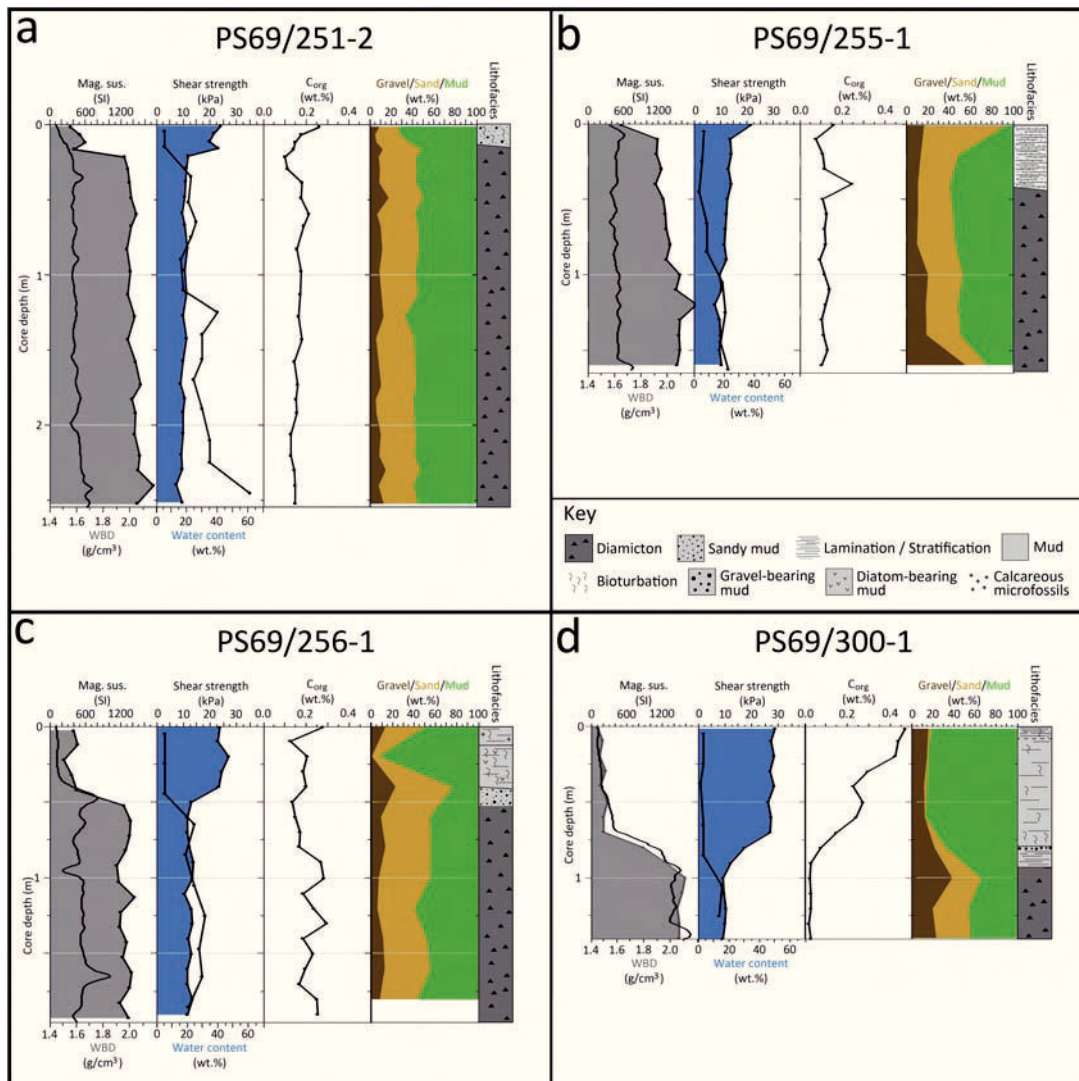


**Figure 3-5.** Core parameters of cores PS69/251-2, 255-1, 256-1, and 300-1 (Magnetic susceptibility (MS), wet-bulk density (WBD), shear strength, water content, total organic carbon (C<sub>org</sub>) content, grain-size composition (Gravel, Sand, Mud), and Lithofacies).

15 kPa), a variable magnetic susceptibility (MS), and medium to high wet-bulk densities (WBD) ( $2.1 \pm 0.1 \text{ g/cm}^3$ ), we interpret it as a glaciomarine and/or subglacial sediment that was subsequently reworked by scouring ice keels (cf. Smith et al. 2011, Klages et al. in review). This supports our interpretation from the bathymetry data that the linear scours formed through ploughing by iceberg or sub-ice shelf keels. Because of their high linearity and pronounced morphological appearance, especially when compared to the randomly-oriented curvilinear iceberg furrows (see Section 3.3.2.10), we suggest free-floating icebergs were not responsible for the origin of the linear scours. Due to the reverse bedslope of the seafloor seaward of a calving front in the outer section of AGT, the draught of an ice shelf or a calved tabular iceberg moving northwards ultimately would have exceeded the local water depth, resulting in scouring of the seabed by grounded ice keels (e.g. Larter et al. 2012), with the linearity of the scours likely facilitated through the bathymetric restriction of the thick floating ice by the trough margins, that, additionally, has a greater immunity to wind and ocean currents. Furthermore, within the axis of several linear ice-shelf/iceberg scours, regular-spaced transverse ridges (wave length  $\sim 200 \text{ m}$ , amplitude 2-3 m) could be identified (Fig. 3-6, inset 'b'). Similar corruga-

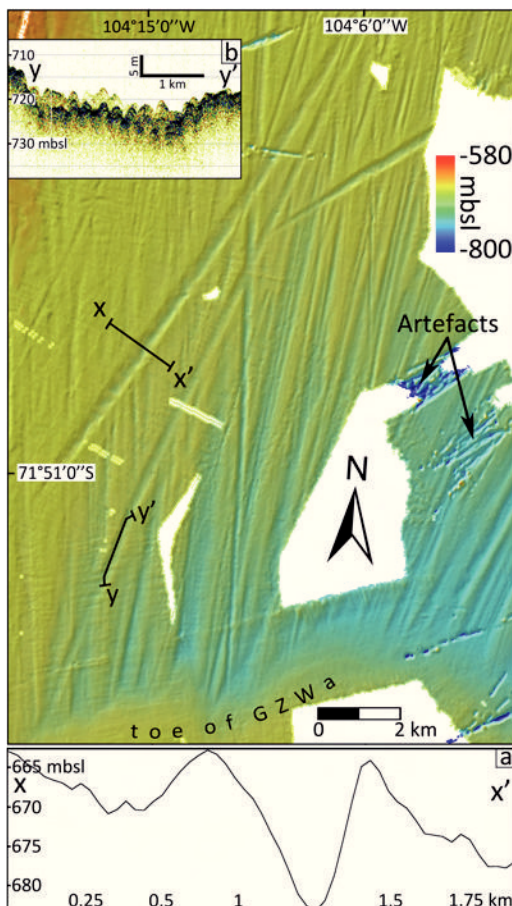


**Figure 3-6.** Linear ice-shelf/iceberg scours and toe of GZWa. Continuous black lines y-y' and x-x' indicate locations of PARASOUND and bathymetric profile shown as inset in same figure, respectively. Grid cell size 30 m. Illuminated from NW.



tions are believed to originate from tidal-controlled, periodic keel grounding beneath a seaward flowing ice shelf (Graham et al. 2013), or at the trailing keel of tabular icebergs (Jakobsson et al. 2011). Jakobsson et al. (2011) also suggested that icebergs may have been embedded within a mélange of sea and brash ice, which may have further restricted the movement of the icebergs and thus contributed to the linear orientation of the resulting scours.

### 3.3.2.3 Drumlinoid features

Under the term ‘drumlinoid features’ we summarize a continuum of streamlined ‘tear-drop’ shaped or oval features, such as drumlins, crag-and-tails, and whalebacks as our data do not allow for a clear distinction between them (Table 3-2). In total, 123 individual drumlinoid landforms have been mapped in the study area that are found in two prominent clusters (Figs. 3-2, 3-3). One of these clusters occurs directly SW of King Peninsula where the elevations of individual features range between 18 and ~200 m (Fig. 3-7). Their streamlined, attenuated, and up to ~6 km long tails point downstream in a NNW direction and often evolve into MSGs. Consequently, the drumlinoid features are most abundant upstream of the MSG sets. The second prominent cluster of drumlinoid features is observed directly WNW of the Demas Ice Tongue, while several minor drumlinoid clusters have been identified along the western side of King Peninsula and north of Thurston Island. The latter cluster is the only cluster within a small tributary trough, where bedforms have a westward orientation (Fig. 3-3). The smallest individual drumlinoid feature has dimensions of 650 m-245 m-15m (L-W-H) and was detected within the minor cluster directly west of King Peninsula at about 73°S. Drumlinoid features in our study area are generally restricted to the deepest parts of central AGT and alternate with zones of MSGs further downstream (Figs. 3-2, 3-3, 3-7), thus they seem to represent regions of fast palaeo-ice flow (cf. Smith et al. 2007) where the resistance of the subglacial substrate has controlled bedform formation (either by influencing ice flow, e.g. producing variations in velocity, or providing direct control on the bedforming mechanism at the ice-bed interface). This is particularly evident when the location of the two main clusters of drumlinoid features is compared to seismic data, which reveals outcropping strata of likely indurated sediments or sedimentary rocks in the corre-

sponding shelf regions (Fig. 3-18). We suggest that the drumlins were eroded into this hard sedimentary substrate or have cores formed of this resistant material.

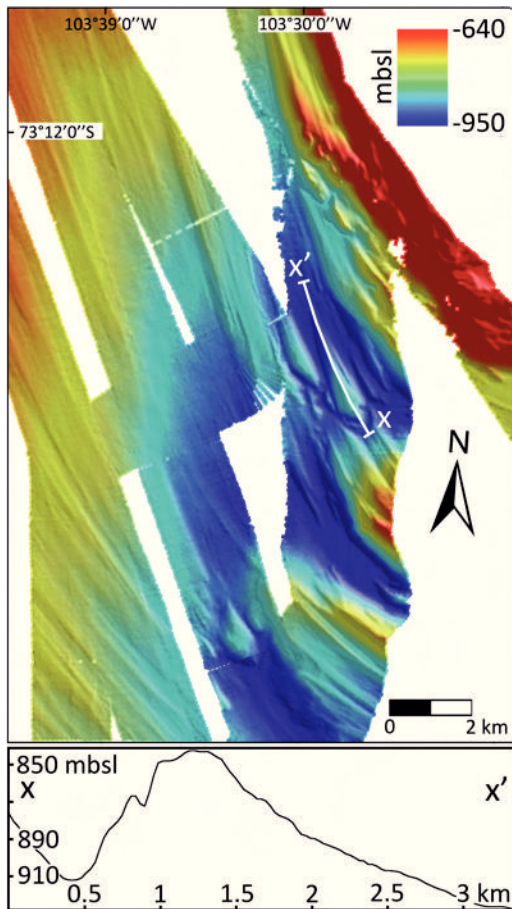


**Figure 3-7.** Drumlinoid features. Continuous white line x-x' indicates location of bathymetric profile shown as inset in same figure. Grid cell size 30 m. Illuminated from NW.

#### 3.3.2.4 Grounding-zone wedges (GZWs)

Based on the characteristics given in Table 3-2, we identified three new grounding zone wedges (GZWs) within AGT. The northern GZW (GZWa) is located WNW of Thurston Island directly north of 72°S (Fig. 3-6), the central GZW (GZWb) is located west of the Demas Ice Tongue, and the southern GZW (GZWc) is located between King Peninsula and Burke Island at 73°S (Figs. 3-2, 3-3). The northern GZW is the most prominent with a length of  $\geq 25$  km, a width of  $\sim 35$  km, a height of  $\geq 90$  m, and a steep lobate-shaped seaward-facing front. The detailed image of the southern GZW (Fig. 3-8) reveals a length of  $\sim 28$  km, a width of  $\sim 11$  km, a height of  $\sim 10$  m, and MSGs on its landward backslope that terminate at the lobate-shaped ridge crest. The steeper lee-sides of all GZWs generally point NNW-NNE-wards indicating the approximate direction of palaeo-ice flow. GZWs record positions where the former grounding lines of ice streams stabilized and subglacial debris was deposited over centuries or a few millennia (e.g. Jakobsson et al.

2012). This accumulation of large amounts of subglacial debris counteracted the reverse bedslope within central AGT that is generally thought to cause inherent instability of marine-based ice streams (e.g. Joughin and Alley 2011). Therefore, GZWs are seen as features that can ‘self-stabilize’ ice streams (e.g. Dowdeswell and Fugelli 2012), especially at locations where the trough geometry is constricted and/or the resistance of the substrate to subglacial erosion influences the ice stream flow (see Section 3.4.6), and document pauses in grounding-line retreat (cf. Gudmundsson et al. 2012; Jamieson et al. 2012). Sediment core PS69/256-1 was recovered from the toe of the northern GZW (Fig. 3-3) and retrieved a homogenous diamicton at its base (Fig. 3-5c; Appendix 1) revealing sedimentological characteristics of a deformation till. However, based on elevated sand contents (>35 wt.%), we assume that the diamicton at site PS69/256-1 was deposited as a glaciogenic debris flow in front of the GZW rather than a subglacial soft till deposited at the base of the ice stream or a glaciomarine diamicton deposited in a sub-ice shelf setting proximal to the grounding line (cf. Smith et al. submitted for publication).

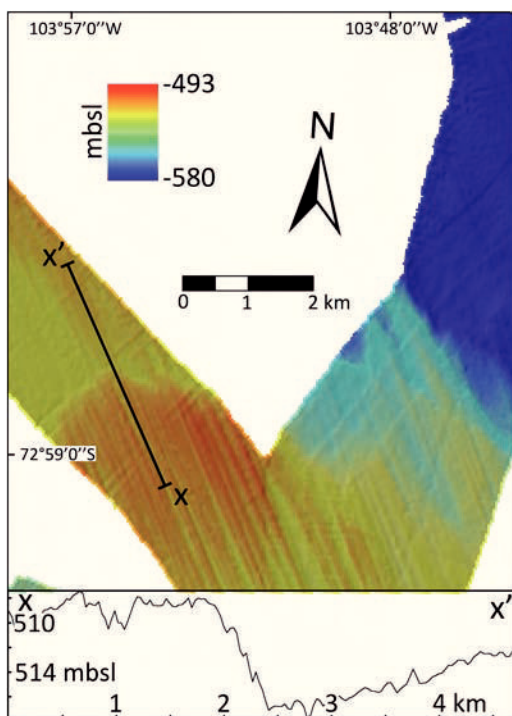


**Figure 3-8. Grounding-zone wedges (GZWs).** Continuous black line x-x' indicates location of bathymetric profile shown as inset in same figure. Grid cell size 30 m. Illuminated from NW.

### 3.3.2.5 Ribbed moraines

North of Burke Island a field of large transverse ridges (Table 3-2), similar in form and distribution to ribbed moraines, has been mapped across a seafloor high (Figs. 3-2, 3-3) that Klages et al. (2013) had previously interpreted as an inter-ice stream ridge separat-

ing the PIT from a tributary trough that was eroded by a minor outlet glacier, the Cosgrove palaeo-ice stream (COPIS). These authors suggested that long-wave ribbing (wavelength  $4.2 \pm 0.1$  km) of a subglacial stiff till was induced by slowly flowing ice on the inter-ice stream ridge. Furthermore, the ribbed moraines form part of an assemblage of landforms that are diagnostic of slow flow and subsequent stagnation on this part of the shelf (see also Sections 3.3.2.6, 3.3.2.7 and 3.3.2.8).

### 3.3.2.6 Recessional moraines

In addition to the recessional moraines that overprint the field of ribbed moraines north of Burke Island (Klages et al. 2013), we identified two more sets of (W)NW-(E)SE-striking 3-15 m high recessional moraines ~18 km NNE of the ribbed moraine field (Figs. 3-2, 3-3, 3-9; Table 3-2). A generally steeper stoss-side results from ice that pushed subglacial sediment NNE-wards, whereas the gentle lee-side was formed by proglacial gravity flows running down the ice-distal slope (e.g. Winkelmann et al. 2010). As the dimensions and orientations of the newly mapped recessional moraines are identical to those reported by Klages et al. (2013), they are also interpreted to reflect minor re-

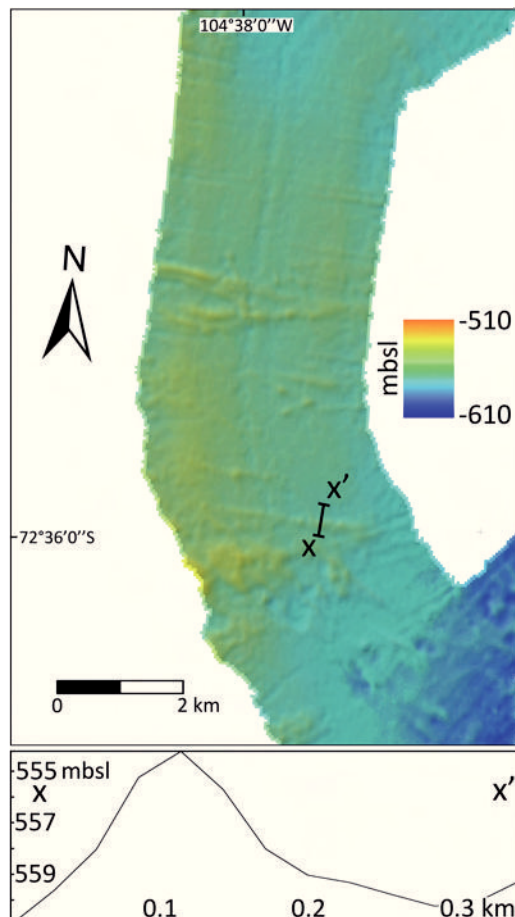


**Figure 3-9.** Recessional moraines. Continuous black line x-x' indicates location of bathymetric profile shown as inset in same figure. Grid cell size 30 m. Illuminated from NW.

advances or stillstands of the ice sheet during a general SSW-ward retreat across the inter-ice stream ridge north of Burke Island.

### 3.3.2.7 Hill-hole pairs and rafts

Recently, three hill-hole pairs have been reported from the inter-ice stream ridge north of Burke Island (see Fig. 2 in Klages et al. 2013). Based on the hills that are generally located NE of the holes, the authors concluded slow and cold-based ice flowing towards NE that thrust up a raft of sediment from its bed, thereby leaving behind a hole, entrained and transported the raft at its base and subsequently deposited the raft downstream, thereby depositing a hill (Klages et al. 2013). In addition to those features, another 14 glaciotectonic hill-hole pairs have been mapped, mainly clustered ~20 km WSW of the Demas Ice Tongue (Figs. 3-2, 3-3, 3-10a). In contrast to the features described from the inter-ice stream ridge, these features are located within central AGT and occur in association with MSGs, which they apparently overprint (Fig. 10a). Their

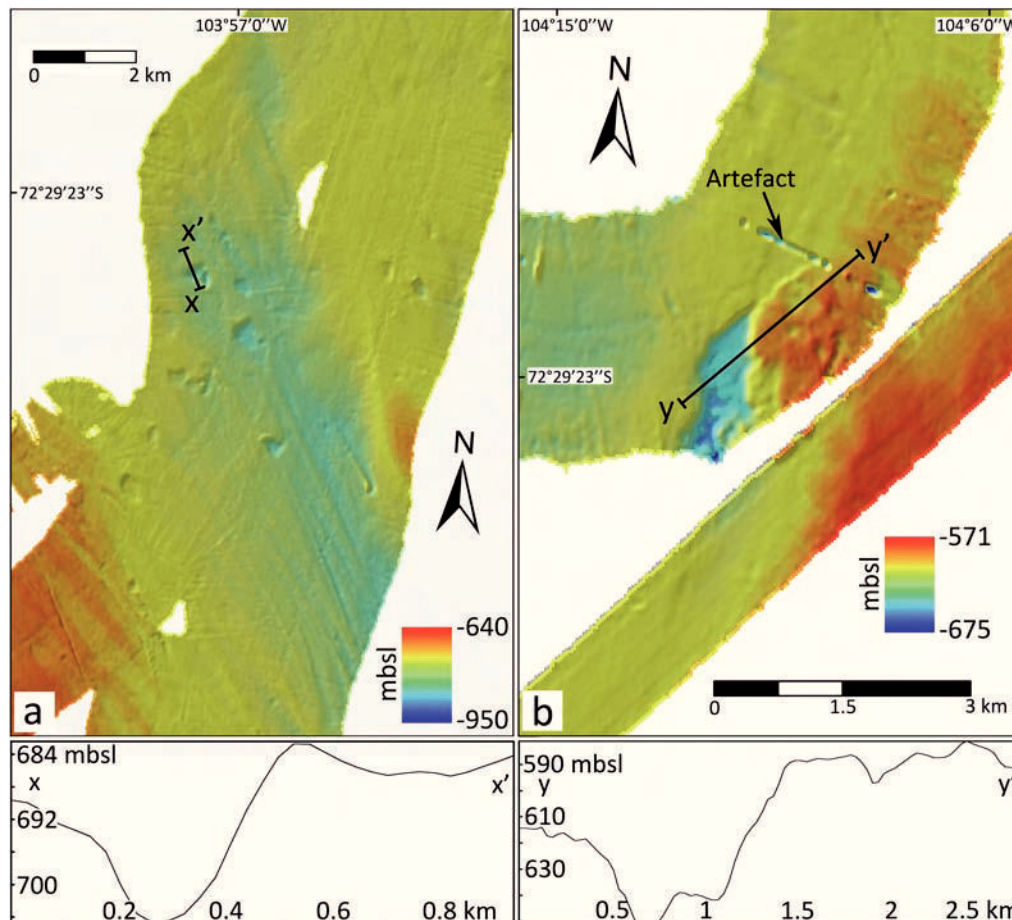


**Figure 3-10.** a) Hill-hole pairs. Continuous black line x-x' indicates location of bathymetric profile shown as inset in same figure. b) Rafts. Continuous black line y-y' indicates location of bathymetric profile shown as inset in same figure. Grid cell size 30 m. Illuminated from NW.



hills were deposited NNW of the holes, recording a palaeo-ice flow direction consistent with the linear bedforms.

Two larger but genetically similar rafts are observed on the NE side of the inter-ice stream ridge north of Burke Island and WSW of the Demas Ice Tongue (Figs. 3-2, 3-3; Table 3-2). The larger western feature indicates that an ~8 km-long, ~2.6 km-wide and ~20 m-high raft of sediment was subglacially thrust NNE-wards by ~0.5 km. Although the eastern sediment raft is smaller (L-W-H: 1 km-1.2 km-25 m), it obviously was thrust by a similar distance (~0.6 km) but in a NE-ward direction (Fig. 3-10b). By assuming the same subglacial transport mechanism as for the hill-hole pairs, the rafts indicate the same NE-NNE-ward palaeo-ice flow on the inter-ice stream ridge as previously inferred by Klages et al. (2013).

### 3.3.2.8 Crevasse-squeeze ridges

A set of highly linear and parallel ridges is located on the inter-ice stream ridge north of Burke Island. These 4-8 m high ridges were previously described by Klages et al. (2013) and interpreted as recording ice-sheet flow stagnation following the deposition of the NE set of recessional moraines, i.e. the ridges were formed when basal till was squeezed into subglacial crevasses facilitated by the pressure of the overlying ice (Table 3-2).

### 3.3.2.9 Grooves

We mapped 21 linear to curvilinear grooves that occur in two groups at the eastern side of the main trough (Figs. 3-2, 3-3) where they are interpreted to reflect ice stream flow around bedrock highs extending W-wards and NW-wards of Thurston Island and the King Peninsula, respectively (Fig. 3-2). The grooves are aligned to the general palaeo-ice flow direction recorded by nearby drumlinoid features and MSGs. In contrast to the latter bedforms, the grooves are much shorter ( $\leq 3.2$  km long) and purely erosive ( $\leq 8$  m deep) (Fig. 3-11; Table 3-2). Both subglacial abrasion and erosion by subglacial meltwater flow might have moulded them into resistant substrate (e.g. Lowe and Anderson 2002).



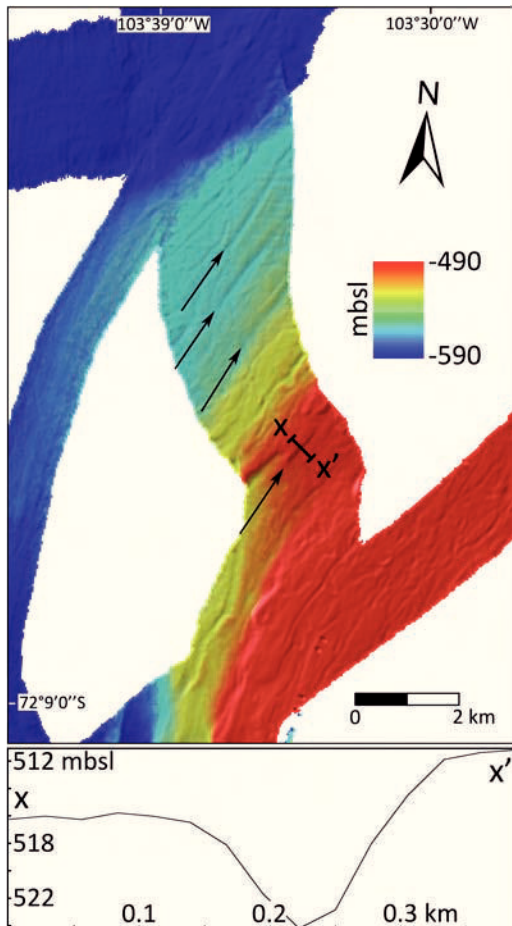


**Figure 3-11.** Grooves (indicated by black arrows). Continuous black line x-x' indicates location of bathymetric profile shown as inset in same figure. Grid cell size 30 m. Illuminated from NW.

### 3.3.2.10 Curvilinear iceberg furrows

Most of the 2001 curvilinear scours interpreted as iceberg furrows have been mapped in the NW part of the study area (Figs. 3-2, 3-3). They generally occur in the shallowest parts of the shelf and are predominantly NE-NW oriented (Fig. 3-3). However, individual furrows are multi-directional because the icebergs scouring them changed drift direction in response to changes in wind and current directions (Fig. 3-12; Table 3-2). Curvilinear iceberg furrows are most common on seafloor with a soft substrate (e.g. Graham et al. 2009) that is shallow enough to enable iceberg grounding, whereas they are rarely found on shallow seabed with resistant substrate such as bedrock or stiff till (Klages et al. 2013). Ehrmann et al. (2011) interpreted a massive diamicton recovered at site PS69/251-2 from the outer shelf of our study area (Fig. 3-2) as a subglacial soft till or as a glaciomarine diamicton that was deposited proximal to the grounding line either as a melt-out diamicton under an ice shelf or as a glaciogenic debris flow. This interpretation was based on the medium to high shear strength (10-35 kPa), low  $C_{org}$  content ( $\leq 0.2$  wt.%), and minor fluctuations in MS, water content, WBD, and grain-size composition

measured for the diamicton (cf. Hillenbrand et al. 2010). However, our new high-resolution bathymetry data reveal that core PS69/251-2 was actually retrieved from intensely iceberg-scoured seafloor (Fig. 3-3), suggesting that the diamicton at this site is an iceberg turbate formed by the reworking of seabed sediments through ploughing iceberg keels (cf. Smith et al. 2011; Klages et al. in review).

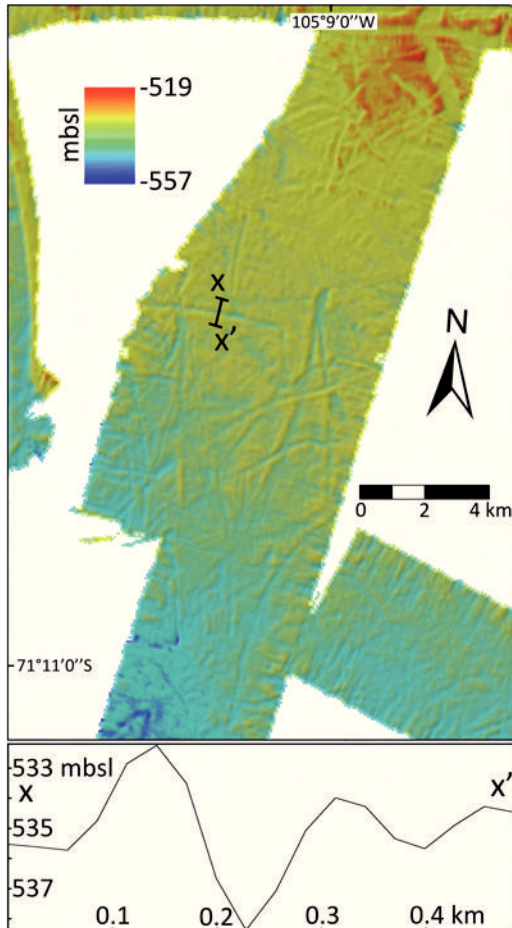


**Figure 3-12.** Curvilinear iceberg furrows. Continuous black line x-x' indicates location of bathymetric profile shown as inset in same figure. Grid cell size 30 m. Illuminated from NW.

### 3.3.2.11 Undifferentiated features

Undifferentiated linear bedforms:

In the NW part of the study area within the extensive fields of curvilinear iceberg furrows a set of crudely aligned, SSW-NNE oriented linear ridges and furrows was mapped (Fig. 3-13a). These elongated ridge/groove features (minimum elongation ratios  $\sim 6/1$  -  $\sim 16/1$ ) co-occur with similar elongated, linear v-shaped scours with berms on either side (amplitudes 5-8 m). The crudely aligned ridges and furrows are located within a slightly deeper part of the outer shelf ( $\sim 600$  mbsl) and extend from  $72^{\circ}0'0''S$  NNE-wards (Figs. 3-2, 3-3). It is not clear, whether the features are incompletely mapped MSGs (Section 3.3.2.1) or linear ice-shelf/iceberg scours (Section 3.3.2.2) (Table 3-2).

In the absence of further diagnostic information from sediment cores, we classify them as ‘undifferentiated linear bedforms’ but recognise that, with better mapping coverage, they may provide information about former ice flow directions and processes.

#### Sediment lobes:

Fan-shaped, stacked sediment lobes are observed ~20 km NE of Burke Island (Fig. 3-13b). These features seem to be depositional, and individual lobes obviously lie on top of other, likely older lobes. The lobes point towards NNE and lie within a small trough that is only slightly deeper than the surrounding seafloor. A lack of data SW and NE of the sediment lobes does not allow a clear classification of the features, but we propose their deposition by glaciogenic debris flows proximal to a palaeo-glacier terminus as they resemble features previously reported from Spitsbergen fjords (e.g. Plassen et al. 2004; Ottesen et al. 2008; Table 3-2).

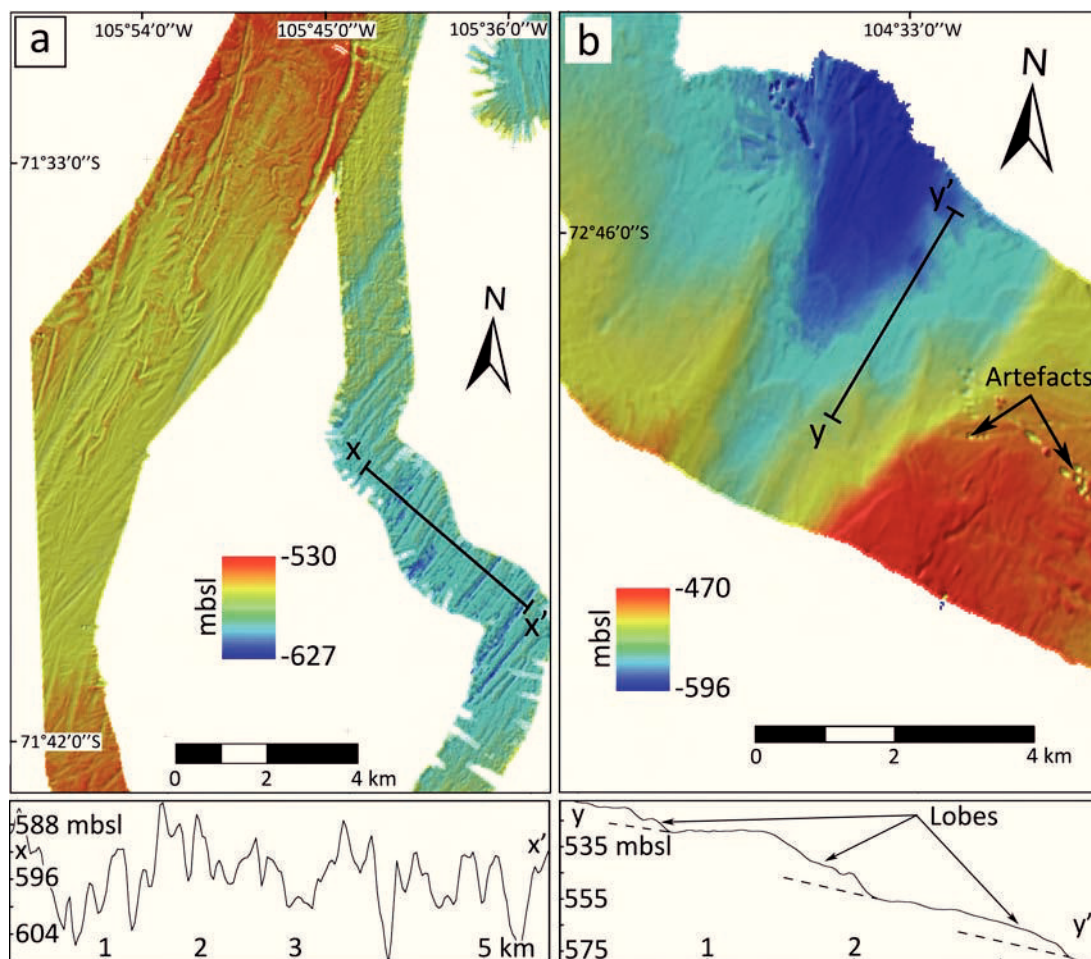


**Figure 3-13.** a) Undifferentiated linear bedforms. Continuous black line x-x' indicates location of bathymetric profile shown as inset in same figure. b) Sediment lobes. Continuous black line y-y' indicates location of bathymetric profile shown as inset in same figure. Grid cell size 30 m. Illuminated from NW.

### 3.3.2.12 Zones of featureless / uninterpreted sea floor

Mainly on the inter-ice stream ridge north of Burke Island some seafloor sections lack any notable bedforms (Fig. 3-14). However, since glaciotectonic features such as hill-hole pairs and rafts are located between these featureless areas (Fig. 3-3), we infer that slowly flowing cold-based ice covered the seafloor here, probably resulting in the deposition of a subglacial stiff till recovered nearby in core PS75/234-1 (Figs. 3-2, 3-3; Klages et al. 2013; Table 3-2).

Other areas that have not been interpreted for this study are situated east of the AGT immediately NW of King Peninsula and N-NW of Thurston Island. Rugged bedrock topography without any overprinting by glacial erosional or depositional processes characterises these areas.

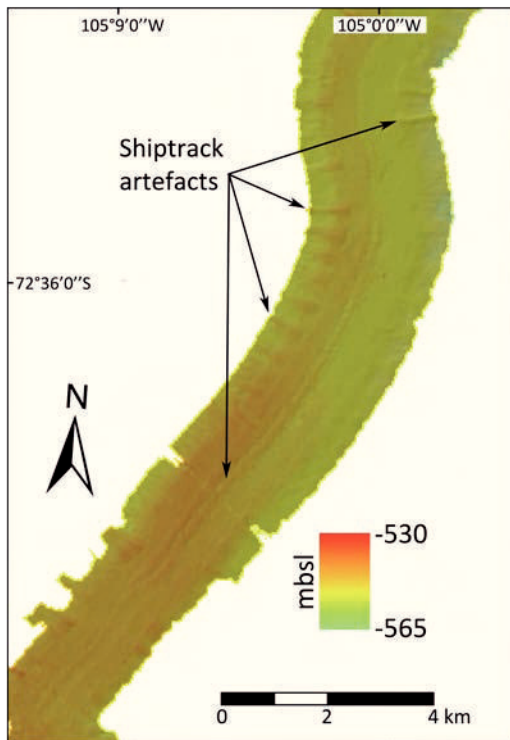


**Figure 3-14.** Featureless / uninterpreted seafloor. Grid cell size 30 m. Illuminated from NW.

## 3.4 Discussion

### 3.4.1 Reconstruction of flow pathways and thermal regime

The detailed mapping of individual subglacial landforms has revealed clusters of particular landform types at certain water depths within the study area (Figs. 3-2, 3-3). Generally, subglacial landforms such as MSGs and drumlinoid features that are aligned parallel to the axis of AGT occur within the trough, whereas hill-hole pairs, rafts, moraines, and iceberg scours are located on the shallower inter-ice stream ridges flanking AGT. This distribution enables us to reconstruct regions of fast and slow (i.e. wet- and cold-based) ice flow (Fig. 3-15), and to set the palaeo-ice flow pattern in our study area into context with palaeo-flow characteristics in the entire ASE (Fig. 3-16).

### 3.4.2 Indicators for regions of fast palaeo-ice flow

The existence of MSGs and drumlinoid features, indicative for fast palaeo-ice flow (e.g. Smith et al. 2007; King et al. 2009), proves that an ice stream occupied the AGT in the recent geological past that flowed from south of King Peninsula along its western coast, continuing west of the Abbot Ice Shelf, from where it flowed in a NNE-ward direction towards the shelf edge. This palaeo-ice stream was fed by two tributary streams, the Cosgrove and Abbot palaeo-ice streams, as well as by at least two minor ice streams that flowed into the system from King Peninsula in NW-ward direction and from Thurston Island in eastward direction, respectively (Fig. 3-15, black arrows). Fast flowing ice is facilitated by a saturated deformable till (e.g. Ó Cofaigh et al. 2005; King et al. 2009), and indicates that areas of MSGs were formed by ‘warm-based’ ice (e.g. Bennett and Glasser 2010). Our detailed mapping also shows that in regions where the trough width narrows from  $\geq 15$  km to  $\geq 5$  km as NW of King Peninsula (Figs. 3-2, 3-3, 3-15), the palaeo-ice stream changed its flow direction, which is indicated by curvilinear MSGs. Downstream of the convergence of the Abbot palaeo-ice stream tributary with that of the Cosgrove palaeo-ice stream, diverging ice flow occurred in a widened trough (width  $\sim 35$  km). However, in contrast to findings by Hochmuth and Gohl (2013), who interpreted “W-shaped” seismic reflections as indication for two individual palaeo-ice streams emana-



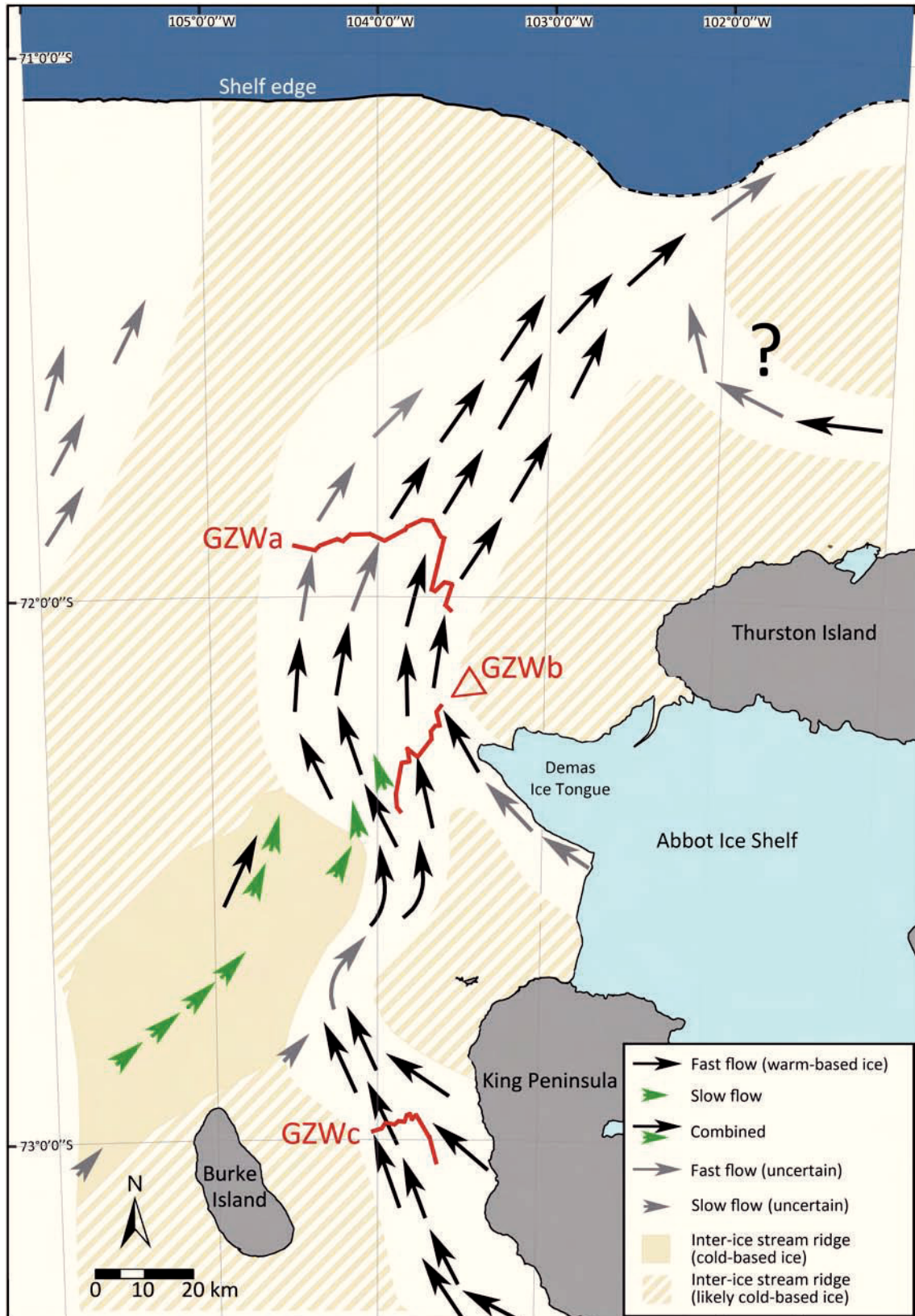


**Figure 3-15.** Reconstruction of palaeo-ice flow pathways and thermal basal ice-sheet regime in the study area during the LGM. Flow indicators digitized based on geomorphological map in Figure 3-3. Long black arrows indicate regions of fast palaeo-ice flow; short green arrows indicate regions of slow palaeo-ice flow; long black combined with short green arrows indicate regions of combined flow (i.e. areas with temporal changes in basal flow regime); grey arrows indicate regions of uncertain flow speed. White areas indicate regions of fast warm-based palaeo-ice flow; light orange shaded areas indicate regions of slow, cold-based ice flow; hatched light orange areas indicate likely cold-based regions. Red lines mark locations of GZWa, GZWb and GZWc. Ice shelves are marked in light blue; land is marked in grey; deep sea is marked in dark blue.



ted from the Abbot Ice Shelf (see Fig. 6 in Hochmuth and Gohl 2013), we found geomorphological evidence for only one tributary, in which ice flowed NW-wards directly southwest of the Demas Ice Tongue (Fig. 3-15). From here the merged Abbot and Cosgrove ice streams flowed towards the NNE in a  $\geq 18$  km-wide trough onto the outermost shelf, to at least  $\sim 10$  km within the shelf edge. However, we consider that within the relatively shallow AGT section directly landward of the shelf break iceberg furrows may have subsequently eradicated any MSGs and therefore we propose that the palaeo-ice stream likely extended to the continental shelf edge. This conclusion is corroborated by the fact that erosion of the trough mouth of AGT into the shelf break is clearly visible in the regional bathymetric data (Fig. 3-2, inset 'i'; cf. Nitsche et al. 2007). Furthermore, we propose that the palaeo-ice stream on the outer shelf north of  $72^{\circ}\text{S}$  was considerably wider during the LGM ( $\sim 40$  km), extending westwards onto a shallower part of AGT to within  $\sim 104^{\circ}30'\text{W}$  as it is indicated by the presence of GZWa which was deposited during post-LGM ice stream retreat (see Sections 3.4.5 and 3.4.6). Again, however, extensive post-LGM linear scouring of the seafloor (see Section 3.3.2.2) likely obliterated any potential pre-existing subglacial bedforms on this shallower part of the shelf. From the several smaller ice streams that were proposed to have spread in a radial pattern from Thurston Island in a N-NNE direction across the outermost shelf (Hochmuth and Gohl 2013), we only found geomorphological evidence for one minor palaeo-ice stream north of Thurston Island and directly west of  $101^{\circ}\text{W}$  that indicates an eastward palaeo-ice flow in a  $\geq 3$  km wide trough. However, due to a general lack of high-resolution bathymetric data on this part of the shelf in combination with strong iceberg scouring, it remains uncertain if other small palaeo-ice streams were present there during the last glacial period. Furthermore, it is unclear whether the ice within the small palaeo-ice stream trough north of Thurston Island converged with the Abbot palaeo-ice stream in the past or terminated at some location on the shelf (Fig. 3-15).

### 3.4.3 Palaeo-ice flow on ice stream margins and inter-ice stream ridges

Iceberg scouring is the process often assumed to be responsible for eradicating glacial landforms on elevated palaeo-ice stream trough margins and inter-ice stream ridges (e.g. Lien et al. 1989; Dowdeswell and Bamber 2007). However, on the shallow inter-ice

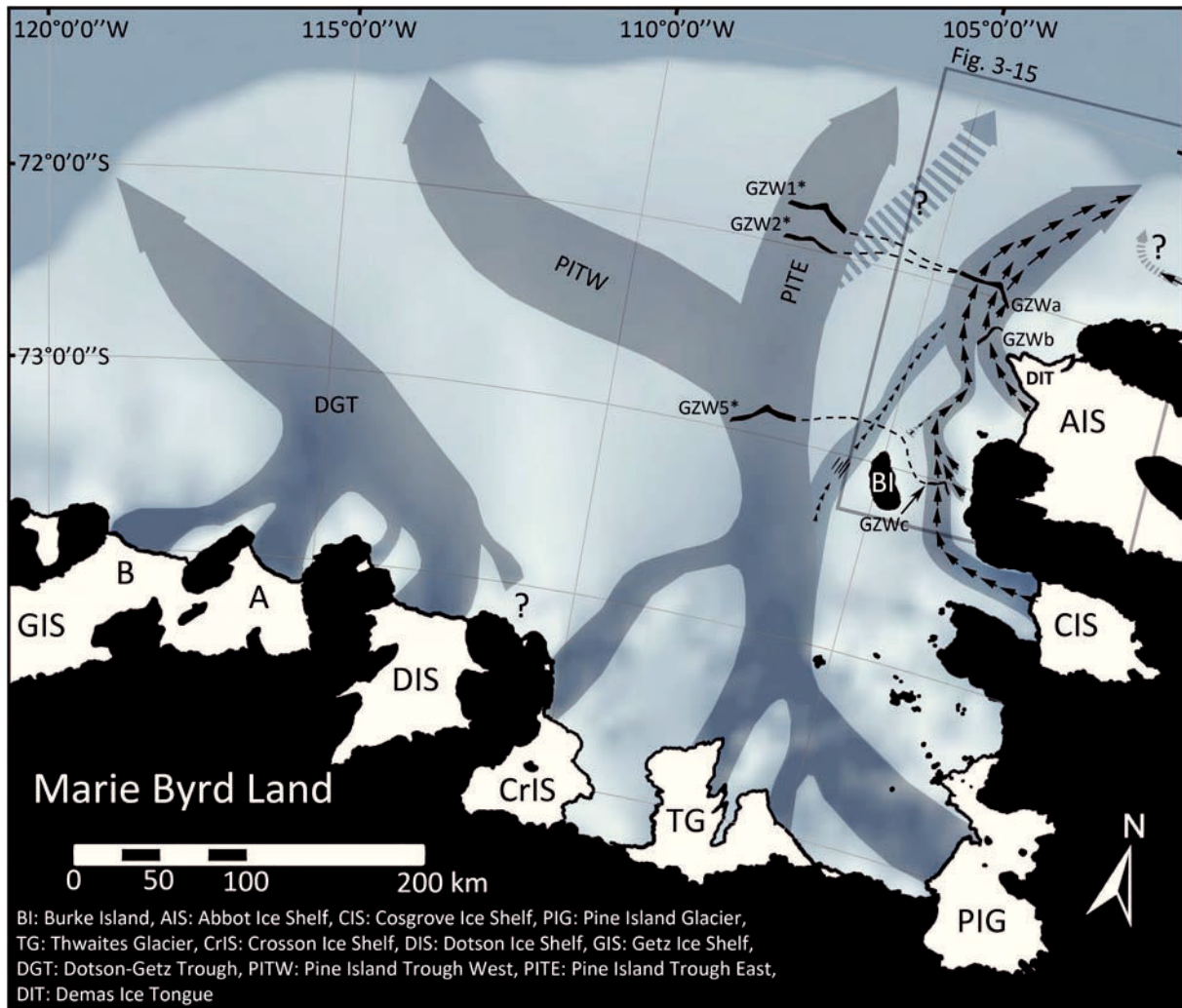


**Figure 3-16.** Reconstruction of palaeo-ice flow pathways in the context of the wider ASE palaeo-ice flow pattern during the LGM. The location of the study area (Figure 3-15) is indicated by the grey frame. Large grey arrows indicate the main palaeo-ice stream pathways. Black arrows mark regions of fast palaeo-ice flow within the study area; small black arrows indicate regions of slow palaeo-ice flow within the study area. Unclear palaeo-ice flow is indicated by dashed grey arrows and/or question marks. Ice shelves are displayed in white; Land is displayed in black. Abbreviations for the main ice shelves and bathymetric troughs are given in the figure. (\* GZW '1, 2 & 5': Graham et al. 2010)

stream ridge north of Burke Island, located between the PIT and AGT, an assemblage of sub- and proglacial landforms has been preserved on an otherwise largely smooth sea-floor that has been interpreted as diagnostic for slowly flowing to stagnant ice (Klages et al. 2013). Besides the hill-hole pairs, which were detected here (Klages et al. 2013) and which are commonly interpreted as recorders of slow and cold-based ice flow (e.g. Ottesen et al. 2005), we also discovered two large sediment rafts ~35 km WSW of the Demas Ice Tongue (Fig. 3-3) that support the interpretation of a slow and cold-based NE to NNE-ward palaeo-ice flow across the inter-ice stream ridge (Figs. 3-15, 3-16). Moreover, Lowe and Anderson (2002) described some SW-NE-oriented grooves at the eastern margin of the PIT at about 73°0'0''S west of Burke Island (Fig. 3-16), which they related

to local ice flow into PIT from the east. However, as the authors were not able to deduce a clear palaeo-ice flow direction from these features, we suggest that a NNE-ward ice flow originating from PIT formed these grooves because they are well aligned with the flow directions inferred from the hill-hole pairs, rafts and the field of ribbed moraines north of Burke Island (Klages et al. 2013). Therefore, slowly NE-NNE-ward ice flow between PIT and AGT across the inter-ice stream ridge appears likely during and/or subsequent to the LGM (Fig. 3-16).

As the eastern raft on the inter-ice stream ridge (Figs. 3-2, 3-10b) is located only ~5 km away from a set of NNW-oriented MSGs, it allows to draw the boundary between cold- and warm-based regions relatively precisely (Figs. 3-3, 3-15). This further hints at an ice stream marginal shear zone in this region, i.e. the former boundary zone between the fast flowing wet-based palaeo-ice stream tributary emanating from Cosgrove Ice Shelf and the slowly moving cold-based ice on the inter-ice stream ridge north of Burke Island (cf. Raymond et al. 2001).

We assume similar basal ice conditions for the remaining marginal- and inter-ice stream areas since they lie in the same water-depth range as the inter-ice stream ridge north of Burke Island. However, direct geomorphological evidence for cold basal conditions is lacking since these regions were heavily scoured by icebergs (Fig. 3-3). Nevertheless, we consider these areas as 'likely cold-based' inter-ice stream ridges (Fig. 3-15). The predominant ENE orientation of iceberg scours on the inter-ice stream areas in the northern part of our study area might have been steered by the westward flowing Antarctic Coastal Current, which controls sea-ice drift in this area today (Assmann et al. 2005).

#### **3.4.4 Evidence for past changes in basal conditions**

One region in our study area that is located ~20 km WSW of the Demas Ice Tongue is characterized by a mixed assemblage of subglacial landforms indicative of both fast (MSGs) and slow palaeo-ice flow (hill-hole pairs) (Figs. 3-2, 3-3, 3-17), suggesting a past change in the basal ice conditions. The holes obviously formed when subglacial till was ripped up at the location where MSGs were already present, and therefore they must be younger than the MSGs. The downstream deposition of the hills NNW of the holes indicates an identical palaeo-ice flow direction as recorded by the MSGs. Consequently, a change in the basal thermal regime to cold-based conditions must have oc-

curred after the formation of the MSGs, to enable subglacial thrusting by ice that was frozen to its bed forming the hill-hole pairs (cf. Hogan et al. 2010). As hill-hole pairs have been previously interpreted as features formed near ice stream margins (e.g. Moran et al. 1980), we suggest that the hill-hole pairs may reflect the thermal conditions at the bed of the ice stream just prior to its landward retreat. Stokes et al. (2008) described a similar process inferred from ribbed moraines that overprint MSGs on the NW Canadian Shield. The authors concluded a change in rheology of the subglacial material from water-saturated soft tills, in which the MSGs had formed, to stiffer more dewatered sediments that enabled ribbed moraine formation under slow compressional ice flow. We conclude an analogue change for the particular region in our study area, as the imaged subglacial landforms are indicative for similar changes in subglacial flow conditions and thermal regimes.

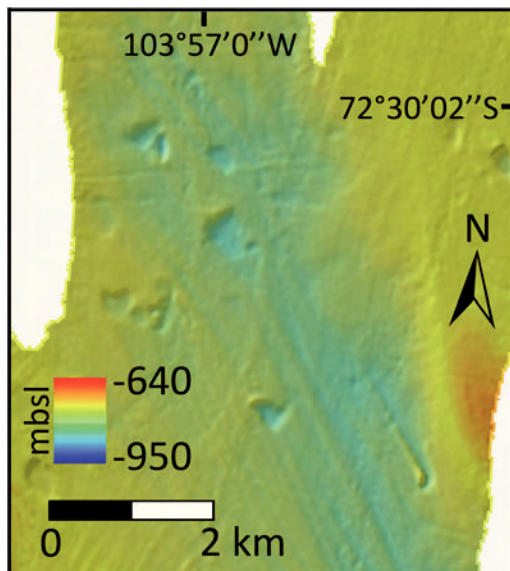


**Figure 3-17.** Hill-hole pairs overlying MSGs. Grid cell size 30 m. Illuminated from NW.

### 3.4.5 Relationships to main palaeo-ice stream flow in PIT

Several studies in the recent past investigated the post-LGM retreat pattern of the WAIS within the main PIT (e.g. Lowe and Anderson 2002; Evans et al. 2006; Graham et al. 2010; Jakobsson et al. 2012; Kirshner et al. 2012) and on adjacent inter-ice stream areas (Klages et al. 2013). Both the fast and slow flowing parts of the ice sheet in the eastern ASE retreated episodically as it is recorded by numerous GZWs within PIT and recessional moraines on the inter-ice stream ridge (e.g. Graham et al. 2010; Jakobsson et al. 2012; Klages et al. 2013). We have mapped three discrete GZWs (GZWs 'a-c' in Figs. 3-3, 3-15, 3-16) within AGT of which the two largest (GZWa and c) are located at similar lati-

tudes as GZW1, GZW2 and GZW5 in PIT (Fig. 3-16; Graham et al. 2010; Jakobsson et al. 2012). This relationship might hint at a related stepped retreat of the palaeo-ice streams in both troughs, whereby both GZW1 and GZW2 in PIT may have formed simultaneously with GZWa in AGT (Fig. 3-16). Unfortunately no bathymetric evidence could be detected yet on the inter-ice stream ridge separating the troughs that would corroborate a coherent grounding line stillstand on the outer shelf of the eastern ASE. Such a coherent pattern, however, may be evident for the middle shelf because on the inter-ice stream ridge between PIT and AGT several sets of recessional moraines are preserved (Figs. 3-2, 3-3) that might relate to the grounding line pauses evident from the formation of GZWc and GZW5 in the neighbouring troughs. This might indicate related phases of grounding-line stabilization between the two troughs and the inter-ice stream ridge (Fig. 3-16), but as reliable chronological information from cores constraining these stillstands are currently unavailable, this hypothesis remains untested.

A direct eastward flow relationship between PIT and AGT north of 72°S has recently been proposed by Hochmuth and Gohl (2013) for past glacial maxima. However, besides the indications for slow palaeo-ice across the inter-ice stream ridge north of Burke Island (Section 3.2.2), we do not observe a direct eastward flow relationship between the two troughs north of 72°N during the LGM. If the undifferentiated linear bedforms were crudely aligned MSGs (Table 3-2), a NNE-ward flow between 105° and 106°W could have been initiated at some point. This potential palaeo-flow pathway, however, does not show a direct relation to the LGM-ice flow in AGT, i.e. no direct connection can be inferred from the available geomorphological record (Figs. 3-2, 3-3, 3-15).

#### 3.4.6 Relation of GZWs to the substrate geology

GZW5 in PIT formed at a location where the trough width is constricted ('bottle neck'-effect) and where a high of probably hard sedimentary strata resistant to subglacial erosion exists (Jakobsson et al. 2012). Generally, ice streams tend to stabilize on seafloor highs that likely act as "stabilizing pinning points" on the ice stream bed (Dowdeswell and Fugelli 2012). Both GZWa and GZWc in AGT are located at locations constricted by distinct bedrock highs from either side, which likely caused a slow down of the ice stream flow velocity. Moreover, both GZWs are underlain by highs, which consist of old, likely lithified sedimentary strata of assumed Neogene age in case of GZWa (Hochmuth



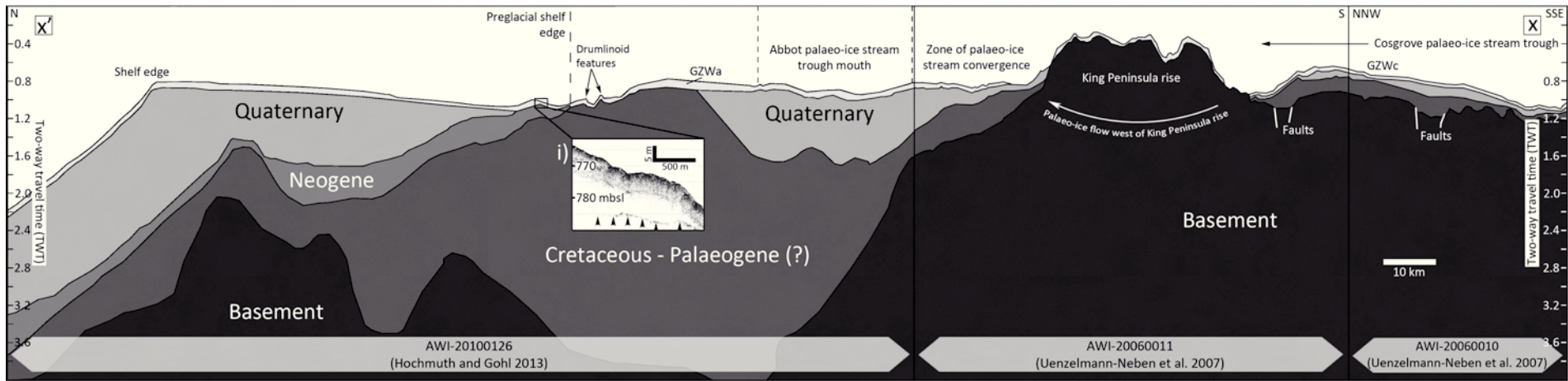


**Figure 3-18.** Interpreted seismic profile across the study area. Location of the profile is indicated by continuous grey line x-x' in Figure 2. Inset 'i' shows a PARASOUND profile section with a sub-bottom reflector (black upward pointing arrows) that likely corresponds to the surface of old, hard sedimentary strata of assumed Neogene age. The figure is based on interpretations derived from Uenzelmann-Neben et al. (2007) and Hochmuth and Gohl (2013).



and Gohl 2013) and acoustic basement that was lifted up tectonically in case of GZWc (Uenzelmann-Neben et al. 2007) (Fig. 3-18). These highs along the ice stream's pathway either counteracted the generally reverse bedslope or slowed it down (e.g. Stokes et al. 2007), causing the ice stream grounding-line to pause during retreat. Inset 'i' in Figure 3-18 illustrates the proximity of these old sedimentary strata near the modern seafloor directly offshore from GZWa. These old sedimentary strata may be overlain by post-LGM glaciomarine sediments (Hochmuth and Gohl 2013), but again age control from marine sediment cores is lacking.

### 3.5 Conclusions

- Our new comprehensive set of high-resolution bathymetry data from the eastern ASE comprising 3010 glacial landforms confirms the existence of the ~250 km-long AGT. AGT hosted a large ice stream at the LGM, which was mainly fed by two tributary ice streams, the Cosgrove and Abbot palaeo-ice streams, and which reached the shelf edge.
- Subglacial landforms indicative of wet or cold basal ice regimes resolve regions of fast and slow palaeo-ice flow, thus pathways of streaming ice could be reconstructed in detail. Furthermore, we located one area, where the thermal regime at the ice bed changed from wet to cold-based, which is evident from hill-hole pairs that formed on top of MSGs.
- Shallower regions along the palaeo-ice stream flow path W and NW of King Peninsula as well as WNW of the Demas Ice Tongue, correspond with three newly mapped GZWs, two of which may correlate with previously mapped GZWs in Pine Island Trough (PIT) and recessional moraines on the inter-ice stream ridge between AGT and PIT. This suggests a uniform pattern of episodic grounding-line retreat across the eastern ASE.
- The locations of the northernmost and southernmost GZWs in AGT correspond to both constrictions in the trough geometry and bathymetric highs that consist of substrate resistant to subglacial erosion, such as bedrock and/or acoustic basement. This relationship suggests geological control on grounding line stillstands during general ice-sheet retreat.

- Our data provide new detailed information on palaeo-ice stream flow pathways across the eastern ASE, east of the main PIT. This information will help to validate ice sheet models that aim to resolve the palaeo-flow characteristics of the WAIS during and since the LGM in order to refine estimations of possible future changes.

### **Acknowledgements**

We thank captains, crews, and scientists who participated in the research cruises that collected the data for this study. Furthermore, we acknowledge J.E. Arndt (AWI) for generating an earlier version of the bathymetric grid, as well as N. Lensch, M. Seebeck, S. Wiebe, and R. Fröhlking for their assistance with coring operations and post-cruise analyses, respectively. The work was financially supported by the Alfred Wegener Institute research program *Polar Regions and Coasts in a changing Earth System* (PACES).

## Chapter 4.

### Retreat of the West Antarctic Ice Sheet from the western Amundsen Sea shelf at a pre- or early LGM stage

J.P. Klages <sup>a,\*</sup>, G. Kuhn <sup>a</sup>, C.-D. Hillenbrand <sup>b</sup>, A.G.C. Graham <sup>c</sup>, J.A. Smith <sup>b</sup>, R.D. Larter <sup>b</sup>, K. Gohl <sup>a</sup>, L. Wacker <sup>d</sup>

<sup>a</sup> Alfred-Wegener-Institut, Helmholtz-Zentrum für Polar- und Meeresforschung, Marine Geology and Paleontology, Am Alten Hafen 26, 27568 Bremerhaven, Germany

<sup>b</sup> British Antarctic Survey, High Cross, Madingley Road, Cambridge CB3 0ET, United Kingdom

<sup>c</sup> College of Life and Environmental Sciences, University of Exeter, Amory Building, Rennes Drive, Exeter EX4 4RJ, United Kingdom

<sup>d</sup> ETH Zürich, Laboratory of Ion Beam Physics, Schafmattstrasse 20, CH-8093 Zürich, Switzerland

Published in *Quaternary Science Reviews* 91 (2014), p. 1-15.

#### Abstract

Recent palaeoglaciological studies on the West Antarctic shelf have mainly focused on the wide embayments of the Ross and Amundsen Seas in order to reconstruct the extent and subsequent retreat of the West Antarctic Ice Sheet (WAIS) since the Last Glacial Maximum (LGM). However, the narrower shelf sectors in between those two major embayments have remained unstudied in previous geological investigations despite them covering extensive areas of the West Antarctic shelf. Here, we present the first systematic marine geological and geophysical survey of a shelf sector offshore from the Hobbs Coast. It is dominated by a large grounding zone wedge (GZW), which fills the base of a palaeo-ice stream trough on the inner shelf and marks a single prolonged stabilization of the grounding line during general WAIS retreat following the last maximum local glaciation (LLGM). Reliable age determinations on calcareous microfossils from the infill of a subglacial meltwater channel superimposing the GZW reveal that grounded ice had retreated landward of the GZW before ~20.88 cal. ka BP with deglaciation of the innermost shelf prior to ~12.97 cal. ka BP. Geophysical sub-bottom information from the inner-, mid- and outer shelf indicates grounded ice extended to the shelf edge prior to the formation of the GZW. Assuming the wedge was deposited during a prolonged stillstand during deglaciation, we infer the timing of maximum grounded ice extent to well before

~20.88 cal. ka BP. Therefore the retreat of the WAIS from the outer shelf must have been initiated early on in the period of Antarctic deglaciation, immediately following the LLGM, with ice retreat already underway during a time corresponding to or even pre-dating the peak of the global LGM (~23-19 cal. ka BP). Our new findings give insights into the regional deglacial behaviour of this understudied part of the West Antarctic shelf area and at the same time support early deglaciation ages recently presented for adjacent drainage sectors of the WAIS. If correct, these findings contrast with the hypothesis that deglaciation of Antarctic Ice Sheets occurred synchronously at ~19 cal. ka BP.

#### 4.1 Introduction

The largely marine-based WAIS drains its ice into the Ross, Amundsen, and Bellingshausen Seas, predominantly in the form of fast-flowing ice streams. Some of those ice streams (e.g. Pine Island and Thwaites Glaciers) are currently undergoing considerable changes including extensive thinning (Joughin and Alley 2011), accelerated ice flow (Rignot et al. 2011), and fast grounding line retreat (Joughin et al. 2010; Tinto and Bell 2011), whereas others have slowed (e.g. Whillans Ice Stream) or even stagnated in recent decades (e.g. Kamb Ice Stream) (Joughin and Alley 2011). To put this variable behaviour today into a long term context, reconstructions of the maximum WAIS extent during the last glacial period and its retreat subsequent to the LGM have been carried out for major palaeo-ice stream troughs in the eastern Ross Sea Embayment (RSE, e.g. Mosola and Anderson 2006; Bart and Cone 2012; Bart and Owolana 2012) and the Amundsen Sea Embayment (ASE, e.g. Larter et al. 2009; Smith et al. 2011; Kirshner et al. 2012; Hillenbrand et al. 2013). All these studies concluded that, in all areas, grounded ice extended to at least the outer shelf during the LGM and retreated episodically from the outer shelf to the modern-day grounding line position (e.g. Mosola and Anderson 2006; Graham et al. 2010; Kirshner et al. 2012). Episodic phases of retreat have often been manifest in the geological record by sedimentary wedge deposits, which accumulated at former ice-stream termini within palaeo-ice stream troughs (termed grounding zone wedges; GZWs) (e.g. Mosola and Anderson 2006; Graham et al. 2010; Dowdeswell and Fugelli 2012). Furthermore, some studies have inferred an early initial retreat from the outer shelf at the end of the last glacial period, dated to before ~30.7 cal. ka BP in the

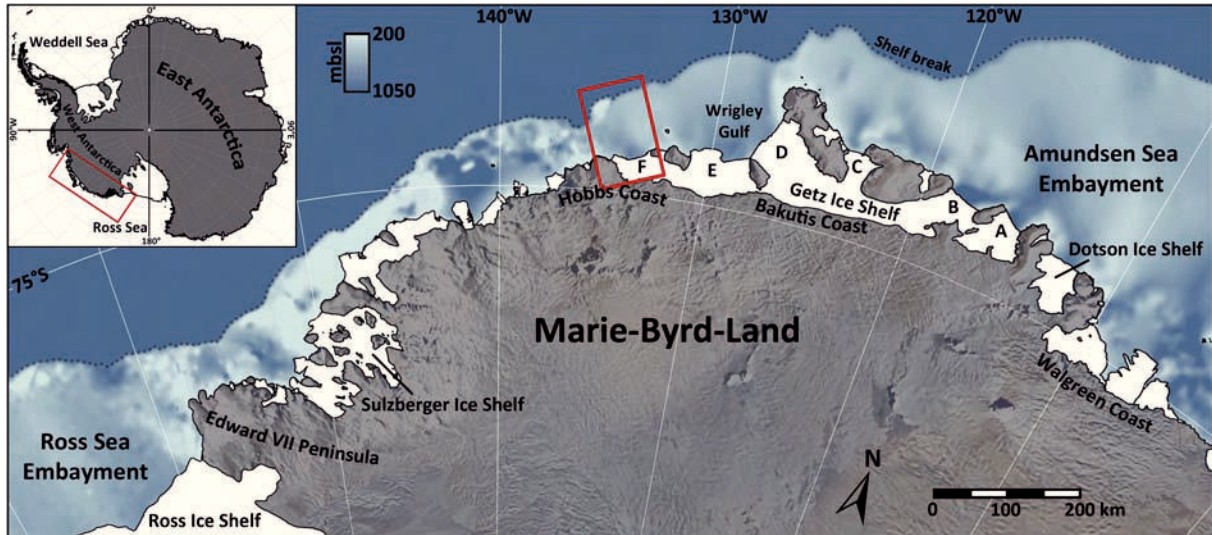


**Figure 4-1.** Overview map showing the location of the study area (in red). The general bathymetry of the West Antarctic shelf is derived from IBCSO data (Arndt et al. 2013; mbsl = metres below sea level). Ice shelves are displayed in white; continental shelf edge is indicated by dark grey dotted line. Nomenclature ‘Getz Ice Shelf 1-5’ was chosen according to previous studies (Larter et al. 2009; Hillenbrand et al. 2013).

southern Bellingshausen Sea (Hillenbrand et al. 2010); before  $\sim 31.6$  cal. ka BP in the eastern Ross Sea Embayment ( $\sim 27.5$   $^{14}\text{C}$  ka BP; Bart and Cone 2012); and to before  $\sim 22.4$  cal. ka BP in the western Amundsen Sea Embayment (Smith et al. 2011). For the eastern ASE, an early deglaciation of the inner shelf by the onset of the Holocene has also been concluded by Hillenbrand et al. (2013). In contrast to these studies, other authors have recently suggested a synchronous deglaciation of Northern Hemisphere and Antarctic ice sheets in which they propose synchronous grounding line retreat of the WAIS at  $\sim 19$  cal. ka BP (Weber et al. 2011).

Further constraints on West Antarctic deglaciation are clearly required to determine the phasing, timing and episodes of global ice sheet retreat. However, in contrast to the comparatively well-studied palaeo-ice stream troughs in the Ross and Amundsen Seas, interjacent shelf sectors still lack coverage of high-resolution bathymetric, seismic, and geologic data: the primary data necessary to interpret grounded ice extent and ice flow dynamics in the geological past, at and since the LGM (referring here to the global LGM;  $\sim 23$ - $19$  ka BP). Without this data a more complete reconstruction of WAIS extent during the last glacial period, which, in turn, is essential to estimate Antarctica’s contribution to the LGM sea level low stand and postglacial meltwater pulses, is not possible.

Here we present new marine geophysical and geological data from a part of the western Amundsen Sea shelf offshore from the Hobbs Coast, between the Ross Sea and Amundsen Sea embayments (Fig. 4-1). A landward deepening trough was incised into the shelf



by a palaeo-ice stream, and subsequently occupied by fast-flowing glaciers during glacial advances. The most recent glacial episode deposited a trough-wide GZW on the inner shelf within the depression. The size and geometry of the GZW is remarkable when compared to other GZWs reported from the Amundsen Sea shelf so far. We aim to: (1) decipher whether the WAIS advanced to the shelf edge in this sector at the LGM; (2) determine the significance and age of the pronounced GZW on the inner shelf. Both the extent and timing of post-LGM retreat are crucial to evaluate past WAIS behaviour for an area, which was largely neglected in previous palaeo-ice sheet studies; (3) provide new data to assess whether the style of WAIS retreat subsequent to the LGM was diachronous or synchronous. This, in turn, offers an additional constraint for ice sheet models that aim to predict the future behaviour of the WAIS.

## 4.2 Study area and methods

The study area is located offshore from the westernmost Getz Ice Shelf ('Getz F' following the nomenclature of Larter et al. 2009 and Hillenbrand et al. 2013) on the western Amundsen Sea shelf and extends from the Hobbs Coast to the shelf edge (Fig. 4-1). The distance from the modern ice shelf edge to the continental shelf edge is ~85 km, meaning the shelf is very narrow when compared to the eastern RSE and western ASE whose shelves are up to ~300 km wide. Maximum water depths of ~1000 m are reached on the innermost shelf, whereas the outer shelf and the trough flanks are between 400 and 500 m deep (Fig. 4-2a).

The marine geophysical and geological data used in this study were mainly acquired on cruise ANT-XXVI/3 of the RV *Polarstern* in early 2010 (Gohl 2010). In contrast to the sparsely mapped outer shelf, the inner part of the continental shelf was mapped completely for this study using multibeam echosounders, providing coverage of an area of ~1300 km<sup>2</sup> (~36 x 36 km). The bathymetry data was collected with a hull-mounted Atlas Hydrosweep DS-2 multibeam swath bathymetry system (59 beams at 15.5 kHz). Depth values and beam ray paths were calibrated during the cruise using sound velocity profiles from the Hydrosweep system itself. The raw data from the bathymetric survey were processed in MB-system (Caress and Chayes 2003) and subsequently gridded at a 30-m cell size. On the inner shelf we combined our new data with swath bathymetry data previously collected aboard RV/IB *Nathaniel B. Palmer* on cruise NBP0001 in early

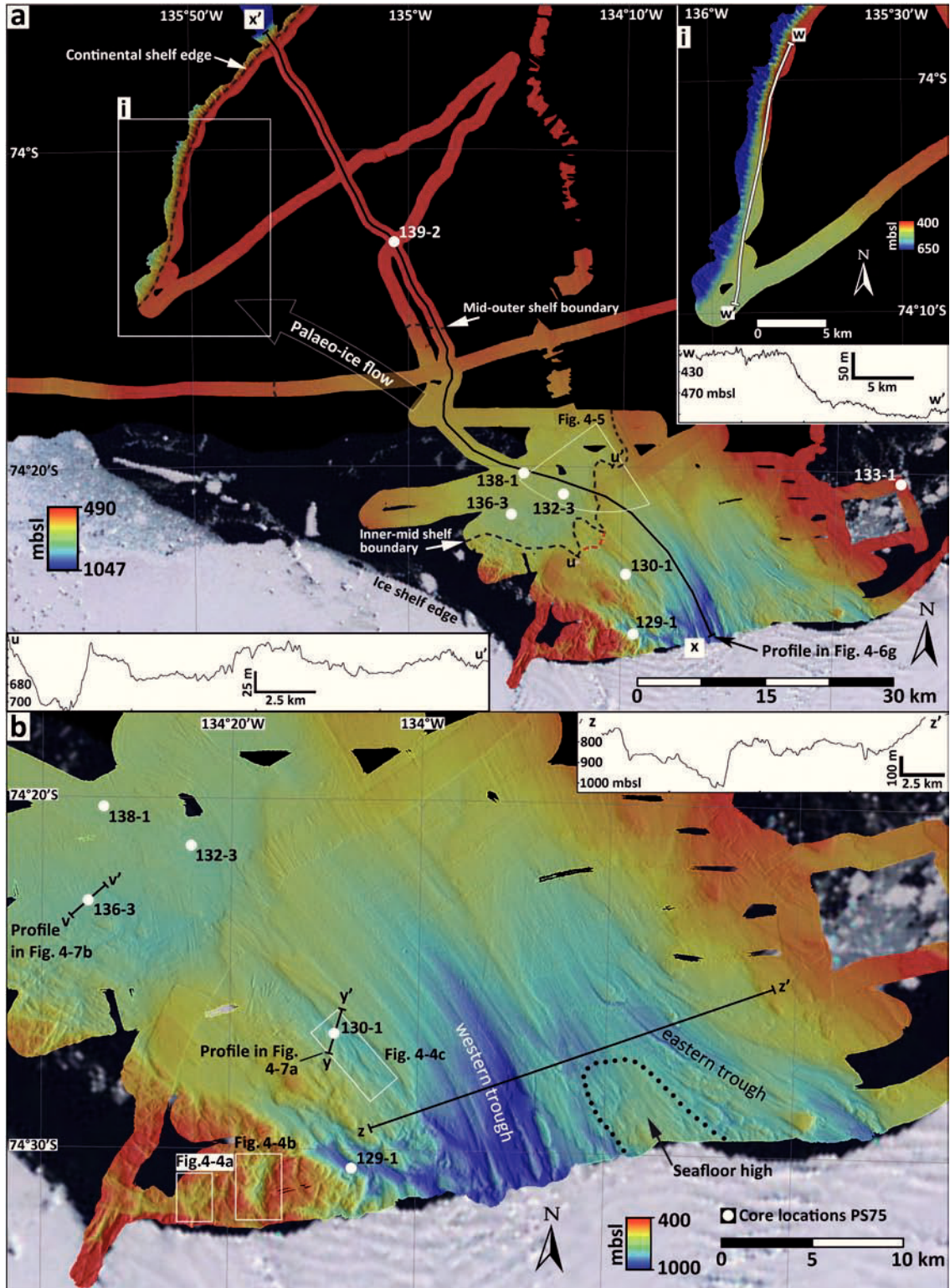


**Figure 4-2.** Detailed bathymetric maps of the study area. (a) Entire study area from inner shelf to continental shelf edge - Inset 'i' displays bathymetric trough mouth at the shelf edge (note the different colour/depth scale). Black dashed lines indicate boundaries between inner-, mid- and outer shelf; Continuous black line x-x' marks the location of the shelf profile in Figure 4-6g. Combined red/black dashed line u-u' marks the location of the profile shown as inset in same figure. Sector symbol indicates the point of view in Figure 4-5; Main estimated palaeo-ice flow direction is indicated by transparent arrow. (b) Close-up of the inner shelf bathymetry. Locations of detailed bathymetry in Figs. 4-4 a-c are indicated by white frames. Locations of PARASOUND profiles in Fig. 4-7 are indicated by profile lines y-y' and v-v'. Profile z-z' is displayed as inset in upper right corner. Core locations in both figures are indicated by full white circles. The sea floor high that separates the two tributary troughs (western and eastern trough) is highlighted by a black dotted line. Grid cell size 30 m. Grid illuminated from NNE. Projected in UTM zone 11S (WGS84).

2000 (Carbotte et al. 2007).

An Atlas PARASOUND acoustic sub-bottom profiler was used simultaneously with the multibeam swath bathymetry system to collect information on the properties of the (sub-)seafloor. A detailed description of the PARASOUND system can be obtained elsewhere (e.g. Melles and Kuhn 1993). In this study, the system only achieved ~5-30 m of penetration at most locations due to a combination of a relatively 'hard' seabed and a highly consolidated homogenous sub-seafloor substrate. In order to acquire sub-seafloor information that exceeded the maximum penetration depth of the PARASOUND system, multi-channel seismic reflection data were acquired with a cluster of 3 GI-guns (0.72 l) towed at 5 m water depth, and recorded with a 3000 m-long Sercel Sentinel digital solid streamer, with 240 channels, towed at 10 m water depth. We utilise only one seismic line here (AWI-20100114). However, more information about the seismic configuration and its implementation during the expedition can be obtained from Gohl et al. (2013).

Sediment cores were recovered with a Kiel-type gravity corer and a giant box corer. The core locations were identified using sub-bottom and multibeam data. Following recovery, the cores were cut into 1 m long sections and sealed. Sections were logged for P-wave velocity ( $V_p$ ), magnetic susceptibility (MS) and wet-bulk density (WBD) with a GEOTEK Multi Sensor Core Logger (MSCL). The core sections were split at the Alfred Wegener Institute (AWI) in Bremerhaven, Germany, and subsequently processed using standard procedures described in *Chapter 2* (in the following referred to as Klages et al. 2013). Accelerator Mass Spectrometry (AMS) radiocarbon dating was carried out exclusively on calcareous microfossils at both the Beta Analytic Radiocarbon Dating Laboratory in Miami, Florida, USA, where the conventional AMS  $^{14}\text{C}$  dating method was applied, and at the Laboratory of Ion Beam Physics at the Swiss Federal Institute of Technology (ETH) in Zürich, Switzerland, where a Caesium sputter negative ion source was used, which is especially applicable for very small carbonate sample sizes (Wacker et al. 2010). All downcore  $^{14}\text{C}$  ages were corrected by subtracting the uncorrected  $^{14}\text{C}$  date of a bivalve from the surface of the giant box core PS75/133-1 (Fig. 2a). This age ( $1420 \pm 30$   $^{14}\text{C}$  yrs) is in good agreement with the modern Antarctic Marine Reservoir effect (MRE,  $1300 \pm 70$  yrs, Berkman and Forman 1996) that we used. We express all radiocarbon dates as calibrated (cal.) yrs BP. All radiocarbon ages were calibrated with the Calib 6.0

software using the Marine09 curve (Reimer et al. 2009). For supplementary information, see doi:10.1594/PANGAEA.818175, *Appendices 1d*, and *2c*.

### 4.3 Results and interpretation

We divided the continental shelf of the study area into three zones corresponding to the inner-, mid- and outer shelf (Fig. 4-2a, boundaries indicated by black dashed lines). We then describe specific morphologic and sub-surface characteristics from each zone.

#### 4.3.1 Seabed geomorphology

##### 4.3.1.1 Inner shelf

The inner shelf is dominated by a large GZW but more generally reveals a highly varied seabed topography, with elongated bedforms in the central part and a rugged and/or channelized topography at the margins (Fig. 4-2b). The deepest part of the inner shelf (maximum water depth ~1000 m) is characterised by a single palaeo drainage trough, which was fed by two converging tributary troughs, referred hereafter to the eastern and western troughs (Fig. 4-2b). The two tributaries are clearly separated by an elevated sea floor high (Fig. 4-2b, dotted line), which is characterized by subtle elongated bedforms and undulating channels. The western tributary is deeper than its eastern counterpart (Fig. 4-2b, Profile z-z'). Streamlined teardrop-shaped features, which we interpret as drumlins/drumlinoid features, are observed within the innermost trough as well as on the intervening sea floor high. They are 20-150 m high, 800-2500 m long and 150-700 m wide and have also been described from other palaeo-ice stream beds in the ASE (e.g. Graham et al. 2009; Nitsche et al. 2013). Further seaward these features become narrower and more elongated before evolving into glacial lineations with average elongation ratios (length/width) of ~30:1, which switch their alignment from NNW to NW (western trough) and NW to NNW (eastern trough) and terminate on a prominent GZW, thus slightly diverge here (Figs. 4-2b, 4-3). The glacial lineations measure lengths of 1-10 km, widths of 150-350 m, and heights of 3-20 m and are separated by a medial feature, which emanates from the elevated sea floor high (Fig. 4-2b). Drumlin-to-lineation forms were likely formed subglacially in water-saturated deformable sediments (Alley



et al. 1989; King et al. 2009) by relatively fast flowing ice (e.g. Clark 1993; Stokes and Clark 2002; King et al. 2009). We base that on their relatively high elongation ratios (10:1 – 80:1) and highly parallel alignment. The slightly divergent alignment of lineations on top of the GZW probably indicates a glacier margin that was close to flotation

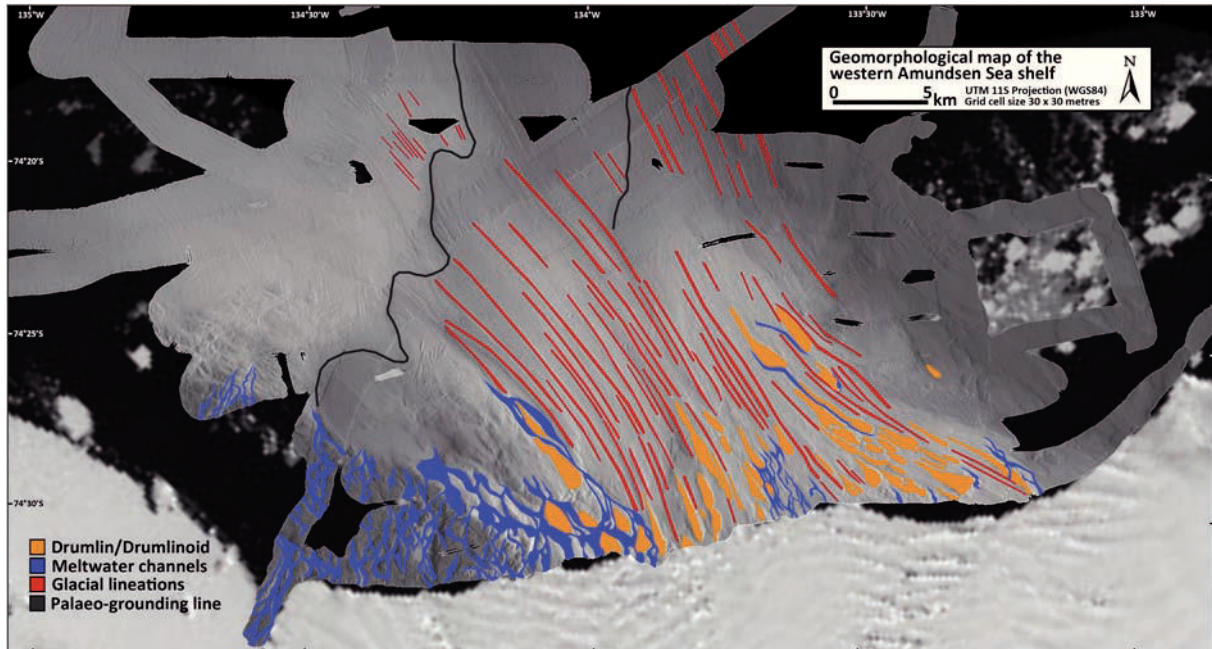


**Figure 4-3.** Geomorphological map of the inner- and mid shelf offshore from the Hobbs coast. Features digitized from 30 m swath bathymetric grid shown in Figure 4-2b. Grid cell size 30 m. Projected in UTM zone 11S (WGS84).

(i.e. at or just behind the grounding line) when the lineations formed (cf. Rebesco et al. 2011; Graham and Smith 2012), with two diverging ice fronts, separated by an accumulative medial feature, e.g. a medial moraine. The GZW is characterised by unequal slopes (stoss-side: gently rising,  $\sim 0.8^\circ$ ; lee-side: steeply dipping,  $\sim 2.3^\circ$ ) and a sinuously shaped (typical of ‘till deltas’, Alley et al. 1987, 1989; Larter and Vanneste 1995), SW-NE striking seaward margin that has been deposited at a palaeo-glacier terminus. The  $\sim 18$  km long and  $\sim 8$  km wide GZW has a  $\sim 80$  m high seaward facing front, which defines the transition to the mid-shelf.

The topography on the western trough flank can be divided into two: a southern elevated bedrock-floored portion (water depth  $\sim 500$  m) is rough and channelized with bedforms lacking a preferred orientation, and a northern deeper region with no bedforms but some channels, on the western edge of the GZW; the two are separated out by a clear geological step (Figs. 4-2, 4-3). On the elevated flank, v- and u-shaped channels (lengths of 1-3 km; depths of 20-300 m; widths of 250-800 m) have seaward dipping, undulating thalwegs (amplitudes up to  $\sim 20$  metres; Fig. 4-4a, b). We suggest that the channels were



incised into the outcropping bedrock by subglacial meltwater. In places their deep incision into resistant bedrock (sometimes up to 300 m, Fig. 4-4b) suggests a reoccupation

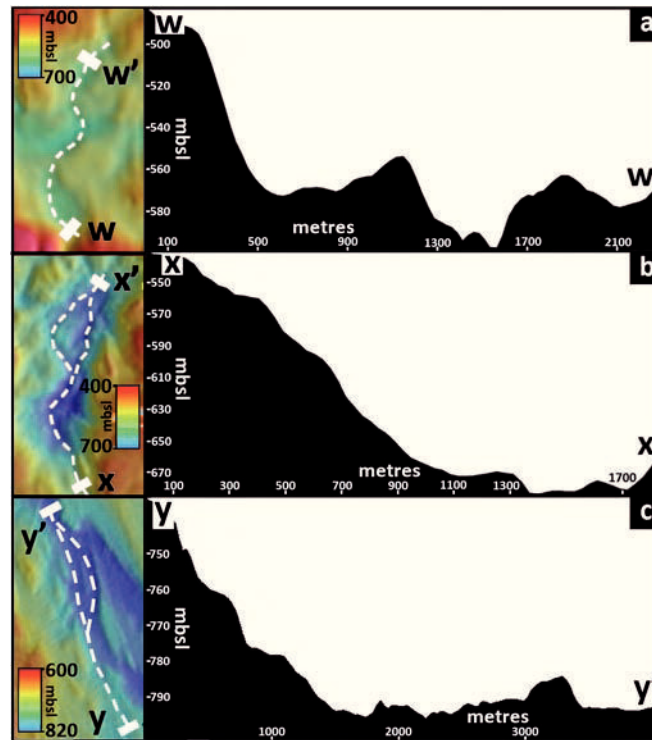


**Figure 4-4.** Detailed bathymetric maps and associated depth profiles of subglacial meltwater channels. Profiles in panels 'b' and 'c' relate to eastern channel pathways. Grid cell size 30 m. Projected in UTM zone 11S (WGS84).

by subglacial meltwater likely during several glacial cycles and a probable geological control on their form (e.g. Lowe and Anderson 2003; Graham et al. 2009; Smith et al. 2009).

Several wider and generally shallower channels have been imaged at the margins of the trough as well as on the high that separates the two tributaries in the centre of the trough (Fig. 4-3). The most prominent example is a SE-NW striking 10 km-long V-shaped channel at the western margin of the trough, which is incised into the sedimentary substrate of the GZW (Figs. 4-2b, 4-4c). It is between 80 and 120 m deep and up to 3 km wide, thus its spatial dimensions clearly differ from the structurally-controlled channels on the western bedrock high (Fig. 4-4a, b). Dowdeswell and Fugelli (2012) recently described similar shaped buried subglacial meltwater channels within GZWs on the Greenland shelf, which they relate to a non-topographically controlled 'high-energy meltwater flow'. Only one other example of a similar (but smaller) feature has been reported so far from a GZW on the Antarctic shelf by McMullen et al. (2006), who interpreted the channel as forming by meltwater flow through a 'breach point'. Generally, meltwater chan-

nels in our study area are located at the margins of the tributary troughs, which is where the highest basal melt rates are likely to occur (e.g. Clark and Stokes 2003). Similar channels to those described here have been mapped on other parts of the Amundsen Sea shelf (e.g. Lowe and Anderson 2003; Graham et al. 2009; Larter et al. 2009; Smith et al. 2009; Nitsche et al. 2013).

#### 4.3.1.2 Mid shelf

We define the mid-shelf to be situated between the seaward front of the GZW and the 550 m water depth-contour line, which lies between  $\sim 74^{\circ} 10' S$  and  $\sim 74^{\circ} 15' S$  (Fig. 4-2a). Here, 20-45 km landward of the shelf edge, the seafloor has gently shoaled seaward from a maximum water depth of  $\sim 720$  m just in front of the GZW by  $\sim 150$  metre to the point we define as the transition from the mid- to the outer shelf (Fig. 4-2a, black dashed line). The seafloor of the adjacent banks remains comparatively shallow ( $\sim 400$ -500 m). By comparison to the inner shelf bathymetry, the seafloor of the mid-shelf is remarkably featureless. However, some subtle SE-NW striking elongated bedforms, interpreted as glacial lineations, are present on the eastern part of the mid-shelf directly offshore from the GZW front (Figs. 4-3, 4-5). Their elongation ratios are up to three times lower than their counterparts on the inner shelf and they are poorly preserved. They appear highly parallel to sub-parallel and trend SE-NW-wards, which aligns with the larger and more pronounced glacial lineations on top of the GZW (inner shelf). In addition to lower elongation ratios, the mid-shelf lineations appear more subdued, which we attribute to a thin sediment cover, perhaps related to mass-wasting processes running down the stoss-side of the wedge (Fig. 4-5). Due to the position of the “faint” lineations offshore from the GZW, we suggest that their formation clearly pre-dates the GZW and thus the formation of glacial lineations on top of it but we attribute them to an LGM advance to the shelf edge rather than an earlier glacial advance (i.e., MIS3, 4 or possibly 6) based on the  $^{14}C$  ages and the sub-bottom stratigraphy discussed below.

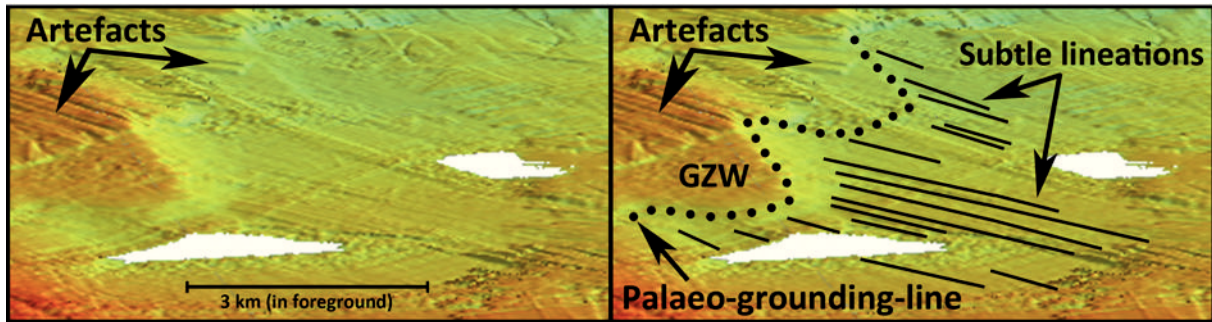


**Figure 4-5.** 3D-view of glacial lineations seaward of the GZW. Colours (red-green) represent a vertical depth range of ~100 metres.

#### 4.3.1.3 Outer shelf

We define the extent of the sparsely mapped outer shelf as the area between the northernmost limit of the mid-shelf and the continental shelf edge (Fig. 4-2a). Compared to the inner- and mid-shelf, the outer shelf is shallower with water depths ranging between 400 and 550 m. Curvilinear to angular grooves and shallow ridges of different orientations dominate the sea floor here. We interpret these features as the imprint of scouring iceberg keels. Similar features were widely imaged and documented from adjacent West Antarctic outer shelf areas (e.g. Lowe and Anderson 2002; Ó Cofaigh et al. 2005; Graham et al. 2009; Graham et al. 2010). The gentle NW-ward rise of the sea floor described for the mid-shelf continues onto the outer shelf to near the shelf edge, where the sea floor remains significantly deeper (~120 m) than the surrounding areas (see Profile w-w' in Fig. 4-2a, inset 'i'). We attribute this depression to be the continuation of a SE-NW trending trough carved by palaeo-ice streams that reached the continental shelf edge during the past (Fig. 4-2a).

#### 4.3.2 Acoustic sub-bottom stratigraphy

We use sub-seafloor information from both high-resolution reflection seismics and acoustic sub-bottom profiling (PARASOUND) to combine deep (below the maximum local penetration depth of the PARASOUND system) and surface or near-surface (higher vertical resolution than multi-channel reflection seismics) information from the zones within our study area (Fig. 4-6).

#### 4.3.2.1 Inner- and mid shelf

Lack of penetration indicates that near-surface sub-bottom information on the inner shelf is sparse. It is almost exclusively restricted to meltwater channel beds that are located on the western GZW margin or the elevated western trough flank. A cross-sectional PARASOUND profile from a wide channel that incised the western GZW margin reveals a 15m-thick sedimentary channel infill (Fig. 4-7a). Two sediment cores (discussed in Section 4.3.3) were recovered from the channel beds north of the elevated western trough flank (PS75/129-1) and from the western GZW margin (PS75/130-1; Fig. 4-7a). Besides the channel beds, the wavy sea floor appears acoustically impenetrable, without any distinct sub-bottom information, thus probably indicating a hard substratum such as bedrock and/or till, in which constructional features such as drumlins and glacial lineations have formed. There is an absence of an acoustically-transparent layer in areas around these channels, which is often associated with an ice-stream deforming bed (e.g. Dowdeswell et al. 2004). However, it is possible that during glacial cover a thin water-saturated deformable layer existed on top of any bedrock-floored regions in the ice-stream pathway (perhaps only a few centimetres thick), thus too thin as to be resolved by our PARASOUND system but still enabled the ice stream to move via basal sliding (Engelhardt and Kamb 1998).

The internal form of the GZW itself is revealed by a seismic reflection profile (AWI-20100114) that crosses the long-axis of the GZW in a SE-NW direction (Figs. 4-2a, 4-6a). A prominent sub-bottom reflector is observed at the base of the GZW (Fig. 4-6a, red line) and although the GZW lacks coherent internal reflections (cf. Alley et al. 1989; Vanneste and Larter 1995), it is still clearly a sedimentary depositional feature. Furthermore, the seismic profile shows a sedimentary high underlying the GZW, which might have acted as a pinning point on the previous palaeo-ice stream bed, where the ice stream grounding line stabilized over a longer time and accumulated sub- and proglacial debris to form the GZW (e.g. Dowdeswell and Fugelli 2012). The reflector at the base of the GZW can be traced seawards as a surface or near-surface reflector towards the mid-shelf, where it truncates seaward-dipping sedimentary strata (dip angle =  $\sim 4^\circ$ , Kalberg and Gohl, in preparation) of Early Pleistocene age (pers. comm. A. Eisenhauer, GEOMAR). This continuous near-surface reflector ( $\sim 2\text{-}3$  mbsf) is clearly visible on the PARASOUND profiles in Figures 4-6b and 4-6c and appears to be overlain by several acoustically transparent

lenses at the seaward toe of the GZW (Fig. 4-6b). In the transitional zone between the mid- and outer shelf, the sub-bottom reflector appears more faint and discontinuous and occasionally lies deeper ( $\leq 10$  mbsf) (Fig. 4-6d, e). But even on the high-resolution PARASOUND profiles, the truncated seaward-dipping strata are locally detectable (Fig. 4-6c, d, tilted arrows). A PARASOUND profile from the mid shelf, which was recorded perpendicular to the profiles in Figure 4-6b-e, allows a deeper look into the sub-sea floor and reveals multiple wavy (dipping) and parallel reflectors that are imaged to  $\sim 30$  m below the seafloor (Fig. 4-7b). Sediment core PS75/136-3 (discussed in Section 4.3.3) partly recovered these sediments.

#### 4.3.2.2 Outer shelf

The faint and discontinuous character of the sub-bottom reflector at the transition between the mid- and outer shelf changes to a strong reflector on the outer shelf that is most prominent between  $\sim 40$  and  $\sim 17$  km away from the shelf edge (Fig. 4-6f). Similar continuous sub-bottom reflectors were reported from several other palaeo-ice-stream troughs in West Antarctica (e.g. Ó Cofaigh et al. 2007; Graham et al. 2010; Reinardy et al. 2011a) and adjacent inter-ice stream ridges (Klages et al. 2013). They are associated with a lithological boundary between glaciogenic sediments near the sea floor. In the past, they have been linked to changes in ice flow velocities (from slow to fast) or to cycles of glacial advance and retreat, in both cases with the reflector indicating a transition from stiff to soft diamicton: A combination of lodgement, deformation (Ó Cofaigh et al. 2007) and/or subglacial traction processes (Evans et al. 2005) are believed to have acted on initially emplaced water-saturated subglacial diamictons (soft tills) or grounding-zone proximal glaciomarine diamictons (Reinardy et al. 2011b). Subsequently, those compacted and de-watered sediments (stiff tills), whose surfaces are often recorded as a sub-bottom reflector in acoustic sub-bottom profiles, have been covered by unconsolidated diamictons. In our study area, these soft diamictons are recorded as a transparent unit between the sub-bottom reflector and the sea floor (Fig. 4-6f). The transparent unit is of varying thickness and characterised by a highly irregular and rough surface topography that has been caused by the grounding and scouring of iceberg keels. At some locations on the outermost shelf the transparent unit is entirely absent. Nevertheless, the persistent presence of the continuous to discontinuous sub-bottom reflector that ex-



tends from beneath the GZW to a location ~17 km away from the shelf edge suggests the reflector is a glacial unconformity recording a single glacial event. We interpret the unconformity to indicate the last maximum advance of grounded ice across the shelf with its shallow stratigraphic level constraining this last advance to a time in the relatively recent past.

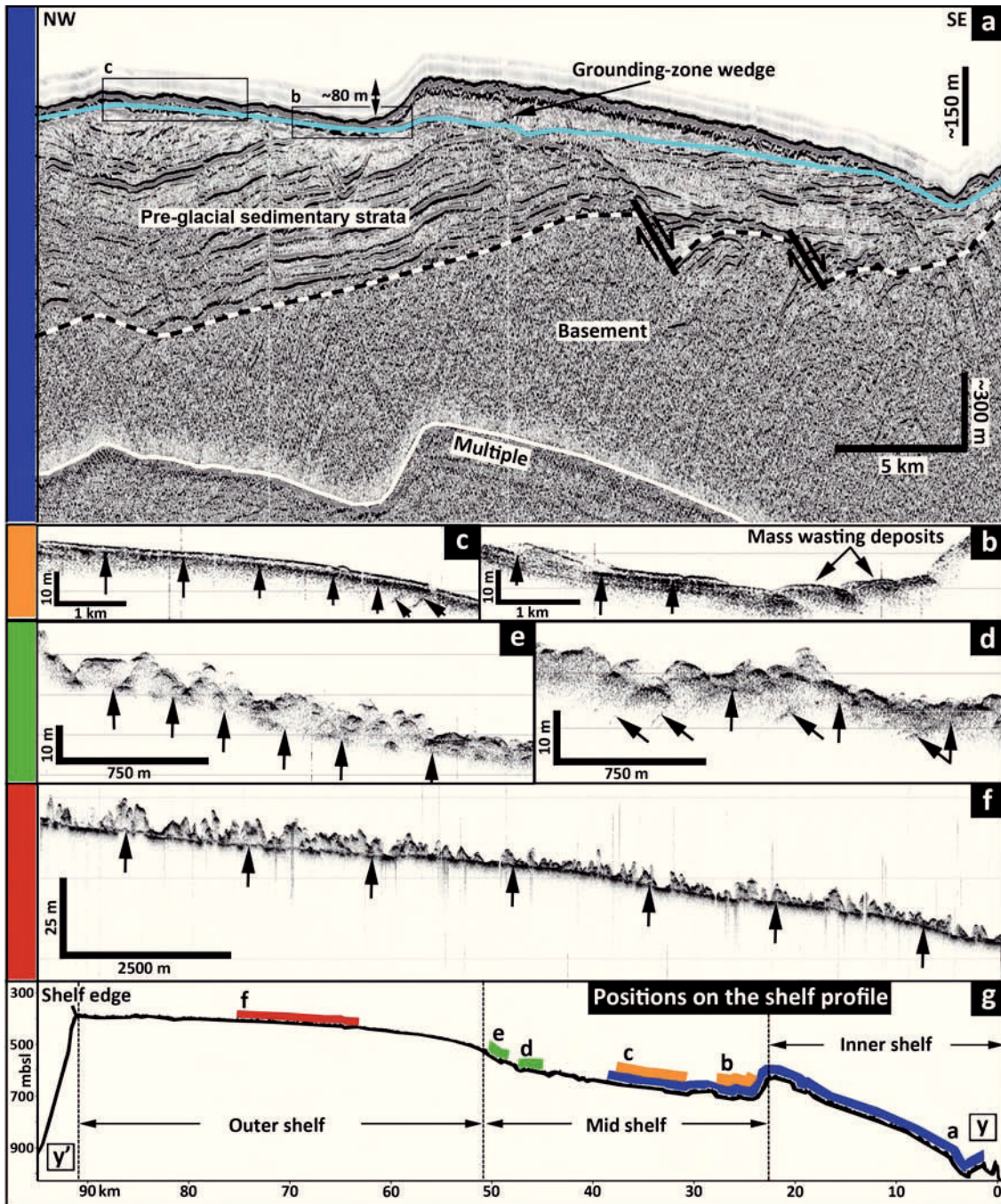


**Figure 4-6.** Extent of the glacial unconformity from the inner- to the outer shelf illustrated from seismic reflection (panel 'a', continuous light blue line) and PARASOUND data (panels 'b-f', black upward pointing arrows). Tilted black arrows in panels 'c' and 'd' highlight seaward dipping strata. Positions of the different sections on the shelf are displayed in panel 'g'. Location of shelf profile y-y' in panel 'g' is indicated in Fig. 4-2a. Distance on x-axis refers to distance from modern ice shelf edge.

### 4.3.3 Sediment cores

In order to constrain the timing of ice sheet variations and GZW formation as well as to ground-truth the geophysical data, we obtained seven sediment cores from the inner (PS75/129-1, 130-1 and 133-1), middle (PS75/132-3, 136-3 and 138-1), and outer shelf (PS75/139-2) (Fig. 4-2, Table 4-1). The inner shelf cores have been recovered from the eastern flank of the trough (PS75/133-1), from a meltwater channel on the western side of the wedge (PS75/130-1, Fig. 4-7a) and from a channel bed in the area directly seaward of the channelized bedrock high (PS75/129-1). Gravity cores PS75/132-3, 136-3 (Fig. 4-7b) and 138-1 were retrieved from the mid-shelf seaward of the GZW. Gravity core PS75/139-2 recovered sediments from the transparent unit overlying the distinct glacial unconformity on the outer shelf (Fig. 4-7c). A bivalve from the sediment surface of giant box core PS75/133-1 provided a radiocarbon age that confirmed the MRE for Antarctic shelf sediments.

**Table 4-1.** Information on sediment core locations. GC = gravity corer, GBC = Giant box corer.

Expedition	Gear	Core	Lat.	Lon.	Water depth (m)	Core recovery (m)
ANT-XXVI/3	GC	PS75/129-1	74° 30.54 S	134° 7.25 W	923	2.58
ANT-XXVI/3	GC	PS75/130-1	74° 26.71 S	134° 9.17 W	794	3.19
ANT-XXVI/3	GC	PS75/132-3	74° 21.97 S	134° 23.16 W	750	1.26
ANT-XXVI/3	GBC	PS75/133-1	74° 20.65 S	133° 4.68 W	474	0.33
ANT-XXVI/3	GC	PS75/136-3	74° 23.15 S	134° 35.59 W	752	2.12
ANT-XXVI/3	GC	PS75/138-1	74° 20.30 S	134° 33.42 W	703	0.95
ANT-XXVI/3	GC	PS75/139-2	74° 6.01 S	135° 3.31 W	449	

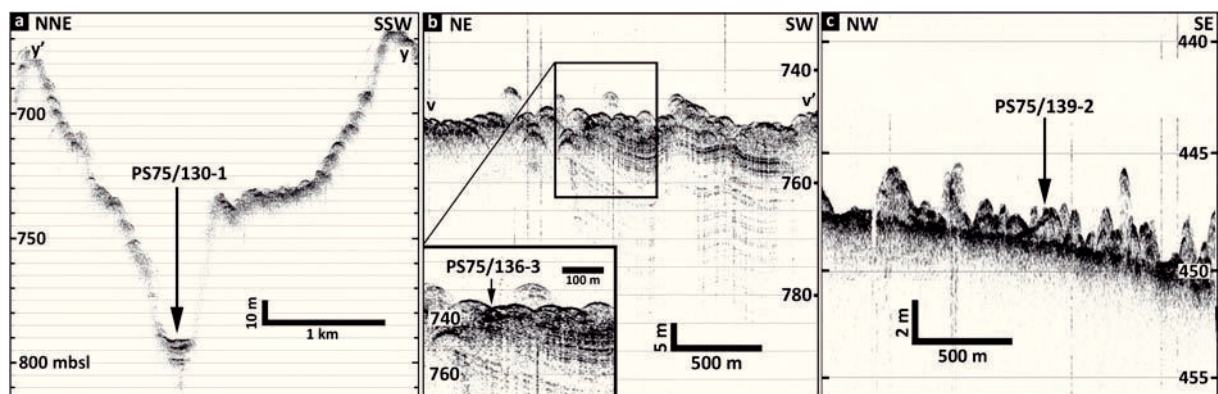


**Figure 4-7.** PARASOUND profiles of selected core locations on the inner- (panel 'a', PS75/130-1), mid- (panel 'b', PS75/136-3) and outer shelf (panel 'c', PS75/139-2). Profile locations in panel 'a' (y-y') and 'b' (v-v') are given in Fig. 4-2b.

#### 4.3.3.1 Lithofacies

Detailed sediment properties as well as lithology and sedimentary structure for all cores are given in Table 4-2 and summarised in Figs. 4-8 and 4-9. The two cores recovered from meltwater channels on the inner shelf (PS75/129-1 and PS75/130-1; Fig. 4-2b) mainly comprise crudely to strongly laminated to stratified mud (Fig. 4-8; Table 4-2, Lithofacies ‘M’) that is occasionally intercalated by sandy layers and/or, in case of core PS75/129-1, by distinct units of graded (gravelly) sandy mud with sharp bases (Fig. 4-8; Table 4-2, Lithofacies ‘Gr’). Based on these characteristics we propose that Lithofacies ‘M’ has been deposited in a sub-sea ice or sub-ice shelf environment with interruptions by rain-out of sandy debris from the base of an ice shelf or, in case of Lithofacies ‘Gr’ (PS75/129-1), with interruptions by sediment-gravity flows that have either been initiated on the proximal channel flanks (cf. Smith et al. 2009) or flowed along the channel thalweg. Sub-sea ice/sub-ice shelf sediments of this type have been described from other parts of the West Antarctic shelf (e.g. Domack et al. 1999; Pudsey and Evans 2001; Lowe and Anderson 2002, 2003; Hillenbrand et al. 2005; McKay et al. 2009; Smith et al. 2009; Kirshner et al. 2012; Hillenbrand et al. 2013). The uppermost muddy section in both cores is moderately to strongly bioturbated and bears gravel grains interpreted as iceberg-rafted debris (IRD) as well as diatoms, and thus indicates deposition in a seasonal-open marine environment (Fig. 4-8, Lithofacies ‘Mb’; see Table 4-2 for further sediment properties). Calcareous microfossils occur in 219 cmbsf (PS75/129-1) and in 319-315 cmbsf, 185-180 cmbsf and 125-120 cmbsf (PS75/130-1).

Three gravity cores were recovered from the mid-shelf and one of them is described here in more detail (Fig. 4-9, PS75/136-3), since the two other cores (PS75/132-3 and PS75/138-1) are shorter and almost identical in their lithology and sedimentary structure (see Supplementary material, doi:10.1594/PANGAEA.818175). Core PS75/136-3 mainly comprises homogenous to crudely stratified mud (Fig. 4-9; Table 4-2, Lithofacies ‘M’) that is unconsolidated between 125 and 0 cmbsf and overcompacted between 212 and 175 cmbsf near the core base (Lithofacies ‘Mc’). We attribute the overcompaction to advance of grounded ice over pre-LGM glaciomarine sediments, but note that the advance did not deposit a till, which could suggest a relatively cold bed (e.g. Atkins et al. 2002). These two mud sections are intercalated by a prominent bed of graded gravelly



**Table 4-2. Summary table of sediment core parameters, interpreted depositional environments and associated lithofacies. (WBD = wet bulk density, MS = magnetic susceptibility, IRD = ice-rafted debris).**

Lithology / Structure	Characteristic parameters	Interpreted depositional environment	Lithofacies
Crudely to strongly laminated to stratified mud occasionally intercalated by coarse-grained layers, sometimes enriched in calcareous microfossils, scarcely bioturbated, occasionally larger clasts incorporated	Medium to high water content, low shear strength, low WBD, low MS, low P-wave velocity, very low $C_{org}$ content	Alternating settling of hemipelagic and meltwater plume material in a sub-sea ice or sub-ice shelf environment, occasional release of IRD from icebergs or the basal layer of an ice shelf:  <b>Sub-sea ice or sub-ice shelf deposit</b>	Mud (M)
Homogenous to crudely stratified mud occasionally enriched in calcareous microfossils	Highly consolidated compared to Facies M (very high shear strength), medium water content, high P-wave velocity, very low $C_{org}$ content, no coarse-grained material (>63 $\mu\text{m}$ )	Alternating settling of fine-grained hemipelagic and meltwater plume material in a marine or glaciomarine environment:  <b>Open marine or glaciomarine deposit</b>	Overcompacted mud (Mc)
Normally graded (gravelly) sandy mud with erosional base, occasionally stratified towards base (PS75/136-3), occasionally enriched in calcareous microfossils	Medium to high water content, low to medium shear strength, medium to high WBD, medium to high MS, medium P-wave velocity, very low to low $C_{org}$ content	Debris flow or release of subglacial debris from basal melting at the grounding zone:  <b>Glaciogenic debris flow or proximal grounding zone deposit</b>	Graded (gravelly) sandy mud (Gr)
Slightly to strongly bioturbated mud, numerous scattered gravel grains, microfossil-bearing	High water content, very low shear strength, low WBD, low MS, low P-wave velocity, high $C_{org}$ content	Hemipelagic settling alternating with IRD deposition released from icebergs in a seasonal-open marine environment distal from the grounding-zone:  <b>Seasonal-open marine sediment</b>	Bioturbated mud (Mb)
Massive diamicton intercalated by a slightly stratified section, occasionally microfossil-bearing	Medium water content, generally low shear strength with several discrete peaks up to ~35 kPa, medium to high WBD, variable MS, low $C_{org}$ content	Reworking of glaciomarine and subglacial material by scouring iceberg keels distal from the grounding zone:  <b>Iceberg turbate</b>	Massive diamicton (Dm)

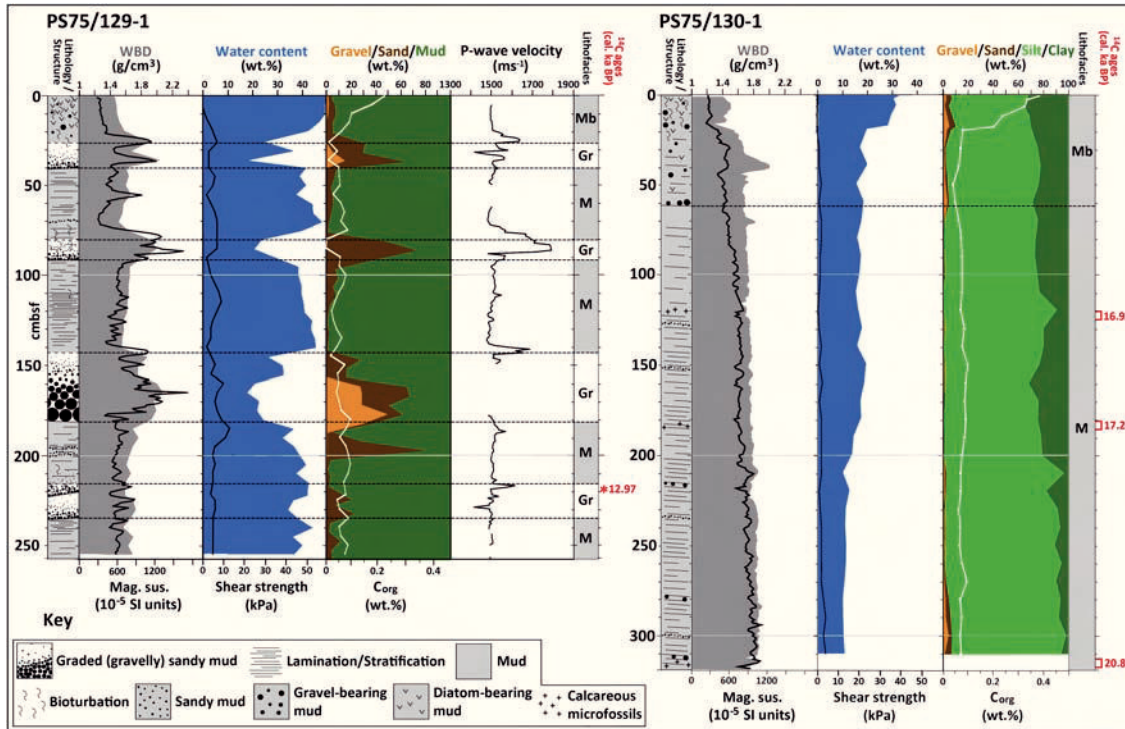


**Figure 4-8.** Core parameters for the inner shelf cores PS75/129-1 and PS75/130-1 (Lithology/structure, Wet-bulk density (WBD), Magnetic susceptibility (Mag. sus.), Water content, Shear strength, Grain-size fractions (Gravel, Sand, Mud [Silt, Clay], Corg content, P-wave velocity (data only available for PS75/129-1)). Dashed lines mark facies boundaries: (M) Sub-sea ice or sub-ice shelf deposit, (Gr) Glaciogenic debris flow or proximal grounding zone deposit, (Mb) Seasonal-open marine sediment. Sampling locations (intervals) for AMS <sup>14</sup>C dating and corresponding (calibrated) ages are indicated with red asterisks and red brackets, respectively.

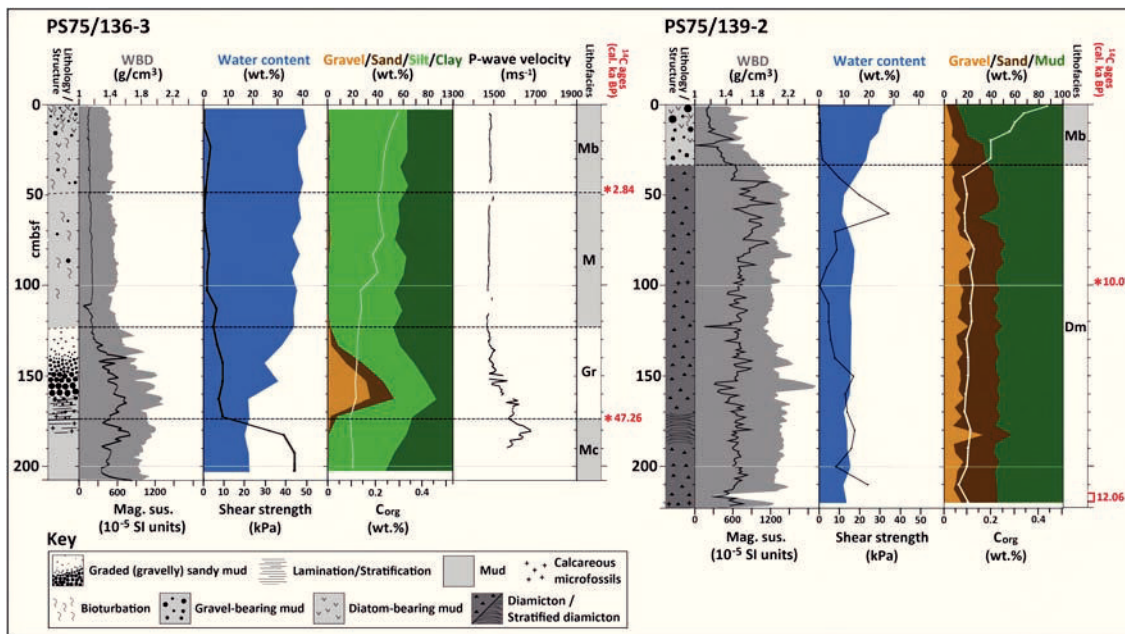


**Figure 4-9.** Core parameters for the mid- and outer shelf cores PS75/136-3 and PS75/139-2 (Lithology/structure, Wet-bulk density (WBD), Magnetic susceptibility (Mag. sus.), Water content, Shear strength, Grain-size fractions (Gravel, Sand, Mud [Silt, Clay], Corg content, P-wave velocity (data only available for PS75/136-3)). Dashed lines mark facies boundaries: (Mc) Open marine or glaciomarine deposit, (Gr) Glaciogenic debris flow or proximal grounding zone deposit, (M) Sub-sea ice or sub-ice shelf deposit, (Mb) Seasonal-open marine sediment, (Dm) Iceberg turbate. Sampling locations (intervals) for AMS <sup>14</sup>C dating and corresponding (calibrated) ages are indicated with red asterisks and red brackets, respectively.



sandy mud with a sharp base (Facies ‘Gr’). In contrast to similar lithological units within the inner shelf core PS75/129-1, this bed overlies a subglacially overcompacted mud (shear strength up to  $\sim 45$  kPa), thus rather indicates deposition of glaciogenic debris released from melting in a grounding zone proximal environment, probably subsequent to the landward retreat of grounded ice from the core location (cf. Lowe and Anderson 2002; Hillenbrand et al. 2013). A moderately to strongly bioturbated gravel- and diatom-bearing mud characterizes the core from 50-0 cmbsf and indicates increasing seasonal-open marine conditions towards the core top with occasional release of IRD in an environment distal from the ice front (Fig. 4-9, Lithofacies ‘Mb’, see Table 4-2 for further sediment properties). Calcareous microfossils occur in 183 cmbsf and 173 cmbsf. Additionally, a fragment of a fishbone was found at 43 cmbsf core depth.

One gravity core (PS75/139-2) was retrieved from the transparent unit that superimposes the glacial unconformity on the outer shelf. The corresponding sediments consist of a massive diamicton (Lithofacies ‘Dm’) that is stratified between 190 and 170 cmbsf (Fig. 4-9). Based on its sedimentary properties (Table 4-2) and its location on the irregular and rough seabed surface of the outer shelf, we propose heavy post-depositional reworking of subglacial and glaciomarine detritus by scouring iceberg keels as the main formation process for Lithofacies ‘Dm’ (cf. Lowe and Anderson 2002; Smith et al. 2011). Physical and sedimentary properties indicating low consolidation, fine-grained lithology, presence of diatoms, IRD, and bioturbation (Fig. 4-9; Table 4-2) from 35-0 cmbsf core depth indicate deposition of those sediments in a seasonal-open marine environment (Lithofacies ‘Mb’).

#### 4.3.3.2 Radiocarbon chronology

Five of the gravity cores and the giant box core from the inner-, mid- and outer shelf provided adequate amounts of calcareous microfossils for reliable AMS  $^{14}\text{C}$  radiocarbon dating (Figs. 4-8, 4-9). All conventional, corrected and calibrated AMS  $^{14}\text{C}$  ages are given in Table 4-3. The inner-shelf cores provided conventional (uncorrected) ages of  $12,190 \pm 60$   $^{14}\text{C}$  yrs BP in 219 cmbsf (PS75/129-1, Lithofacies ‘Gr’) and  $18,832 \pm 169$   $^{14}\text{C}$  yrs BP in 319-315 cmbsf,  $15,498 \pm 120$   $^{14}\text{C}$  yrs BP in 185-180 cmbsf and  $15,096 \pm 112$   $^{14}\text{C}$  yrs BP in 125-120 cmbsf (PS75/130-1, Lithofacies ‘M’), respectively. The conventional (uncorrected) radiocarbon ages from the mid-shelf sediment core PS75/136-3 span the

**Table 4-3. Conventional, corrected and calibrated AMS  $^{14}\text{C}$  ages obtained from sediment cores with additional information on core location, water depth, and dated material. The entire  $1\sigma$  range for each calibrated age is indicated by 'Min, Max', but only the mean age is quoted throughout the text and figures.**

Core	Publication code	Lat.	Lon.	Water depth (m)	Core depth (cmbsf)	Material dated	Conventional $^{14}\text{C}$ age (yrs BP)	$\pm 1\sigma$	Correction	Corrected $^{14}\text{C}$ age (yrs BP)	Calibrated $^{14}\text{C}$ age (yrs BP)	$\pm 1\sigma$ (min.)	(max.)	$\delta^{13}\text{C}$ (‰)
PS75/129-1	Beta-284598	-74,509	-134,1208	923	219	Bryozoans, unspec. calcareous shell fragments	12190	60	1420	10770	12967	12599	13335	-
PS75/130-1	ETH-50197	-74,445	-134,153	794	317	Benthic and planktic foraminifera	18832	169	1420	17412	20875	20468	21282	5,5
PS75/130-1	ETH-50908	-74,445	-134,153	794	182,5	Benthic and planktic foraminifera, bivalves	15498	120	1420	14078	17284	16962	17607	-0,3
PS75/130-1	ETH-50907	-74,445	-134,153	794	122,5	Benthic and planktic foraminifera, bivalves	15096	112	1420	13676	16917	16726	17108	5,5
PS75/133-1	Beta-332589	-74,344	-133,078	474	Surface	Bivalve	1420	30	N/A	0	0			-1,2
PS75/136-3	ETH-50198	-74,386	-134,593	752	173	Benthic and planktic foraminifera	46431	2595	1420	45011	47259	46228	48290	7,8
PS75/136-3	Beta-332590	-74,386	-134,593	752	43	Fishbone fragment	3950	40	1420	2530	2845	2678	3012	-24
PS75/139-2	ETH-50199	-74,1	-135,055	449	219	Benthic and planktic foraminifera	11622	91	1420	10202	12061	11792	12330	3
PS75/139-2	Beta-332591	-74,1	-135,055	449	98	Bryozoan	10180	50	1420	8760	10067	9859	10275	-5,1

time from  $46,431 \pm 2595$  ('radiocarbon-dead') to  $3950 \pm 40$   $^{14}\text{C}$  yrs BP. The presence of 'radiocarbon-dead' samples in Facies 'Mc' from core PS75/136-3 indicates that old glaciomarine sediments, deposited prior to MIS1-3 have been subsequently overridden by grounded ice and most likely during the LGM (Fig. 4-9). Two radiocarbon ages in Lithofacies 'Dm' of the outer shelf core PS75/139-2 provide conventional (uncorrected) ages of  $11622 \pm 91$   $^{14}\text{C}$  yrs BP and  $10180 \pm 50$   $^{14}\text{C}$  yrs BP. The similarity of ages in this unit together with absence of older  $^{14}\text{C}$  ages in these sediments, which directly overlie a prominent shallow glacial unconformity, indicates a young postglacial sediment cover that is likely to have accumulated since the last glacial advance and has then been re-worked by scouring iceberg keels (see Section 4.3.1.3).

## 4.4 Discussion

### 4.4.1 Extent of grounded ice during the last glacial period

The understanding of maximum glacial extent and subsequent retreat dynamics is important to decipher Antarctica's input to post-LGM meltwater pulses (MWP). Recently, Anderson et al. (2013) emphasized the problem of sparse information about the glacial and post-glacial behaviour of palaeo-ice streams that flowed onto the continental shelf in between the Dotson-Getz palaeo-ice stream and the eastern RSE. For the East Antarctic Ice Sheet (EAIS) it is known, that grounded ice did not extend to the shelf edge in Prydz Bay, the western Ross Sea Embayment and offshore from the George V. Land during the LGM (Licht et al. 1996; Domack et al. 1998, 1999; Shipp et al. 1999; Beaman and Harris 2003). This however is widely assumed for the WAIS (e.g. Anderson 1999; Conway et al. 1999; Graham et al. 2010; Smith et al. 2011), although recently a debate has arisen about the maximum LGM extent of the WAIS in both the Weddell Sea (e.g. Bentley et al. 2010, Hein et al. 2011, Hillenbrand et al. 2012, Larter et al. 2012) and the eastern Ross Sea (e.g. Mosola and Anderson 2006, Bart and Cone 2012).

The prominent glacial unconformity that was imaged beneath the GZW on the inner shelf (Fig. 4-6a) can be traced as a semi-continuous surface or near-surface reflector towards the mid- and outer shelf (Fig. 4-6 b-f), and is interpreted here to record a shelf-wide glaciation (e.g. Mosola and Anderson 2006; Dowdeswell and Fugelli 2012) that at least reached a position  $\sim 17$  km away from the modern continental shelf edge. Since the

GZW on the inner shelf clearly overlies this glacial unconformity, its deposition must post-date the shelf-wide glaciation. Furthermore, the presence of glacial lineations that are situated seaward of the GZW (Figs. 4-3, 4-5) indicate glacial flow beyond the GZW at some point prior to wedge formation. While the remaining areas of the mid- and outer shelf lack similar direct geomorphological evidence for glacial flow, this is likely a consequence of scouring by grounded iceberg keels that eradicated any potential pre-existing bedforms here, rather than evidence against prior ice grounding (cf. Graham et al. 2009). Generally, the overall bedform distribution in our study area deviates from other West Antarctic drainage sectors where glacial lineations often reach outer shelf or even shelf edge positions (e.g. Marguerite Trough, Ó Cofaigh et al. 2005; Pine Island Bay, Graham et al. 2010; eastern Ross Sea, Mosola and Anderson, 2006). Nevertheless, the combination of the pervasive, semi-continuous glacial unconformity and observation of glacial lineations beyond the GZW strongly suggests glacial flow to at least ~17 km away from the continental shelf edge. Further, the shallow stratigraphic level of the glacial unconformity on the mid- and outer shelf as well as the preservation of glacial lineations seaward of the GZW argue for extensive glaciation in the relatively recent geological past, which we suggest was during the last glacial period. The apparent subdued nature of the glacial lineations in front of the GZW suggests they have been overprinted by glaciomarine sediment, possibly released as gravity-flows as the wedge developed (Figs. 4-5, 4-6b). In turn, glacial bedforms on the backslope of the GZW, such as glacial lineations and meltwater channels (Fig. 4-3), are well preserved and distinct when compared to the lineations beyond the GZW, and are thus clearly of younger age.

#### 4.4.2 Timing and pattern of WAIS retreat offshore from the Hobbs Coast

In order to reconstruct the timing of WAIS extent and subsequent retreat along the Hobbs Coast continental shelf, we dated carbonate material from four sediment cores from the outer, middle, and inner shelf. Dating the sediments overlying the semi-continuous shallow glacial unconformity on the outer shelf should provide a reliable minimum age for the maximum expansion of the WAIS in this sector. If the GZW was an LGM feature then we would expect to find pre-LGM age sediments. However, this is not the case because none of our cores seems to contain sediments of pre-LGM age (Figs. 4-8, 4-9; Table 4-3). For example, an iceberg-turbated glaciomarine diamicton at site

PS75/139-2 contains calcareous microfossils whose ages span late glacial (~12 cal. ka BP at core base) to early Holocene times (~10 cal. ka BP at 98 cmbsf) indicating deposition in an (seasonal) open-marine environment after the grounding line had retreated. Core PS75/136-3, recovered seaward of the wedge, also provides additional support for a more extensive glacial advance in the recent past. Overcompacted glaciomarine sediments containing ‘radiocarbon-dead’ foraminifera (Fig. 4-9, Facies ‘Mc’) are overlain by younger glacier proximal sediments (Fig. 4-9, Facies ‘Gr’), which are in turn overlain by Holocene-age (~2.84 cal. ka BP at 43 cmbsf; Table 4-3) glaciomarine muds (Fig. 4-9, Facies ‘M’ and ‘Mb’). We suggest that this stratigraphic sequence records an LGM advance of grounded ice over pre-existing glaciomarine sediments deposited during an earlier phase of (seasonal) open-marine conditions. The absence of a subglacial till is also potentially significant and could indicate an erosive or cold-based ice sheet bed. Thus, while we cannot completely rule out the possibility that older sediments exist on the outer shelf (but have been obliterated by icebergs or just not recovered during coring), their apparent absence in our investigation leads us to the conclusion that there was a previously more extensive LLGM advance, and hence the GZW is a stabilisation feature formed during retreat. As clearly shown by our seismic data, the GZW overlies the glacial unconformity stratigraphically (Fig. 4-6a), and thus its formation must post-date the LLGM (Fig. 4-10b, c).

The size of the GZW is also instructive when assessing if the feature marks the maximum extent of ice at the LGM or was deposited during retreat. The Hobbs Coast wedge is considerably smaller than other GZWs that mark LGM grounding-zone positions elsewhere on the Antarctic shelf (e.g. WPC-1 in Prydz Bay, East Antarctica; Domack et al. 1998; O’Brien et al. 1999), which goes some way to support the interpretation that the feature in the western Amundsen Sea records a stillstand during general WAIS retreat rather than the position of maximum advance. However, the wedge we have imaged is notably larger than GZWs recording a stepped retreat elsewhere in the ASE, e.g. within the Pine Island Trough (Graham et al. 2010; Jakobsson et al. 2012). Indeed by comparing the long-axis cross-sectional area of the GZW (~0.72 km<sup>2</sup> per m width) we can show that the single GZW on the Hobbs Coast inner shelf is approximately equivalent in size to the combined area of five GZWs that formed during WAIS retreat within Pine Island Trough (~1.0 km<sup>2</sup>). This observation additionally suggests either a relatively prolonged phase of



grounding-zone stabilization or, alternatively, an extremely high sediment flux during a brief stillstand.

Age determinations on calcareous microfossils from the backslope of the wedge reveal that ice must have already retreated from the wedge before  $\sim 20.88$  cal. ka BP (Fig. 4-8, core PS75/130-1) and to the innermost shelf by  $\sim 12.97$  cal. ka BP (Fig. 4-8, core PS75/129-1). This older age in core PS75/130-1 is supported by two additional radiocarbon ages that are in stratigraphic order (Fig. 4-8; Table 4-3). Thus the wedge must have formed prior to  $\sim 20.88$  cal. ka BP. Together with our geophysical data (subtle glacial lineations beyond the GZW and shallow stratigraphic level of glacial unconformity), these ages suggest that grounded ice extended beyond the GZW within  $\sim 17$  km of the shelf-edge location at some point before  $\sim 20.88$  cal. ka BP. In the absence of additional age constraints from the outer shelf it remains difficult to fully assess when the shelf-wide glacial unconformity may have exactly formed, i.e. the ice reached its maximum expansion. However, Jakobsson et al. (2012) estimated that the largest GZW in the Pine Island Bay took between 600-2000 years to form. If we assume a similar rate of formation for the much larger wedge in the Hobbs Coast trough, then deglaciation of the outer shelf would have occurred sometime before  $\sim 24$  cal. ka BP. This would imply a relatively early initial retreat and possibly before or during the time-interval commonly assumed to define the LGM in Antarctica ( $\sim 23$ -19 cal. ka BP), since our calculation does not take into account the time required for grounding line retreat from the shelf edge to the inner shelf (along with subsequent GZW formation), which may have been considerable.

Thus, our findings point to early phases of retreat of the WAIS in the Hobbs Coast sector, from both the maximum shelf-edge position, and from a later stillstand position on the inner shelf. Comparable early shelf-edge advance and onset of retreat have been documented in nearby WAIS drainage basins including the Dotson-Getz Trough (Smith et al. 2011), the Belgica Trough (Hillenbrand et al. 2010), and the eastern Ross Sea embayment (Bart and Cone 2012), giving us confidence in our interpretations.

#### **4.4.3 Model for the glacial retreat offshore from the Hobbs Coast**

Combining geophysical observations with the interpretations of timing set out above, we present a reconstruction of the history and glaciological conditions along the Hobbs

Coast during the last glacial period and ensuing retreat (Fig. 4-10). We have documented an early shelf-edge glaciation offshore from the Hobbs Coast region (the LLGM, Fig. 4-10a) as described in Section 4.4.2, and inferred an early onset of deglaciation and inland retreat (Fig. 4-10b). Because eustatic sea level and atmospheric temperatures during the last (global) deglaciation did not rise before ~16-18 cal. ka BP (e.g. Deschamps et al. 2012; Shakun et al. 2012), a possible explanation for the hypothesised early onset of post-LLGM deglaciation in the western Amundsen Sea could be via inflow of relatively warm Circumpolar Deep Water (CDW) that was able to enter the shelf through deeper parts of the continental margin. A ~500 m-deep trough mouth (LGM depth ~400 m) exists today at the continental shelf edge in the Hobbs Coast study area (Fig. 4-2a, inset 'i'). Presently, CDW may enter bathymetric troughs where they are deeper than ~300 m (Wåhlin et al. 2010). Thus, a 400 m-deep trough mouth would have been plausibly deep to enable CDW flow onto the shelf at an initial stage of deglaciation. However, the feasibility of this explanation remains an open question because the upwelling intensity of CDW is assumed to be weaker during glacial periods (Tschumi et al. 2011 and references therein).

Retreat inland was followed by a major phase of grounding-zone stabilization on the inner shelf before ~20.88 cal. ka BP, during which the GZW was formed, thereby prograding to its maximum seaward extent (Fig. 4-10c). Fast and wet-based ice flow conditions were dominant during the final stages of GZW formation (e.g. Graham et al. 2010), as it is recorded by well-preserved elongate glacial lineations on top of the GZW (e.g. Stokes and Clark, 2002; Clark et al. 2003; King et al. 2009; Fowler 2010). The incision of a wide meltwater channel on top of the GZW's western margin suggests active subglacial meltwater flow during or shortly after the final phase of GZW formation. The presence of meltwater supports our interpretation of fast and wet-based ice drainage on a thin layer of water-saturated deformable sediments (cf. Engelhardt and Kamb 1998; King et al. 2009) that also acted as the mechanism for building up the GZW. The well-preserved bedforms that terminate at the GZW crest provide evidence that there were no subsequent re-advances beyond this palaeo-grounding zone after the stillstand (Todd et al. 2007), i.e. not after ~20.88 cal. ka BP. Following GZW formation, the grounding line retreated across the inner shelf until it reached the modern coastline (Fig. 4-10d, e). Meltwater channels may well have been active during this phase of retreat. Cores collected from the post-glacial infill of the subglacial meltwater channel on the GZW's western

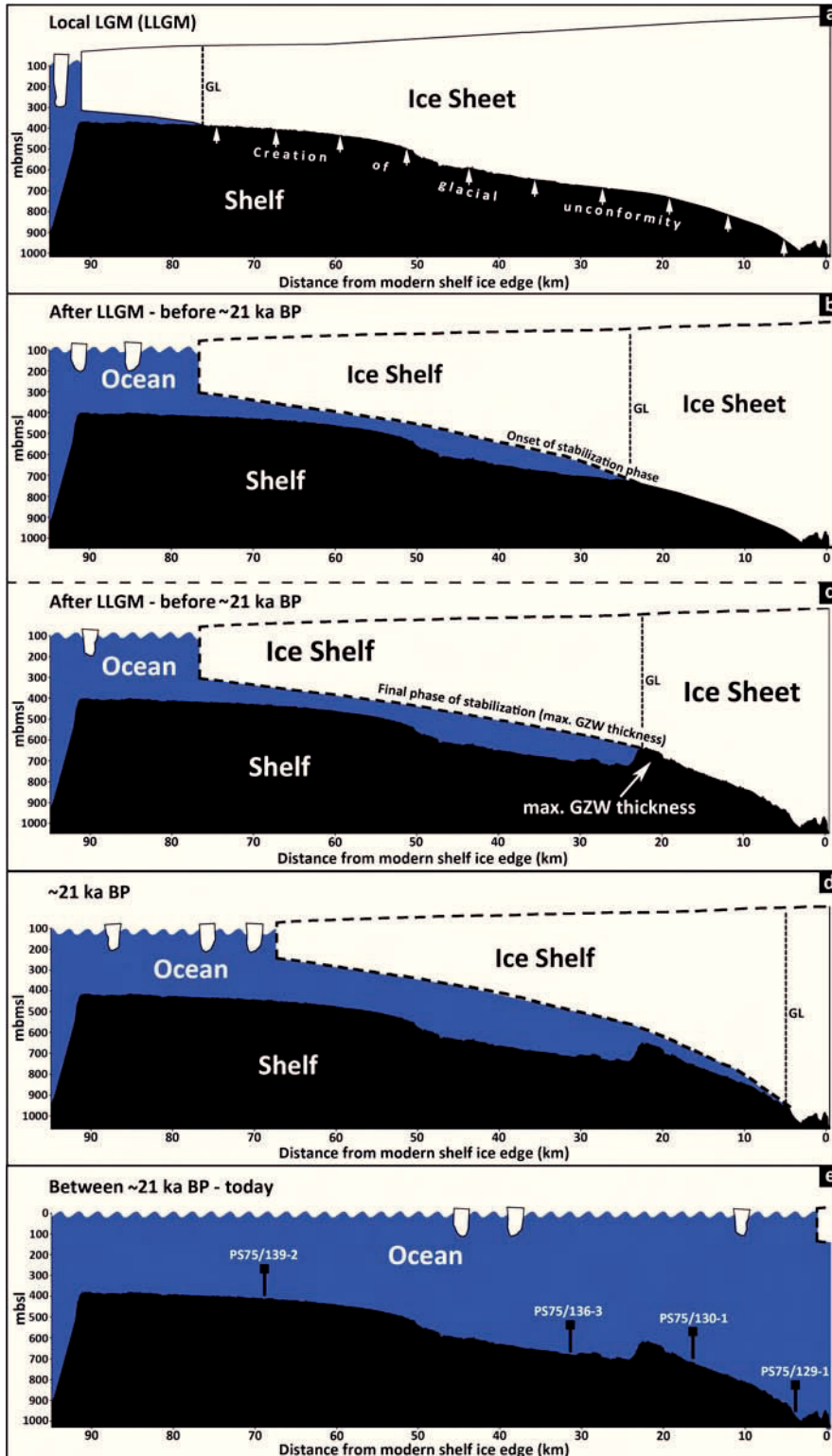


**Figure 4-10.** Conceptual model for the deglaciation of the shelf offshore from the Hobbs Coast in five phases, (a) Maximum extent of grounded ice during the local LGM (LLGM), when the shelf-wide glacial unconformity was created (white upward pointing arrows), (b, c) Post-LLGM retreat of the grounding line to an inner-/mid-shelf position where it stabilized and successively deposited the GZW prior to ~20.88 cal. ka BP, (d) Grounded ice evacuated the GZW at around ~20.88 cal. ka BP. An ice shelf may have been present in the following time, (e) Between ~20.88 cal. ka BP and today the grounding line and ice shelf edge retreated to its modern position, thus the imaged continental shelf has been ice-free since an early stage (since ~20.88 cal. ka BP). Vertical dashed lines indicate the estimated minimum position of the grounding line (GL) based on our data. Distance on x-axis refers to distance from modern ice shelf edge. Positions of core locations are indicated with simplified ‘gravity corer’-symbol. (mbmsl = metres below modern sea level; mbsl = metres below sea level; GL = grounding line).

margin (Figs. 4-2b, 4-4c, 4-7a) recovered fine-grained sediments with low IRD and microfossil content that were probably deposited in a sub-ice shelf or perennial sea-ice environment (cf. Domack et al. 1999, 2005; Kirshner et al. 2012). Thus, we interpret ice shelves to have also been present at least intermittently when the ice sheet retreated landward from the GZW. Laminated to stratified glaciomarine muds, which are occasionally intercalated by thin sandy layers underlying the muds, might reflect a combination of meltwater-plume deposition and rain-out of basal debris from the overlying ice shelf during this phase. In contrast, the homogeneity of the overlying muds probably indicates deposition near the ‘null point’ (cf. Domack et al. 1999), i.e. the zone that is half-way and thus distal from both the grounding line and the calving line. Overlying sediments with higher water content and higher contents of biogenic components indicate a transition to seasonal-open marine conditions consistent with an eventual retreat or loss of the ice shelf (Fig. 4-10e), and establishment of the grounding-line at its modern-day location.

#### 4.4.4 Wider context of post-glacial WAIS retreat in the Hobbs Coast region

The model we have proposed for retreat in the Hobbs Coast region (Fig. 4-10) suggests a relatively early WAIS retreat in this sector. The fact that the initial retreat was before ~20.88 cal. ka BP, and possibly as early as ~24 cal. ka BP, our findings appear to contradict the hypothesis that deglaciation of the Antarctic continent occurred synchronously at ~19 cal. ka BP (Weber et al. 2011). A minimum retreat age older than ~20.88 cal. ka BP is in agreement with minimum initial deglaciation ages presented for drainage sectors nearby (before ~30.7 cal. ka BP in the southern Bellingshausen Sea, Hillenbrand et al. 2010; before ~31.6 cal. ka BP (~27.5 <sup>14</sup>C ka BP) in the eastern Ross Sea Embayment, Bart and Cone 2012; before ~22.4 cal. ka BP in the western Amundsen Sea Embayment, Smith et al. 2011). Livingstone et al. (2012) compiled chronological information about the onset of Antarctic deglaciation and showed that the corresponding ages are highly variable, ranging broadly from 31 to 8 cal. ka BP. Our new data support their interpretation that WAIS retreat was time-transgressive diachronous between different sectors and even between different and adjacent drainage basins. The diachrony can be seen as similar (though over longer timescales) to modern responses of marine terminating West Antarctic ice streams that in some areas undergo considerable changes as fast

## Chapter 5.

### General conclusions and future perspectives

#### 5.1 New insights into the palaeo-glaciology of the Amundsen Sea shelf

Prior to this thesis, large areas of the formerly glaciated Amundsen Sea shelf remained unexplored, thus hampering more precise ice sheet reconstructions significantly. Reliable data was particularly lacking from inter-ice stream ridges, and middle and outer shelf regions that are both crucial in terms of understanding and reconstructing past ice sheet flow pattern and dynamics more fully. In this thesis I have presented sedimentological and geophysical data from three formerly unstudied parts of the Amundsen Sea shelf that reveal new detailed insights into their glacial history, enhancing our understanding WAIS dynamics at and since the LGM. I achieved the aims of the thesis introduced in *Chapter 1.3* by:

- 1) showing that a ENE-ward ice flow across the inter-ice stream ridge during the LGM was significantly slower when compared to the neighbouring troughs, as we detected the theoretically predicted ‘mega-scale ribbed moraines’ (cf. Dunlop et al. 2008) for the first time on the Antarctic shelf. In combination with sub- and proglacial landforms that stratigraphically overlie this ribbed moraine (Hill-hole pairs, recessional moraines, and crevasse-squeeze ridges), I was able to characterize the inter-ice stream ridge as having been influenced by slowly flowing, subsequently stagnating, and episodically-retreating cold-based ice. While ice was flowing NNE-wards in the main PITPIS trough, the ice flow direction on the inter-ice stream ridge must have slightly switched from ENE to NNE in between the LGM and final deglaciation, likely initiated shortly after 14.6 <sup>14</sup>C ka BP. It can be concluded that although palaeo-ice sheet dynamics have been entirely different on the inter-ice stream ridge, the timing of ice sheet retreat seems to have been largely synchronous with the PITPIS trough. These new findings close an important gap of understanding about past WAIS dynamics as by now the ice retreat from these inter-ice stream ridges was poorly understood, and thus sometimes wrongly interpreted (e.g. Lowe and Anderson 2002). The new results from



the inter-ice stream ridge are well supported and augmented by studying more extensive detailed bathymetric data from the surrounding shelf areas, as:

- 2) revealing detailed palaeo-flow pathways across the easternmost ASE for the first time using a comprehensive high-resolution bathymetry dataset compiled from 11 research cruises. Thorough mapping of 3010 individual glacial landforms enabled me to clearly identify regions of fast and slow palaeo-ice flow during the LGM and the following retreat. These data confirm the existence of the ~250 km-long AGT that hosted a large ice stream at the LGM, mainly fed by the Cosgrove and Abbot palaeo-ice streams, flowing across the middle and outer shelf where it reached the continental shelf edge. Through several smaller troughs ice was drained into the main ice stream from the adjacent banks. However, in contrast to previous studies, no active LGM tributary from the PITPIS trough could be detected (cf. Hochmuth and Gohl 2013). Outside these warm-based regions of fast palaeo-ice flow, cold-based ice conditions as evident from the previously investigated inter-ice stream ridge could be confirmed across a larger area, thus enabling the distinction of different thermal regimes on the shelf in the past. With the newly mapped raft features in the NE of the inter-ice stream ridge, a NNE slow and cold-based palaeo-ice flow across the ridge that was already inferred from the ribbed moraine and the orientation of hill-hole pairs further SW could be confirmed. Furthermore, this new information clarified the uncertain origin of previously described SSW-NNE-oriented groove features at the eastern margin of PIT (Lowe and Anderson 2002), and indicates a slow-flowing connection between the PIT and AGT across the inter-ice stream ridge during the last glacial. Within the main AGT shallower sea floor features within the palaeo-ice stream pathway could be identified as GZWs. These features indicate an episodic post-LGM retreat pattern from the easternmost ASE shelf, which is consistent with a similar ice retreat in the main PIT. There is confidence in this interpretation because two of the newly mapped GZWs correlate with previously mapped GZWs and with recessional moraines on the inter-ice stream ridge. These new findings reveal a uniform pattern of stepped grounding line retreat across the entire eastern ASE. This retreat pattern is also evident for the so far unstudied westernmost Amundsen Sea shelf as here

3) a large GZW has been discovered likely recording one, rather prolonged grounding line stabilization phase on the inner shelf offshore from the Hobbs Coast subsequent to the maximum extent of local glaciation. This is based on the fact that its size is in the same order of magnitude as e.g. the combined size of the five GZWs in PIT, and a prominent continuous sub-bottom reflector, interpreted as glacial unconformity, has been detected reaching from beneath the GZW to a location ~17 km landward of the continental shelf edge, thereby indicating a glacial ice sheet advance towards the outer shelf prior to GZW deposition. Glaciomarine sediments that cover this shallow outer shelf glacial unconformity only bear calcareous microfossils of late Holocene age. The shallow stratigraphic level of the unconformity in combination with the drape only bearing sediments of Holocene age indicates a shelf-wide glaciation during the last glacial period. This maximum glaciation, however, is constrained by data to a time either prior to the commonly defined Antarctic LGM period (~23-19 ka BP) or to its early phase, as undisturbed glaciomarine sediments overlying the GZW reveal a basal age of ~20.88 cal. ka BP. By assuming a similar rate of GZW formation as estimated for the largest GZW in PIT (600-2000 years; Jakobsson et al. 2012), the minimum age for initial deglaciation from the outer shelf would be ~24 cal. ka BP, leading me to conclude a LLGM for the area. The innermost shelf was evacuated by grounded ice by ~12.9 cal. ka BP.

## 5.2 Implications of the new findings

The findings of this thesis provided new detailed insights into palaeo-ice sheet flow pattern and dynamics of the region and most importantly revealed that 1) the WAIS reached the shelf edge in both the easternmost and westernmost ASE, 2) a palaeo-ice stream in the easternmost ASE flowed along the ~250 km-long AGT trough and was subject to considerable changes in widths along its flow path as trough geometries highly vary, 3) regions outside the troughs were influenced by slowly flowing cold-based ice that stabilized the ice streams in both AGT and PIT, 4) trough constrictions in combination with changes of the subglacial geology within AGT led the ice stream to stabilize for at least 3 times on its landward retreat towards the modern grounding line, thereby

highlighting the importance of trough / seabed geometries (e.g. Dutrieux et al. 2014) and subglacial geology (e.g. Stokes et al. 2007; Golledge et al. 2013) for ice stream stability, 5) deglaciation from the inter-ice stream ridges has followed the retreat of the neighbouring ice streams, as ages for minimum grounding line retreat are similar, and GZWs in both the PIT and AGT correlate with recessional moraines on the inter-ice stream ridge, 6) therefore the WAIS likely retreated uniformly and in steps across the entire eastern ASE shelf, 7) a similar pattern of episodic retreat applies to a formerly unstudied palaeo-ice stream offshore from the Hobbs Coast, 8) within Hobbs Coast Trough, one stabilization phase probably equals five phases in PIT, 9) the associated GZW must have deposited well before  $\sim 20.88$  cal. ka BP, hence indicating an early initial deglaciation from the outer shelf at a pre- or early LGM stage, which supports interpretations from other WAIS drainage basins (e.g. Hillenbrand et al. 2010; Smith et al. 2011; Bart and Owolana 2012), and may point to the importance of local drivers for initial WAIS retreat, such as trough mouth depths at the shelf edge, facilitating a relatively early inflow of CDW, 10) deglaciation of the inner shelf offshore the Hobbs Coast was completed by  $\sim 12.9$  cal. ka BP, thus supporting recent conclusions that inner shelf regions in the Amundsen Sea sector must have been already deglaciated prior to or by the onset of the Holocene (Hillenbrand et al. 2013). 11) My new minimum deglaciation ages thus support a diachronous (cf. Livingstone et al. 2012; Anderson et al. 2013b; Larter et al. 2013) rather than a synchronous (Weber et al. 2011) initial WAIS retreat following the LGM, although external forcings as ocean and air temperatures as well as eustatic sea-level rise are assumed to have affected the Amundsen Sea region in the same manner (Larter et al. 2013, and references therein).

The major contribution of this thesis will help to diminish previous mismatches between model results and empirical data on the Amundsen Sea shelf (Golledge et al. 2013). Advancements in the knowledge of LGM ice sheet extent, palaeo-ice flow pathways, and ice flow pattern development over the past 10-20,000 years will ultimately facilitate 1) a better evaluation of recent rapid cryospheric changes in the region and 2) improvements in the reliability of ice sheet models predicting future WAIS behaviour, especially future contributions of the ice sheet to global eustatic sea level.

### 5.3 Perspectives for future work on the Amundsen Sea shelf

In contrast to other regions of Antarctica, the continental shelf of the Amundsen Sea has only begun to have been surveyed systematically over the past decade. During this time, palaeo-glaciological studies predominantly focused on palaeo-ice stream troughs on inner and middle shelf regions. This thesis contributed the first systematic surveys from regions on the continental shelf that previously remained sparsely studied or entirely disregarded, highlighting how crucial palaeo-ice sheet reconstructions in these regions are in order to gain a better understanding of past WAIS dynamics as a whole. I am able to show that a future neglect of inter-ice stream areas and outer shelf regions will significantly hamper attempts that seek to reconstruct WAIS dynamics more precisely – the only way to reliably test and validate future projections of this inherently unstable ice sheet. The findings of this thesis highlight the urgent need to make these regions the focus of future surveys.

Recently, new methods to reliably date glaciomarine sediments from the Antarctic shelf have been established (Wacker et al. 2010) – the backbone of robust palaeo-ice sheet reconstructions. Previous dating approaches to constrain minimum ages for grounding line retreat remained challenging as calcareous microfossils, known as the most reliable age indicator, quickly dissolve in the corrosive waters of Antarctic continental shelves. Hence sufficient sample sizes as needed for ‘traditional’ radiocarbon dating are difficult to find. An alternative dating approach that is often taken is to analyse the AIO fraction of sediments. However, these samples tend to be contaminated by fossil carbon and often result in erroneous age constraints, although robust deglacial chronologies of Antarctic shelves with AIO dating are possible given careful consideration and correction of the dating suite (e.g. western ASE: Smith et al. 2011, eastern ASE: Smith et al. submitted for publication). While achievable in some places, these authors have recently stated that sediments from outer shelf regions in particular seem to show the strongest rates of contamination, thereby casting strong doubt over age determinations on initial post-LGM deglaciation that are essential in order to define LGM ice limits. Although it is generally assumed that LGM ice limits in the Amundsen Sea sector were at the shelf edge (e.g. Larter et al. 2013), the well-stratified postglacial drape covering the shallowest glacial unconformity seaward of GZWa in the AGT (see Figs. 3-15, 3-16 in *Chapter 3*) is unusually thick (~6 m), thus possibly indicating sub-ice shelf or seasonal-open marine dep-

osition outlasting the last glacial period. To test this hypothesis, I will continue to collaborate with colleagues from the MICADAS radiocarbon dating facility at the ETH Zürich, who are able to date extremely small sample sizes of calcareous microfossils (Wacker et al. 2010). One such sample, I could extract from the base of a 2.96 m-long gravity core recovered from this drape. If the age reveals old, pre-LGM sediments then our previous assumptions on LGM limits in the easternmost ASE have to be revised, which, in turn, would have direct implications for LGM ice sheet models (e.g. Golledge et al. 2013), estimates on Antarctica's LGM ice volume (e.g. Denton and Hughes 2002), and its contribution to post-LGM sea-level rise. It would additionally contribute to the ongoing debate of whether or not, and where, biological refugia could have existed on Antarctic continental shelves during the last glacial period, enabling benthic life to survive extensive glaciations (e.g. Barnes and Kuklinski 2010; Graham and Smith 2012).

The need for a better coverage of high-resolution geophysical and geological data from West Antarctic shelves has been iterated several times during this thesis, as only this information can reveal flow, configuration, and style and timing of subsequent retreat of the past ice sheet, i.e. testing model simulations against these empirical data facilitates confidence in aiming to project the future WAIS. Golledge et al. (2013) recently simulated the LGM ice sheet using a high-resolution model and highlighted the need for more comprehensive data, since models that are fed by observational data only covering the past 30-40 years of ice sheet change (e.g. Favier et al. 2014) cannot fully elucidate future developments.

This effort, however, requires significant fieldwork funding. It can only be achieved if funding for future marine fieldwork in the region will continue. Successful campaigns such as RV *Polarstern* expedition ANT-XXVI/3 in early 2010 already resulted in relevant publications that emphasize the significance of the Amundsen Sea region in order to understand past and modern WAIS changes (e.g. Gohl et al. 2013; Hillenbrand et al. 2013; Klages et al. 2013; Nakayama et al. 2013). Ice streams that drain the WAIS into the Amundsen Sea seem to play a key role in controlling the stability of the entire ice sheet. In order to reconstruct time periods during which the WAIS may have been entirely absent (possibly during the late Pleistocene; Barnes and Hillenbrand 2010), shallow and deep drilling campaigns such as MeBo (Freudenthal and Wefer 2007) or IODP have been proposed and will have the potential to unravel the processes and trigger mechanisms leading to such a potential disintegration of the WAIS. Longer drillcore records could



also significantly help to understand WAIS fluctuations over past glacial cycles more generally (Gohl et al. 2013). This knowledge would be to help evaluate future WAIS development, providing new estimates on the evolution of future sea level, with the utmost relevance for our global community.

## **Data handling**

All data presented in this thesis are stored electronically and available in the PANGAEA database:

Chapter 2    doi:10.1594/PANGAEA.779863

Chapter 4    doi:10.1594/PANGAEA.818175

Multibeam bathymetry and PARASOUND data presented in Chapter 3 are available via the references given in Table 3-1. Core data will be stored in the PANGAEA database (doi registration in progress).

## References

- Alley, R.B., Blankenship, D.D., Bentley, C.R., Rooney, S.T., 1987. Till beneath ice stream B; 3, Till deformation: Evidence and implications. *Journal of Geophysical Research* 92, 8921–8929.
- Alley, R.B., Blankenship, D.D., Rooney, S.T., Bentley, C.R., 1989. Sedimentation beneath ice shelves—The view from ice stream B. *Marine Geology* 85, 101–120.
- Alley, R.B., Anandakrishnan, S., Dupont, T.K., Parizek, B.R., Pollard, D., 2007. Effect of Sedimentation on Ice-Sheet Grounding-Line Stability. *Science* 30, 1838-1841.
- Anandakrishnan, S., Alley, R.B., 1997. Tidal forcing of basal seismicity of ice stream C, West Antarctica, observed far inland. *Journal of Geophysical Research* 102, doi: 10.1029/97JB01073.
- Anderson, J.B., 1999. *Antarctic Marine Geology*. Cambridge University Press, Cambridge, UK, 289 p.
- Anderson, J.B., Shipp, S.S., Lowe, A.L., Smith Wellner, J., Mosola, A.B., 2002. The Antarctic Ice Sheet during the Last Glacial Maximum and its subsequent retreat history: a review. *Quaternary Science Reviews* 21, 49-70.
- Anderson, J.B., Jakobsson, M., OSO0910 Scientific Party, 2010. Oden Southern Ocean 0910: Cruise Report. In: *Meddelanden från Stockholms universitets institution för geologiska vetenskaper* 341, pp. 134.
- Anderson, J.B., Kirshner, A., Simms, A.R., 2013. Constraints on the Antarctic Ice Sheet configuration during and following the Last Glacial Maximum and its episodic contribution to sea-level rise. In: Hambrey, M.J., Barker, P.F., Bowman, V., Davies, B., Smellier, J.L., Tranter, M. (eds.). *Antarctic Palaeoenvironments and Earth-Surface Processes*, Geological Society of London Special Publication 381, doi: 10.1144/SP381.13.
- Anderson, J.B., Conway, H., Bart, P.J., Witus, A.E., Greenwood, S.L., McKay, R.M., Hall, B.L., Ackert, R.P., Licht, K., Jakobsson, M., Stone, J.O., 2013b. Ross Sea paleo-ice sheet drainage and deglacial history during and since the LGM. *Quaternary Science Reviews*, doi: 10.1016/j.quascirev.2013.08.020.
- Arndt, J.E., Schenke, H.W., Jakobsson, M., Nitsche, F.-O., Buys, G., Goleby, B., Rebesco, M., Bohoyo, F., Hong, J.K., Black, J., Greku, R.K., Udintsev, G.B., Barrios, F., Reynoso-Peralta, W., Taisei, M., Wigley, R., 2013. The International Bathymetric Chart of the Southern Ocean Version 1.0 - A new bathymetric compilation covering circum-Antarctic waters. *Geophysical Research Letters* 40, 1-7.
- Assmann, K.M., Hellmer, H.H., Jacobs, S.S., 2005. Amundsen Sea ice production and transport. *Journal of Geophysical Research* 110, C12013, doi:10.1029/2004JC002797.
- Atkins, C.B., Barrett, P.J., Hicock, S.R., 2002. Cold glaciers erode and deposit: Evidence from Allan Hills, Antarctica. *Geology* 30, 659-662.

- Aylsworth, J.M., Shilts, W.W., 1989. Bedforms of the Keewatin Ice Sheet, Canada. *Sedimentary Geology* 62, 407-428.
- Bamber, J.L., Riva, R.E.M., Vermeersen, B.L.A., LeBrocq, A.M., 2009. Reassessment of the Potential Sea-Level Rise from a Collapse of the West Antarctic Ice Sheet. *Science* 324, 901-903.
- Barnes, P.W., Lien, R., 1988. Icebergs rework shelf sediments to 500 m off Antarctica. *Geology* 16, 1130-1133.
- Barnes, D.K.A., Hillenbrand, C.-D., 2010. Faunal evidence for a late quaternary trans-Antarctic seaway. *Global Change Biology* 16, 3297-3303.
- Barnes, D.K.A., Kuklinski, P., 2010. Bryozoans of the Weddell Sea continental shelf, slope and abyss: did marine life colonize the Antarctic shelf from deep water, outlying islands or in situ refugia following glaciations? *Journal of Biogeography*
- Bart, P.J., Cone, A.N., 2012. Early stall of West Antarctic Ice Sheet advance on the eastern Ross Sea middle shelf followed by retreat at 27,500 <sup>14</sup>C yrs BP. *Palaeogeography Palaeoclimatology Palaeoecology* 335-336, 52-60.
- Bart, P., Owolana, B., 2012. On the duration of West Antarctic ice sheet grounding events in Ross Sea during the Quaternary. *Quaternary Science Reviews* 47, 101-115.
- Beaman, R., Harris, P., 2003. Seafloor morphology and acoustic facies of the George V Land shelf. *Deep Sea Research Part II* 50, 1343-1355.
- Bennett, M.M., Glasser, N.F., 2009. *Glacial Geology: Ice Sheets and Landforms*, 2nd Edition. Wiley-Blackwell, Hoboken (USA), pp. 400.
- Bentley, M.J., Fogwill, C.J., Le Brocq, A.M., Hubbard, A.L., Sugden, D.E., Dunai, T.J., Freeman, S.P.H.T., 2010. Deglacial history of the West Antarctic Ice Sheet in the Weddell Sea embayment: Constraints on past ice volume change. *Geology* 38, 411-414.
- Bentley, M.J., Ó Cofaigh, C., Anderson, J.B., Conway, H., Davies, B., Graham, A.G.C., Hillenbrand, C.-D., Hodgson, D.A., Jamieson, S.S.R., Larter, R.D., Mackintosh, A., Smith, J.A., Verleyen, E., Ackert, R.P., Bart, P.J., Berg, S., Brunstein, D., Canals, M., Colhoun, E.A., Crosta, X., Dickens, W.A., Domack, E., Dowdeswell, J.A., Dunbar, R., Ehrmann, W., Evans, J., Favier, V., Fink, D., Fogwill, C.J., Glasser, N.F., Gohl, K., Golledge, N.R., Goodwin, I., Gore, D.B., Greenwood, S.L., Hall, B.L., Hall, K., Hedding, D.W., Hein, A.S., Hocking, E.P., Jakobsson, M., Johnson, J.S., Jomelli, V., Jones, R.S., Klages, J.P., Kristoffersen, Y., Kuhn, G., Leventer, A., Licht, K., Lilly, K., Lindow, J., Livingstone, S.J., Massé, G., McGlone, M.S., McKay, R.M., Melles, M., Miura, H., Mulvaney, R., Nel, W., Nitsche, F.O., O'Brien, P.E., Post, A.L., Roberts, S.J., Saunders, K.M., Selkirk, P.M., Simms, A.R., Spiegel, C., Stollendorf, T.D., Stone, J.O., Sugden, D.E., van der Putten, N., van Ommen, T., Verfaillie, D., Vyverman, W., Wagner, B., White, D.A., Witus, A.E., Zwartz, D., in press. A community-based reconstruction of Antarctic Ice Sheet deglaciation since the Last Glacial Maximum. *Quaternary Science Reviews*.

- Berkman, P.A., Forman, S.L., 1996. Pre-bomb radiocarbon and the reservoir correction for calcareous marine species in the Southern Ocean. *Geophysical Research Letters* 23, 363-366.
- Bluemle, J.P., Clayton, L.E.E., 1984. Large-scale glacial thrusting and related processes in North Dakota. *Boreas* 13, 279-299.
- Boulton, G.S., Van der Meer, J.J.M., Hart, J., Beets, D., Ruegg, G.J.H., Van der Wateren, F.M., Jarvis, J., 1996. Till and moraine emplacement in a deforming bed surge - an example from a marine environment. *Quaternary Science Reviews* 15, 961-987.
- Bouchard, M.A., 1989. Subglacial landforms and deposits in central and northern Quebec, Canada, with emphasis on Rogen moraines. *Sedimentary Geology* 62, 293-308.
- Bromwich, D.H., Nicolas, J.P., Monaghan, A.J., Lazzara, M.A., Keller, L.M., Weidner, G.A., Wilson, A.B., 2013. Central West Antarctica among the most rapidly warming regions on Earth. *Nature Geoscience* 6, 139-145.
- Carbotte, S.M., Ryan, W.B.F., O'Hara, S., Arko, R., Goodwillie, A., Melkonian, A., Weissel, R.A., and Ferrini, V.L., 2007. Antarctic Multibeam Bathymetry and Geophysical Data Synthesis: An On-Line Digital Data Resource for Marine Geoscience Research in the Southern Ocean. U.S. Geological Survey Open-File Report 2007, 1047 p., doi: 10.3133/of2007-1047.srp002.
- Caress, D.W., Chayes, D.N., 2003. MB-system, 5 ed. <http://www.ldeo.columbia.edu/pi/MB-System>, p. Open source software distributed from the MBARI and LDEO web sites.
- Clark, C.D., 1993. Mega-scale lineations and cross-cutting ice-flow landforms. *Earth Surface Processes and Landforms* 18, 1-29.
- Clark, C.D., 1999. Glaciodynamic context of subglacial bedform generation and preservation. *Annals of Glaciology* 28, 23-32.
- Clark, C.D., Meehan, R.T., 2001. Subglacial bedform geomorphology of the Irish Ice Sheet reveals major configuration changes during growth and decay. *Journal of Quaternary Science* 16, 483-496.
- Clark, C.D., Stokes, C.R., 2003. Palaeo-ice stream landsystem. In: Evans, D.J.A. (Ed.), *Glacial Landsystems*. Arnold, London, pp. 204-227.
- Clark, C.D., Tulaczyk, S.M., Stokes, C.R., Canals, M., 2003. A groove-ploughing theory for the production of mega-scale glacial lineations, and implication for ice stream mechanics. *Journal of Glaciology* 49, 240-256.
- Conway, H., Hall, B.L., Denton, G.H., Gades, A.M., Waddington, E.D., 1999. Past and Future Grounding-Line Retreat of the West Antarctic Ice Sheet. *Science* 286, 280-283.
- Denton, H.G., Hughes, T.J., 2002. Reconstructing the Antarctic Ice Sheet at the Last Glacial Maximum. *Quaternary Science Reviews* 21, 193-202.



- Deschamps, P., Durand, N., Bard, E., Hamelin, B., Camoin, G., Thomas, A., Henderson, G., Okuno, J., Yokoyama, Y., 2012. Ice sheet collapse and sea-level rise at the Bølling warming 14,600 yr ago. *Nature* 483, 559-564.
- Domack, E., O'Brien, P., Harris, P., Taylor, F., Quilty, P.G., De Santis, L., Raker, B., 1998. Late Quaternary sediment facies in Prydz Bay, East Antarctica and their relationship to glacial advance onto the continental shelf. *Antarctic Science* 10, 236-246.
- Domack, E., Jacobson, E.A., Shipp, S., Anderson, J.B., 1999. Late Pleistocene–Holocene retreat of the West Antarctic Ice-Sheet system in the Ross Sea: Part 2—Sedimentologic and stratigraphic signature. *Geological Society of America Bulletin* 111, 1517-1536.
- Domack, E.W., Duran, D., Leventer, A., Ishman, S., Doane, S., McCallum, S., Amblas, D., Ring, J., Gilbert, R., Prentice, M., 2005. Stability of the Larsen B ice shelf on the Antarctic Peninsula during the Holocene epoch. *Nature* 436, 681–685.
- Dowdeswell, J.A., Ó Cofaigh, C., Pudsey, C.J., 2004. Thickness and extent of the subglacial till layer beneath an Antarctic paleo-ice stream. *Geology* 32, 13-16.
- Dowdeswell, J.A., Bamber, J.L., 2007. Keel depths of modern Antarctic icebergs and implications for sea-floor scouring in the geological record. *Marine Geology* 243, 120-131.
- Dowdeswell, J.A., Fugelli, E.M.G., 2012. The seismic architecture and geometry of grounding-zone wedges formed at the marine margins of past ice sheets. *Geological Society of America Bulletin* 124, 1750-1761.
- Dunlop, P., Clark, C.D., 2006. The morphological characteristics of ribbed moraine. *Quaternary Science Reviews* 25, 1668-1691.
- Dunlop, P., Clark, C.D., Hindmarsh, R.C.A., 2008. Bed Ribbing Instability Explanation: Testing a numerical model of ribbed moraine formation arising from coupled flow of ice and subglacial sediment. *Journal of Geophysical Research* 113, F03005.
- Dupont, T.K., Alley, R.B., 2005. Assessment of the importance of ice-shelf buttressing to ice-sheet flow. *Geophysical Research Letters* 32, L04503. doi:10.1029/2004GL022024.
- Dutrieux, P., Vaughan, D.G., Corr, H.F.J., Jenkins, A., Holland, P.R., Joughin, I., Fleming, A.H., 2013. Pine Island glacier ice shelf melt distributed at kilometre scales. *The Cryosphere* 7, 1543-1555.
- Dutrieux, P., De Rydt, J., Jenkins, A., Holland, P.R., Kyung Ha, H., Hoon Lee, S., Steig, E.J., Ding, Q., Abrahamsen, E.P., Schröder, M., 2014. Strong Sensitivity of Pine Island Ice-Shelf Melting to Climatic Variability. *Science* 343, 174-178.
- Ehrmann, W., Hillenbrand, C.-D., Smith, J.A., Graham, A.G.C., Kuhn, G., Larter, R.D., 2011. Provenance changes between recent and glacial-time sediments in the Amundsen Sea embayment, West Antarctica: clay mineral assemblage evidence. *Antarctic Science* 23, 471-486.

- Engelhardt, H.F., Kamb, B., 1998. Sliding velocity of Ice Stream B. *Journal of Glaciology* 43, 207-230.
- Evans, D.J.A., Rea, B.R., 1999. Geomorphology and sedimentology of surging glaciers: a land-systems approach. *Annals of Glaciology* 28, 75-82.
- Evans, J., Pudsey, C.J., 2002. Sedimentation associated with Antarctic Peninsula ice shelves: implications for palaeoenvironmental reconstructions of glacial marine sediments. *Journal of the Geological Society, London* 159, 233-237.
- Evans, J., Pudsey, C.J., Ó Cofaigh, C., Morris, P., Domack, E., 2005. Late Quaternary glacial history, flow dynamics and sedimentation along the eastern margin of the Antarctic Peninsula Ice Sheet. *Quaternary Science Reviews* 24, 741-774.
- Evans, J., Dowdeswell, J.A., Ó Cofaigh, C., Benham, T.J., Anderson, J.B., 2006. Extent and dynamics of the West Antarctic Ice Sheet on the outer continental shelf of Pine Island Bay during the last glaciation. *Marine Geology* 230, 53-72.
- Evans, J., Ó Cofaigh, C., Dowdeswell, J.A., Wadhams, P., 2009. Marine geophysical evidence for former expansion and flow of the Greenland Ice Sheet across the north-east Greenland continental shelf. *Journal of Quaternary Science* 23, 279-293.
- Favier, L., Durand, G., Cornford, S.L., Gudmundsson, G.H., Gagliardini, O., Gillet-Chaulet, F., Zwinger, T., Payne, A.J., Le Brocq, A.M., 2014. Retreat of Pine Island Glacier controlled by marine ice-sheet instability. *Nature Climate Change*, doi:10.1038/nclimate2094.
- Fowler, A.C., 2010. The formation of subglacial streams and mega-scale glacial lineations. *Proceedings of the Royal Society A: Mathematical, Physical & Engineering Science* 466, 3181-3201.
- Freudenthal, T., Wefer, G., 2007. Scientific Drilling with the Sea Floor Drill Rig MeBo. *Scientific Drilling* 5, 63-66.
- Fricker, H.A., Scambos, T., 2009. Connected subglacial lake activity on lower Mercer and Whillans Ice Streams, West Antarctica, 2003-2008. *Journal of Glaciology* 55, 303-315.
- Gladstone, R.M., Lee, V., Rougier, J., Payne, A.J., Hellmer, H., Le Brocq, A., Shepherd, A., Edwards, T.L., Gregory, J., Cornford, S.L., 2012. Calibrated prediction of Pine Island Glacier retreat during the 21<sup>st</sup> and 22<sup>nd</sup> centuries with a coupled flowline model. *Earth and Planetary Science Letters* 333-334, 191-199.
- Gohl, K., 2007. The expedition ANT-XXIII/4 of the Research Vessel Polarstern in 2006, *Berichte zur Polar- und Meeresforschung (Reports on Polar and Marine Research)*, 557, 166 pp, <http://epic.awi.de/26756/>.
- Gohl, K., 2010. The expedition of the Research Vessel "Polarstern" to the Amundsen Sea, Antarctica, in 2010 (ANT-XXVI/3), *Berichte zur Polar- und Meeresforschung (Reports on Polar and Marine Research)*, 617, 173pp.
- Gohl, K., Uenzelmann-Neben, G., Larter, R.D., Hillenbrand, C.-D., Hochmuth, K., Kalberg, T., Weigelt, E., Davy, B., Kuhn, G., Nitsche, F.O., 2013. Seismic stratigraphic record of the

Amundsen Sea Embayment shelf from pre-glacial to recent times: Evidence for a dynamic West Antarctic Ice Sheet. *Marine Geology* 344, 115-131.

Golledge, N.R., Levy, R.H., McKay, R.M., Fogwill, C.J., White, D.A., Graham, A.G.C., Smith, J.A., Hillenbrand, C.-D., Licht, K.J., Denton, G.H., Ackert Jr., R.P., Maas, S.M., Hall, B.L., 2013. Glaciology and geological signature of the Last Glacial Maximum Antarctic ice sheet. *Quaternary Science Reviews* 78, 225-247.

Graham, A.G.C., Larter, R.D., Gohl, K., Hillenbrand, C.D., Smith, J.A., Kuhn, G., 2009. Bed-form signature of a West Antarctic palaeo-ice stream reveals a multi-temporal record of flow and substrate control. *Quaternary Science Reviews* 28, 2774-2793.

Graham, A.G.C., Larter, R.D., Gohl, K., Dowdeswell, J.A., Hillenbrand, C.-D., Smith, J.A., Evans, J., Kuhn, G., Deen, T., 2010. Flow and retreat of the Late Quaternary Pine Island-Thwaites palaeo-ice stream, West Antarctica. *Journal of Geophysical Research* 115.

Graham, A. G. C., Nitsche, F. O., Larter, R. D., 2011. An improved bathymetry compilation for the Bellingshausen Sea, Antarctica, to inform ice-sheet and ocean models. *The Cryosphere* 5, 95-106.

Graham, A.G.C., Smith, J.A., 2012. Palaeoglaciology of the Alexander Island ice cap, western Antarctic Peninsula, reconstructed from marine geophysical and core data. *Quaternary Science Reviews* 35, 63-81.

Graham, A.G.C., Dutrieux, P., Vaughan, D.G., Nitsche, F.O., Gyllencreutz, R., Greenwood, S.L., Larter, R.D., Jenkins, A., 2013. Sea-bed corrugations beneath an Antarctic ice shelf revealed by autonomous underwater vehicle survey: origin and implications for the history of Pine Island Glacier. *Journal of Geophysical Research* 118.

Greenwood, S.L., Kleman, J., 2010. Glacial landforms of extreme size in the Keewatin sector of the Laurentide Ice Sheet. *Quaternary Science Reviews* 29, 1894-1910.

Gudmundsson, G.H., Krug, J., Durand, G., Favier, L., Gagliardini, O., 2012. The stability of grounding lines on retrograde slopes. *The Cryosphere* 6, 1497-1505.

Hättestrand, C., 1997. Ribbed moraines in Sweden - distribution pattern and palaeoglaciological implications. *Sedimentary Geology* 111, 41-56.

Hein, A.S., Fogwill, C.J., Sugden, D.E., Xu, S., 2011. Glacial/interglacial ice-stream stability in the Weddell Sea embayment, Antarctica. *Earth and Planetary Science Letters* 307, 211-221.

Heroy, D.C., Anderson, J.B., 2005. Ice-sheet extent of the Antarctic Peninsula region during the Last Glacial Maximum (LGM)—Insights from glacial geomorphology. *Geological Society of America Bulletin* 117, 1497.

Hillenbrand, C.-D., Baesler, A., Grobe, H., 2005. The sedimentary record of the last glaciation in the western Bellingshausen Sea (West Antarctica): Implications for the interpretation of diamictos in a polar-marine setting. *Marine Geology* 216, 191-204.

- Hillenbrand, C.-D., Larter, R.D., Dowdeswell, J.A., Ehrmann, W., Ó Cofaigh, C., Benetti, S., Graham, A.G.C., Grobe, H., 2010. The sedimentary legacy of a palaeo-ice stream on the shelf of the southern Bellingshausen Sea: Clues to West Antarctic glacial history during the Late Quaternary. *Quaternary Science Reviews* 29, 2741-2763.
- Hillenbrand, C.-D., Melles, M., Kuhn, G., Larter, R.D., 2012. Marine geological constraints for the grounding-line position of the Antarctic Ice Sheet on the southern Weddell Sea shelf at the Last Glacial Maximum. *Quaternary Science Reviews* 32, 25-47.
- Hillenbrand, C.-D., Kuhn, G., Smith, J.A., Gohl, K., Graham, A.G.C., Larter, R.D., Klages, J.P., Downey, R., Moreton, S.G., Forwick, M., Vaughan, D.G., 2013. Grounding-line retreat of the West Antarctic Ice Sheet from inner Pine Island Bay. *Geology* 41, 35-38.
- Hochmuth, K., Gohl, K., 2013. Glacio-marine sedimentation dynamics of the Abbot glacial trough of the Amundsen Sea Embayment shelf, West Antarctica. Geological Society, London, Special Publications 381.
- Hogan, K.A., Dowdeswell, J.A., Noormets, R., Evans, J., Ó Cofaigh, C., 2010. Evidence for full-glacial flow and retreat of the Late Weichselian Ice Sheet from the waters around Kong Karls Land, eastern Svalbard. *Quaternary Science Reviews* 29, 3563-3582.
- Holland, P.R., Jenkins, A., Holland, D.M., 2008. The response of ice shelf basal melting to variation in ocean temperature. *Journal of Climate* 21, 2558-2572.
- Hughes T., 1981. The weak underbelly of the West Antarctic Ice Sheet. *Journal of Glaciology* 27, 518-525.
- Hulbe, C.L., MacAyeal, D.R., 1999. A new numerical model of coupled inland ice sheet, ice stream, and ice shelf flow and its application to the West Antarctic Ice Sheet. *Journal of Geophysical Research* 104, 25349-25366.
- Intergovernmental Panel On Climate Change (IPCC), 2013. Climate Change 2013 – The Physical Science Basis. Draft Version, June 2013, <http://www.climatechange2013.org/>.
- Jacobs, S.S., Hellmer, H.H., Jenkins, A., 1996. Antarctic ice sheet melting in the Southeast Pacific. *Geophysical Research Letters* 23, 957-960.
- Jacobs, S.S., Jenkins, A., Giulivi, C.F., Dutrieux, P., 2011. Stronger ocean circulation and increased melting under Pine Island Glacier ice shelf. *Nature Geoscience* 4, 519-523.
- Jakobsson, M., Anderson, J.B., Nitsche, F.O., Dowdeswell, J.A., Gyllencreutz, R., Kirchner, N., Mohammad, R., O'Regan, M., Alley, R.B., Anandakrishnan, S., Eriksson, B., Kirshner, A., Fernandez, R., Stollendorf, T., Minzoni, R., Majewski, W., 2011. Geological record of ice shelf break-up and grounding line retreat, Pine Island Bay, West Antarctica. *Geology* 39, 691-694.
- Jakobsson, M., Anderson, J.B., Nitsche, F.O., Gyllencreutz, R., Kirshner, A.E., Kirchner, N., O'Regan, M., Mohammad, R., Eriksson, B., 2012. Ice sheet retreat dynamics inferred from glacial morphology of the central Pine Island Bay Trough, West Antarctica. *Quaternary Science Reviews* 38, 1-10.

- Jamieson, S.S.R., Vieli, A., Livingstone, S.J., Ó Cofaigh, C., Stokes, C.R., Hillenbrand, C.-D., Dowdeswell, J.A., 2012. Ice-stream stability on a reverse bed slope. *Nature Geoscience* 5(11), 799–802.
- Jamieson, S.S.R., Vieli, A., Stokes, C.R., Ó Cofaigh, C., Livingstone, S.J., Hillenbrand, C.-D., in press. Understanding controls on rapid ice-stream retreat during the last deglaciation of Marguerite Bay, Antarctica, using a numerical model. *Journal of Geophysical Research, Earth Surface*.
- Jenkins, A., Dutrieux, P., Jacobs, S.S., McPhail, S.D., Perrett, J.R., Webb, A.T., White, D., 2010. Observations beneath Pine Island Glacier in West Antarctica and implications for its retreat. *Nature Geoscience* 3, 468-472.
- Joughin, I., Smith, B. E., Holland, D. M., 2010. Sensitivity of 21st century sea level to ocean-induced thinning of Pine Island Glacier, Antarctica. *Geophysical Research Letters* 37, L20502, doi:10.1029/2010GL044819.
- Joughin, I., Alley, R.B., 2011. Stability of the West Antarctic ice sheet in a warming world. *Nature Geoscience* 4, 506-513.
- Katz, R.F., Worster, M.G., 2010. Stability of ice-sheet grounding lines. *Proceedings of the Royal Society A: Mathematical, Physical and Engineering Science*.
- Kellogg, D.E., Kellogg, T.B., 1987a. Microfossil distributions in modern Amundsen Sea sediments. *Marine Micropaleontology* 12, 203-222.
- Kellogg, T.B., Kellogg, D.E., 1987b. Late Quaternary deglaciation of the Amundsen Sea: implications for ice sheet modelling. *Physical Basis of Ice Sheet Modelling, Proceedings of the Vancouver Symposium, Vancouver*, pp. 349-357.
- King, E.C., Hindmarsh, R.C.A., Stokes, C.R., 2009. Formation of mega-scale glacial lineations observed beneath a West Antarctic ice stream. *Nature Geoscience* 2, 585-588.
- Kirshner, A.E., Anderson, J.B., Jakobsson, M., O'Regan, M., Majewski, W., Nitsche, F.O., 2012. Post-LGM deglaciation in Pine Island Bay, West Antarctica. *Quaternary Science Reviews* 38, 11-26.
- Klages, J.P., Kuhn, G., Hillenbrand, C.-D., Graham, A.G.C., Smith, J.A., Larter, R.D., Gohl, K., 2013. First geomorphological record and glacial history of an inter-ice stream ridge on the West Antarctic continental shelf. *Quaternary Science Reviews* 61, 47-61.
- Klages, J.P., Kuhn, G., Hillenbrand, C.-D., Graham, A.G.C., Smith, J.A., Larter, R.D., Gohl, K., Wacker, L., in review. Retreat of the West Antarctic Ice Sheet from the western Amundsen Sea shelf at a pre- or early LGM stage. *Quaternary Science Reviews*.
- Larter, R.D., Vanneste, L.E., 1995. Relict subglacial deltas on the Antarctic Peninsula outer shelf. *Geology* 23, 33–36.



- Larter, R.D., Graham, A.G.C., Gohl, K., Kuhn, G., Hillenbrand, C.-D., Smith, J.A., Deen, T.J., Livermore, R.A., Schenke, H.-W., 2009. Subglacial bedforms reveal complex basal regime in a zone of paleo-ice stream convergence, Amundsen Sea Embayment, West Antarctica. *Geology* 37, 411-414.
- Larter, R.D., Graham, A.G.C., Hillenbrand, C.-D., Smith, J.A., Gales, J.A., 2012. Late Quaternary grounded ice extent in the Filchner Trough, Weddell Sea, Antarctica: new marine geophysical evidence. *Quaternary Science Reviews* 53, 111-122.
- Larter, R.D., Anderson, J.B., Graham, A.G.C., Gohl, K., Hillenbrand, C.D., Jakobsson, M., Johnson, J.S., Kuhn, G., Nitsche, F.O., Smith, J.A., Witus, A.E., Bentley, M.J., Dowdeswell, J.A., Ehrmann, W., Klages, J.P., Lindow, J., Ó Cofaigh, C., Spiegel, C., 2013. Reconstruction of changes in the Amundsen Sea and Bellingshausen Sea sector of the West Antarctic Ice Sheet since the Last Glacial Maximum. *Quaternary Science Reviews*, <http://dx.doi.org/10.1016/j.quascirev.2013.10.016>.
- Licht, K.J., Jennings, A.E., Andrews, J.T., Williams, K.M., 1996. Chronology of late Wisconsin ice retreat from the western Ross Sea, Antarctica. *Geology* 24, 223-226.
- Licht, K.J., Dunbar, N.W., Andrews, J.T., Jennings, A.E., 1999. Distinguishing subglacial till and glacial marine diamictos in the western Ross Sea, Antarctica: Implications for a last glacial maximum grounding line. *Geological Society of America Bulletin* 111, 91-103.
- Lien, R., Solheim, A., Elverhøi, A., Rokoengen, K., 1989. Iceberg scouring and sea bed morphology on the eastern Weddell Sea shelf, Antarctica. *Polar Research* 7, 43-57.
- Livingstone, S.J., Ó Cofaigh, C., Stokes, C.R., Hillenbrand, C.-D., Vieli, A., Jamieson, S.S.R., 2012. Antarctic palaeo-ice streams. *Earth-Science Reviews* 111, 90-128.
- Livingstone, S.J., Ó Cofaigh, C., Stokes, C.R., Hillenbrand, C.-D., Vieli, A., Jamieson, S.S.R., 2013. Glacial Geomorphology of Marguerite Bay Palaeo-Ice Stream, western Antarctic Peninsula. *Journal of Maps* 9(4), 558-572.
- Lowe, A.L., Anderson, J.B., 2002. Reconstruction of the West Antarctic ice sheet in Pine Island Bay during the Last Glacial Maximum and its subsequent retreat history. *Quaternary Science Reviews* 21, 1879-1897.
- Lowe, A.L., Anderson, J.B., 2003. Evidence for abundant subglacial meltwater beneath the paleo-ice sheet in Pine Island Bay, Antarctica. *Journal of Glaciology* 49, 125-138.
- Lundqvist, J., 1997. Rogen moraine - an example of two-step formation of glacial landscapes. *Sedimentary Geology* 111, 27-40.
- Marich, A., Batterson, M., Bell, T., 2005. The morphology and sedimentological analyses of Rogen moraines, Central Avalon Peninsula, Newfoundland, Current Research. Geological Survey, Newfoundland and Labrador Department of Natural Resources, pp. 1-14.
- McKay, R., Browne, G., Carter, L., Cowan, E., Dunbar, G., Krissek, L., Naish, T., Powell, R., Reed, J., Talarico, F., Wilch, T., 2009. The stratigraphic signature of the late Cenozoic Ant-

arctic ice sheets in the Ross Embayment. *Geological Society of America Bulletin* 121, 1537–1561.

McMullen, K., Domack, E., Leventer, A., Olson, C., Dunbar, R., Brachfeld, S., 2006. Glacial morphology and sediment formation in the Mertz Trough, East Antarctica. *Palaeogeography, Palaeoclimatology, Palaeoecology* 231, 169–180.

Meer van der, J.J.M., Menzies, J., Rose, J., 2003. Subglacial till: the deforming glacier bed. *Quaternary Science Reviews* 22, 1659-1685.

Melles, M., Kuhn, G., 1993. Subbottom profiling and sedimentological studies in the southern Weddell Sea, Antarctica - evidence for large-scale erosional depositional processes. *Deep-Sea Research Part I-Oceanographic Research Papers* 40, 739-760.

Miller, H., Grobe, H., 1996. Die Expedition ANTARKTIS-XI/3 mit FS "Polarstern" 1994 = The expedition ANTARKTIS-XI/3 of RV "Polarstern" in 1994. *Berichte zur Polarforschung (Reports on Polar Research)*, Bremerhaven, Alfred Wegener Institute for Polar and Marine Research 188, 115 pp, <http://epic.awi.de/26366/>.

Möller, P., 2010. Melt-out till and ribbed moraine formation, a case study from south Sweden. *Sedimentary Geology* 232, 161-180.

Moran, S.R., Clayton, L., Hooke, R.L., Fenton, M.M., Andriashek, L.D., 1980. Glacierbed landforms of the prairie region of North America. *Journal of Glaciology* 25, 457-476.

Mosola, A.B., Anderson, J.B., 2006. Expansion and rapid retreat of the West Antarctic Ice Sheet in eastern Ross Sea: possible consequence of over-extended ice streams? *Quaternary Science Reviews* 25, 2177-2196.

Nakayama, Y., Schröder, M., Hellmer, H.H., 2013. From circumpolar deep water to the glacial meltwater plume on the eastern Amundsen Shelf. *Deep Sea Research Part I: Oceanographic Research Papers* 77, 50-62.

Nitsche, F.O., Jacobs, S.S., Larter, R.D., Gohl, K., 2007. Bathymetry of the Amundsen Sea continental shelf: Implications for geology, oceanography, and glaciology. *Geochem. Geophys. Geosyst.* 8, Q10009, doi:10.1029/2007GC001694.

Nitsche, F.O., Gohl, K., Larter, R.D., Hillenbrand, C.-D., Kuhn, G., Smith, J.A., Jacobs, S., Anderson, J.B., Jakobsson, M., 2013. Paleo ice flow and subglacial meltwater dynamics in Pine Island Bay, West Antarctica. *Cryosphere* 7, 249-262.

O'Brien, P.E., De Santis, L., Harris, P.T., Domack, E., Quilty, P.G., 1999. Ice shelf grounding zone features of western Prydz Bay, Antarctica: sedimentary processes from seismic and sidescan images. *Antarctic Science* 11, 78-91.

Ó Cofaigh, C., Pudsey, C.J., Dowdeswell, J.A., Morris, P., 2002. Evolution of subglacial bedforms along a paleo-ice stream, Antarctic Peninsula continental shelf. *Geophysical Research Letters* 29, 1-4.

- Ó Cofaigh, C., Dowdeswell, J.A., Allen, C.S., Hiemstra, J.F., Pudsey, C.J., Evans, J., Evans, D., 2005. Flow dynamics and till genesis associated with a marine-based Antarctic palaeo-ice stream. *Quaternary Science Reviews* 24, 709-740.
- Ó Cofaigh, C., Evans, J., Dowdeswell, J.A., Larter, R.D., 2007. Till characteristics, genesis and transport beneath Antarctic paleo-ice streams. *Journal of Geophysical Research* 112, doi:10.1029/2006JF000606.
- Ottesen, D., Dowdeswell, J.A., Rise, L., 2005. Submarine landforms and the reconstruction of fast-flowing ice streams within a large Quaternary ice sheet: the 2500-km-long Norwegian-Svalbard margin (57°-80° N). *Geological Society of America Bulletin* 117, 1033-1050.
- Ottesen, D., Dowdeswell, J.A., 2006. Assemblages of submarine landforms produced by tidewater glaciers in Svalbard. *Journal of Geophysical Research* 111, doi:10.1029/2005JF000330.
- Ottesen, D., Dowdeswell, J.A., Benn, D.I., Kristensen, L., Christiansen, H.H., Christensen, O., Hansen, L., Lebesbye, E., Forwick, M., Vorren, T.O., 2008. Submarine landforms characteristic of glacier surges in two Spitsbergen fjords. *Quaternary Science Reviews* 27, 1583-1599.
- Ottesen, D., Dowdeswell, J.A., 2009. An inter-ice-stream glaciated margin: Submarine landforms and a geomorphic model based on marine-geophysical data from Svalbard. *Geological Society of America Bulletin* 121, 1647-1665.
- Plassen, L., Vorren, T.O., Forwick, M., 2004. Integrated acoustic and coring investigation of glacial deposits in Spitsbergen fjords. *Polar Research* 23, 89-110.
- Pritchard, H.D., Arthern, R.J., Vaughan, D.G., Edwards, L.A., 2009. Extensive dynamic thinning on the margins of the Greenland and Antarctic ice sheets. *Nature* 461, 971-975.
- Pritchard, H.D., Luthcke, S.B., Fleming, A.H., 2011. Understanding ice-sheet mass balance: progress in satellite altimetry and gravimetry. *Journal of Glaciology* 56, 1151-1161.
- Pritchard, H.D., Ligtenberg, S.R.M., Fricker, H.A., Vaughan, D.G., van den Broeke, M.R., Padman, L., 2012. Antarctic ice-sheet loss driven by basal melting of ice shelves. *Nature* 484, 502-505.
- Pudsey, C.J., Evans, J., 2001. First survey of Antarctic sub-ice shelf sediments reveals mid-Holocene ice shelf retreat. *Geology* 29, 787-790.
- Putnam, A.E., Denton, G.H., Schaefer, J.M., Barrell, D.J.A., Andersen, B.G., Finkel, R.C., Schwartz, R., Doughty, A.M., Kaplan, M.R., Schluchter, C., 2010. Glacier advance in southern middle-latitudes during the Antarctic Cold Reversal. *Nature Geoscience* 3, 700-704.
- Raymond, C.F., Echelmeyer, K.A., Whillans, I.M., Doake, C.S.M., 2001. Ice stream shear margins. In: *The West Antarctic Ice Sheet: Behaviour and Environment*. Antarctic Research Series 77, Alley, R.B., Bindshadler, R.A. (eds), American Geophysical Union, Washington, DC, 137-155.

- Rebesco, M., Liu, Y., Camerlenghi, A., Winsborrow, M., Laberg, J.S., Caburlotto, A., Diviacco, P., Accettella, D., Sauli, C., Wardell, N., Tomini, I., 2011. Deglaciation of the western margin of the Barents Sea Ice Sheet - A swath bathymetric and sub-bottom seismic study from the Kveitola Trough. *Marine Geology* 279, 141-147.
- Reimer, P.J., Baillie, M.G.L., Bard, E., Bayliss, A., Beck, J.W., Blackwell, P.G., Bronk Ramsey, C., Buck, C.E., Burr, G.S., Edwards, R.L., Friedrich, M., Grootes, P.M., Guilderson, T.P., Hajdas, I., Heaton, T.J., Hogg, A.G., Hughen, K.A., Kaiser, K.F., Kromer, B., McCormac, F.G., Manning, S.W., Reimer, R.W., Richards, D.A., Southon, J.R., Talamo, S., Turney, C.S.M., van der Plicht, J., Weyhenmeyer, C.E., 2009. IntCal09 and Marine09 radiocarbon age calibration curves, 0–50,000 years cal BP. *Radiocarbon* 51(4), 1111–1150.
- Reinardy, B.T.I., Hiemstra, J.F., Murray, T., Hillenbrand, C.-D., Larter, R.D., 2011a. Till genesis at the bed of an Antarctic Peninsula palaeo-ice stream as indicated by micromorphological analysis. *Boreas* 40, 498-517.
- Reinardy, B.T.I., Larter, R.D., Hillenbrand, C.-D., Murray, T., Hiemstra, J.F., Booth, A., 2011b. Streaming flow of an Antarctic Peninsula palaeo-ice stream, both by basal sliding and deformation of substrate. *Journal of Glaciology* 57, 1-13.
- Rignot, E., 1998. Fast Recession of a West Antarctic Glacier. *Science* 281, 549-551.
- Rignot, E., Jacobs, S.S., 2002. Rapid Bottom Melting Widespread near Antarctic Ice Sheet Grounding Lines. *Science* 296, 2020-2023.
- Rignot, E., Bamber, J.L., van den Broeke, M.R., Davis, C., Li, Y., van de Berg, W.J., van Meijgaard, E., 2008. Recent Antarctic ice mass loss from radar interferometry and regional climate modelling. *Nature Geoscience* 1, 106-110.
- Rignot, E., Velicogna, I., van den Broeke, M. R., Monaghan, A., Lenaerts, J. T. M., 2011. Acceleration of the contribution of the Greenland and Antarctic ice sheets to sea level rise. *Geophysical Research Letters* 38, L05503, doi:10.1029/2011GL046583.
- Rignot, E., Jacobs, S., Mouginot, J., Scheuchl, B., 2013. Ice-Shelf Melting Around Antarctica. *Science* 19, 266-270.
- Scambos, T.A., Bohlander, J.A., Shuman, C.A., Skvarca, P., 2004. Glacier acceleration and thinning after ice shelf collapse in the Larsen B embayment, Antarctica. *Geophysical Research Letters* 31, L18402, doi:10.1029/2004GL020670.
- Schoof, C., 2007. Ice sheet grounding line dynamics: Steady states, stability, and hysteresis. *Journal of Geophysical Research: Earth Surface* 112, doi:10.1029/2006JF000664.
- Shakun, J., Clark, P., He, F., Marcott, S., Mix, A., Liu, Z., Otto-Bliesner, B., Schmittner, A., Bard, E., 2012. Global warming preceded by increasing carbon dioxide concentrations during the last deglaciation. *Nature* 484, 49–54.
- Shepherd, A., 2004. Warm ocean is eroding West Antarctic Ice Sheet. *Geophysical Research Letters* 31.

- Shipp, S., Anderson, J.B., Domack, E.W., 1999. Late Pleistocene- Holocene retreat of the West Antarctic ice-sheet system in the Ross Sea; Part 1, Geophysical results. *Geological Society of America Bulletin* 111, 1468-1516.
- Smith, A.M., Murray, T., Nicholls, K.W., Makinson, K., Adalgeirsdottir, G., Behar, A.E., Vaughan, D.G., 2007. Rapid erosion, drumlin formation, and changing hydrology beneath an Antarctic ice stream. *Geology* 35, 127–130.
- Smith, A.M., Murray, T., 2009. Bedform topography and basal conditions beneath a fast-flowing West Antarctic ice stream. *Quaternary Science Reviews* 28, 584-596.
- Smith, J.A., Hillenbrand, C.-D., Larter, R.D., Graham, A.G.C., Kuhn, G., 2009. The sediment infill of subglacial meltwater channels on the West Antarctic continental shelf. *Quaternary Research* 71, 190-200.
- Smith, J.A., Hillenbrand, C.-D., Kuhn, G., Larter, R.D., Graham, A.G.C., Ehrmann, W., Moreton, S.G., Forwick, M., 2011. Deglacial history of the West Antarctic Ice Sheet in the western Amundsen Sea Embayment. *Quaternary Science Reviews* 30, 488-505.
- Smith, J.A., Hillenbrand, C.-D., Kuhn, G., Klages, J.P., Graham, A.G.C., Larter, R.D., Ehrmann, W., Moreton, S.G., Wiers, S., submitted. New constraints on the timing of West Antarctic Ice Sheet retreat in the eastern Amundsen Sea since the Last Glacial Maximum. *Quaternary Science Reviews*.
- Stokes, C.R., Clark, C.D., 2001. Palaeo-ice streams. *Quaternary Science Reviews* 20, 1437-1457.
- Stokes, C.R., Clark, C.D., 2002. Are long subglacial bedforms indicative of fast ice flow?. *Boreas* 31, 239–249.
- Stokes, C.R., Clark, C.D., Lian, O.B., Tulaczyk, S., 2007. Ice stream sticky spots: A review of their identification and influence beneath contemporary and palaeo-ice streams. *Earth Science Reviews* 81, 217-249.
- Stokes, C.R., Lian, O.B., Tulaczyk, S., Clark, C.D., 2008. Superimposition of ribbed moraines on a palaeo-ice stream: implications for ice stream shutdown. *Earth Surface Processes and Landforms* 33, 593-609.
- Tinto, K.J., Bell, R.E., 2011. Progressive unpinning of Thwaites Glacier from newly identified offshore ridge: Constraints from aerogravity. *Geophys. Res. Lett.*, 38, L20503, doi:10.1029/2011GL049026.
- Todd, B.J., Valentine, P.C., Longva, O., Shaw, J., 2007. Glacial landforms on German Bank, Scotian Shelf: evidence for late Wisconsinan ice-sheet dynamics and implications for the formation of De Geer moraines. *Boreas* 36, 148–169.
- Tschumi, T., Joos, F., Gehlen, M., Heinze, C., 2011. Deep ocean ventilation, carbon isotopes, marine sedimentation and the deglacial CO<sub>2</sub> rise. *Climate of the Past* 7, 771-800.



Uenzelmann-Neben, G., Gohl, K., Larter, R.D., Schlüter, P., 2007. Differences in Ice Retreat across Pine Island Bay, West Antarctica, since the Last Glacial Maximum: Indications from Multichannel Seismic Reflection Data. U.S. Geological Survey and The National Academies. USGS OF-2007-1047, Short Research Paper 084, <http://dx.doi.org/10.3133/of2007-1047.srp084>.

Vanneste, L.E., Larter, R.D., 1995. Deep-tow boomer survey on the Antarctic Peninsula Pacific margin: an investigation of the morphology and acoustic characteristics of the late Quaternary sedimentary deposits on the outer continental shelf and upper slope. In: Cooper, A.K., Barker, P.F., Brancolini, G. (Eds.), *Geology and Seismic Stratigraphy of the Antarctic Margin*. Antarctic Research Series, vol. 68, American Geophysical Union, Washington D.C., pp. 97-121.

Vaughan, D.G., Arthern, R., 2007. Why is it hard to predict the future of ice sheets?. *Science* 315, 1503–1504.

Vaughan, D.G., 2008. West Antarctic Ice Sheet collapse – the fall and rise of a paradigm. *Climatic Change* 91, 65-79.

Wacker, L., Bonani, G., Friedrich, M., Hajdas, I., Kromer, B., Němec, M., Ruff, M., Suter, M., Synal, H.-A., Vockenhuber, C., 2010. MICADAS: routine and high-precision radiocarbon dating. *Radiocarbon* 52, 252–262.

Wåhlin, A.K., Yuan, X., Bjork, G., Nohr, C., 2010. Inflow of Warm Circumpolar Deep Water in the Central Amundsen Shelf. *Journal of Physical Oceanography* 40, 1427-1434.

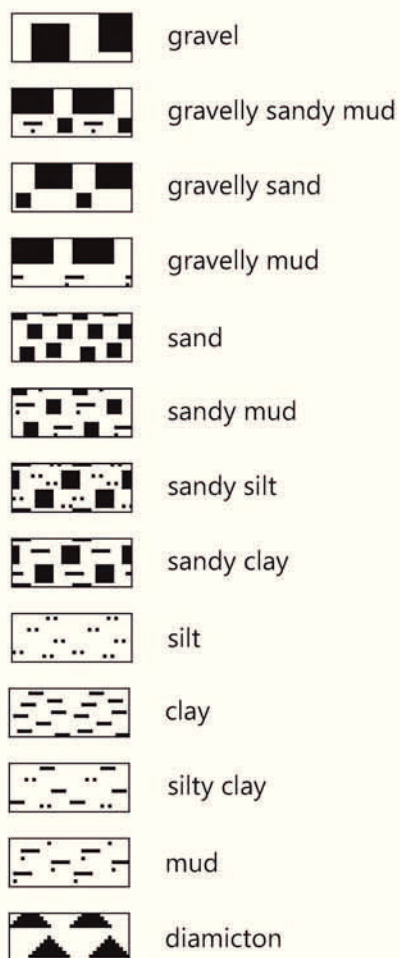
Weber, M.E., Clark, P.U., Ricken, W., Mitrovica, J.X., Hostetler, S.W., Kuhn, G., 2011. Interhemispheric Ice-Sheet Synchronicity During the Last Glacial Maximum. *Science* 334, 1265-1269.

Winkelmann, D., Jokat, W., Jensen, L., Schenke, H.-W., 2010. Submarine end moraines on the continental shelf off NE Greenland: Implications for Lateglacial dynamics. *Quaternary Science Reviews* 29, 1069-1077.

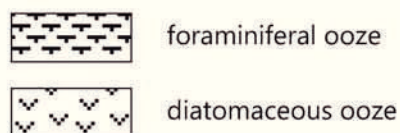
Witus, A.E., Branecky, C.M., Anderson, J.B., Szczuciński, W., Schroeder, D.M., Blankenship, D.D., Jakobsson, M., 2014. Meltwater intensive glacial retreat in polar environments and investigation of associated sediments: example from Pine Island Bay, West Antarctica. *Quaternary Science Reviews* 85, 99-118.

# Appendix 1a - Key for core descriptions

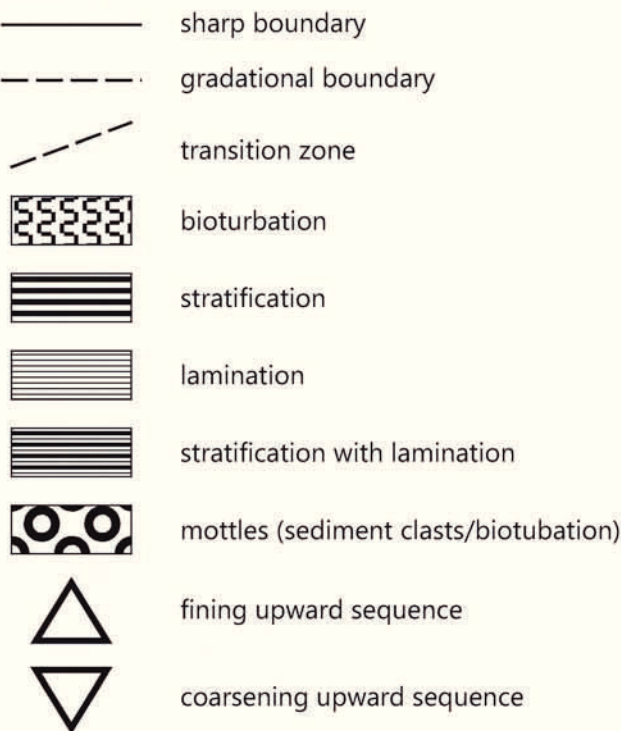
## Lithology:



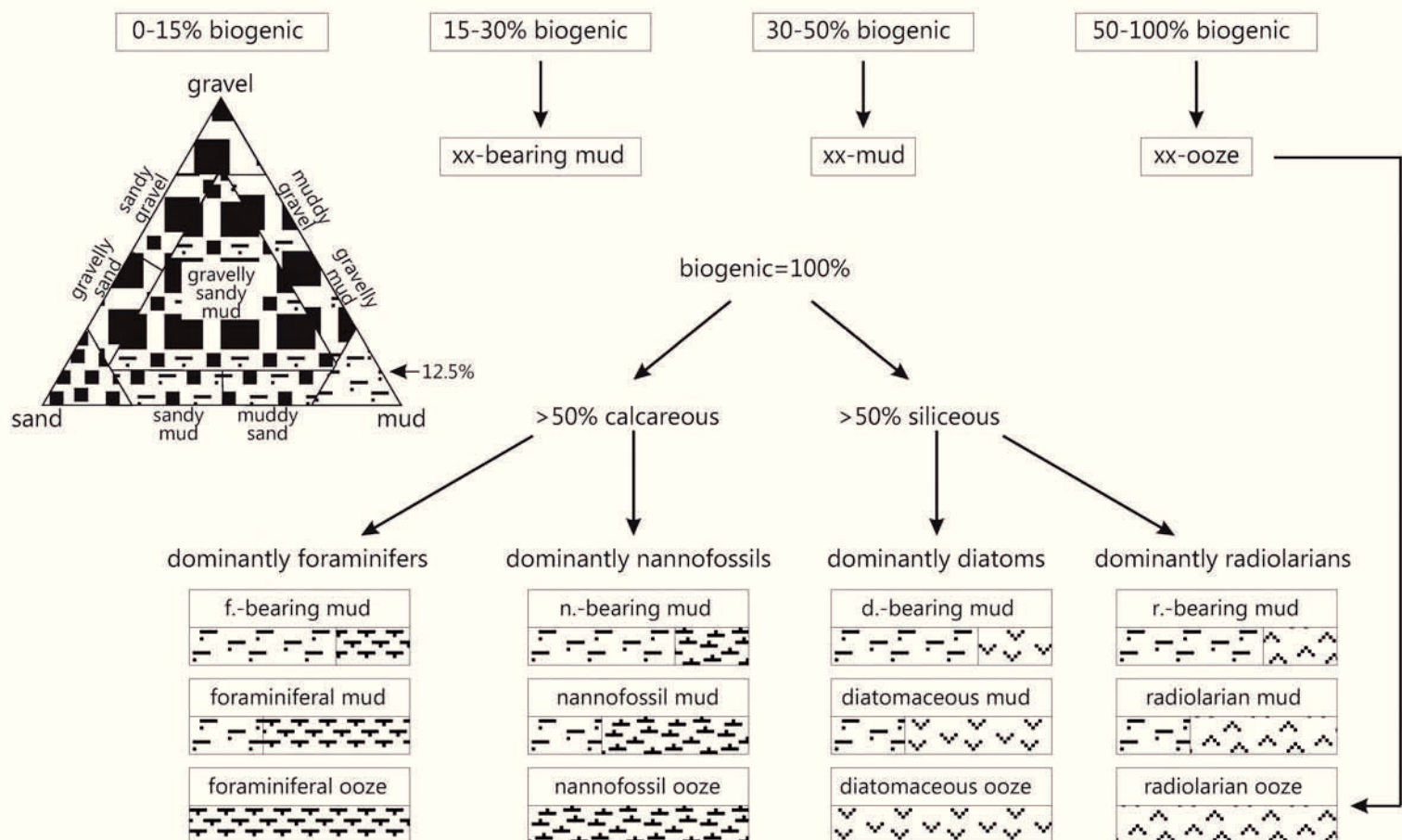
## Lithology:



## Structure:



## Nomenclature:



PS75/233-1 SL

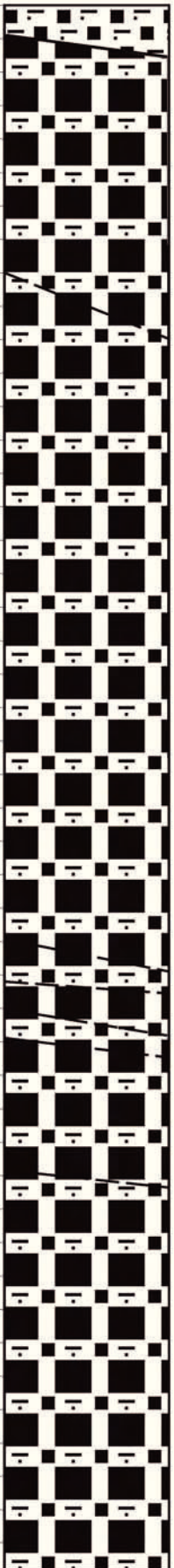

North of Burke Island, Pine Island Bay

ANT-XXVI/3

Recovery: 2.34 m

72°45.19'S, 105°01.08'W

Water depth: 559,6 m

	Lithology	Structure	Color	Description	
0			5Y 5/4	0-(4.5/7) cmbsf: <b>diatom-bearing sandy mud</b> , olive, homogenous	
10			5Y 4/4	(4.5/7)-(40/49.5) cmbsf: <b>gravelly sandy mud</b> , olive, homogenous, between 6 and 7 cm brownish reddish patch (~1cm diameter), high IRD content (diameters between 1 mm and 7 cm), poorly sorted	
20					
30					
40					
50					
60					
70					
80					
90					
100					
110					
120					
130					
140					
150					
160					
170					
180					
190					
200					
210					
220					
230					



PS75/234-1 SL

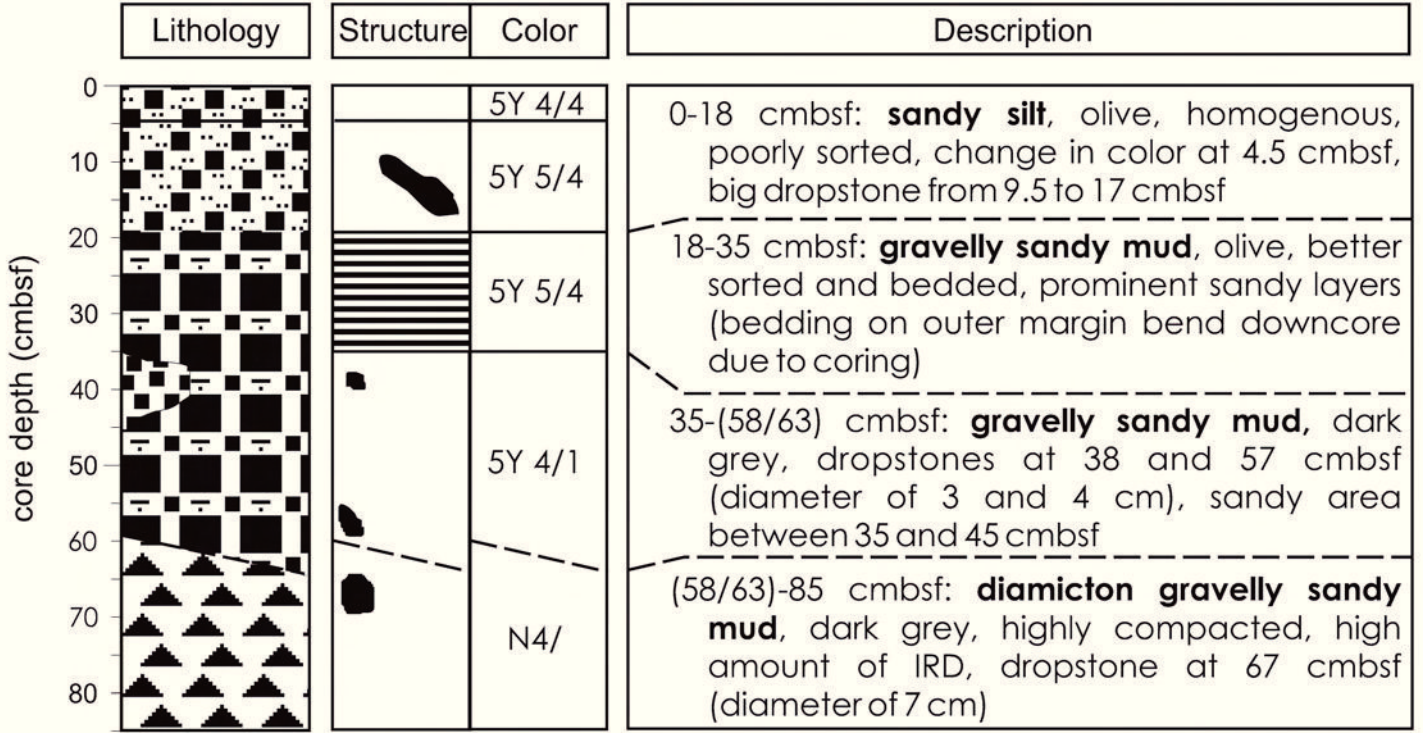
North of Burke Island, Pine Island Bay

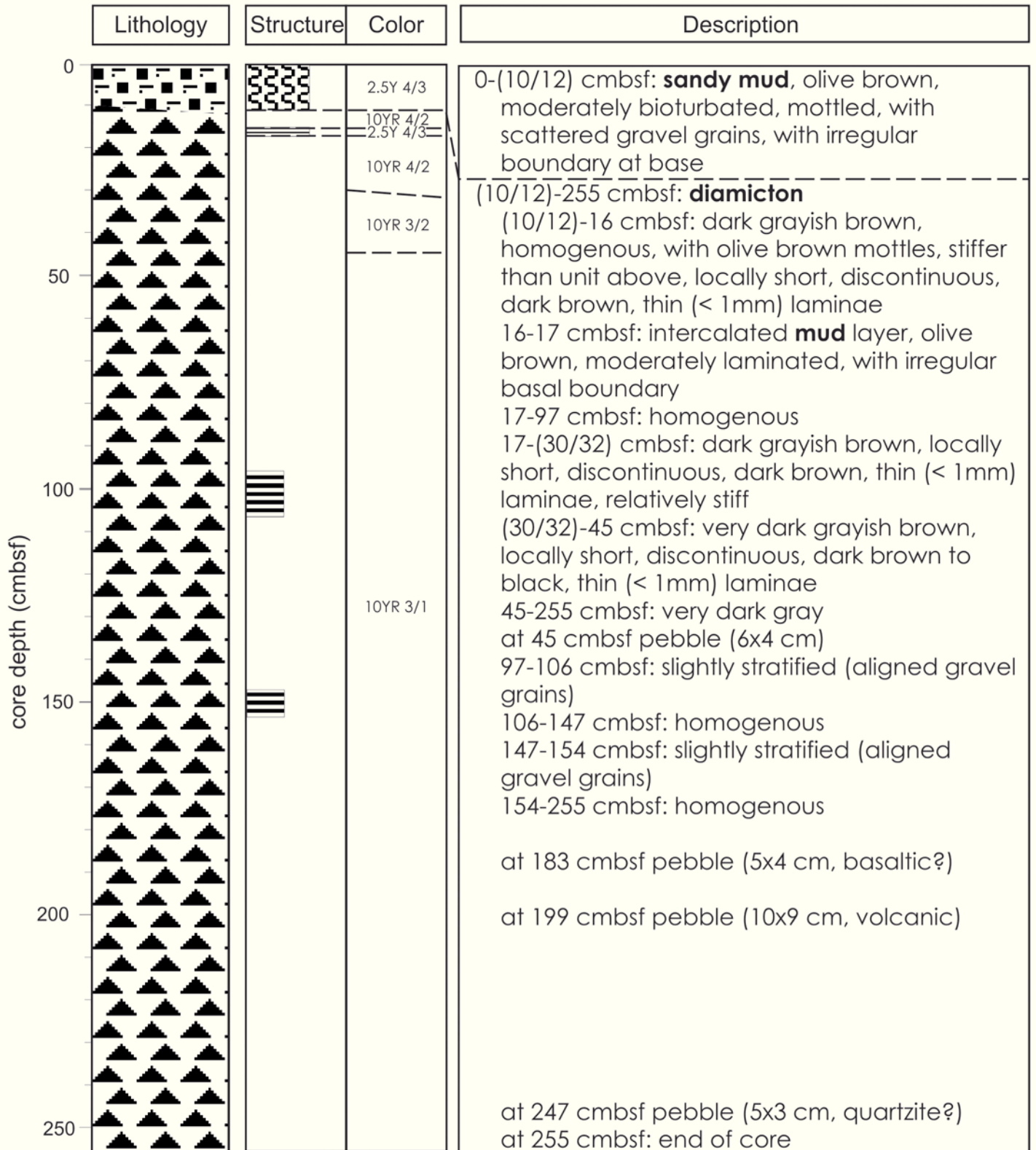
ANT-XXVI/3

Recovery: 0.85 m

74°47.03'S, 105°06.56'W

Water depth: 583.5 m







PS69/255-1 SL

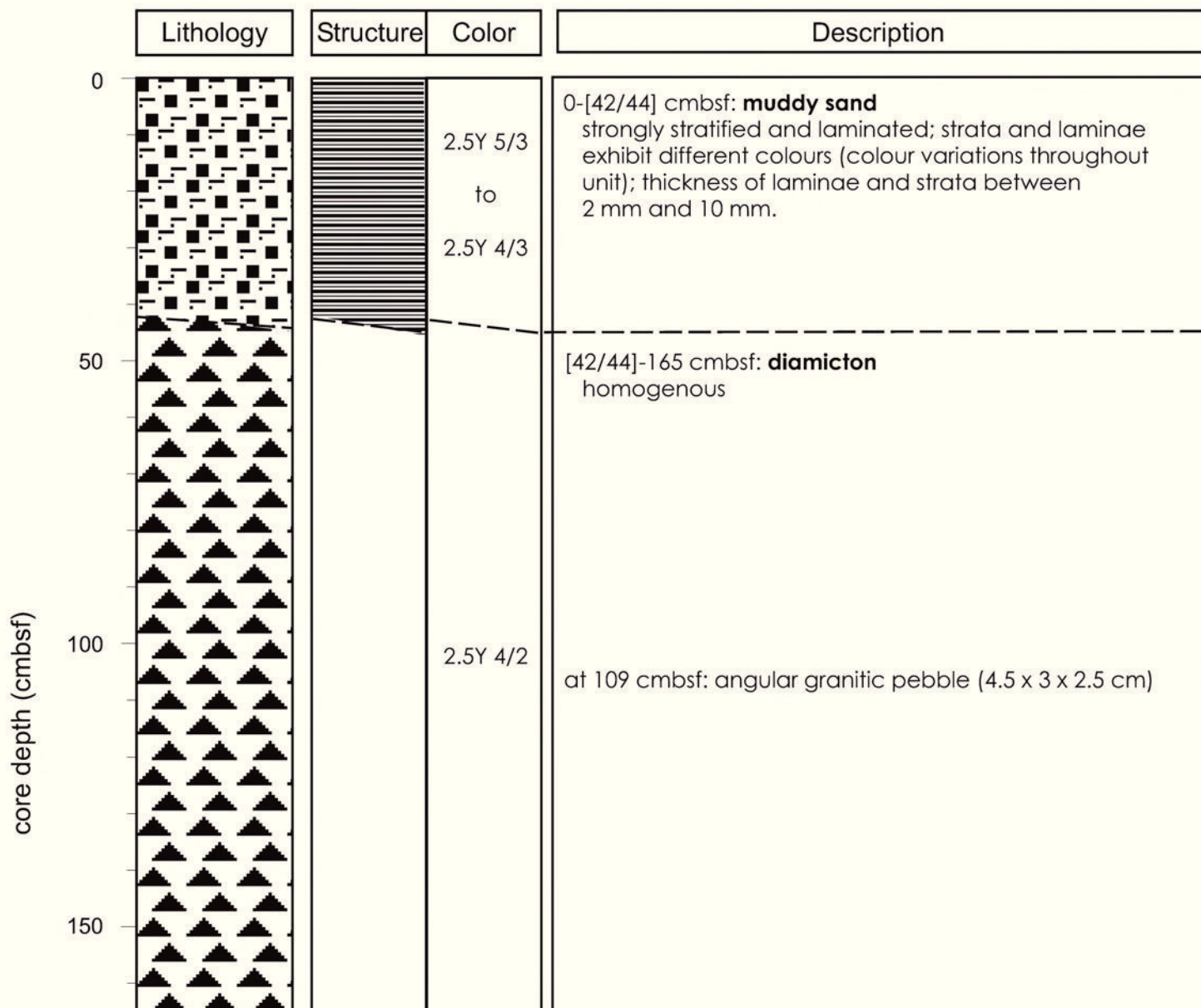
Outer shelf in eastern Amundsen Sea

ANT-XXIII/4

Recovery: 1.65 m

71°48.08'S, 104°21.09'W

Water depth: 657 m



Lithology	Structure	Color	Description
		2.5Y 4/3	0-13.5 cmbsf: <b>foraminifera-bearing mud</b> , with scattered, partly Mn-coated gravel grains; 0-10 cmbsf: slightly bioturbated (mottled) 10-13.5 cmbsf: slightly laminated (discontinuous, dark brown laminae)
		5Y 5/3	13.5-[41/43] cmbsf: <b>silty clay</b> ; with traces of sponge spicules and diatom fragments; moderately bioturbated (mottled) and slightly laminated, with discontinuous brown laminae (in particular between 13.5 and 21.5 cmbsf)
		2.5Y 4/3	[41/43]-58.5 cmbsf: <b>gravelly-sandy mud</b> ; homogenous at 42-51 cmbsf: black, subangular, basaltic pebble (10 x 6 x 5 cm),
		2.5Y 4/2	58.5-296 cmbsf: <b>diamicton</b> ; homogenous with scattered gravel grains and pebbles throughout 58.5-71 cmbsf: color 2.5Y 4/2 dominates, but with patches of grey sediment inbetween.
		N4/	at 61 cmbsf: subangular pebble (5 x 4 x 2.5 cm), garnet-bearing meta-sandstone or amphibolite/pyroxenite at 64 cmbsf: subrounded to subangular granitic pebble (2.5 x 3.5 x 4.5 cm) at 76 cmbsf: angular pebble (1 x 1.5 x 3 cm), breccia (?) at 139 cmbsf: well-rounded, platy, basaltic (?) gravel grain (diameter ca. 1.5 cm) within bright beige clayey matrix 93-96 cmbsf: core gap (all sample depths are uncorrected)

PS69/300-1 SL

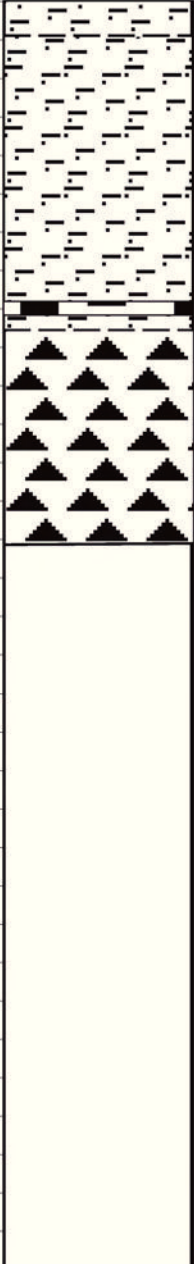

Pine Island Bay (transect)

ANT-XXIII/4

Recovery: 1.41 m

73°16.23'S, 103°40.76'W

Water depth: 766 m

	Lithology	Structure	Color	Description
core depth (cmbsf)			5Y 4/3	0-9 cmbsf: <b>mud</b> ; with some sponge spicules and traces of diatoms; moderately laminated and slightly bioturbated/mottled
			5GY 5/1	9-78.5 cmbsf: <b>mud</b> ; with traces of sponge spicules and with color variations
			5Y 4/1	9-70 cm: slightly bioturbated/mottled and slightly laminated; with scattered circular holes (diameters only a few mm)
			5Y 4/1	70-78.5 cmbsf: moderately bioturbated; with circular holes (diameters a few mm), with two black, oval mottles (diameters ca. 1cm)
			5Y 4/1	78.5-86 cmbsf: <b>mud</b> ; moderately laminated; with mm-thick <b>fine sand</b> laminae and lenses at 78.5-80.5 cmbsf: <b>gravelly</b> layer
			5Y 4/1	86-141 cmbsf: <b>diamicton</b> ; homogenous at 89, 111, 123 cmbsf: rust red aggregates (diameters only a few mm) 107-109 cmbsf: angular, granitic pebble (3.5 x 2.5 x 2 cm) 123-125 cmbsf: subrounded, granitic pebble (3.5 x 2.5 x 1.5 cm) 135-139 cmbsf: subangular, rhyolitic pebble (7 x 5 x 4.5 cm)
				141 cmbsf: end of core



PS75/129-1 GC

Amundsen Sea embayment (inner shelf)

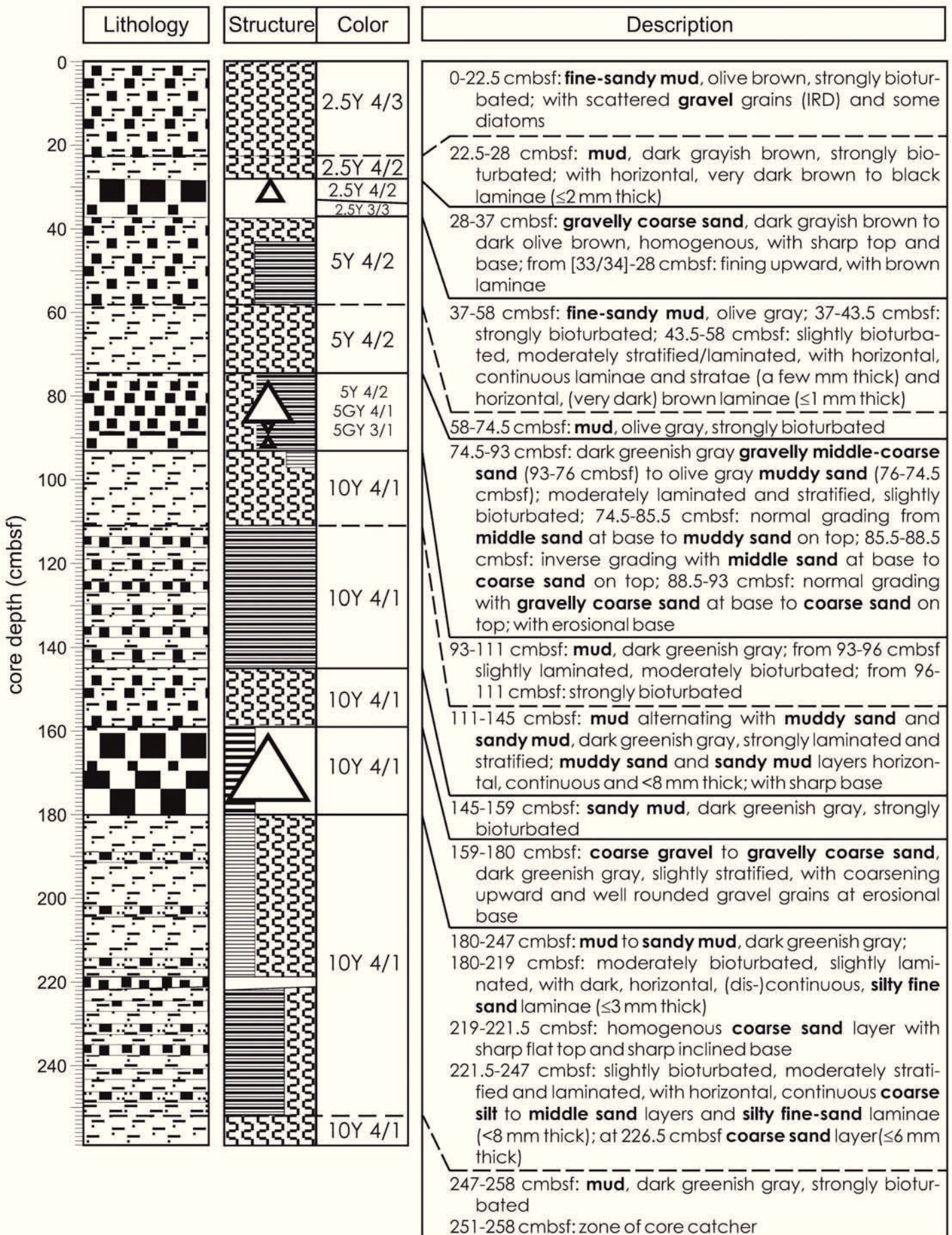
N' of westernmost Getz Ice Shelf

ANT-XXVI/3

Recovery: 2.58 m

74°30.54'S, 134°07.25'W

Water depth: 923 m









PS75/132-3 GC

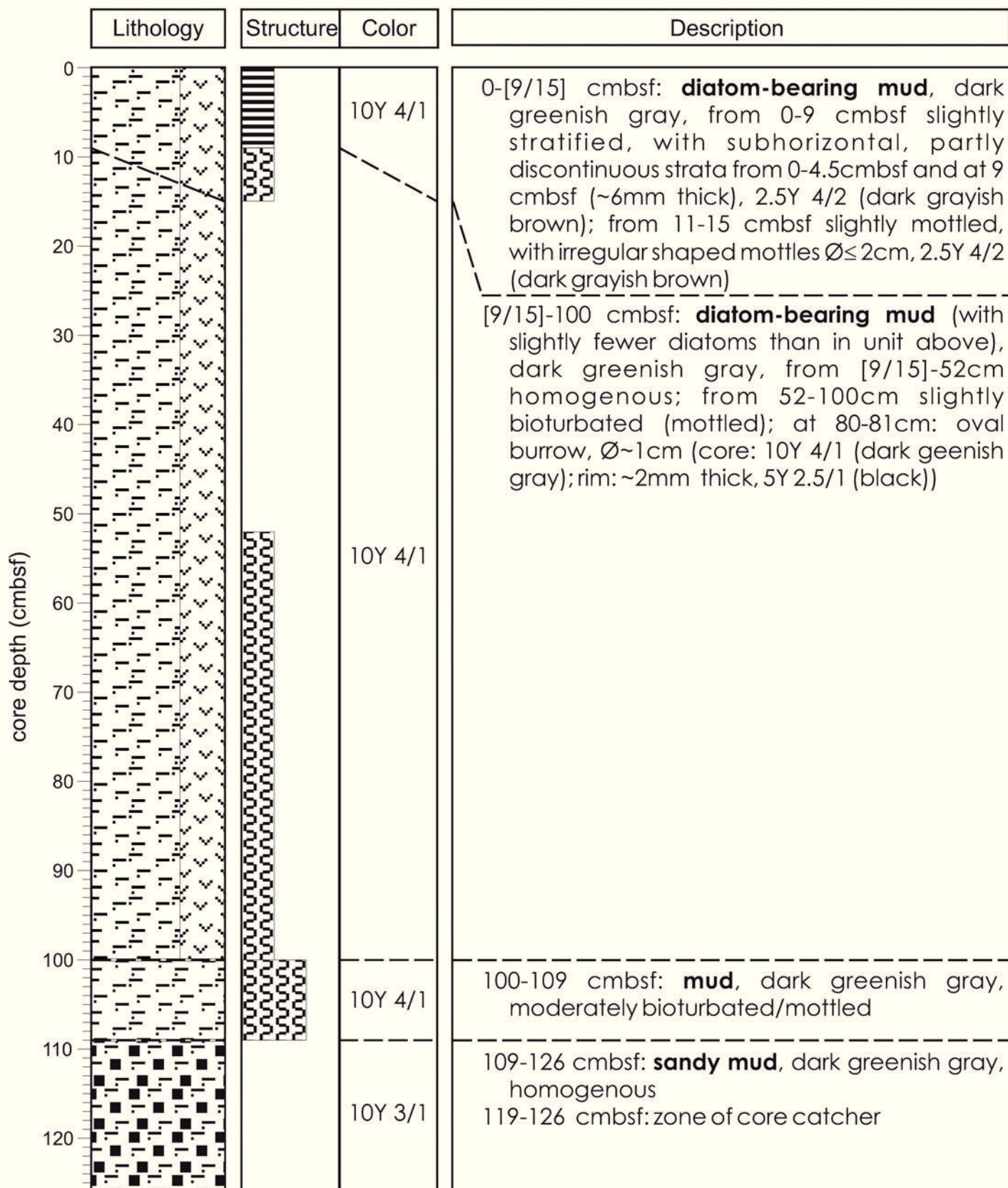
Westernmost Getz Trough

ANT-XXVI/3

Recovery: 1.26 m

74°21.97'S, 134°23.16'W

Water depth: 750 m



PS75/136-3 GC

Westernmost Getz Trough

ANT-XXVI/3

Recovery: 2.115 m

74°23.15'S, 134°35.59'W

Water depth: 752 m

	Lithology	Structure	Color	Description
core depth (cmbsf)				0-(8/13) cmbsf: <b>diatom-bearing mud</b> , dark greenish gray, homogenous, but with brownish mottles at 0-2 cmbsf and 7.5-10 cmbsf (size of mottles up to 3.5x4 cm; 2.5Y 4/4, olive brown)
				(8/13)-38 cmbsf: <b>diatom-bearing mud</b> , homogenous, but with local occurrence of mud pellets ( $\varnothing \leq 2$ mm)
			10Y 4/1	38-(123/126) cmbsf: <b>mud</b> (stiffer than mud in unit above), with a few diatoms from 38-76.5 cmbsf with abundant mud pellets ( $\varnothing \leq 2$ mm) from 38-51.5 cmbsf slightly laminated from 51.5-(123/126) cmbsf homogenous 76.5-(123/126) cmbsf with local occurrence of mud pellets ( $\varnothing \leq 2$ mm), thereby pellets decrease downcore to the base of the unit
			5Y 3/2	(123/126)-(169/171) cmbsf: <b>diamicton</b> , dark olive gray, homogenous  (169/171)-175.5 cmbsf: <b>sandy mud</b> , olive, strongly stratified, with horizontal continuous layers (~5 mm-10 mm thick)
			5Y 4/3 5Y 4/2	175.5-(183/186) cmbsf: <b>mud</b> , olive gray, slightly stratified (only color stratification between bright olive near top and dark olive near base), stiff/consolidated
		10Y 4/1	(183/186)-211.5 cmbsf: <b>mud</b> , dark greenish gray, slightly mottled (only in color, between brighter olive mottles and black mottles); stiff/consolidated	



PS75/138-1

Westernmost Getz Trough

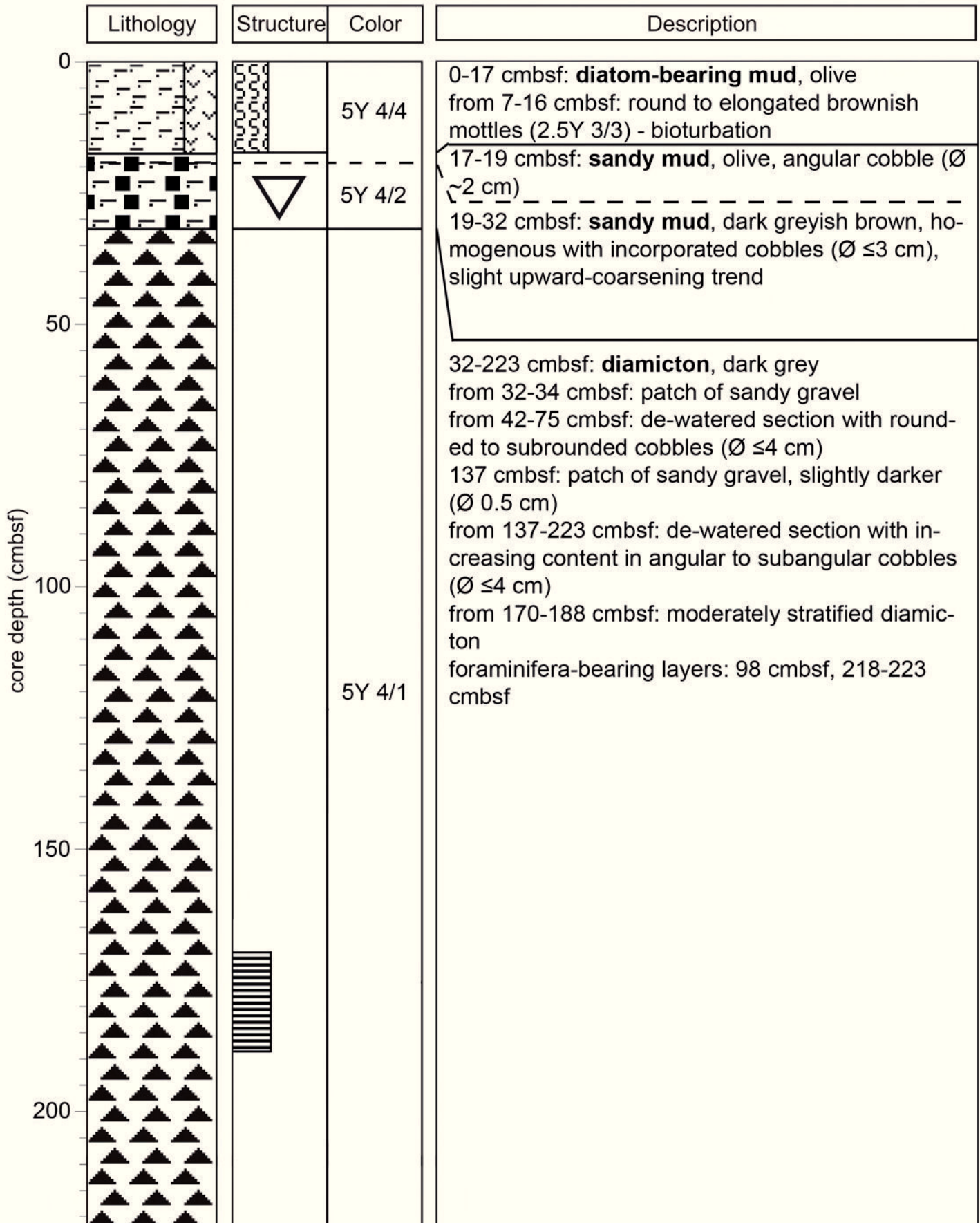
ANT-XXVI/3

Recovery: 0.95 m

74° 20.30'S, 134° 33.42'W

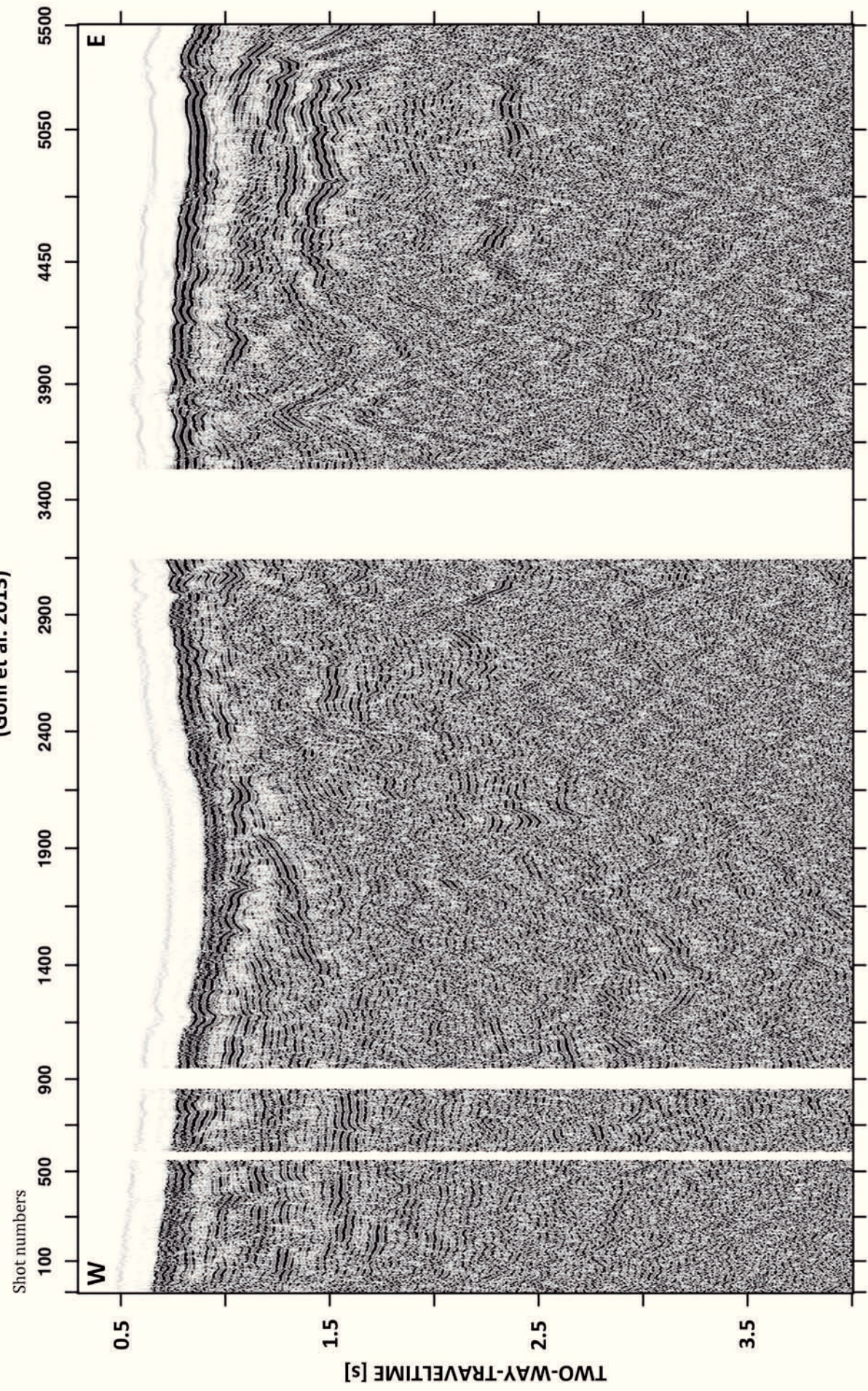
Water depth: 703 m

Lithology	Structure	Color	Description
		<p>5Y 4/2</p>	<p>0-75 cmbsf: <b>mud</b>, olive gray, homogenous, stiffer towards top            from 0-1 cmbsf: traces of diatoms            from 31-32 cmbsf: continuous layer of gravelly sand (black gravel grains: basaltic?)</p> <p>75-78 cmbsf: <b>silty clay</b>, olive gray, homogenous</p> <p>75-78 cmbsf: <b>diamicton</b>, structureless</p>

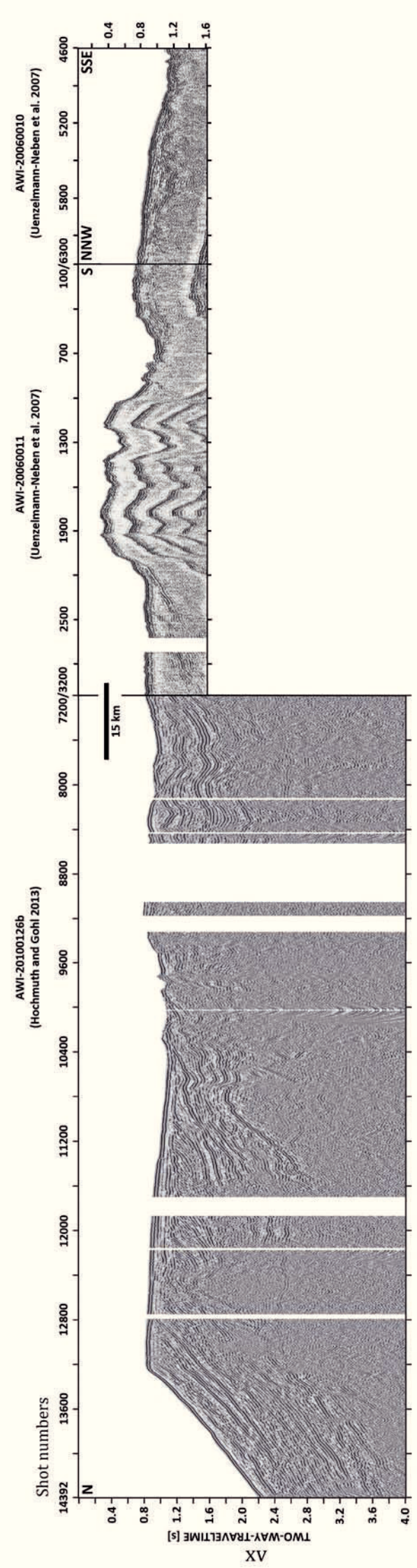




AWI-20100126a  
(Gohl et al. 2013)











# Grounding-line retreat of the West Antarctic Ice Sheet from inner Pine Island Bay

Claus-Dieter Hillenbrand<sup>1\*</sup>, Gerhard Kuhn<sup>2</sup>, James A. Smith<sup>1</sup>, Karsten Gohl<sup>2</sup>, Alastair G.C. Graham<sup>1</sup>, Robert D. Larter<sup>1</sup>, Johann P. Klages<sup>2</sup>, Rachel Downey<sup>1</sup>, Steven G. Moreton<sup>3</sup>, Matthias Forwick<sup>4</sup>, and David G. Vaughan<sup>1</sup>

<sup>1</sup>British Antarctic Survey, Natural Environment Research Council, High Cross, Madingley Road, Cambridge CB3 0ET, UK

<sup>2</sup>Alfred Wegener Institute for Polar and Marine Research (AWI), Helmholtz Association, Am Alten Hafen 26, D-27568 Bremerhaven, Germany

<sup>3</sup>NERC Radiocarbon Laboratory (Environment), Scottish Enterprise Technology Park, Rankine Avenue, East Kilbride G75 0QF, UK

<sup>4</sup>University of Tromsø, Department of Geology, N-9037 Tromsø, Norway

## ABSTRACT

Ice loss from the marine-based, potentially unstable West Antarctic Ice Sheet (WAIS) contributes to current sea-level rise and may raise sea level by  $\leq 3.3$  m or even  $\leq 5$  m in the future. Over the past few decades, glaciers draining the WAIS into the Amundsen Sea Embayment (ASE) have shown accelerated ice flow, rapid thinning, and fast retreat of the grounding line (GL). However, the long-term context of this ice loss is poorly constrained, limiting our ability to accurately predict future WAIS behavior. Here we present a new chronology for WAIS retreat from the inner continental shelf of the eastern ASE, based on radiocarbon dates from three marine sediment cores. The ages document a retreat of the GL to within  $\sim 100$  km of its modern position before ca. 10,000 calibrated (cal.) yr B.P. This early deglaciation is consistent with ages for GL retreat from the western ASE. Our new data demonstrate that, in contrast to the Ross Sea, WAIS retreat from the ASE shelf was largely complete by the start of the Holocene. Our results further suggest either slow GL retreat from the inner ASE shelf throughout the Holocene, or that any episodes of fast GL retreat must have been short-lived. Thus, today's rapid retreat may be exceptional during the Holocene and may originate in recent changes in regional climate, ocean circulation, or ice-sheet dynamics.

## INTRODUCTION

Pine Island Glacier, Thwaites Glacier, and Smith Glacier drain the West Antarctic Ice Sheet (WAIS) into Pine Island Bay in the eastern Amundsen Sea Embayment (ASE) (Fig. 1). Ice loss from this sector of the WAIS is currently raising global sea level at a rate of  $\sim 0.15$ – $0.30$  mm/yr, making it Antarctica's main contributor to present sea-level rise (Joughin and Alley, 2011, and references therein). Continued WAIS melting in the ASE sector has the potential to raise global sea level by  $\leq 1.5$  m, and thus to dominate sea-level change over coming centuries (Vaughan, 2008; Wingham et al., 2009). The current negative mass balance, which is mainly attributed to significant sub-ice shelf melting by upwelling of relatively warm Circumpolar Deep Water (e.g., Rignot and Jacobs, 2002; Pritchard et al., 2012), is characterized by fast grounding line (GL) retreat (Pine Island Glacier,  $\sim 25$  km from 1992 to 2009; Joughin et al., 2010; Thwaites Glacier,  $\leq 14.5$  km from 1992 to 2009; Tinto and Bell, 2011), accelerated ice discharge (Rignot, 2008; Joughin et al., 2010), and rapid thinning of grounded ice and ice shelves draining into the ASE (e.g., Joughin and Alley, 2011). However, it is unknown if the contemporary dynamic changes are simply part of long-term WAIS retreat since the Last Glacial Maximum (LGM, ca. 23,000–19,000 cal. yr B.P.), or solely recent phenomena.

The deglacial history in the ASE sector since the LGM is poorly constrained. Subglacial bedforms mapped by multibeam bathymetry and information from marine sediment cores revealed that Pine Island, Thwaites, and Smith Glaciers coalesced on the inner shelf during the LGM to form a major ice stream that advanced through a bathymetric trough to the outer shelf (Lowe and Anderson, 2002; Graham et al., 2010; Jakobsson et al., 2012). Radiocarbon ages from the sediment cores constrain deglaciation of

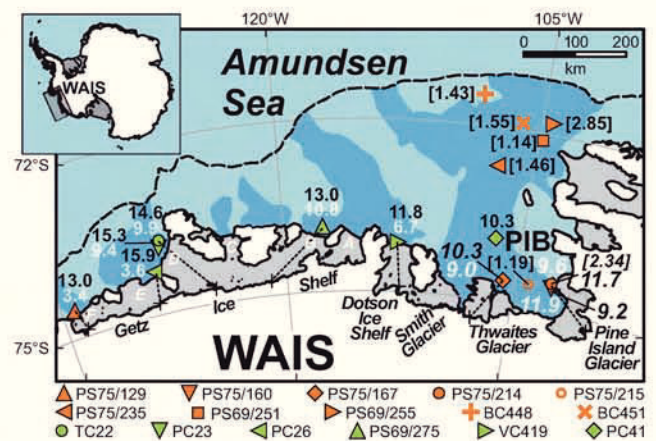


Figure 1. Map of Amundsen Sea Embayment, Antarctica, showing shelf break (black dashed line), locations of paleo-ice stream trough systems (dark blue), ice shelves (gray shaded), modern grounding line (GL; black continuous line, from Rignot et al., 2011), sediment core sites from the shelf, core-top  $^{14}\text{C}$  dates (from calcareous microfossils) used for establishing the regional marine reservoir effect (in uncorrected  $^{14}\text{C}$  kyr B.P.; black numbers in brackets), minimum ages for GL retreat (in calibrated kyr B.P.; black numbers), and maximum rates for GL retreat from core sites to modern GL of the West Antarctic Ice Sheet (WAIS) (in m/yr; white numbers). Core locations presented here for first time are highlighted by orange symbols (cores discussed in detail are highlighted by ages and retreat rates given in italics), while those from previously published studies are marked by green symbols (details and references in Table DR1; see footnote 1). Distances of core sites from present GL were measured from furthest landward GL point upflow from each site (black crosses) along trajectories marked by black dotted lines. Inset map shows location of study area within wider context of Antarctica. PIB—Pine Island Bay.

the middle shelf at  $\sim 73^\circ\text{S}$  to before 12,503 cal. yr B.P., while just a single  $^{14}\text{C}$  date from core NBP99–02 PC41 (Fig. 1) constrains the timing of grounded ice retreat within  $\sim 250$  km of the modern GL of Pine Island Glacier to before 10,256 cal. yr B.P. (Lowe and Anderson, 2002; Kirshner et al., 2012). Our study investigates whether rapid GL retreat similar to the modern GL retreat has typified WAIS retreat from the ASE shelf during the Holocene. This knowledge will improve our understanding of current mass loss of West Antarctic glaciers and model-based predictions of future changes.

## MATERIALS

During R/V *Polarstern* expedition ANT-XXVI/3 in 2010, we collected three sediment cores (PS75/160, PS75/167, and PS75/214) at inner shelf locations in Pine Island Bay to reconstruct the history of post-LGM WAIS retreat (Table DR1 in the GSA Data Repository<sup>1</sup>). The three core sites are located on shallow ridges flanking the paleo-ice stream trough

<sup>1</sup>GSA Data Repository item 2013012, Table DR1 (radiocarbon dates from the ASE cores) and Appendix DR1 (methods and laboratory techniques), is available online at [www.geosociety.org/pubs/ft2013.htm](http://www.geosociety.org/pubs/ft2013.htm), or on request from editing@geosociety.org or Documents Secretary, GSA, P.O. Box 9140, Boulder, CO 80301, USA.

\*E-mail: [hilc@bas.ac.uk](mailto:hilc@bas.ac.uk).



and are 110, 112, and 93 km offshore from the modern GLs of Pine Island Glacier (PS75/160, PS75/214) and Thwaites Glacier (PS75/167), respectively (Fig. 1). As in other paleo-ice stream troughs around West Antarctica (e.g., Livingstone et al., 2012), grounded ice and subglacial meltwater eroded a deep basin in the most landward trough section over numerous glacial cycles (Lowe and Anderson, 2003). Consequently, inner Pine Island Bay is characterized by rugged seafloor topography with only localized patches of sediment cover, and water depths of  $\leq 1600$  m. Crystalline bedrock is exposed over most of its seafloor (Lowe and Anderson, 2003); however, we identified small sediment pockets suitable for gravity coring on highs above 800 m water depth, where sediments contain biogenic carbonate (Hauck et al., 2012). Calcareous microfossils are usually absent from Antarctic shelf sediments, but provide the most reliable  $^{14}\text{C}$  ages (e.g., Anderson et al., 2002; Domack et al., 2005).

## RESULTS AND DISCUSSION

### Facies Analysis

All three cores contained soft, predominantly fine-grained, muddy to sandy sediments with common abundances of foraminifera (Fig. 2). In accordance with previous studies on sediments from ice-marginal settings, we investigated their lithological composition, sedimentary structures, grain-size distribution, and physical properties (Appendix DR1 in the Data Repository) to assign them to six different glaciomarine facies types (Table 1). We attributed coarse-grained sediments to a depositional setting proximal to the GL and fine-grained sediments to a depositional setting distal from the GL, following previously published facies analyses on Antarctic shelf sediments (e.g., Lowe and Anderson, 2002, 2003; McKay et al., 2009; Hillenbrand et al., 2010; Passchier et al., 2011). Near the core top, the sediments at all three sites consist of bioturbated mud (facies M) with some diatom frustules, likely deposited by hemipelagic settling in a seasonal open-marine environment distal from the GL, although perennial coverage by floating ice (e.g., Domack et al., 2005) cannot be ruled out. Physical property values of facies M resemble those of underlying

terrigenous muds interlaminated with thin silt layers (facies MSi) present at site PS75/214 (Fig. 2), which are interpreted as meltwater plume sediments deposited at some distance from grounded ice (cf. Lowe and Anderson, 2002). In contrast, a massive sandy gravel unit (facies GS) at site PS75/167, a slightly bioturbated sand unit (facies S) at site PS75/160, and muds interstratified with sandy layers (facies MSa) recovered in all three cores are characterized by both lower water contents and higher values of wet-bulk density, shear strength, and magnetic susceptibility (Fig. 2). The coarse-grained intervals of facies S and MSa are occasionally characterized by fining upward and erosional basal contacts suggesting their formation by gravity flows, turbidity currents, meltwater plumes, and/or current winnowing in a setting proximal to the GL (Table 1). The deposition of facies GS probably resulted from similar processes, or a high accumulation of ice-rafted debris combined with current winnowing.

The sedimentary sequences retrieved at sites PS75/214 and PS75/167 document a transition from a setting proximal to the GLs of Pine Island and Thwaites Glaciers to a distal seasonal open-marine environment (Fig. 2; Table 1). The more complex stratigraphy in core PS75/160 also contains facies MC. Facies MC is characterized by deformed and sheared pebblesized muddy to sandy soft sediment clasts that are randomly orientated in a muddy matrix. This facies probably results from iceberg furrowing, because the modern average iceberg keel depth at the floating part of Pine Island Glacier is  $\sim 500$  m (e.g., Jenkins et al., 2010), greatly exceeding the 337 m water depth at site PS75/160. Alternatively, facies MC may have been formed by debris flows or slumps or melt-out of soft sediment clasts from icebergs or the base of an ice shelf. We rule out that facies MC formed as a glacioteconite (i.e., a subglacially deformed and sheared deposit consisting of till and reworked ice-marginal sediments that have retained some of the structural characteristics of the parent material; e.g., Ó Cofaigh et al., 2011), because facies MC lacks some key features of glacioteconites, such as interbedding with subglacial diamicton, orientated fabric of soft-sediment clasts, and clear evidence for erosional unconformities.

Notably, the three cores recovered exclusively foraminifera-bearing muddy to sandy sediments that are normally consolidated and show a range

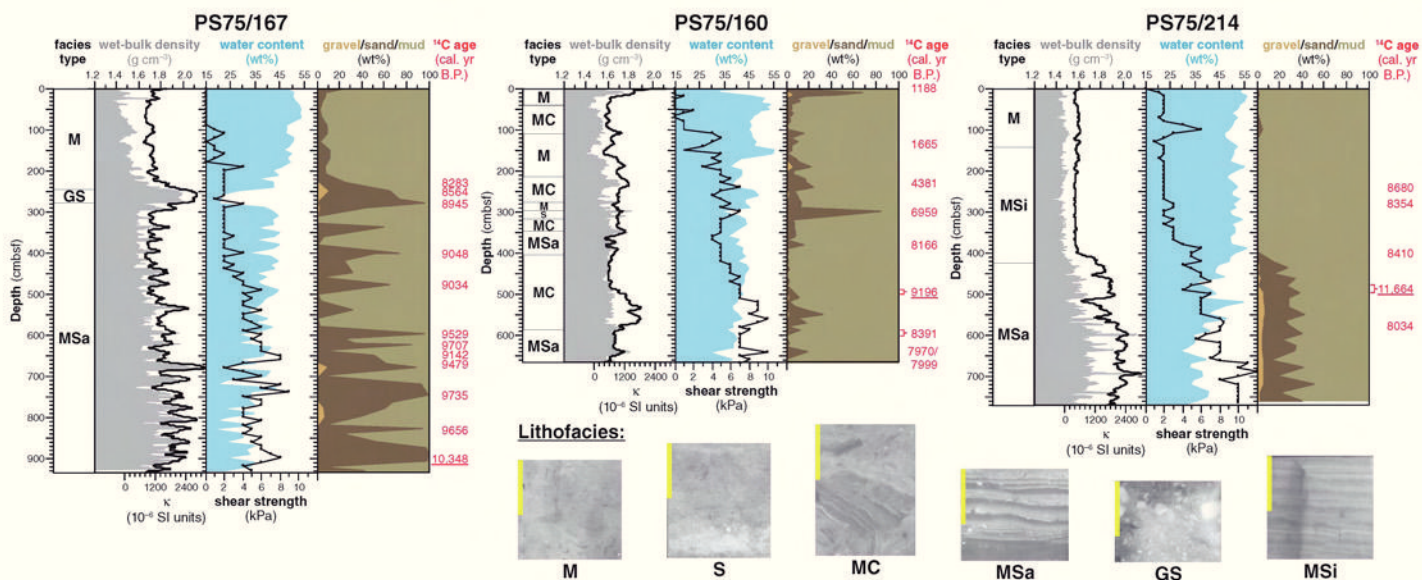


Figure 2. Facies (described in detail in Table 1), physical properties (wet-bulk density, volume-specific magnetic susceptibility  $\kappa$ , water content, shear strength), grain-size distribution (gravel/sand/mud ratios) and calibrated (cal.) accelerator mass spectrometry  $^{14}\text{C}$  ages on calcareous microfossils in sediment cores PS75/167, PS75/160, and PS75/214 (oldest age at each site is underscored; cmbsf—centimeters below seafloor). Examples of X-ray radiographs (negatives) for six facies types are also shown (yellow scale bars in upper left corners = 5 cm). X-ray radiograph examples for facies M (bioturbated mud), MSa (muds interstratified with sandy layers), and MSi (terrigenous muds interlaminated with thin silt layers) are from core PS75/214, those for facies S (slightly bioturbated sand) and MC (deformed, sheared pebblesized muddy to sandy soft sediment clasts randomly orientated in muddy matrix) are from core PS75/160, and example for facies GS (massive sandy gravel) is from core PS75/167.



TABLE 1. SUMMARY OF FACIES IDENTIFIED IN THE STUDIED SEDIMENT CORES, AND INFERRED PROCESSES AND PALEOENVIRONMENTS

Facies	Lithology	Sedimentary structures	Physical properties	Processes and paleoenvironments
M	mud and/or sandy mud, with diatom frustules and/or calcareous microfossils; occasionally with a few dispersed gravel grains	slightly to strongly bioturbated, slightly to moderately laminated and/or stratified	high water content, low shear strength, low wet bulk density, low to medium magnetic susceptibility	hemipelagic suspension settling with deposition of IRD in an open-marine setting or under sea-ice and/or thin ice shelf distal from the grounding line (references A, B, C, D, F, G, H)
MSi	mud alternating with layers and lenses of silt and/or sandy silt; coarse-grained layers occasionally enriched in calcareous microfossils	moderately to strongly laminated and/or stratified, slightly bioturbated	high water content, low shear strength, low wet bulk density, low magnetic susceptibility	hemipelagic suspension settling alternating with settling from meltwater plumes under sea-ice and/or ice-shelf cover in a setting distal from the grounding line (references D, F, G)
GS	sandy gravel (with a few pebbles), enriched in calcareous microfossils	massive, with coarsening upward	low water content, low shear strength, high wet bulk density, high magnetic susceptibility	high-energy gravity flows (references C, F, H) or meltwater flows (reference E), high IRD accumulation (reference G), high-energy current winnowing of glaciomarine sediment (reference D) under sea-ice and/or ice-shelf cover proximal to the grounding line
S	sand (with a few gravel grains), enriched in calcareous microfossils	slightly bioturbated, moderately stratified	low water content, high shear strength, medium wet bulk density, medium magnetic susceptibility	high-density gravity flows (references C, D, F, G, H), current winnowing of glaciomarine sediment (references D, G) under sea-ice and/or ice-shelf cover proximal to the grounding line
MSa	mud alternating with layers and lenses of sand and/or gravelly sand; coarse-grained layers occasionally enriched in calcareous microfossils	moderately to strongly stratified and/or laminated; coarse-grained layers occasionally massive with fining upward and erosional base	low water content, high shear strength, high wet bulk density, medium to high magnetic susceptibility	hemipelagic suspension settling alternating with turbidity currents (references C, F, G, H), settling from meltwater plumes (reference F), current winnowing of glaciomarine sediment (reference D) under sea-ice and/or ice-shelf cover proximal to the grounding line
MC	soft sediment clasts of mud and/or sandy mud and sand and/or muddy sand in a muddy matrix, occasionally with calcareous microfossils	randomly orientated deformed and sheared mottles of massive to laminated and/or stratified soft sediment clasts	medium to high water content, variable shear strength, medium wet bulk density, variable magnetic susceptibility	iceberg turbation of glaciomarine sediments in an open-marine setting distal from the grounding line (references D, H), melt-out of clasts from an ice-shelf base in a proximal sub-ice shelf setting (references A, B), debris flow or slump (references C, D, F, G)

Note: IRD—ice-rafted debris. References: A—Anderson et al., 2002; B—Domack et al., 2005; C—Hillenbrand et al., 2010; D—Lowe and Anderson, 2002; E—Lowe and Anderson, 2003; F—McKay et al., 2009; G—Passchier et al., 2011; H—Smith et al., 2011.

of sedimentary structures (Table 1). We do not observe massive terrigenous diamictos resembling subglacial till recovered in other cores from the ASE (Lowe and Anderson, 2002; Smith et al., 2011; Kirshner et al., 2012) and other parts of the West Antarctic shelf (e.g., Anderson et al., 2002; Livingstone et al., 2012). Therefore, we are certain that the sedimentary sequences recovered in our cores are of glaciomarine origin and that their deposition must postdate the last GL advance across the core sites. However, the occurrence of microfossils in the sediments does not necessarily exclude the presence of an ice shelf (e.g., Domack et al., 2005) that may have covered inner Pine Island Bay until the 1930s (Steig et al., 2012).

### Radiocarbon Chronology

A unique feature of our cores is the common abundance of calcareous microfossils, mainly benthic and planktonic foraminifera tests (Table DR1). We obtained accelerator mass spectrometry  $^{14}\text{C}$  dates on calcareous microfossils taken from all facies types (Fig. 2; Appendix DR1). In accordance with uncorrected  $^{14}\text{C}$  ages from core-top sediments in the ASE (Fig. 1; Table DR1) and previous Antarctic studies (e.g., Livingstone et al., 2012, and references therein), we corrected the  $^{14}\text{C}$  dates by subtracting a marine reservoir effect of  $1100 \pm 200$  yr (Berkman and Forman, 1996; Domack et al., 2005). The  $^{14}\text{C}$  ages of core PS75/160 span the time from 1188 to 9196 cal. yr B.P. (Fig. 2; Table DR1). The  $^{14}\text{C}$  dates of core PS75/214 range from 8034 to 11,664 cal. yr B.P., and those of core PS75/167 range from 8283 to 10,348 cal. yr B.P., suggesting that a hiatus in sedimentation may have occurred at both sites during the mid-late Holocene, or that sediments accumulated at very low rates. We observe minor  $^{14}\text{C}$  age reversals at sites PS75/160 and PS75/214 below ~5 m core depth (Fig. 2) that probably result from sediment reworking by downslope processes, strong current activity, and/or iceberg scouring (Table 1), but do not affect our deglacial chronology or our paleoenvironmental

interpretation. All other age reversals are within the uncertainty of the reservoir correction and the analytical error (Table DR1).

### TIMING OF INNER SHELF DEGLACIATION AND RATE OF HOLOCENE GL RETREAT

Regardless of their subsequent redeposition from nearby, shallower shelf areas by gravitational downslope transport, the calcareous microfossils can only have lived near a core site after grounded ice had retreated further landward. Therefore, our  $^{14}\text{C}$  dates constitute reliable minimum ages for GL retreat. Consequently, the GL must have retreated before 9196 cal. yr B.P. from site PS75/160, before 11,664 cal. yr B.P. from site PS75/214, and before 10,348 cal. yr B.P. from site PS75/167 (Fig. 2). Combining our reconstruction of GL retreat from inner Pine Island Bay with existing minimum deglaciation ages from near-coastal core locations in the western ASE indicates consistent grounded ice-sheet retreat across the inner shelf before at least ~10,000 cal. yr B.P. (Fig. 1; Table DR1). In contrast to the steady pattern of GL retreat from the Ross Sea shelf (Conway et al., 1999), the WAIS had already retreated to the inner ASE shelf before the start of the Holocene, achieving a configuration close to the modern remarkably early.

Given that there is currently no evidence from the ASE sector of the WAIS for a Holocene GL position landward of the modern position or a Holocene readvance of the GL onto the inner shelf, the calculation of retreat rates from the core sites to the present-day GL position allows us to characterize the long-term context of WAIS retreat. Our calculated retreat rates are maxima (they are based on minimum deglaciation ages) and range from  $3.4 \pm 0.1$  m/yr to  $11.9 \pm 0.7$  m/yr; the highest rate is observed in Pine Island Bay (Fig. 1). It is significant that all retreat rates are more than two orders of magnitude lower than the recent GL retreat of Pine Island and Thwaites Glaciers (Joughin et al., 2010; Tinto and Bell, 2011), and thus indicate that today's rapid retreat is exceptional in a Holocene context.



However, our rates are averaged over thousands of years. The presence of grounding-zone wedges and radiocarbon dates from sediment cores in the mid-shelf part of the Pine Island paleo-ice stream trough document that post-LGM ice-sheet retreat there was episodic (Graham et al., 2010; Jakobsson et al., 2012; Kirchner et al., 2012). Similarly, the recent episode of rapid GL retreat of Pine Island Glacier, attributed to its decoupling from a transverse seafloor ridge at some time between A.D. 1975 and 1982, may have followed an extended period of GL stability (Jenkins et al., 2010; Joughin et al., 2010). Even if the Holocene deglaciation of inner Pine Island Bay was characterized by long-term GL stability interrupted by brief (i.e., ~25–30 yr) episodes of rapid retreat comparable to those recently recorded for Pine Island Glacier, our results would imply that no more than 3–4 such episodes could have occurred between ~10,000 cal. yr B.P. and A.D. 1992, because otherwise the GL would have retreated landward of its modern position. Sedimentary wedges deposited during potential long-term still-stands of the GL are not present between our core sites and the modern calving fronts of Pine Island and Thwaites Glaciers (e.g., Lowe and Anderson, 2003), suggesting that the present rapid retreat may be unprecedented during the Holocene.

We conclude that the current rapid deglaciation of the ASE sector is probably a recent phenomenon driven by changes in glacier-bed interaction (Jenkins et al., 2010), atmospheric warming (Ding et al., 2011), and a strengthening of Circumpolar Deep Water inflow (Jacobs et al., 2011), which may have been forced by an increase of westerly wind stress (Steig et al., 2012), rather than being a continued ice-sheet response to much earlier changes. Our data provide the first geological constraints on past ice retreat from the coastal vicinity of a key drainage sector of the WAIS, and reveal for the first time a pattern of deglaciation that forms the critical context for present and future ice-sheet changes.

#### ACKNOWLEDGMENTS

We thank the captain and crew participating in R/V *Polarstern* expedition ANT-XXVI/3, and H. Blagbrough, D. Baqu , R. Fr hliking, M. Gutjahr, P. Jernas, N. Lensch, I. MacNab, M. Seebeck, S. Wiebe, and S. Wiers for their assistance. This work was financially supported by the UK Natural Environment Research Council and the Alfred Wegener Institute research program Polar Regions and Coasts in a Changing Earth System. We thank A. Rodger, J. Johnson, and two anonymous reviewers for their constructive comments.

#### REFERENCES CITED

Anderson, J.B., Shipp, S.S., Lowe, A.L., Wellner, J.S., and Mosola, A.B., 2002, The Antarctic Ice Sheet during the Last Glacial Maximum and its subsequent retreat history: A review: *Quaternary Science Reviews*, v. 21, p. 49–70, doi:10.1016/S0277-3791(01)00083-X.

Berkman, P.A., and Forman, S.L., 1996, Pre-bomb radiocarbon and the reservoir correction for calcareous marine species in the Southern Ocean: *Geophysical Research Letters*, v. 23, p. 363–366, doi:10.1029/96GL00151.

Conway, H., Hall, B.L., Denton, G.H., Gades, A.M., and Waddington, E.D., 1999, Past and future grounding-line retreat of the West Antarctic Ice Sheet: *Science*, v. 286, p. 280–283, doi:10.1126/science.286.5438.280.

Ding, Q., Steig, E.J., Battisti, D.S., and K ttel, M., 2011, Warming in West Antarctica caused by central tropical Pacific warming: *Nature Geoscience*, v. 4, p. 398–403, doi:10.1038/ngeo1129.

Domack, E., Duran, D., Leventer, A., Ishman, S., Doanne, S., McCallum, S., Amblas, D., Ring, J., Gilbert, R., and Prentice, M., 2005, Stability of the Larsen B ice shelf on the Antarctic Peninsula during the Holocene epoch: *Nature*, v. 436, p. 681–685, doi:10.1038/nature03908.

Graham, A.G.C., Larter, R.D., Gohl, K., Dowdeswell, J.A., Hillenbrand, C.-D., Smith, J.A., Evans, J., Kuhn, G., and Deen, T., 2010, Flow and retreat of the late Quaternary Pine Island–Thwaites palaeo-ice stream, West Antarctica: *Journal of Geophysical Research*, v. 115, F03025, doi:10.1029/2009JF001482.

Hauck, J., Gerdes, D., Hillenbrand, C.-D., Hoppema, M., Kuhn, G., Nehrke, G., V lker, C., and Wolf-Gladrow, D.A., 2012, Distribution and mineralogy of carbonate sediments on Antarctic shelves: *Journal of Marine Systems*, v. 90, p. 77–87, doi:10.1016/j.jmarsys.2011.09.005.

Hillenbrand, C.-D., Smith, J.A., Kuhn, G., Esper, O., Gersonde, R., Larter, R.D., Maher, B., Moreton, S.G., Shimmield, T.M., and Korte, M., 2010, Age assignment of a diatomaceous ooze deposited in the western Amundsen Sea Embayment after the Last Glacial Maximum: *Journal of Quaternary Science*, v. 25, p. 280–295, doi:10.1002/jqs.1308.

Jacobs, S.S., Jenkins, A., Giulivi, C.F., and Dutrieux, P., 2011, Stronger ocean circulation and increased melting under Pine Island Glacier ice shelf: *Nature Geoscience*, v. 4, p. 519–523, doi:10.1038/ngeo1188.

Jakobsson, M., Anderson, J.B., Nitsche, F.O., Gyllencreutz, R., Kirchner, A., Kirchner, N., O'Regan, M.A., Mohammad, R., and Eriksson, B., 2012, Ice sheet retreat dynamics inferred from glacial morphology of the central Pine Island Bay Trough, West Antarctica: *Quaternary Science Reviews*, v. 38, p. 1–10, doi:10.1016/j.quascirev.2011.12.017.

Jenkins, A., Dutrieux, P., Jacobs, S.S., McPhail, S.D., Perrett, J.R., Webb, A.T., and White, D., 2010, Observations beneath Pine Island Glacier in West Antarctica and implications for its retreat: *Nature Geoscience*, v. 3, p. 468–472, doi:10.1038/ngeo890.

Joughin, I., and Alley, R.B., 2011, Stability of the West Antarctic ice sheet in a warming world: *Nature Geoscience*, v. 4, p. 506–513, doi:10.1038/ngeo1194.

Joughin, I., Smith, B.E., and Holland, D.M., 2010, Sensitivity of 21st century sea level to ocean-induced thinning of Pine Island Glacier, Antarctica: *Geophysical Research Letters*, v. 37, L20502, doi:10.1029/2010GL044819.

Kirchner, A.E., Anderson, J.B., Jakobsson, M., O'Regan, M., Majewski, W., and Nitsche, F.O., 2012, Post-LGM deglaciation in Pine Island Bay, West Antarctica: *Quaternary Science Reviews*, v. 38, p. 11–26, doi:10.1016/j.quascirev.2012.01.017.

Livingstone, S.J.,   Cofaigh, C., Stokes, C.R., Hillenbrand, C.-D., Vieli, A., and Jamieson, S.S.R., 2012, Antarctic palaeo-ice streams: *Earth-Science Reviews*, v. 111, p. 90–128, doi:10.1016/j.earscirev.2011.10.003.

Lowe, A.L., and Anderson, J.B., 2002, Reconstruction of the West Antarctic ice sheet in Pine Island Bay during the Last Glacial Maximum and its subsequent retreat history: *Quaternary Science Reviews*, v. 21, p. 1879–1897, doi:10.1016/S0277-3791(02)00006-9.

Lowe, A.L., and Anderson, J.B., 2003, Evidence for abundant subglacial meltwater beneath the paleo-ice sheet in Pine Island Bay, Antarctica: *Journal of Glaciology*, v. 49, p. 125–138, doi:10.3189/172756503781830971.

McKay, R., Browne, G., Carter, L., Cowan, E., Dunbar, G., Krissek, L., Naish, T., Powell, R., Reed, J., Talarico, F., and Wilch, T., 2009, The stratigraphic signature of the late Cenozoic Antarctic ice sheets in the Ross Embayment: *Geological Society of America Bulletin*, v. 121, p. 1537–1561, doi:10.1130/B265401.

  Cofaigh, C., Evans, D.J.A., and Hiemstra, J.F., 2011, Formation of a stratified subglacial ‘till’ assemblage by ice-marginal thrusting and glacier overriding: *Boreas*, v. 40, p. 1–14, doi:10.1111/j.1502-3885.2010.00177.x.

Passchier, S., Browne, G., Field, B., Fielding, C.R., Krissek, L.R., Panter, K., and Pekar, S.F., and the ANDRILL-SMS Science Team, 2011, Early and Middle Miocene Antarctic glacial history from the sedimentary facies distribution in the AND-2A drill hole, Ross Sea, Antarctica: *Geological Society of America Bulletin*, v. 123, p. 2352–2365, doi:10.1130/B30334.1.

Pritchard, H.D., Ligtenberg, S.R.M., Fricker, H.A., Vaughan, D.G., van den Broeke, M.R., and Padman, L., 2012, Antarctic ice-sheet loss driven by basal melting of ice shelves: *Nature*, v. 484, p. 502–505, doi:10.1038/nature10968.

Rignot, E., 2008, Changes in West Antarctic ice stream dynamics observed with ALOS PALSAR data: *Geophysical Research Letters*, v. 35, L12505, doi:10.1029/2008GL033365.

Rignot, E., and Jacobs, S.S., 2002, Rapid bottom melting widespread near Antarctic Ice Sheet grounding lines: *Science*, v. 296, p. 2020–2023, doi:10.1126/science.1070942.

Rignot, E., Mouginot, J., and Scheuchl, B., 2011, Antarctic grounding line mapping from differential satellite radar interferometry: *Geophysical Research Letters*, v. 38, L10504, doi:10.1029/2011GL047109.

Smith, J.A., Hillenbrand, C.-D., Kuhn, G., Larter, R.D., Graham, A.G.C., Ehrmann, W., Moreton, S.G., and Forwick, M., 2011, Deglacial history of the West Antarctic Ice Sheet in the western Amundsen Sea Embayment: *Quaternary Science Reviews*, v. 30, p. 488–505, doi:10.1016/j.quascirev.2010.11.020.

Steig, E.J., Ding, Q., Battisti, D.S., and Jenkins, A., 2012, Tropical forcing of Circumpolar Deep Water Inflow and outlet glacier thinning in the Amundsen Sea Embayment, West Antarctica: *Annals of Glaciology*, v. 53, p. 19–28, doi:10.3189/2012AoG60A110.

Tinto, K.J., and Bell, R.E., 2011, Progressive unpinning of Thwaites Glacier from newly identified offshore ridge: Constraints from aerogravity: *Geophysical Research Letters*, v. 38, L20503, doi:10.1029/2011GL049026.

Vaughan, D.G., 2008, West Antarctic Ice Sheet collapse—The fall and rise of a paradigm: *Climatic Change*, v. 91, p. 65–79, doi:10.1007/s10584-008-9448-3.

Wingham, D.J., Wallis, D.W., and Shepherd, A., 2009, Spatial and temporal evolution of Pine Island Glacier thinning, 1995–2006: *Geophysical Research Letters*, v. 36, L17501, doi:10.1029/2009GL039126.

Manuscript received 29 March 2012

Revised manuscript received 3 July 2012

Manuscript accepted 3 July 2012

Printed in USA





Contents lists available at ScienceDirect

## Quaternary Science Reviews

journal homepage: [www.elsevier.com/locate/quascirev](http://www.elsevier.com/locate/quascirev)

Invited review

## Reconstruction of changes in the Amundsen Sea and Bellingshausen Sea sector of the West Antarctic Ice Sheet since the Last Glacial Maximum

Robert D. Larter<sup>a,\*</sup>, John B. Anderson<sup>b</sup>, Alastair G.C. Graham<sup>a,c</sup>, Karsten Gohl<sup>d</sup>, Claus-Dieter Hillenbrand<sup>a</sup>, Martin Jakobsson<sup>e</sup>, Joanne S. Johnson<sup>a</sup>, Gerhard Kuhn<sup>d</sup>, Frank O. Nitsche<sup>f</sup>, James A. Smith<sup>a</sup>, Alexandra E. Witus<sup>b</sup>, Michael J. Bentley<sup>g</sup>, Julian A. Dowdeswell<sup>h</sup>, Werner Ehrmann<sup>i</sup>, Johann P. Klages<sup>d</sup>, Julia Lindow<sup>j</sup>, Colm Ó Cofaigh<sup>g</sup>, Cornelia Spiegel<sup>j</sup>

<sup>a</sup> British Antarctic Survey, High Cross, Madingley Road, Cambridge CB3 0ET, UK<sup>b</sup> Department of Earth Sciences, Rice University, 6100 Main Street, Houston, TX 77005, USA<sup>c</sup> College of Life and Environmental Sciences, University of Exeter, Exeter EX4 4RJ, UK<sup>d</sup> Alfred Wegener Institute, Helmholtz-Centre for Polar and Marine Research, Am Alten Hafen 26, D-27568 Bremerhaven, Germany<sup>e</sup> Department of Geological Sciences, Stockholm University, 106 91 Stockholm, Sweden<sup>f</sup> Lamont-Doherty Earth Observatory of Columbia University, Palisades, NY, USA<sup>g</sup> Department of Geography, Durham University, South Road, Durham DH1 3LE, UK<sup>h</sup> Scott Polar Research Institute, University of Cambridge, Cambridge CB2 1ER, UK<sup>i</sup> Institute of Geophysics and Geology, University of Leipzig, Talstraße 35, D-04103 Leipzig, Germany<sup>j</sup> Department of Geosciences, University of Bremen, Bremen, Germany

## ARTICLE INFO

## Article history:

Received 28 March 2013

Received in revised form

4 October 2013

Accepted 15 October 2013

Available online xxx

## Keywords:

Ice sheet

Last Glacial Maximum

Holocene

Ice stream

Grounding line

Radiocarbon

Cosmogenic isotope

Surface exposure age

Multibeam swath bathymetry

Sediment

Glacimarine

Diamicton

Continental shelf

Circumpolar deep water

Subglacial meltwater

Sea level

## ABSTRACT

Marine and terrestrial geological and marine geophysical data that constrain deglaciation since the Last Glacial Maximum (LGM) of the sector of the West Antarctic Ice Sheet (WAIS) draining into the Amundsen Sea and Bellingshausen Sea have been collated and used as the basis for a set of time-slice reconstructions. The drainage basins in these sectors constitute a little more than one-quarter of the area of the WAIS, but account for about one-third of its surface accumulation. Their mass balance is becoming increasingly negative, and therefore they account for an even larger fraction of current WAIS discharge. If all of the ice in these sectors of the WAIS were discharged to the ocean, global sea level would rise by ca 2 m.

There is compelling evidence that grounding lines of palaeo-ice streams were at, or close to, the continental shelf edge along the Amundsen Sea and Bellingshausen Sea margins during the last glacial period. However, the few cosmogenic surface exposure ages and ice core data available from the interior of West Antarctica indicate that ice surface elevations there have changed little since the LGM. In the few areas from which cosmogenic surface exposure ages have been determined near the margin of the ice sheet, they generally suggest that there has been a gradual decrease in ice surface elevation since pre-Holocene times. Radiocarbon dates from glacimarine and the earliest seasonally open marine sediments in continental shelf cores that have been interpreted as providing approximate ages for post-LGM grounding-line retreat indicate different trajectories of palaeo-ice stream recession in the Amundsen Sea and Bellingshausen Sea embayments. The areas were probably subject to similar oceanic, atmospheric and eustatic forcing, in which case the differences are probably largely a consequence of how topographic and geological factors have affected ice flow, and of topographic influences on snow accumulation and warm water inflow across the continental shelf.

Pauses in ice retreat are recorded where there are "bottle necks" in cross-shelf troughs in both embayments. The highest retreat rates presently constrained by radiocarbon dates from sediment cores are found where the grounding line retreated across deep basins on the inner shelf in the Amundsen Sea, which is consistent with the marine ice sheet instability hypothesis. Deglacial ages from the Amundsen

\* Corresponding author.

E-mail addresses: [rdla@bas.ac.uk](mailto:rdla@bas.ac.uk), [rdlarter@gmail.com](mailto:rdlarter@gmail.com) (R.D. Larter).



Sea Embayment (ASE) and Eltanin Bay (southern Bellingshausen Sea) indicate that the ice sheet had already retreated close to its modern limits by early Holocene time, which suggests that the rapid ice thinning, flow acceleration, and grounding line retreat observed in this sector over recent decades are unusual in the context of the past 10,000 years.

© 2013 Elsevier Ltd. All rights reserved.

## 1. Introduction

### 1.1. Recent ice sheet change

Over recent decades, rapid changes have occurred in the sector of the West Antarctic Ice Sheet draining into the Amundsen and Bellingshausen seas (Fig. 1). These changes include thinning of ice shelves and thinning, flow velocity acceleration and grounding line retreat of ice streams feeding into them (Rignot, 1998, 2008; Pritchard et al., 2009, 2012; Scott et al., 2009; Wingham et al., 2009; Bingham et al., 2012). Ice shelves and ice streams in the ASE have exhibited the highest rates of change. These ice streams

include Pine Island Glacier (PIG) and Thwaites Glacier, which are the outlets from large drainage basins in the centre of the WAIS with a combined area of 417,000 km<sup>2</sup> (basin “GH”; Rignot et al., 2008). This amounts to about 60% of the area of the entire Amundsen-Bellingshausen sector as defined in Fig. 1 (ca 700,000 km<sup>2</sup>).

Modern snow accumulation rates in the sector are, on average, more than twice those in the drainage basins of the Siple Coast ice streams that flow into the Ross Ice Shelf (Arthern et al., 2006). Consequently, although the Amundsen-Bellingshausen sector comprises just a little more than a quarter of the area of the WAIS, it collects about one-third of the total accumulation. If the ice sheet

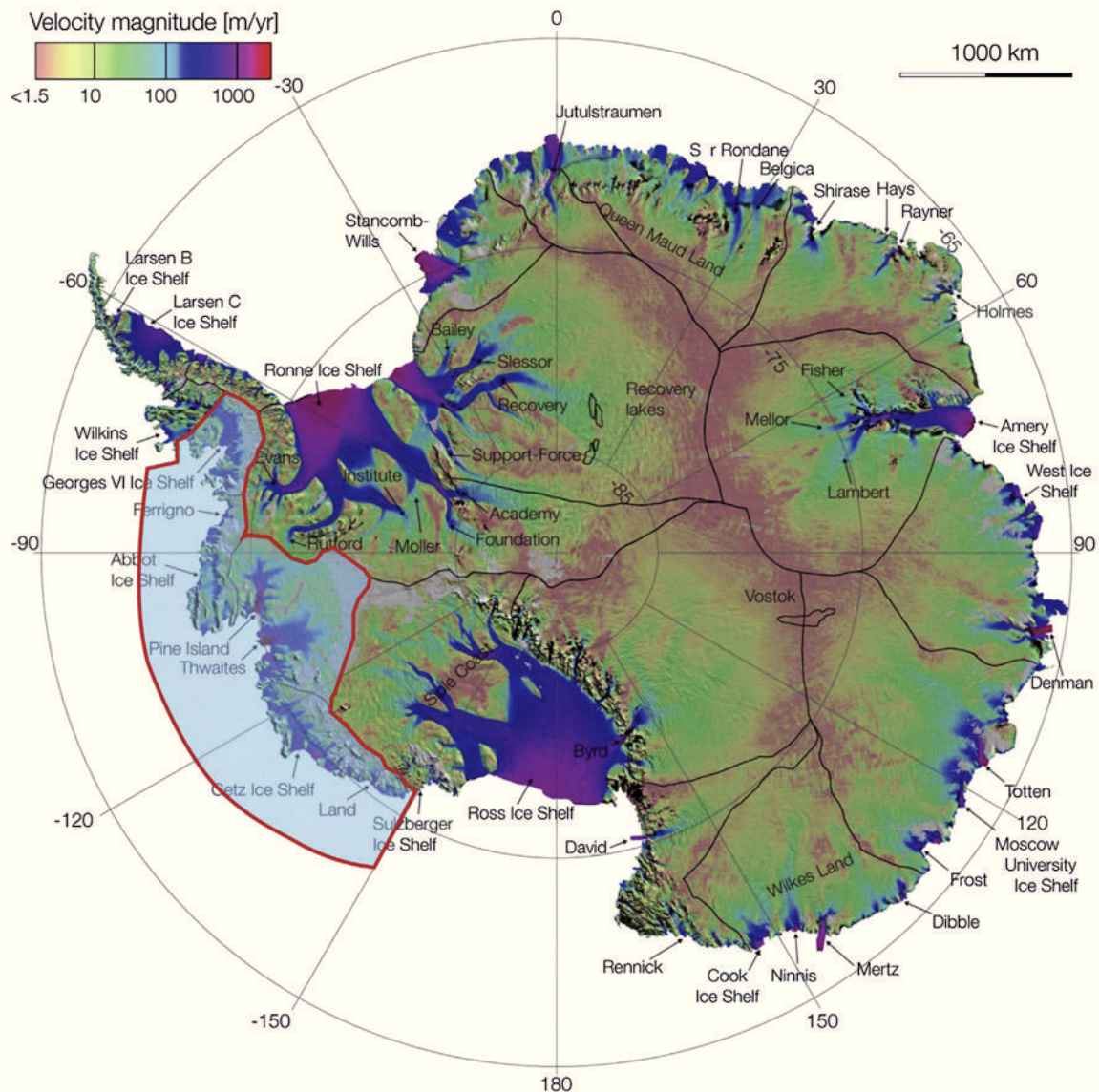


Fig. 1. Amundsen-Bellingshausen sector limits (red outline with semi-transparent blue fill) overlaid on map of Antarctic ice flow velocities and ice divides (black lines) from Rignot et al. (2011).



was in balance, this would imply that the sector also accounted for one-third of the total ice discharge. However, mass loss from the sector has increased over recent decades, such that by 2006 basin “GH” contributed  $37 \pm 2\%$  of the entire outflow from the WAIS ( $261 \pm 4 \text{ Gt yr}^{-1}$  out of a total of  $700 \pm 23 \text{ Gt yr}^{-1}$  according to Rignot et al., 2008). Since 2006 the rate of mass loss has continued to increase (Shepherd et al., 2012).

The accelerating changes to ice shelves and glaciers in the ASE over recent decades have focused renewed attention on concerns that climate change could eventually cause a rapid deglaciation, or “collapse”, of a large part of the WAIS (Mercer, 1978; Hughes, 1981; Bindschadler, 1998; Oppenheimer, 1998; Vaughan, 2008; Joughin and Alley, 2011). The total potential contribution to global sea level rise from the WAIS is 4.3 m, whereas the potential contribution from ice in the WAIS grounded below sea level, and therefore widely considered to be most vulnerable, is 3.4 m (Bamber et al., 2009b; Fretwell et al., 2013). The Pine Island and Thwaites drainage basins alone contain enough ice to raise sea level by 1.1 m (Rignot et al., 2002; Holt et al., 2006; Vaughan et al., 2006), and the total potential contribution from the whole Amundsen-Bellingshausen sector may be as much as 2 m. Future rapid dynamical changes in ice flow were identified as the largest uncertainty in projections of sea level rise in the Fourth Assessment Report of the Intergovernmental Panel on Climate Change, and it was stated in the report that the recently-observed accelerations in West Antarctic ice streams were an important factor underlying this uncertainty (Solomon et al., 2007).

Even before the above-described changes in ASE ice shelves and glaciers were known, Hughes (1981) had suggested a chain of events whereby reduction of ice shelf buttressing in Pine Island Bay (PIB) could cause flow acceleration of PIG and Thwaites Glacier, drawing down ice from their drainage basins, and ultimately leading to disintegration of the WAIS. This hypothesis developed from the realisation that the two ice streams drain large basins in the centre of the WAIS and are not buttressed by a confined and pinned ice shelf. Hughes (1981) encapsulated the hypothesis by coining the memorable description of the region as “The weak underbelly of the West Antarctic Ice Sheet”.

### 1.2. The need for long-term records of change

Recent rates of change in the Amundsen-Bellingshausen sector are undoubtedly too fast to be a simple continuation of a progressive deglaciation that started shortly after the LGM (23–19 cal ka BP). For example, grounding line retreat at a rate of  $>1 \text{ km/yr}$ , as measured on PIG (Rignot, 1998, 2008), would have resulted in deglaciation of the entire continental shelf within 500 years. Without considering records spanning thousands of years, however, there can be no certainty that the recent changes are not the latest phase of a step-wise retreat resulting from internal ice dynamic processes or variations in forcing parameters, or a combination of both. There is a growing consensus that the recent changes have been driven by increased inflow of relatively warm Circumpolar Deep Water (CDW) across the continental shelf, which has increased basal melting of ice shelves (Jacobs et al., 1996, 2011; Shepherd et al., 2004; Arneborg et al., 2012; Pritchard et al., 2012). However, historical observations do not provide any indication of when the inflow started to increase, and leave open the question of whether or not there have been previous periods since the LGM when similar inflow has driven phases of rapid retreat. Moreover, whereas some aspects of ice sheet response to external forcing occur within decades, other aspects of their response take centuries to millennia (e.g. conduction of surface temperature and advection of accumulated snow to the bed; changes in surface configuration resulting from shifting accumulation patterns; Bamber et al., 2007;

Bentley, 2010). Therefore, it is important to consider long-term records of change in order to fully test and calibrate ice sheet models, and improve confidence in their skill to predict future ice sheet contributions to sea-level rise. Records of ice sheet change spanning millennia are also important for modelling the glacial isostatic adjustment of the lithosphere, which is essential for calculating recent ice mass changes from satellite-measured changes in the Earth’s gravity field (Ivins and James, 2005; King et al., 2012; Lee et al., 2012; Whitehouse et al., 2012).

The amount of data available to constrain ice sheet change in the Amundsen-Bellingshausen sector over the past 25 ka has increased greatly since the start of this century. In this review we use the available data to inform a set of reconstructions depicting changes in the ice sheet in 5 ka steps. On the basis of the synthesis we also highlight significant data gaps and suggest some priorities for future research.

### 1.3. Sector definition

The divides between ice drainage sectors, which are now mostly well-defined from satellite remote sensing data (Bamber et al., 2009a), provide a practical basis for defining sector boundaries for ice sheet reconstruction studies. For the purposes of this review, we have used ice divides to define most of the Amundsen-Bellingshausen sector boundary (Fig. 1). At the western limit of the sector we extended the boundary with the Ross Sea sector northwards across the narrow continental shelf from where it meets the coast. At the eastern boundary of the sector, there must have been a palaeo-divide extending from Palmer Land across George VI Sound and Alexander Island, as marine geological and geophysical data provide compelling evidence that palaeo-ice streams flowed out of each end of George VI Sound (Ó Cofaigh et al., 2005a, 2005b; Hillenbrand et al., 2010a; Kilfeather et al., 2011; Bentley et al., 2011). The deglacial history of the northern arm of George VI Sound suggests that this divide must have been located on the southern part of Alexander Island (Bentley et al., 2005, 2011; Smith et al., 2007), although its position is not precisely constrained. We have tentatively drawn the palaeo-divide along the length of Latady Island and then northwards across the continental shelf (Fig. 1).

### 1.4. Geological factors that may influence ice dynamics

Following earlier development at the active Pacific margin of Gondwana, West Antarctica has been affected by several phases of rifting since mid-Cretaceous time, possibly continuing until as recently as the Middle Miocene (Cande et al., 2000; Siddoway et al., 2005; Granot et al., 2010). As a consequence, most of the continental crust in the Amundsen-Bellingshausen sector is relatively thin and dissected by rift basins (Gohl et al., 2007, 2013a; Jordan et al., 2010; Bingham et al., 2012; Gohl, 2012). Gohl (2012) and Gohl et al. (2013a) postulated that tectonic lineaments inherited from continental breakup and rift basins have influenced the major ice-flow paths of the Amundsen Sea shelf. Bingham et al. (2012) proposed that intersections of rift basins with the ice sheet margin have steered palaeo-ice streams paths across the shelf, and that many of the cross shelf troughs eroded by the ice streams now channel inflow of CDW to the grounding line. The parts of the grounding line in such troughs are likely to be particularly vulnerable to retreat due to reverse gradients on the ice bed leading back to the deepest parts of the basins, and possibly also elevated geothermal heat flow as a legacy of the Neogene rifting (Bingham et al., 2012).

Tomographic inversions of earthquake seismic data show that much of West Antarctica overlies a region of relatively warm upper



mantle centred beneath Marie Byrd Land (Danesi and Morelli, 2000; Shapiro and Ritzwoller, 2004). The warm mantle is probably associated with elevated geothermal heat flow (Shapiro and Ritzwoller, 2004), but there are no published heat flow measurements to confirm this. The region is volcanically active, and eruptions since mid-Oligocene time have constructed 18 large volcanoes in Marie Byrd Land with exposed volumes up to 1800 km<sup>3</sup> (LeMasurier et al., 1990). Although volcanic edifices beyond Marie Byrd Land are smaller, the alkaline volcanic province they are part of extends across the entire Amundsen-Bellingshausen sector and along the Antarctic Peninsula (Hole and LeMasurier, 1994; Finn et al., 2005). Of the large volcanoes in Marie Byrd Land, Mount Berlin and Mount Takahē are known to have erupted since the LGM (Wilch et al., 1999). A volcano in the Hudson Mountains, north of PIG, erupted only ca 2200 year ago (Corr and Vaughan, 2008). There may have been other eruptions in the sector since the LGM that are yet to be detected. In addition to local effects around the eruption sites and a temporary, more widespread effect of tephra deposition on ice surface albedo, eruptions could have affected ice dynamics by supplying meltwater to the ice sheet bed.

## 2. Methods

### 2.1. Marine survey data

Echo sounding data collected over many decades and multi-beam swath bathymetry data collected during the past two decades have been collated to produce regional bathymetric grids for the Amundsen Sea (Nitsche et al., 2007, 2013) and Bellingshausen Sea (Graham et al., 2011). These grids have recently been incorporated into Bedmap2 (Fretwell et al., 2013), which we have used to produce the regional basemaps for this review.

We have used more detailed, local grids generated from multi-beam swath bathymetry data to map areas in which streamlined bedforms occur and the positions of features such as grounding zone wedges (GZWs) that represent past limits of grounded ice extent. Multibeam data have been collected on the continental shelf in the sector on numerous research cruises of RVIB *Nathaniel B. Palmer*, RV *Polarstern*, RRS *James Clark Ross* and *IB Oden*. The extent of individual surveys is described in subsequent sections. Most data were collected using Kongsberg multibeam systems (EM120/EM122) that transmit at ca 12 kHz. Surveys before 2002 on RVIB *Nathaniel B. Palmer* were conducted using a Seabeam 2112 system, which also transmits at 12 kHz, whereas Hydrosweep DS-1 and DS-2 systems that transmit at 15 kHz were used on RV *Polarstern*. These systems are all capable of surveying swaths with a width more than three times the water depth and collecting data with vertical precision better than a metre at the depths on the continental shelf. The spatial accuracy of the data, referenced to ship positions determined using GPS, is better than a few metres.

Acoustic sub-bottom profiler data were also collected during most multibeam swath bathymetry surveys, and on many other cruises, using systems that transmit signals in the range 1.5–5 kHz. These data provide information about the physical nature of the upper few metres, or sometimes several tens of metres, of seabed sediments, which is helpful in interpreting geomorphic features observed in multibeam data (e.g. Graham et al., 2010; Klages et al., 2013) and also valuable for selecting sediment core sites. On many parts of the continental shelf, hemipelagic sediments deposited since glacial retreat in seasonally open water conditions have an acoustically-laminated character on sub-bottom profiles. Such sediments are often observed to overlie less well-laminated or acoustically-transparent units, which sediment cores typically reveal as being deglacial transitional sediments or low-shear-

strength diamictos (e.g. Dowdeswell et al., 2004; Ó Cofaigh et al., 2005b). On some parts of the continental shelf these latter types of sediments occur with little or no cover of acoustically-laminated sediments, whereas in other areas any acoustic stratigraphy that was once present has been disrupted as a result of ploughing by iceberg keels. In still other areas bedrock or high-shear-strength diamictos, which sub-bottom profiler signals cannot penetrate, occur with little or no glacial marine sediment cover.

Seismic reflection profiles acquired using airgun sources have been collected on the continental shelf during several research cruises on RV *Polarstern*, RRS *James Clark Ross* and RVIB *Nathaniel B. Palmer* over the past two decades. Airgun sources generate signals with frequencies that range from less than 10 Hz to a few hundred Hz, and these penetrate much further into the subsurface than the higher frequencies transmitted by acoustic sub-bottom profiling systems. The primary aim in collecting such data has usually been to study geological structure and patterns of sediment erosion and deposition over millions of years. However, airgun seismic data also provide a means of examining the thickness and internal stratigraphy of sedimentary units deposited during the last glacial cycle that are too thick, too coarse grained or too compacted for acoustic sub-bottom profiler signals to penetrate (e.g. high shear strength diamictos, GZWs and meltwater channel infills).

### 2.2. Continental shelf sediment cores

Sediment cores have been collected on the Amundsen-Bellingshausen sector continental shelf on many research cruises using a range of different coring devices, including gravity corers, piston corers, kasten corers, vibrocorers and box corers. [Supplementary Table 1](#) lists all cores collected on the continental shelf that recovered more than 1 m of sediment. Cores that recovered <1 m of sediment, but from which radiocarbon dates have been obtained are also included in [Supplementary Table 1](#).

Shelf sediment cores have typically recovered a succession of facies in which diamictos are overlain by gravelly and sandy muds, which are in turn overlain by a layer of predominantly terrigenous mud bearing scarce diatoms, foraminifera and ice-rafted debris (IRD) that varies in thickness from a few centimetres to a few metres. This succession of facies has been widely interpreted as recording grounding line retreat (Wellner et al., 2001; Hillenbrand et al., 2005, 2010a, 2013; Smith et al., 2009, 2011; Kirshner et al., 2012; Klages et al., 2013). Some diamictos have been interpreted as having been deposited in a proximal glacial marine setting (e.g. ones containing scarce microfossils or some stratification), whereas others have been interpreted as having formed subglacially (Wellner et al., 2001; Hillenbrand et al., 2005; Smith et al., 2011; Kirshner et al., 2012). Within diamictos interpreted as having a subglacial origin, particularly in cores from cross-shelf troughs, a downward transition is often observed from low shear strength diamicton (“soft till”; usually < 25 kPa) to diamicton with higher shear strength (“stiff till”; Wellner et al., 2001; Ó Cofaigh et al., 2007; Hillenbrand et al., 2005, 2010a; Smith et al., 2009, 2011; Kirshner et al., 2012; Klages et al., 2013). The soft tills probably formed as dilated sediment layers like those observed beneath some modern ice streams (Alley et al., 1987; Tulaczyk et al., 1998; Kamb, 2001; Dowdeswell et al., 2004; Smith and Murray, 2009; Smith et al., 2013). The uppermost mud facies is generally considered to have been deposited in a setting distal from the grounding line in seasonally open water conditions (Wellner et al., 2001; Hillenbrand et al., 2005; Kirshner et al., 2012).

Locally, cores have recovered a variety of other facies types that are significant for reconstructing processes and the progress of deglaciation. A few examples are: (1) in deep inner shelf basins in



the western ASE, a diatom ooze layer was deposited soon after ice had retreated from the area (Hillenbrand et al., 2010b; Smith et al., 2011); (2) in the mid-shelf part of Pine Island Trough, a homogenous mud unit that contains very little IRD has been interpreted as a sub-ice shelf facies (Kirshner et al., 2012); (3) in the axis of a seabed channel in PIB, a unit comprising well-sorted sands and gravels has been interpreted as having been deposited from subglacial meltwater (Lowe and Anderson, 2003).

### 2.3. Dating of core samples

Supplementary Table 2 lists 207 published accelerator mass spectrometry (AMS)  $^{14}\text{C}$  dates obtained on samples from sediment cores collected in this sector. These comprise 41 dates on sea-floor surface (or near-surface) samples and 166 dates on samples taken down core. One of the surface dates and three of the down-core dates are previously unpublished.

It is widely accepted that calcareous microfossils provide the most reliable AMS  $^{14}\text{C}$  dates from marine sediments, but the scarcity of such microfossils in many Antarctic sediment cores has driven researchers to attempt to date other carbon-bearing materials (Andrews et al., 1999; Heroy and Anderson, 2007; Rosenheim et al., 2008). Where present, other carbonate materials (e.g. bryozoans or shell fragments) have been dated, but in many cores these are also lacking and the only carbon available is in organic matter from bulk sediment samples. Acid-insoluble organic matter (AIOM) is mainly derived from diatomaceous organic matter, and its dating has been widely applied to provide age models for sediment cores recovered from the Antarctic shelf (e.g. Licht et al., 1996, 1998; Andrews et al., 1999; Domack et al., 1999; Ó Cofaigh et al., 2005a; Pudsey et al., 2006; Hillenbrand et al., 2010a, 2010b).

AMS  $^{14}\text{C}$  dates on AIOM, however, are often biased by fossil carbon derived from glacial erosion of the Antarctic continent and by reworking of unconsolidated sediments. Such contamination by fossil carbon can be demonstrated in sea-floor surface sediments by paired AMS  $^{14}\text{C}$  dating of AIOM and foraminifera (where foraminifera are present) or comparison of  $^{14}\text{C}$  dates on AIOM to  $^{210}\text{Pb}$  profiles (e.g. Hillenbrand et al., 2010a, 2010b). Circumstantial evidence of such contamination is also provided by the fact that dates on AIOM in surface sediments vary by up to several thousand years between different regions of the Antarctic shelf and even between different core sites in the same region (e.g. Andrews et al., 1999; Pudsey et al., 2006).

Even for cores where several down-core AMS  $^{14}\text{C}$  dates on AIOM yield ages in correct stratigraphic order, a sharp increase in reported ages with depth within deglacial transitional sediments (typically sandy gravelly muds) is often observed. This sharp increase has been referred to as a “dog leg”, and interpreted as the result of a down-core increase in fossil carbon contamination within the transitional unit, implying that the dates from its lower part are unreliable (Pudsey et al., 2006; Heroy and Anderson, 2007). While such a rapid increase in AMS  $^{14}\text{C}$  ages with depth could result from much slower sedimentation rates in the deglacial unit than in the overlying sediments, glacial marine sedimentation models (e.g. Powell, 1984) generally imply that relatively high sedimentation rates are expected in this unit, and therefore the “dog-leg” is unlikely to result from a down-core change in sedimentation rate.

The occurrence of old surface ages combined with potential variability in the amount of fossil carbon contamination down core complicates the reliability of age models derived from AMS  $^{14}\text{C}$  dating of AIOM for Antarctic post-LGM sedimentary sequences. Usually, down-core AIOM ages are corrected by subtracting the core-top age (e.g. Andrews et al., 1999; Domack et al., 1999; Mosola and Anderson, 2006; Pudsey et al., 2006). This approach assumes that (1) the core top represents modern sedimentation, and (2) the

contribution of reworked fossil carbon from the hinterland remained constant through time. The first assumption can be validated by deploying coring devices that are capable of recovering undisturbed sediment samples from the modern seabed surface (e.g. box and multiple corers), paired  $^{14}\text{C}$  dating of the AIOM and calcareous microorganisms (if present) and application of  $^{210}\text{Pb}$  dating in addition to AIOM  $^{14}\text{C}$  dating (e.g. Harden et al., 1992; Andrews et al., 1999; Domack et al., 2001, 2005; Pudsey et al., 2006). The validity of the second assumption might be tested by paired  $^{14}\text{C}$  down-core dating of both AIOM and calcareous material, if the latter is present in any cores in a study area (e.g. Licht et al., 1998; Domack et al., 2001; Licht and Andrews, 2002; Rosenheim et al., 2008).

In Supplementary Table 2, most dates on AIOM have been corrected by subtracting a core-top age from the same or a nearby core. A few dates on AIOM from sediment cores in the Bellingshausen Sea have been corrected by subtracting the difference between paired core-top ages on AIOM and foraminifera. In each case the correction procedure is explained in the “Comments” column in Supplementary Table 2. Age calibrations to convert  $^{14}\text{C}$  years to calendar years were carried out using the CALIB Radiocarbon Calibration Program version 6.1.0. We used the Marine09 calibration dataset (Reimer et al., 2009) and a marine reservoir effect correction of  $1300 \pm 70$  years (Berkman and Forman, 1996) for consistency with age calibrations in other sector reviews in this volume, although the range of ages from the 14 calcareous core-top samples listed in Supplementary Table 2 is somewhat greater than the quoted uncertainty. Ages quoted in subsequent sections are calibrated ages unless stated otherwise.

The oldest AMS  $^{14}\text{C}$  age in each core that was considered as providing a reliable constraint on deglaciation by the authors who originally published it is shown in bold type in Supplementary Table 2. Older ages that occur in some cores are either on diamicton or from transitional deglacial sediments in which the age may be significantly biased by fossil carbon (i.e. part of a “dog leg” in down-core age progression). It is important to bear in mind that the ages shown in bold type in Supplementary Table 2 are *minimum* ages for grounding line retreat. In contrast, ages obtained on diamicton recovered at the base of some cores are likely to represent maximum ages for the preceding ice advance, since the dated material was probably derived from previously deposited shelf sediments that were incorporated into the diamicton (Hillenbrand et al., 2010a).

Relative palaeomagnetic intensity measurements have been used to provide additional constraints on age of deglaciation for a small number of cores recovered in the western ASE (Hillenbrand et al., 2010b).

### 2.4. Onshore survey data

Airborne and oversnow radio echo sounding data and oversnow seismic soundings collected over many decades have recently been collated into Bedmap2 (Fretwell et al., 2013). The PIG and Thwaites Glacier drainage basins are covered by systematic airborne surveys with 15–30 km line spacing (Holt et al., 2006; Vaughan et al., 2006), but in some other parts of the sector sounding data remain very sparse (Fretwell et al., 2013).

### 2.5. Terrestrial exposure age data

Published terrestrial data on the timing of deglaciation of this sector is limited to 16  $^{10}\text{Be}$  and 3  $^{26}\text{Al}$  surface exposure ages. Some published ages are also available from locations outside, but close to, the margins of the sector, for example from the Ford Ranges of Marie Byrd Land, Mount Waesche in the interior of West Antarctica,

XXV



and Two Step Cliffs in eastern Alexander Island, so we have included those in addition. These ages are shown in [Supplementary Table 3](#), with data used to calculate the  $^{10}\text{Be}$  and  $^{26}\text{Al}$  ages in [Supplementary Table 4](#). All  $^{10}\text{Be}$  and  $^{26}\text{Al}$  concentrations reported are blank-corrected. We have recalculated the published  $^{10}\text{Be}$  and  $^{26}\text{Al}$  ages in order to make them comparable across the sector. This was achieved by incorporating the published information about each sample into version 2.2 of the CRONUS-Earth online exposure age calculator ([Balco et al., 2008](#)). We applied the erosion rate that the original authors assumed (zero in all cases), quartz density of  $2.7\text{ g cm}^{-3}$  for each sample, and used the Antarctic pressure flag ('ant') for the input file. We took  $^{10}\text{Be}$  and  $^{26}\text{Al}$  concentrations, sample thicknesses, and shielding corrections from the original papers.

We have chosen to report all the  $^{10}\text{Be}$  and  $^{26}\text{Al}$  exposure ages in reference to the global production rates ([Balco et al., 2008](#); CRONUS v.2.2), since these are currently the most widely used. Since the calibration sites on which this  $^{10}\text{Be}$  production rate is based are in the Northern Hemisphere,  $^{10}\text{Be}$  exposure ages from sites in Antarctica have to be calculated by extrapolating production rates from the Northern Hemisphere to the Southern Hemisphere using one of five published scaling schemes ('St': [Lal, 1991](#); [Stone, 2000](#); 'De': [Desilets et al., 2006](#); 'Du': [Dunai, 2001](#); 'Li': [Lifton et al., 2005](#); 'Lm': [Lal, 1991](#); [Stone, 2000](#); [Nishiizumi et al., 1989](#)). Here we report exposure ages based on the most commonly-used scaling scheme, 'St'. We did not apply a geomagnetic correction. The  $^3\text{He}$  and  $^{36}\text{Cl}$  ages from Mt Waesche ([Ackert et al., 1999](#)) reported here have not been recalculated.

## 2.6. Ice core constraints on past ice surface elevation

Past ice surface elevations can be estimated from total gas content in ice cores, as this is a function of past atmospheric pressure (elevation of the site) and, to a lesser extent, palaeo-temperature ([Raynaud and Lebel, 1979](#); [Martinierie et al., 1992](#)). The latter variable can be constrained by parameters measured on the ice cores themselves, such as oxygen and hydrogen isotope ratios. The WAIS Divide ice core site at  $79^\circ 28' \text{ S}$ ,  $112 05' \text{ W}$  ([Fig. 2](#)), where drilling started in 2005 and has recently been completed (austral summer 2012–2013; <http://www.waisdivide.unh.edu/>; [WAIS Divide Project Members, 2013](#)), is the only location from which a deep ice core has been recovered in the Amundsen–Bellingshausen sector, but no palaeo-elevation estimates based on it have yet been published. Results from the Byrd Station ice core, (drilled at  $80^\circ 01' \text{ S}$ ,  $119^\circ 31' \text{ W}$  in the Ross Sea sector of the WAIS; [Fig. 2](#)), however, provide valuable constraints on changes in ice surface elevation since the LGM in the interior of the WAIS (see [Section 3.2](#) for details).

## 3. Datasets

### 3.1. Amundsen Sea marine studies

#### 3.1.1. Geophysical surveys and geomorphological studies

The first marine geoscientific investigations on the Amundsen Sea continental shelf ([Fig. 2](#)) were carried out on the "Deep Freeze" cruises on the USCGC *Glacier* in 1981 and 1985 ([Anderson and Myers, 1981](#); [Kellogg and Kellogg, 1987a, 1987b](#)). Echo sounding data and sub-bottom profiles collected with a sparker system on the 1985 cruise revealed deep troughs on the inner shelf in the eastern part of the ASE, which [Kellogg and Kellogg \(1987a\)](#) suggested represent paths of palaeo-ice streams.

The first systematic echo sounding survey on the ASE shelf was carried out during the 'South Pacific Rim International Tectonic Expedition' (SPRITE) aboard RV *Polar Sea* in 1992. This provided a

preliminary bathymetric map of a cross-shelf trough extending from inner PIB to the mid-shelf ([SPRITE Group and Boyer, 1992](#)), which we refer to as Pine Island Trough (PIT; [Fig. 3](#)). In 1994, single beam echo-sounding data from the outer shelf in the eastern ASE and from the outer and middle shelf in the western ASE were collected during expedition ANT-XI/3 with RV *Polarstern* ([Miller and Grobe, 1996](#)). The first multichannel seismic profile extending onto the shelf in the region was also collected in the eastern ASE during the same expedition ([Nitsche, 1998](#); [Nitsche et al., 1997, 2000](#); [Gohl et al., 2013b](#)).

The first multibeam swath bathymetry data from the ASE were collected on RVIB *Nathaniel B. Palmer* Cruise NBP9902 in 1999 ([Anderson et al., 2001](#); [Wellner et al., 2001](#); [Lowe and Anderson, 2002, 2003](#)). A single-channel seismic reflection profile extending along PIT from the inner shelf to the shelf edge was collected on the same cruise ([Lowe and Anderson, 2002, 2003](#); [Jakobsson et al., 2012](#); [Gohl et al., 2013b](#)). Using these data, [Lowe and Anderson \(2002, 2003\)](#) identified a set of geomorphic zones along PIT, from glacially-scoured crystalline basement on the inner shelf, through glacially lineated surfaces over sedimentary strata and a large GZW on the middle shelf, to a pervasively iceberg-furrowed surface on the outer shelf. [Wellner et al. \(2001\)](#) and [Lowe and Anderson \(2002, 2003\)](#) also presented multibeam swath bathymetry data that revealed evidence of an extensive subglacial meltwater drainage network having been active in PIB.

Subglacial bedforms revealed by sparse swath bathymetry data covering parts of the seabed directly offshore from the easternmost Getz Ice Shelf were presented by [Wellner et al. \(2001\)](#) and led these authors and [Anderson et al. \(2001\)](#) to the conclusion that another palaeo-ice stream trough is present in this part of the ASE, which we refer to as Dotson-Getz Trough (DGT; [Fig. 3](#)). Sparse swath bathymetry data collected still farther west, in Wrigley Gulf, were interpreted by [Anderson et al. \(2001\)](#) as evidence of another palaeo-ice stream trough, which we refer to as Wrigley Gulf Trough (WGT; [Fig. 2](#)). Seismic reflection data collected on the same cruise revealed a significant geological boundary running across the ASE, between acoustic basement underlying the inner shelf and sedimentary strata underlying middle and outer shelf areas ([Wellner et al., 2001, 2006](#); [Lowe and Anderson, 2002](#)). [Wellner et al. \(2001, 2006\)](#) observed that this boundary coincided with a change in the types of bedforms observed in multibeam swath bathymetry data and suggested that it had exerted a significant influence on past ice dynamics.

Early in 2000, further multibeam swath bathymetry data were collected on RVIB *Nathaniel B. Palmer* Cruise NBP0001. The most significant addition to swath bathymetry coverage during this cruise was over the former subglacial meltwater drainage network in PIB ([Nitsche et al., 2013](#)).

[Evans et al. \(2006\)](#) presented multibeam swath bathymetry showing elongated bedforms near the shelf edge in a trough that branches off from PIT in a northwestward direction, and which we refer to as Pine Island Trough West (PITW). The authors interpreted these bedforms as having formed at the base of a fast flowing ice stream ([Fig. 4](#)). These data were collected on RRS *James Clark Ross* Cruise JR84 in 2003. Acoustic sub-bottom profiler data collected on the same cruise did not reveal any discernible post-glacial sediment layer overlying the bedforms, and [Evans et al. \(2006\)](#) interpreted this as evidence that the WAIS grounding line had advanced to the shelf edge during the last glaciation.

Co-ordinated cruises on RRS *James Clark Ross* (JR141) and RV *Polarstern* (ANT-XXIII/4) early in 2006 collected extensive multibeam bathymetry, sub-bottom profiler and seismic reflection data off the Dotson and eastern Getz ice shelves in the western part of the ASE ([Larter et al., 2007](#); [Gohl, 2007](#); [Weigelt et al., 2009, 2012](#)). The multibeam data revealed a varied assemblage of landforms,



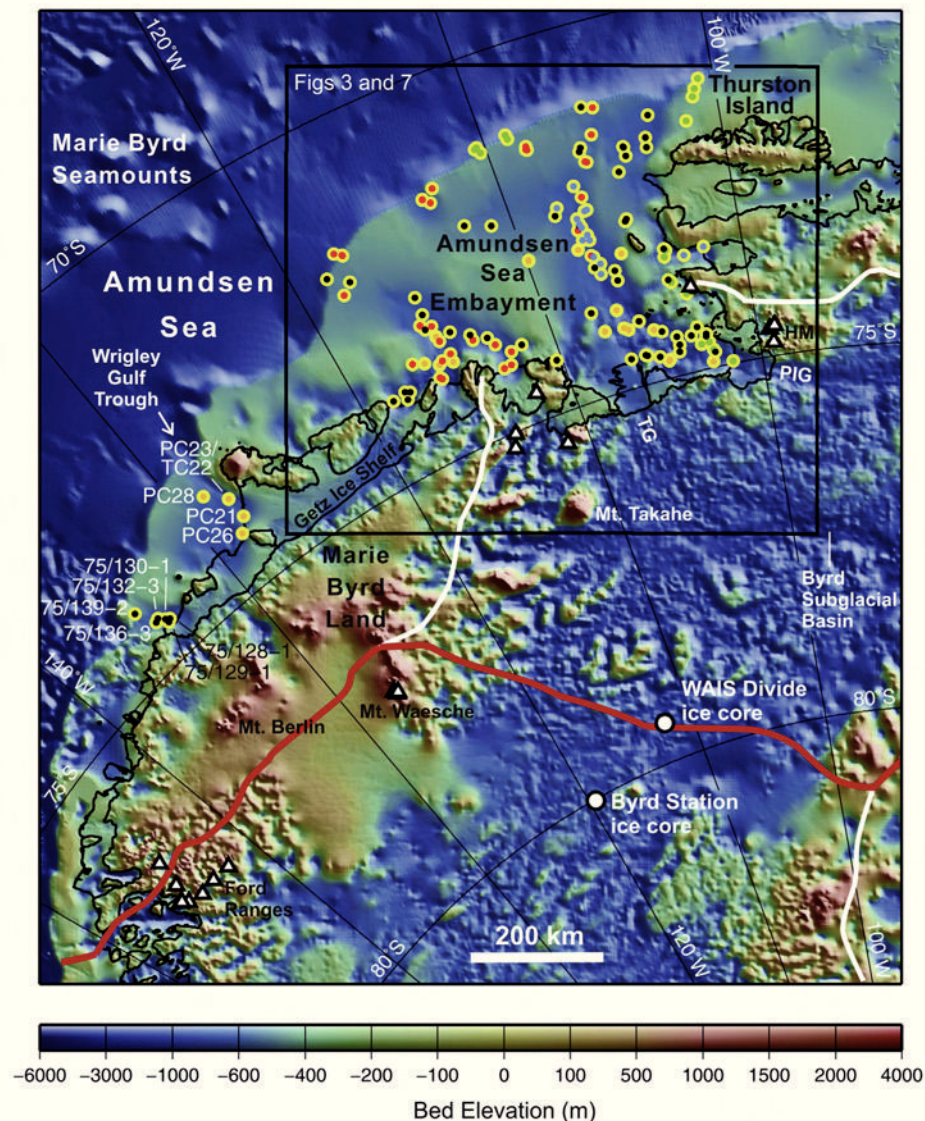


**Fig. 2.** Map of the Amundsen Sea region showing continental shelf sediment core sites (yellow circles), cosmogenic surface exposure age sample locations (white-filled triangles) and deep ice core sites (white-filled circles), overlaid on Bedmap2 ice sheet bed and bathymetry (Fretwell et al., 2013), which is displayed with shaded-relief illumination from the upper right. Sediment core sites are shown for cores that recovered more than 1 m of sediment and for shorter cores from which AMS  $^{14}\text{C}$  dates have been obtained. Core site symbol fill colour indicates ship the core was collected on: green – USCGC *Glacier*; orange – RVIB *Nathaniel B. Palmer*; red – RRS *James Clark Ross*; black – RV *Polarstern*; blue – IB *Oden*. Thick red line marks sector limit, along the main ice divide between the Amundsen Sea and the Ross Sea. Thick white lines mark other major ice divides. Black rectangle outlines area shown in greater detail in Figs. 3 and 7. Core sites outside the area shown in Figs. 3 and 7 are labelled with the core ID. PIG – Pine Island Glacier; TG – Thwaites Glacier; HM – Hudson Mountains.

some of which were indicative of formerly extensive fast ice flow in three glacially-eroded troughs that merge into the DGT (Fig. 3), even though acoustic basement is exposed at the sea floor across most of the inner shelf (Graham et al., 2009; Larter et al., 2009). This implies that the onset of fast flow was not fixed at the geological boundary identified by Wellner et al. (2001) throughout past glacial periods. Graham et al. (2009) interpreted multibeam data together with acoustic sub-bottom profiles and seismic profiles from the DGT and its tributaries, and argued that the varied assemblage of landforms observed over the inner shelf represents a multi-temporal record of past ice flow, not simply a “snapshot” of conditions immediately prior to the last deglaciation. The absence of any morphological features on bathymetric profiles along the outer shelf part of the DGT that could potentially represent a limit of grounding line advance during the LGM was interpreted by Larter et al. (2009) as evidence that the last advance reached the shelf edge.

Multibeam data over the innermost part of one of the troughs in front of the eastern Getz Ice Shelf revealed evidence of an extensive channel network interpreted as having been eroded by subglacial meltwater, similar to the one previously described in PIB (Graham et al., 2009; Larter et al., 2009). During the JR141 and ANT-XXIII/4 research cruises, additional acoustic and seismic profiles were also collected from outer continental shelf and slope of the ASE (Gohl, 2007; Gohl et al., 2007; Larter et al., 2007). RV *Polarstern* also reached inner PIB, and multichannel seismic profiles collected in PIB and along a corridor near the eastern coast of the ASE were interpreted as indicating differences in rate of glacial retreat and basal meltwater activity between these two areas (Uenzelmann-Neben et al., 2007).

Nitsche et al. (2007) compiled all of the single beam and multibeam echo sounding data available up to 2007, producing a continuous gridded regional bathymetry map of the Amundsen Sea that provided the first accurate representation of the continental



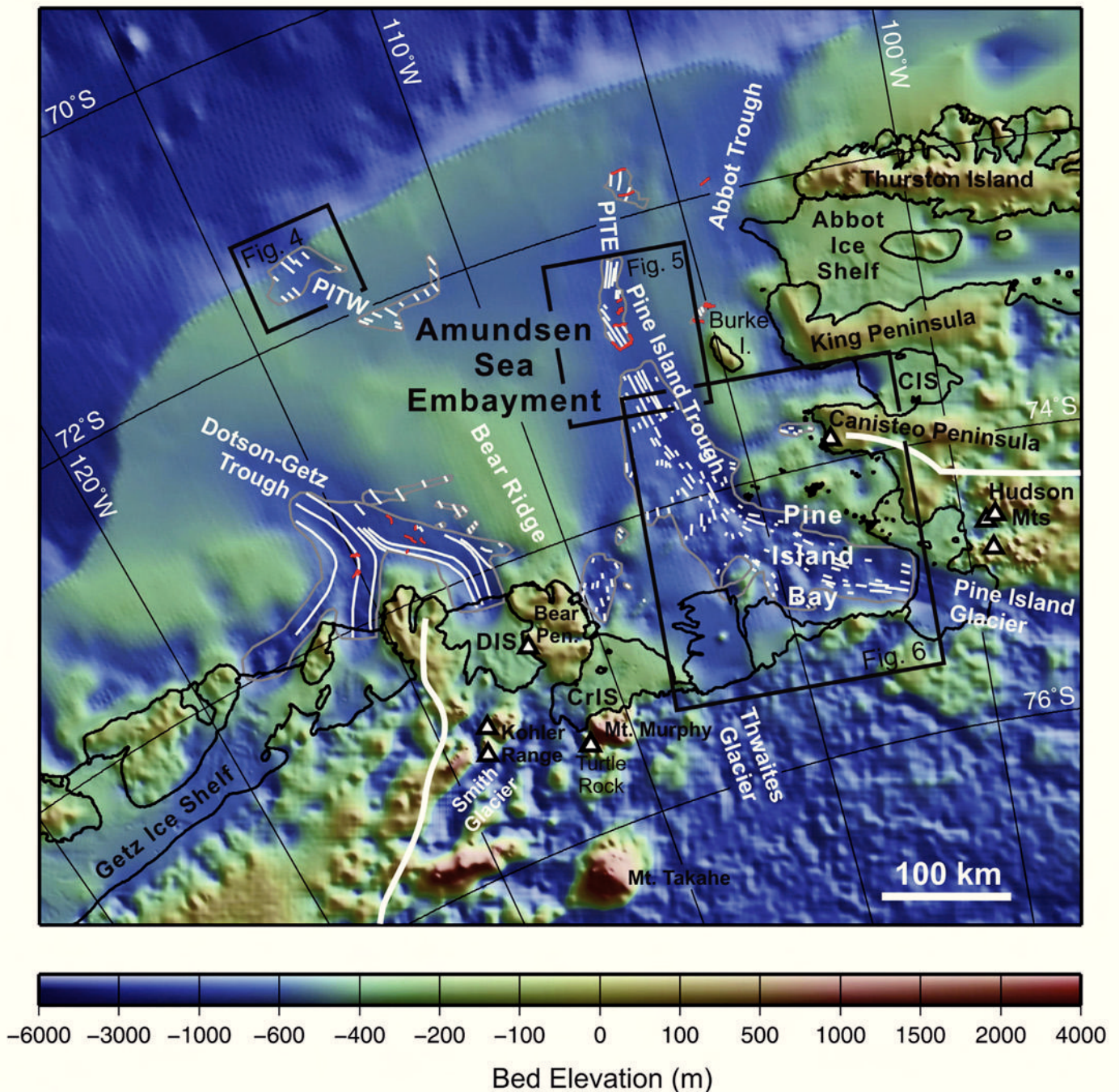


**Fig. 3.** Map of the Amundsen Sea Embayment showing main geomorphological features on the continental shelf and cosmogenic surface exposure age sample locations onshore, overlaid on Bedmap2 ice sheet bed and bathymetry (Fretwell et al., 2013), which is displayed with shaded-relief illumination from the upper right. Grey outlines mark areas in which bedforms indicative of past ice flow direction are observed in multibeam swath bathymetry data. Thin white lines indicate flow alignment. Red lines mark the crests of grounding zone wedges and moraines that represent past grounding line positions. Thick white lines mark major ice divides. Black rectangles outline areas shown in greater detail in Figs. 4–6. CIS – Cosgrove Ice Shelf; CrIS – Crosson Ice Shelf; DIS – Dotson Ice Shelf; PITE – Pine Island Trough East; PITW – Pine Island Trough West.

slope and major cross shelf troughs (Figs. 2 and 3). In addition to PIT, PITW, DGT and WGT, the data also showed additional troughs that extend seawards from other ice shelf fronts along the eastern

ASE coast (e.g. a trough extending NNE-wards from the Abbot Ice Shelf, which is referred to as 'Abbot Trough' by Hochmuth and Gohl, 2013; Gohl et al., 2013b), the Crosson Ice Shelf and various sections

xxviii



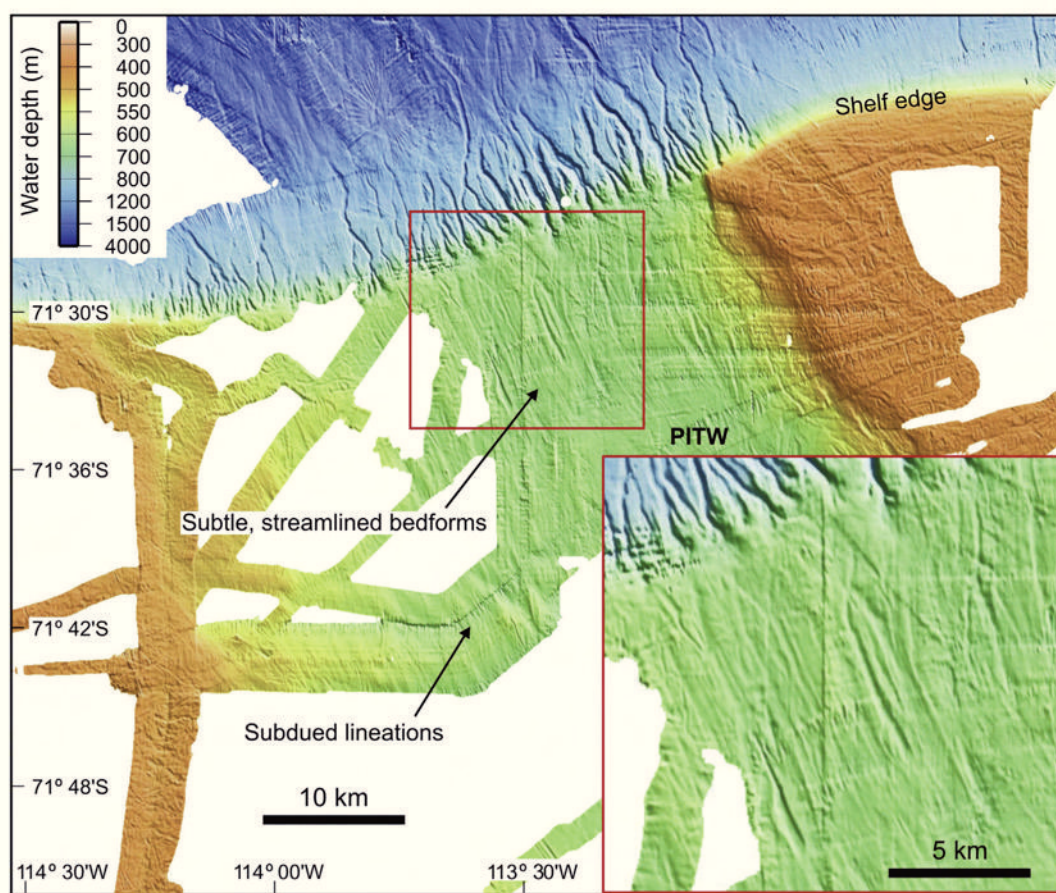


**Fig. 4.** Multibeam swath bathymetry data from the outer part of Pine Island Trough West showing streamlined bedforms. Data shown were collected on RRS *James Clark Ross* cruises JR84 and JR141, RVIB *Nathaniel B. Palmer* cruises NBP0001 and NBP0702, and RV *Polarstern* cruise ANT-XXIII/4. The grid was generated using a near neighbour algorithm, has a cell size of 50 m and is displayed with shaded-relief illumination from 65° (modified from Graham et al., 2010).

of the Getz Ice Shelf (e.g. a small glacial trough extending north-westwards from the westernmost Getz Ice Shelf). A possible tectonic basement control for the locations of the main palaeo-ice stream troughs in the ASE has recently been suggested by Gohl (2012). One multibeam swath bathymetry dataset included in the compilation by Nitsche et al. (2007) that has not been mentioned above was collected early in 2007 on RVIB *Nathaniel B. Palmer* cruise NBP0702. The additional multibeam data collected on that cruise improved definition of the continental shelf break and augmented previous coverage of inner shelf areas, including PIB (Nitsche et al., 2007).

Guided by the Nitsche et al. (2007) bathymetry map, multibeam swath bathymetry data were collected in a continuous corridor from the continental shelf edge along the axis of the eastern branch of PIT (PITE; Fig. 3) and the main trunk of the trough to PIB on RRS *James Clark Ross* Cruise JR179 early in 2008. Two overlapping swaths were collected along most of this corridor and in places the coverage also overlapped with data collected on previous cruises (NBP9902, NBP0001, JR141 and ANT-XXIII/4). Streamlined landforms observed along this corridor confirmed that it represented a flow-line of former ice motion, at least to within 68 km of the shelf edge (Graham et al., 2010). The presence of other streamlined landforms along PITW (Fig. 4), as previously reported by Evans et al. (2006), was interpreted by Graham et al. (2010) as evidence of palaeo-ice stream flow switching on the outer shelf. Graham et al. (2010) also described five sediment bodies that they interpreted as GZWs, two of which are in the axis of PITE, whereas the other three are located in a “bottle neck” in PIT, just landward of where it

divides into its two outer shelf branches (Figs. 3 and 5). The most landward of these GZWs was the one previously identified by Lowe and Anderson (2002). The existence of multiple GZWs implies that the retreat history of the ice stream was punctuated by pauses in landward migration of the grounding line and minor re-advances (Graham et al., 2010).

Bathymetry data collected early in 2009 beneath the ice shelf that extends from the grounding line of PIG, using the Autosub3 autonomous underwater vehicle (AUV), revealed a transverse ridge (Jenkins et al., 2010). Bedforms imaged on the crest of the ridge using the multibeam echo sounding system on the AUV were interpreted by Jenkins et al. (2010) as evidence that it was a former grounding line, and the smooth surface on the seaward slope was interpreted as having formed by deposition of sediment scoured from the crest. Jenkins et al. (2010) also interpreted a bump in the ice surface seen in a 1973 Landsat image as an ice rumple caused by contact between the ice and the highest point of the ridge. By 2005 the grounding line was more than 30 km upstream of that point (Vaughan et al., 2006), but combining the AUV observations with grounding line retreat and ice shelf thinning rates measured since the mid-1990s (Rignot, 1998, 2008; Wingham et al., 2009) implies that these rates must have been slower over the preceding 20 years. Inversion of airborne gravimetry data collected by the NASA Ice-bridge project provided additional constraints on the geometry of the ridge and the sub-ice-shelf cavity on its upstream side (Studinger et al., 2010). The inversion, however, predicts a shallower ridge than observed in the AUV data, which implies that the ridge consists mainly of dense bedrock rather than being a GZW



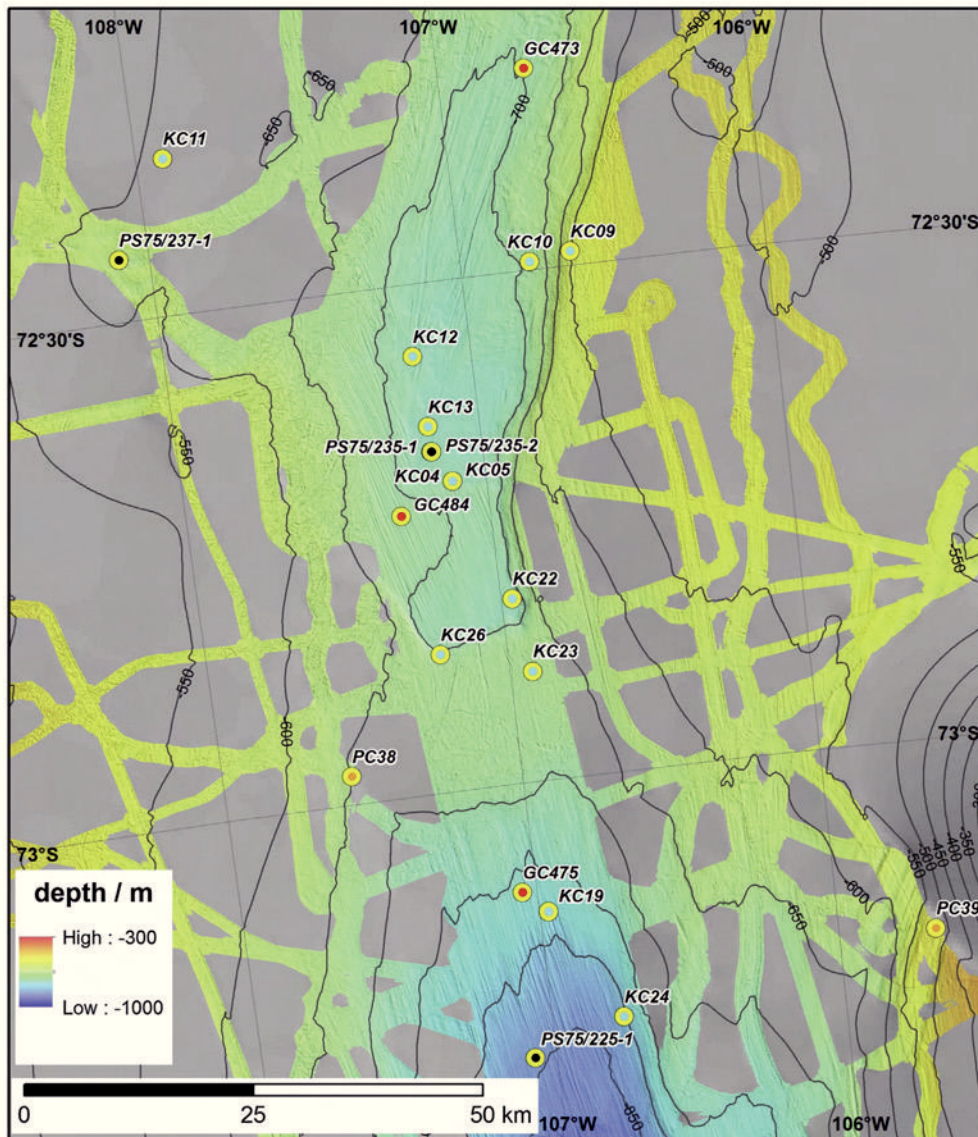


**Fig. 5.** Map of the mid-shelf part of Pine Island Trough showing shelf sediment core sites overlaid on multibeam swath bathymetry (Lowe and Anderson, 2002; Graham et al., 2010; Jakobsson et al., 2011, 2012). Bathymetry contours from a regional compilation (Nitsche et al., 2007) are shown at 50 m intervals and highlight the “bottle neck” in this part of Pine Island trough. Sediment core sites are shown and labelled with the core ID for cores that recovered more than 1 m of sediment and for shorter cores from which AMS  $^{14}\text{C}$  dates have been obtained. Core site symbol fill colour indicates ship the core was collected on, as in Fig. 2.

built by deposition of glacial sediments. By modelling the gravimetry data, however, Muto et al. (2013) estimated a sediment thickness of  $479 \pm 143$  m beneath the crest of the ridge, and their model shows that the bathymetric crest is offset about 8 km upstream from the crest of a buried bedrock ridge. Inversion of airborne gravimetry data over the ice shelf that extends seaward from Thwaites Glacier (Fig. 3) also revealed a submarine ridge that undulates between 300 and 700 m below sea level and has an average relief of 700 m (Tinto and Bell, 2011).

Autosub3 was deployed from RVIB *Nathaniel B. Palmer* during Cruise NBP0901 to collect the sub-ice shelf data described above. At the time of the AUV missions, PIB was unusually clear of sea ice, and this allowed almost complete swath bathymetry coverage of inner PIB to be achieved using the hull-mounted multibeam echo sounding system. These data showed that the former subglacial meltwater drainage network identified by Lowe and Anderson (2002, 2003) was more extensive than previously realised, and received substantial subglacial meltwater inflow from the east as well as from the Pine Island and Thwaites glaciers (Fig. 6; Nitsche

et al., 2013). The swath bathymetry data also revealed a zone of relatively smooth topography directly in front of Pine Island ice shelf, which was shown to be the surface of 300 m-thick sedimentary deposits by multichannel seismic profiles collected on RV *Polarstern* a year later (Nitsche et al., 2013).

Early in 2010, a second successive austral summer with unusually sparse sea ice cover on the Amundsen Sea continental shelf allowed systematic multibeam swath bathymetry survey over the mid-shelf part of PIT on IB *Oden* (OSO0910; Jakobsson et al., 2011, 2012) and acquisition of an extensive network of multichannel seismic lines on RV *Polarstern* (ANT-XXVI/3; Gohl, 2010; Gohl et al., 2013b).

Using the multibeam bathymetry data collected over the mid-shelf part of PIT on OSO0910 (Fig. 5), Jakobsson et al. (2011, 2012) were able to map the full extent of the GZWs and associated bedforms previously identified by Lowe and Anderson (2002) and Graham et al. (2010). Jakobsson et al. (2011) identified unusual 1–2 m-high “corrugation ridges” associated with and transverse to curvilinear-linear furrows in the axis of PIT, seaward of the mid-

XXX



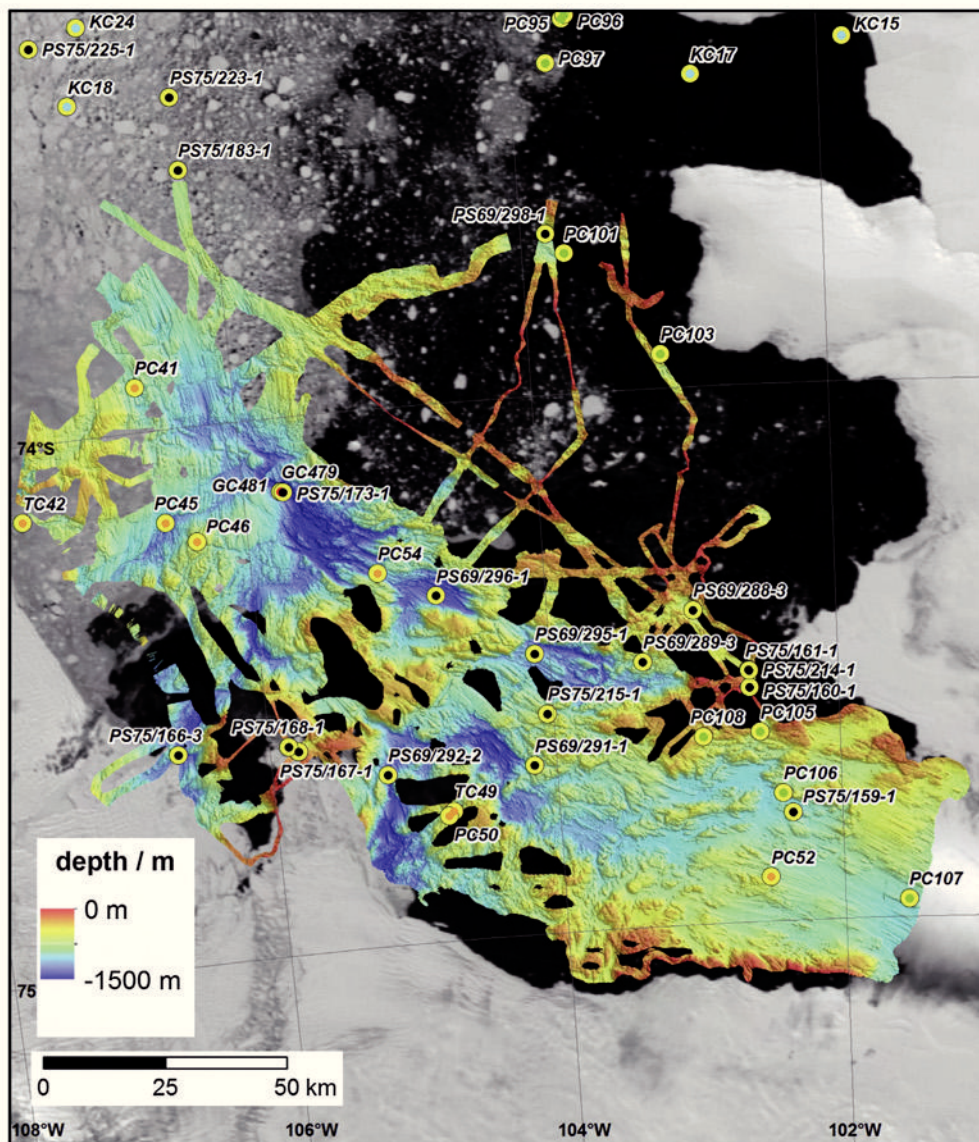


**Fig. 6.** Map of Pine Island Bay showing shelf sediment core sites overlaid on multibeam swath bathymetry (Nitsche et al., 2013). Sediment core sites are shown and labelled with the core ID for cores that recovered more than 1 m of sediment and for shorter cores from which AMS  $^{14}\text{C}$  dates have been obtained. Core site symbol fill colour indicates ship the core was collected on, as in Fig. 2. In most cases, where a box core or giant box core from which only a surface sample has been dated is co-located (within 50 m) with another core, only the other core is labelled (see co-ordinates in Supplementary Table 1 to identify co-located cores).

shelf GZWs, and interpreted these as having been generated by tidal motion of icebergs resulting from ice shelf collapse and calving directly at the grounding line. The area in which the corrugation ridges occur is seaward of, and at greater water depth than the mid-shelf GZWs, implying that the hypothesized ice shelf break-up must have occurred before formation of the GZWs. Jakobsson et al. (2012) interpreted palaeo-ice stream flow as having switched from PITW to PITE at an early stage during the last deglaciation, and estimated the length of time required for the largest GZW to develop as between 600 and 2000 years, assuming that sediment flux rates at the bed of the palaeo-ice stream were between  $500$  and  $1650 \text{ m}^3 \text{ a}^{-1} \text{ m}^{-1}$ .

Klages et al. (2013) presented multibeam swath bathymetry data, acoustic sub-bottom profiles, a multichannel seismic profile, and results of analyses of two sediment cores collected on a bank to the east of PIT and north of Burke Island on ANT-XXVI/3 (Fig. 3). The authors interpreted the unusual assemblage of bedforms revealed by the multibeam data as indicating that the bank supported an inter-ice stream ridge during the LGM, and recording two still-

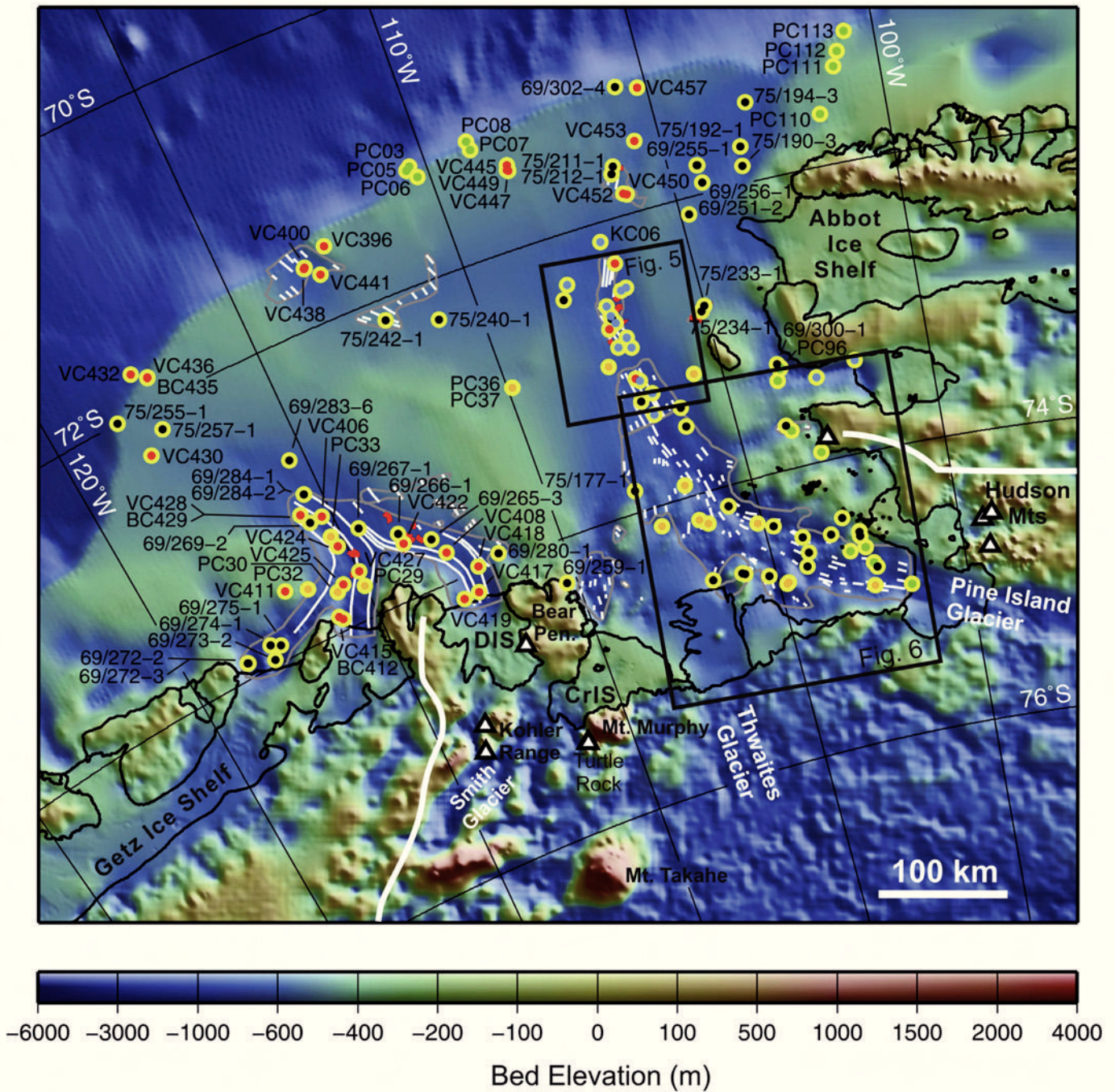
stands or minor re-advances of the grounding line during the last deglaciation.

### 3.1.2. Sediment core studies and geochronological data

The first sediment cores from the Amundsen Sea continental shelf were collected on the “Deep Freeze” cruises on the USCGC *Glacier* in 1981 and 1985 (Fig. 7; Anderson and Myers, 1981; Kellogg and Kellogg, 1987a, 1987b). On the 1981 cruise, three piston cores on the outer shelf recovered glacial deposits, and five piston cores on the continental slope recovered a variety of glacial marine sediments and mass flow deposits, such as debris flows and turbidites (Anderson and Myers, 1981; Dowdeswell et al., 2006; Kirshner et al., 2012). AMS  $^{14}\text{C}$  dating was carried out recently on foraminifera in samples from one of the shelf cores (Kirshner et al., 2012).

Kellogg and Kellogg (1987a, 1987b) reported results from micropalaeontological and sedimentological examination of 20 sediment cores collected on the continental shelf during the Deep Freeze 85 cruise, and inferred from the widespread occurrence of





- |   |  |
|---|--|
| Palaeo-ice flow alignment indicated by bedforms | Crest of grounding zone wedge or moraine |
| Site sampled for cosmogenic isotope analysis    | USCGC <i>Glacier</i> core site           |
| RVIB <i>Nathaniel B. Palmer</i> core site       | RRS <i>James Clark Ross</i> core site    |
| RV <i>Polarstern</i> core site                  | IB <i>Oden</i> core site                 |

**Fig. 7.** Map of the Amundsen Sea Embayment showing continental shelf sediment core sites (yellow circles) and cosmogenic surface exposure age sample locations (white-filled triangles), overlaid on geomorphological features (see Fig. 3 for details) and Bedmap2 ice sheet bed and bathymetry (Fretwell et al., 2013), which is displayed with shaded-relief illumination from the upper right. Sediment core sites are shown for cores that recovered more than 1 m of sediment and for shorter cores from which AMS  $^{14}\text{C}$  dates have been obtained. Core site symbol fill colour indicates ship the core was collected on, as in Fig. 2. In most cases, where a box core or giant box core from which only a surface sample has been dated is co-located (within 50 m) with another core, only the other core is labelled (see co-ordinates in Supplementary Table 1 to identify co-located cores). Thick white lines mark major ice divides. Black rectangles outline area shown in greater detail in Figs. 5 and 6. Core sites outside the area shown in Figs. 5 and 6 are labelled with the core ID. CrIS – Crosson Ice Shelf; DIS – Dotson Ice Shelf.



“compact” diamicton, and sub-bottom profiles collected with a sparker system on the same cruise, that grounded ice had advanced to the continental shelf edge. Although no radiometric age constraints had been obtained from the cores, Kellogg and Kellogg (1987a) suggested that the last advance may have occurred during the LGM. Kellogg and Kellogg (1987b) observed that sediments in four cores recovered from inner PIB were almost barren of microfossils, and attributed this to deposition beneath a former extension of the floating terminus of PIG. They further suggested that ice shelf retreat from inner PIB occurred within the preceding century, and speculated that the “Thwaites Iceberg Tongue” (iceberg B-10), grounded north of the terminus of Thwaites Glacier at that time, might have originated from PIG. This latter hypothesis was assessed by Ferrigno et al. (1993) as being unlikely, on the basis that the crevassing pattern on the iceberg seen in Landsat images was a better match to that observed downstream of the grounding line on Thwaites Glacier than on PIG. This conclusion by Ferrigno et al. (1993) has subsequently been strengthened by the observation that a similar large iceberg calved from Thwaites Glacier in 2002 (iceberg B-22A) ran aground in the same position that iceberg B-10 had occupied for more than two decades before it drifted away in 1992 (Rabus et al., 2003).

Seabed surface sediments were collected from the outer shelf in the eastern ASE and from the outer and middle shelf in the western ASE during expedition ANT-XI/3 with RV *Polarstern* (Miller and Grobe, 1996). Results of various sedimentological, mineralogical, geochemical and micropalaeontological analyses on these samples were published as part of larger geographical compilations (Hillenbrand et al., 2003; Esper et al., 2010; Ehrmann et al., 2011; Hauck et al., 2012; Mackensen, 2012).

Piston cores were collected from inner and middle shelf areas during RVIB *Nathaniel B. Palmer* Cruise NBP9902 in 1999, and samples from these cores yielded the first radiocarbon dates from the region constraining ice retreat since the LGM (Anderson et al., 2002; Lowe and Anderson, 2002; Supplementary Table 2).

Lowe and Anderson (2002) used the ages and other data from the cores in the PIT region, such as the presence of subglacially deposited tills, together with multibeam swath bathymetry data and a single-channel seismic reflection profile collected on the same cruise (Anderson et al., 2001; Wellner et al., 2001; Lowe and Anderson, 2003), as the basis for a reconstruction of grounded ice extent at the LGM and the subsequent history of ice sheet retreat. They considered that the grounding line probably advanced to the shelf break during the LGM, but also defined a minimum LGM grounding line position near the boundary between the middle and outer parts of the continental shelf, at a latitude of about 72° 30'S. Lowe and Anderson (2002) interpreted subsequent retreat as having reached a mid-shelf position by about 16 ka BP (uncorrected <sup>14</sup>C years), on the basis of an AMS <sup>14</sup>C date on foraminifera from a core (PC39; Fig. 5) recovered to the west of Burke Island, at which point the grounding line retreat paused and a GZW started to develop. The precise age of these events remained quite uncertain because the 1-sigma uncertainty in the reported deglacial date from PC39 was ±3900 yr, and the age we obtain from calibration is 17,203 ± 9430 cal yr BP (Supplementary Table 2).

In their reconstruction of ice retreat, Lowe and Anderson (2002) interpreted grounding line unpinning from the mid-shelf GZW as having occurred between 16 and 12 ka BP (uncorrected <sup>14</sup>C years, equivalent to 18.0 to 12.6 cal ka BP with the calibration parameters used in this paper), and suggested that subsequent retreat into PIB may have been rapid. A date of 10,086 ± 947 cal yr BP (Supplementary Table 2) on foraminifera from glacial marine sediment in a core (PC41; Fig. 6) recovered 250 km from the modern grounding line of PIG showed that ice had retreated at least as far as the outer part of PIB by early Holocene time.

Anderson et al. (2002) published additional AMS <sup>14</sup>C dates on foraminifera from cores (TC22, TC/PC23, PC26) recovered farther west, in Wrigley Gulf (Fig. 2). The radiocarbon dates showed that ice had retreated to the inner shelf in WGT before the start of the Holocene (ages between 15,610 ± 651 and 14,321 ± 536 cal yr BP, Supplementary Table 2).

A core (PC46; Fig. 6) from the axis of one of the former subglacial channels in PIB recovered well-sorted sands and gravels at shallow depth below the sea floor (Lowe and Anderson, 2003). These well-sorted sediments were probably deposited from meltwater in either a subglacial or proglacial setting, but they suggest that subglacial meltwater flow was active in PIB during the last glacial period or deglaciation (Lowe and Anderson, 2003).

In contrast, sediment cores collected in 2006 on Cruise JR141, from the axes of channels located directly offshore from the Dotson and eastern Getz ice shelves, recovered sedimentary facies that do not support meltwater activity in those channels during the LGM or the last deglaciation (Smith et al., 2009). One of the cores collected from the axis of a channel offshore from the Getz Ice Shelf (VC415; Fig. 7) even recovered a sequence that typically records the retreat of a grounding line (i.e. subglacial till overlain by transitional sandy mud, overlain in turn by diatom-bearing mud deposited in seasonal open marine conditions similar to today), indicating that the channel floor was overridden by grounded ice since it was last active as a meltwater conduit (Smith et al., 2009).

A diatom ooze layer overlying glacial and deglacial transition sediments was recovered in several cores collected from inner shelf tributaries of DGT on JR141 and ANT-XXIII/4 (Fig. 7). AMS <sup>14</sup>C dates on AIOM from samples of this layer yielded consistent AMS <sup>14</sup>C ages which, when calibrated, are between 14,312 ± 510 and 11,881 ± 455 cal yr BP (Hillenbrand et al., 2010b; Supplementary Table 2). The low terrigenous sediment component of the ooze means that these ages are less likely to be affected by significant fossil organic carbon contamination. Constraints from relative palaeomagnetic intensity (RPI) records of cores penetrating the ooze layer, however, suggest that the oldest ages from the ooze must be affected by some contamination, and the ages considered to be most reliable from ooze samples range between 12,816 and 11,881 cal yr BP (Hillenbrand et al., 2010b; Smith et al., 2011). Radiocarbon dates obtained on two samples of acid-cleaned diatom tests from the ooze layer yielded ages that are significantly younger and inconsistent with constraints from RPI records (Hillenbrand et al., 2010b), probably due to adsorption of atmospheric CO<sub>2</sub> on the highly reactive opal surfaces of the extracted diatom tests prior to sample graphitisation and combustion for AMS <sup>14</sup>C dating (cf. Zheng et al., 2002). The dates obtained on the conventionally-treated ooze samples show that the ice margin had retreated from much of the inner shelf in the DGT before the start of the Holocene.

Smith et al. (2011) integrated the ages from the diatom ooze layer with a large dataset of radiocarbon ages obtained from glacial marine sediments in cores retrieved along transects in DGT and its tributaries during JR141 and ANT-XXIII/4. The collated ages on both AIOM and, where present, foraminifera samples record rapid deglaciation across the middle and inner shelf from about 13,779 cal yr BP to within c.10–12 km of the present ice shelf front between 12,549 and 10,175 cal yr BP (Smith et al., 2011; calibrated ages from Supplementary Table 2). The distinction between glacial marine and subglacial facies in the studied cores was based on a dataset comprising sedimentological parameters, physical properties and proxies for sediment provenance (Smith et al., 2011). Clay mineral changes between subglacial and postglacial sediments in cores retrieved from near-coastal sites in the ASE led Ehrmann et al. (2011) to the conclusion that the drainage basins of palaeo-ice streams discharging into the ASE have varied through time.

xxxiii



In 2010, sediment cores were also collected on both IB *Oden* (OSO0910) and RV *Polarstern* (ANT-XXVI/3): Kasten cores were collected from 27 sites during OSO0910, mostly in the mid-shelf part of PIT (Fig. 5; Kirshner et al., 2012), whereas 37 gravity cores, eight giant box cores and one multiple core were collected from various locations on the ASE shelf during ANT-XXVI/3 (Gohl, 2010; Hillenbrand et al., 2013; Klages et al., 2013).

Majewski (2013) analysed benthic foraminifera assemblages in the core tops of sediment cores collected on OSO0910, and Kirshner et al. (2012) carried out multi-proxy analyses on both the OSO0910 cores and cores collected previously on DF81 and NBP9902. The latter study included detailed identification and mapping of sedimentary facies and then established a chronostratigraphic framework constrained by previously published and 23 new AMS  $^{14}\text{C}$  dates. The authors also developed an updated reconstruction of ASE deglaciation, incorporating their new results. This reconstruction followed Graham et al. (2010) in interpreting the LGM limit of grounded ice in PITE as having been somewhere between the most seaward GZW and the continental shelf edge. An AMS  $^{14}\text{C}$  date on planktonic foraminifera from a core (DF81, PC07; Fig. 7) near the shelf edge farther west showed that glacial marine sediments began accumulating on the eastern ASE outer shelf before 16.4 cal ka BP (Supplementary Table 2), and this is therefore a minimum age for the start of grounding line retreat (Kirshner et al., 2012). A mud-dominated facies containing very little sand and devoid of pebbles, interpreted by Kirshner et al. (2012) as representing sub-ice shelf deposition, was recovered in cores from the inshore flank of the largest and most landward GZW in the mid-shelf part of PIT. AMS  $^{14}\text{C}$  dates on monospecific juvenile planktonic foraminifera from this unit indicate that it was deposited between 12.3 and 10.6 cal ka BP (Supplementary Table 2), which implies that the GZWs in the mid-shelf part of the trough all formed before 12.3 cal ka BP and that an ice shelf was present over the mid-shelf region for almost 2000 years (Kirshner et al., 2012). Kirshner et al. (2012) further suggested that during this interval the grounding line in PIT was likely to have been at the sedimentary to crystalline bedrock transition previously identified by Lowe and Anderson (2002). Sedimentological changes at the end of this interval (Kirshner et al., 2012) and geomorphological features (Jakobsson et al., 2012) have been interpreted as indicating that it was followed by ice shelf break-up and rapid grounding line retreat into inner PIB. Break-up of the ice shelf has been attributed to inflow of a warm water mass onto the shelf (Jakobsson et al., 2012; Kirshner et al., 2012). An abrupt change in sedimentation to a draping silt unit began between  $\sim 7.8$  and 7.0 cal ka BP. This terrigenous silt unit has been interpreted as a meltwater-derived facies (Kirshner et al., 2012).

Hillenbrand et al. (2013) presented a detailed facies analysis of three sediment cores collected from relatively shallow water sites in inner PIB on ANT-XXVI/3 (Fig. 5), and integrated this with 33 new radiocarbon dates to argue that the grounding line had retreated into inner PIB, to within 112 km of the modern PIB grounding line, before  $11,664 \pm 653$  cal yr BP. This age was obtained by calibration of an AMS  $^{14}\text{C}$  date of  $11,090 \pm 50$  yr BP (uncorrected  $^{14}\text{C}$  years) on mixed benthic and planktonic foraminifera from a facies consisting of mud alternating with layers and lenses of sand and/or gravelly sand in core PS75/214-1, the sandy layers being interpreted as turbidites. Hillenbrand et al. (2013) calibrated this date by following the same procedure as used in this paper, apart from assuming a different marine reservoir age ( $1100 \pm 200$  years, cf.  $1300 \pm 70$  years used in this paper). The age for the same sample in Supplementary Table 2 is  $11,157 \pm 248$  cal yr BP, highlighting the fact that, for some time intervals, small differences in the assumed reservoir age can propagate into larger differences in calibrated age. Although our calibrated age for this sample is more than 500 years

younger than that derived by Hillenbrand et al. (2013), the uncertainty range of the age still does not overlap with that of the date Kirshner et al. (2012) use to constrain the younger limit of the period of ice shelf cover over the mid-shelf area. If these two dates and the published interpretations of the dated facies are accepted, they imply that an ice shelf extending more than 200 km from the grounding line persisted after the grounding line retreated into inner PIB. Alternatively, one or other of the ages or facies interpretations must be misleading.

AMS  $^{14}\text{C}$  dates on carbonate samples from two other cores in inner PIB that support an interpretation of an early Holocene retreat of the grounding line to within c. 100 km of its present position were also presented by Hillenbrand et al. (2013). The oldest date from another core only c. 2 km from site PS75/214, yields an age of  $9015 \pm 251$  cal yr BP from the calibration in this paper, and the oldest date from a core only 93 km from the modern grounding line of Thwaites Glacier corresponds to an age of  $10,124 \pm 269$  cal yr BP (Supplementary Table 2). The oldest dates from two of the three inner PIB cores studied by Hillenbrand et al. (2013) are not from the dated samples deepest in the core (although the age of 10,124 cal yr BP is the deepest of 12 dated samples from the same core that are all in stratigraphic order, within the uncertainty of the calibrated ages), but these authors argue that regardless of subsequent redeposition from nearby, shallower shelf areas by gravitational downslope transport, the dated calcareous microfossils can only have lived near the core sites after the grounding line had retreated farther landward. Although it is theoretically possible that reworking of older foraminifera could have biased the oldest date (11,157 cal yr BP) determined from the inner PIB cores, contamination with 10% of very old ("radiocarbon dead") foraminifera would be required to increase the measured age by 1000 years, and an age bias of this magnitude would require an even higher level of contamination with foraminifera that lived just before the LGM. Such extensive contamination would imply the existence of a significant 'reservoir' of pre-LGM microfossils somewhere in PIB, for which there is no evidence. If such a reservoir was shown to exist, this would reduce confidence in many other dates from sites in PIB and farther offshore.

Hillenbrand et al. (2013) also collated minimum ages of deglaciation from inner shelf cores collected in other parts of the Amundsen Sea that had previously been published by Anderson et al. (2002), Hillenbrand et al. (2010b) and Smith et al. (2011), and presented one new radiocarbon date on a carbonate sample from a core recovered from the inner shelf part of the small glacial trough offshore from the westernmost Getz Ice Shelf (PS75/129-1; Fig. 2; age  $12,825 \pm 236$  cal yr BP, Supplementary Table 2). The collated deglacial ages showed that WAIS retreat from the entire Amundsen Sea shelf was largely complete by the start of the Holocene.

Klages et al. (2013) presented six new AMS  $^{14}\text{C}$  dates on AIOM samples from the two sediment cores collected on a bank to the east of PIT and north of Burke Island on ANT-XXVI/3 (Fig. 7), and the ones they interpreted as minimum ages of deglaciation are  $19,146 \pm 269$  and  $17,805 \pm 578$  cal yr BP (Supplementary Table 2). These ages are older, but not incompatible with, the minimum age for the start of deglaciation of the outer shelf of 16.4 cal ka BP obtained by Kirshner et al. (2012), and suggest that deglaciation of the inter-ice stream ridge proceeded in parallel with retreat of the flanking ice streams.

### 3.2. Amundsen Sea region terrestrial studies

Before 2004, the subglacial topography of the ASE was only known from a few widely-spaced oversnow traverses and a handful



of airborne survey flights (e.g. Lythe et al., 2001). Radio echo sounding data density was greatly increased as a result of a collaborative US/UK airborne campaign that undertook a systematic geophysical survey during the austral summer of 2004/05 (Holt et al., 2006; Vaughan et al., 2006). In the PIG drainage basin these new data revealed that whereas there is a deep, inland sloping bed beneath the trunk of PIG, the lower basin of the glacier is surrounded by areas in which the bed is relatively shallow. After deglaciation and isostatic rebound, these shallow bed areas could rise above sea level and would impede ice-sheet collapse initiated near the grounding line (Vaughan et al., 2006). This contrasts with the survey results from the Thwaites Glacier drainage basin where, except for short-wavelength roughness, the bed slopes inland monotonically from the grounding line to the interior of the basin, continuing to the deepest part of the Byrd Subglacial Basin at 2300 m below sea level (Fig. 2; Holt et al., 2006).

The first constraints on changes in ice surface elevations in the ASE spanning thousands of years were published by Johnson et al. (2008), who obtained cosmogenic surface exposure ages on glacial erratic boulders collected from sites around PIB. From the resulting ages (Supplementary Table 3), these authors inferred average ice thinning rates of  $3.8 \pm 0.3 \text{ cm yr}^{-1}$  over the past 4.7 ka on Mount Manthe, in the Hudson Mountains near PIG, and  $2.3 \pm 0.2 \text{ cm yr}^{-1}$  over the past 14.5 ka on Turtle Rock, which lies between Smith and Pope glaciers near Mount Murphy (Figs. 3 and 7). An exposure age of  $2.2 \pm 0.2 \text{ ka}$  was obtained from an erratic boulder exposed at 8 m above sea level (m.a.s.l.) on an unnamed island near the tip of Canisteo Peninsula (Fig. 3), but it was not clear if this age represents retreat of the local ice margin or glacio-isostatic emergence (Johnson et al., 2008; Supplementary Table 3). Paired  $^{10}\text{Be}$  and  $^{26}\text{Al}$  cosmogenic surface exposure results on a sample of striated bedrock from 470 m.a.s.l. on Hunt Bluff, Bear Peninsula (on the southern coast of the ASE; Figs. 3 and 7) yielded ages in excess of 100 ka (Johnson et al., 2008; Supplementary Table 3). On a two-isotope diagram the results from this sample plot slightly below the “erosion island”, but as they are within error of one another they could plausibly represent continuous exposure throughout the last glacial period. However, as these are results from a single sample, we need to treat them with caution.

More extensive collections of glacial erratic samples from the Hudson Mountains (Figs. 3 and 7) obtained by a field party in the austral summer of 2007/08 and from sites accessed by helicopter during RV *Polarstern* expedition ANT-XXVI/3 in 2010 have provided surface exposure ages that indicate a more detailed history of surface elevation change. These ages suggest that there was a decrease in ice surface elevation in this area to near the modern level in the early Holocene (Bentley et al., 2011; Johnson et al., 2012).

Glacial erratic samples were also collected from sites in the Kohler Range that were accessed by helicopter during ANT-XXVI/3 (Figs. 3 and 7). From the cosmogenic surface exposure ages obtained from these samples, Lindow et al. (2011) inferred an average thinning rate of ca  $3 \text{ cm yr}^{-1}$  over the past 13 ka. This is similar to the thinning rate inferred by Johnson et al. (2008) for Turtle Rock, which lies about 70 km to the east (Figs. 3 and 7). However, each of these thinning rates is inferred from a very small sample set, so they must be treated with caution.

The Ford Ranges in western Marie Byrd Land straddle the ice divide between the Amundsen Sea and Ross Sea sectors (Fig. 2). Stone et al. (2003) published cosmogenic surface exposure ages from numerous nunataks in the Ford Ranges that indicated ice thinning rates in the inland part of the range of  $2.5\text{--}9 \text{ cm yr}^{-1}$  over the past 10.4 ka. Around the most seaward peaks, the surface exposure ages indicated gradual ice thinning up to 3.5 ka ago, then greatly increased thinning rates for about 1200 years. Stone et al.

(2003) interpreted these changes as resulting from retreat of the grounding line and consequent landward migration of a relatively steep ice surface gradient upstream of it (see also Anderson et al., 2013).

No surface exposure ages from the interior of the Amundsen Sea sector of the WAIS have yet been published, but in the Ross Sea sector about 70 km from the ice divide, important constraints on past ice surface elevations have been obtained from Mount Waesche (Fig. 2) by Ackert et al. (1999). These authors interpreted  $^3\text{He}$  and  $^{36}\text{Cl}$  surface exposure ages obtained from a lateral moraine on Mount Waesche, together with geomorphological observations, as indicating that the ice sheet was up to 45 m thicker in this area ca 10 ka ago. Furthermore, Ackert et al. (1999) suggested that the surface position 10 ka ago represents a highstand, and showed that increasing ice thickness in the area during the early stages of post-LGM Antarctic deglaciation can be simulated with a non-equilibrium ice sheet model (see also Anderson et al., 2013). Recently published results from a more sophisticated ice sheet modelling study are consistent with this scenario (Ackert et al., 2013).

Past ice surface elevations in the interior of the WAIS have also been estimated from total gas content, V, in the Byrd Station ice core (drilled at  $80^\circ 01' \text{ S}$ ,  $119^\circ 31' \text{ W}$  in the Ross Sea sector of the WAIS; Fig. 2), with variable results. A complicating factor for this ice core is that the site was not located near an ice divide, so the ice at depth in the core will have come from an upstream location that has a higher modern elevation. Using an early, sparse set of V measurements and without correcting for ice flow, Jenssen (1983) calculated ice surface elevations that were 400–500 m higher than present between 19 and 11 ka ago. However, Raynaud and Whillans (1982) presented new, more densely sampled V measurements, applied a correction for ice flow to them, and calculated that ice surface elevations were 200–250 m lower than present at the end of the LGM. Furthermore, Raynaud and Whillans (1982) inferred a thickening of the ice with time since the LGM, which they attributed to an increase in accumulation rate. Using the same V dataset, Lorius et al. (1984) revised the increase in surface elevation since the LGM down to 175–205 m as a result of using a new estimate of surface temperature increase since the LGM of  $10^\circ \text{ C}$  (cf.  $7^\circ \text{ C}$  used by Raynaud and Whillans, 1982). New estimates of past ice surface elevation in the interior of the WAIS may be expected soon from the WAIS Divide ice core (Fig. 2; <http://www.waisdivide.unh.edu/>; WAIS Divide Project Members, 2013).

Studies of the configuration of internal ice sheet layers detected in radio-echo sounding profiles have allowed conclusions about current and past migrations of the ice divides between the Amundsen Sea and Weddell Sea sectors (Ross et al., 2011) and the Amundsen Sea and Ross Sea sectors (Neumann et al., 2008; Conway and Rasmussen, 2009), respectively. Chronological constraints were inferred from modern rates of ice accumulation, compaction and flow velocity (Ross et al., 2011) or from correlation with dated ice cores (Neumann et al., 2008).

### 3.3. Bellingshausen Sea embayment marine studies

#### 3.3.1. Geophysical surveys and geomorphological studies

Although the southern Bellingshausen Sea continental shelf (Fig. 8) was the site of the first overwintering expedition in Antarctica, after the *Belgica* became beset by ice there in 1898 (Cook, 1909; Declair, 1999), no extensive marine geoscientific investigations were carried out there for nearly a century. The region remains less intensively studied than the neighbouring ASE. A brief reconnaissance over the outer continental shelf between  $80^\circ$  and  $83^\circ \text{ W}$  was carried out during USNS *Eltanin* Cruise 42 in 1970, but only echo sounding data were collected on the shelf, whereas



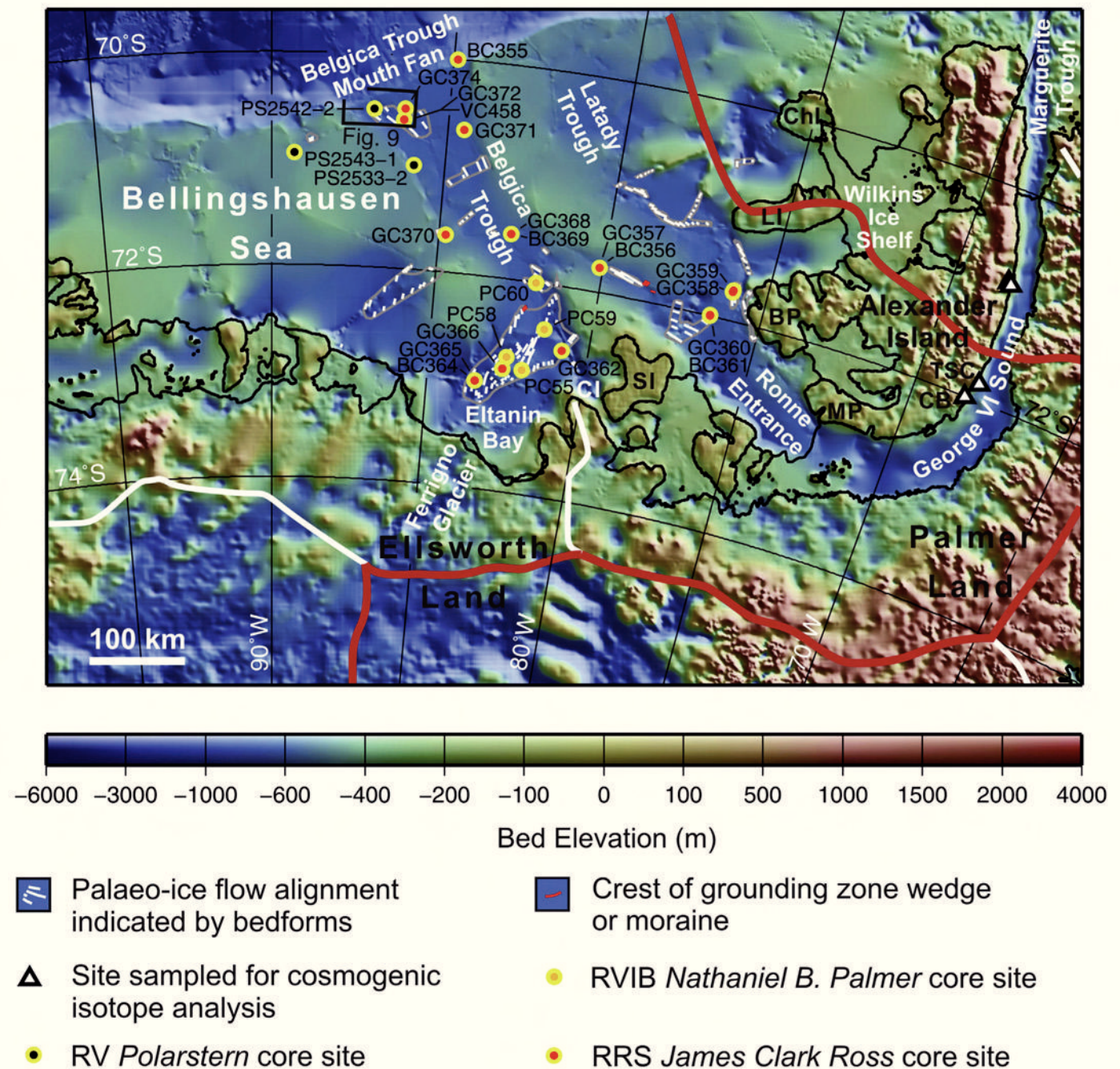


**Fig. 8.** Map of the Bellingshausen Sea region showing continental shelf sediment core sites (yellow circles), cosmogenic surface exposure age sample locations (white-filled triangles) and the main geomorphological features on the continental shelf, overlaid on Bedmap2 ice sheet bed and bathymetry (Fretwell et al., 2013), which is displayed with shaded-relief illumination from the upper right. Grey outlines mark areas in which bedforms indicative of past ice flow direction are observed in multibeam swath bathymetry data. Thin white lines indicate flow alignment. Thin red lines mark the crests of grounding zone wedges and moraines that represent past grounding line positions. Sediment core sites are shown and labelled with the core ID for cores that recovered more than 1 m of sediment and for shorter cores from which AMS  $^{14}\text{C}$  dates have been obtained. Core site symbol fill colour indicates ship the core was collected on, as in Fig. 2. Thick red line marks sector limit, along main modern ice divide between the Bellingshausen Sea and the Weddell Sea and an inferred palaeo-ice divide across Alexander Island. Thick white lines mark other major ice divides. In most cases, where a box core or giant box core from which only a surface sample has been dated is co-located (within 50 m) with another core, only the other core is labelled (see co-ordinates in Supplementary Table 1 to identify co-located cores). Black rectangle outlines area shown in greater detail in Fig. 9. BP – Beethoven Peninsula; CB – Citadel Bastion; CI – Carroll Inlet; CHL – Charcot Island; LI – Latady Island; MP – Monteverti Peninsula; SI – Smyley Island; TSC – Two Step Cliffs.

single-channel seismic profiles were collected across the slope and rise (Tucholke and Houtz, 1976).

In the austral summers of 1992/93 and 1993/94 the first research cruises of the modern era to investigate the continental shelf in this region were conducted on RRS *James Clark Ross* (JR04) and RV *Polarstern* (ANT-XI/3). Multichannel seismic profiles collected on these two cruises revealed an extensively prograded

outer continental shelf, an unusually deep shelf edge, and a low-gradient continental slope in the area now known to be the mouth of Belgica Trough (Cunningham et al., 1994, 2002; Nitsche et al., 1997, 2000). Acoustic sub-bottom profiles were also collected on both cruises, and some isolated swaths of multibeam bathymetry data were collected on ANT-XI/3 (Miller and Grobe, 1996).

xxxvi



Early in 1994, single beam echo sounding data were collected as RVIB *Nathaniel B. Palmer* Cruise NBP9402 traversed the southern Bellingshausen Sea continental shelf and reached the ice front in the Ronne Entrance. Further single-beam echo sounding surveys, with a particular focus on the Ronne Entrance and Carroll Inlet (Fig. 8), were carried out on HMS *Endurance* in 1996.

The first published multibeam swath bathymetry data from the region were collected early in 1999 on RVIB *Nathaniel B. Palmer* Cruise NBP9902, and revealed bedforms produced by glacial erosion in a deep trough in Eltanin Bay, separated by a drumlin field from mega-scale glacial lineations (MSGL) farther offshore (Wellner et al., 2001, 2006). Early in 2004, multibeam swath bathymetry data and sub-bottom profiler data were collected from several parts of the continental shelf and slope on RRS *James Clark Ross* Cruise JR104. Subglacial bedforms revealed by the multibeam and sub-bottom profiler data showed that past ice flow from the Ronne Entrance and Eltanin Bay had converged to form a large palaeo-ice stream in the Belgica Trough that advanced to, or close to, the shelf edge (Fig. 9; Ó Cofaigh et al., 2005b). Extensive multibeam swath bathymetry data collected over the part of the continental slope adjacent to the mouth of the Belgica Trough demonstrated the presence of a trough mouth fan (Dowdeswell et al., 2008). Systematic changes in the spatial density and size of upper slope gullies from the centreline of the trough to its margins were interpreted by Noormets et al. (2009) as indicating that the gullies were eroded by hyperpycnal flows initiated by sediment-laden subglacial meltwater discharges from a grounding line at the shelf edge. Further analysis of the fan geomorphology by Gales et al. (2013) supported this conclusion.

Graham et al. (2011) compiled all of the single beam and multibeam echo sounding data available at that time to produce a continuous gridded regional bathymetry map of the Bellingshausen Sea that provided the first accurate representation of the continental slope and major cross shelf troughs. Prior to this work the representation of the bathymetry of the region had been quite poor even in relatively recent circum-Antarctic bathymetry and

subglacial topography compilations (e.g. IOC, IHO and BODC, 2003; Le Brocq et al., 2010). Inclusion of some multibeam swath bathymetry datasets that have not been mentioned above helped improve definition of the continental shelf and slope. These included data collected on RRS *James Clark Ross* cruises JR141 and JR179, in early 2006 and early 2008, respectively. Other multibeam data that augmented coverage of inner shelf areas were collected early in 2007 on RRS *James Clark Ross* Cruise JR165.

### 3.3.2. Sediment core studies and geochronological data

The first sediment cores from the southern Bellingshausen Sea continental shelf were collected on RV *Polarstern* expedition ANT-XI/3 in the austral summer of 1993/94 (Miller and Grobe, 1996). Five giant box cores, three gravity cores and four multiple cores were collected from nine sites on the continental shelf, with additional gravity cores and multiple cores being collected from four sites on a transect across the adjacent continental slope (Hillenbrand et al., 2003, 2005, 2010a). Cores from both the shelf and the slope contain a similar succession of facies, with massive, homogenous diamictons overlain by terrigenous sandy muds, which are in turn overlain by bioturbated foraminifer-bearing muds. Although no radiocarbon dates were available on samples from the cores, Hillenbrand et al. (2005) inferred that the diamictons were of LGM age, interpreting the diamicton cored on the shelf as deformation till overlain by glacial marine diamicton, and the diamictons on the slope as glacial debris flow deposits. The sandy muds were interpreted as representing a deglaciation stage, and the bioturbated foraminifera-bearing muds as having been deposited in seasonally open water conditions like those that pertain today (Hillenbrand et al., 2005).

Piston cores collected on RV *Nathaniel B. Palmer* Cruise NBP9902 in 1999 from an area where MSGL were observed on the middle shelf recovered diamictons with moderate shear strength (<34 kPa), interpreted as tills, overlain by a thin cover of very soft diamicton with more abundant microfossils (Wellner et al., 2001).

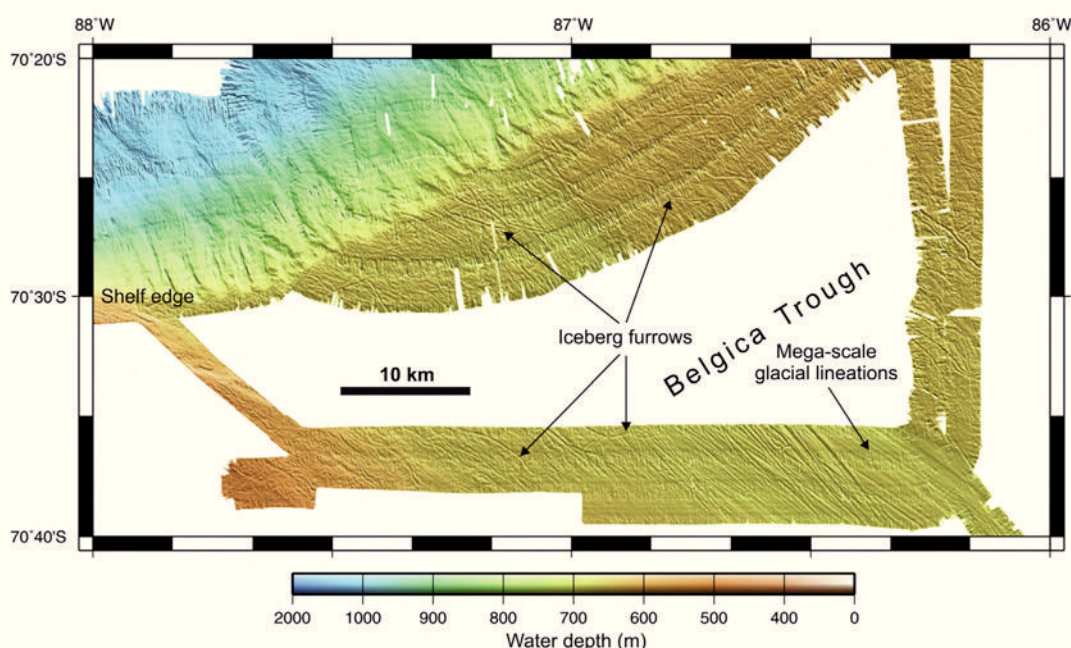


Fig. 9. Multibeam swath bathymetry data from the outer part of Belgica Trough showing mega-scale glacial lineations that extend to within 30 km of the continental shelf edge. Data shown were collected on RRS *James Clark Ross* cruises JR104 and JR141. The grid was generated using a near neighbour algorithm, has a cell size of 40 m and is displayed with shaded-relief illumination from 50°.



Early in 2004, gravity cores and box cores were collected from several parts of the continental shelf and slope on RRS *James Clark Ross* Cruise JR104. Samples from these extensively analysed cores yielded the only radiocarbon dates presently available from the region constraining ice retreat since the LGM (Hillenbrand et al., 2010a). Although planktonic foraminifera are present in sea-floor sediments (Hillenbrand et al., 2003, 2005) and radiocarbon dates were obtained from them (Hillenbrand et al., 2010a), their abundance decreases rapidly downcore and none of the earliest seasonally open-marine or deglacial sandy muds recovered in the JR104 cores contained enough foraminifera for AMS  $^{14}\text{C}$  dating. Therefore, minimum ages of grounding line retreat were obtained by AMS  $^{14}\text{C}$  dating of AIOM samples from the cores. Hillenbrand et al. (2005, 2009) analysed down-core changes of clay mineral assemblages, and Hillenbrand et al. (2010a) used this information to identify the deepest levels in the postglacial sediments at which the mineralogical provenance, and therefore the likely extent of fossil carbon contamination, were similar to those of recent seabed sediments. The calibrated ages suggest early ice retreat from the outermost part of Belgica Trough, starting before the global LGM (ages  $30,758 \pm 2262$  and  $29,585 \pm 1780$  cal yr BP, Supplementary Table 2), followed by a gradual retreat along the outer and middle shelf part of the trough, with the inner shelf tributaries in Eltanin Bay and the Ronne Entrance becoming free of grounded ice in the earliest and late Holocene, respectively (Hillenbrand et al., 2010a). While it is possible that a change in the amount of fossil carbon contamination independent of clay mineral provenance might be responsible for the surprisingly old ages from the outer shelf, it seems unlikely that such changes could account for the gradual retreat indicated by ages from the core transects.

The apparent continuation of gradual grounding line retreat towards the Ronne Entrance through the late Holocene contrasts not only with the retreat history indicated by data from Eltanin Bay, but also with those from neighbouring regions in the Amundsen Sea and southern Antarctic Peninsula, where the ice margin had retreated close to modern limits by early Holocene time (Heroy and Anderson, 2007; Smith et al., 2011; Hillenbrand et al., 2010a, 2013; Kilfeather et al., 2011; Bentley et al., 2011; Livingstone et al., 2012; Ó Cofaigh et al., in review). It is also difficult to reconcile with biological studies that have indicated the presence of a diversity hotspot in nematode fauna and microbial diversity in southern Alexander Island (Lawley et al., 2004; Maslen and Convey, 2006), implying that a glacial refuge has persisted somewhere in the area through several glacial cycles (Convey et al., 2008, 2009). The gradual retreat is, however, consistent with an ice history model that reconstructs an ice dome to the south of the Ronne Entrance persisting into the Holocene (Ivins and James, 2005).

Analyses of clay mineral assemblages in sediment cores recovered from the continental shelf and slope on ANT-XI/3 and JR104 provided evidence of past changes in sediment provenance (Hillenbrand et al., 2005, 2009). The geographical heterogeneity of clay mineral assemblages in sub- and pro-glacial diamictos and gravelly deposits recovered on the shelf was interpreted by Hillenbrand et al. (2009) as indicating that they were eroded from underlying sedimentary strata of different ages. Furthermore, Hillenbrand et al. (2009) interpreted the clay mineralogical heterogeneity of soft tills recovered on the shelf as evidence that the drainage area of the palaeo-ice stream flowing through Belgica Trough changed through time.

### 3.4. Bellingshausen Sea region terrestrial constraints

Subglacial topography in the part of West Antarctica to the south of the Bellingshausen Sea remains relatively poorly known, as there have been no systematic, regional airborne geophysical surveys like

those conducted in the Amundsen Sea region. A recent over-snow radio-echo sounding survey and data collected by the NASA Ice-bridge project have improved knowledge of subglacial topography in the drainage basin of the Ferrigno Ice Stream, which flows into Eltanin Bay (Fig. 8; Bingham et al., 2012). The new subglacial topography data, together with modelling of potential field data collected during earlier reconnaissance aerogeophysical surveys (Bingham et al., 2012), are consistent with a previous interpretation that the region contains Cenozoic basins formed by extension along a continuation of the West Antarctic Rift System that connected to a subduction zone along the Pacific margin of the Antarctic Peninsula (Eagles et al., 2009). The presence of these basins can be expected to influence the dynamic behaviour of this part of the WAIS, both through topographic effects on ice sheet stability and elevated heat flow (Bingham et al., 2012).

No surface exposure ages or ice core data have been published that constrain past surface elevations of the WAIS in the Bellingshausen Sea region. However, surface exposure ages have been published from several locations on Alexander Island, including some that lie just within the boundary of the sector under consideration, as defined in Fig. 1 (Bentley et al., 2006, 2011; Hodgson et al., 2009; Supplementary Table 3). These ages are on samples collected from sites close to the southern part of George VI Sound, at Two Step Cliffs and Citadel Bastion (Fig. 8). Ages on samples from a col below Citadel Bastion, at an elevation of 297 m, suggest that some ice thinning had occurred in that area by 13 ka ago, whereas ages of ca 10 ka on samples collected from the 465 m-high summit were interpreted by Hodgson et al. (2009) as representing the retreat of a plateau icefield. The recalculated ages in Supplementary Table 3 on samples from 370 to 380 m elevation at Two Step Cliffs, which are based on  $^{10}\text{Be}$  and  $^{26}\text{Al}$  concentrations reported by Bentley et al. (2006), range between 7.1 and 8.7 ka. The simplest interpretation of these ages would be that grounded ice was still present in southern George VI Sound until this time, even though there had been rapid ice thinning and retreat of the calving front along the northern part of George VI Sound by 9.6 ka ago (Bentley et al., 2005, 2011; Smith et al., 2007; Ó Cofaigh et al., in review). However, Bentley et al. (2011) point out that the Two Step Cliffs samples were collected from high, rather flat-topped ridges, and therefore the possibility that they represent retreat of another perched icefield cannot be ruled out. If this latter interpretation is correct it means that the grounding line could have retreated from the northern end of George VI Sound as far as Citadel Bastion in the early Holocene (Bentley et al., 2011).

## 4. Timeslice reconstructions

We have used the data sources summarized above as the basis for reconstructions of the Amundsen Sea and Bellingshausen Sea sector of the WAIS at 5 ka intervals since 25 ka ago (Figs. 10–15). The reconstructions described below have been made consistent with available data constraints, as far as this is possible. In instances where it is difficult or impossible to reconcile all of the available data, we explain the factors that were considered in deciding what is shown in the reconstruction for a particular time. It must be remembered that ages labelled next to core sites on Figs. 10–14 are *minimum* ages of deglaciation, and therefore when interpreting the position of the ice sheet limit, greatest weight has been placed on ages older than the time of the particular reconstruction. The reconstructions only show ice extent in the Amundsen Sea and Bellingshausen Sea sector, as reconstructions of neighbouring sectors are discussed in other papers in this volume (Anderson et al., 2013; Ó Cofaigh et al., in review; Hillenbrand et al., 2013).



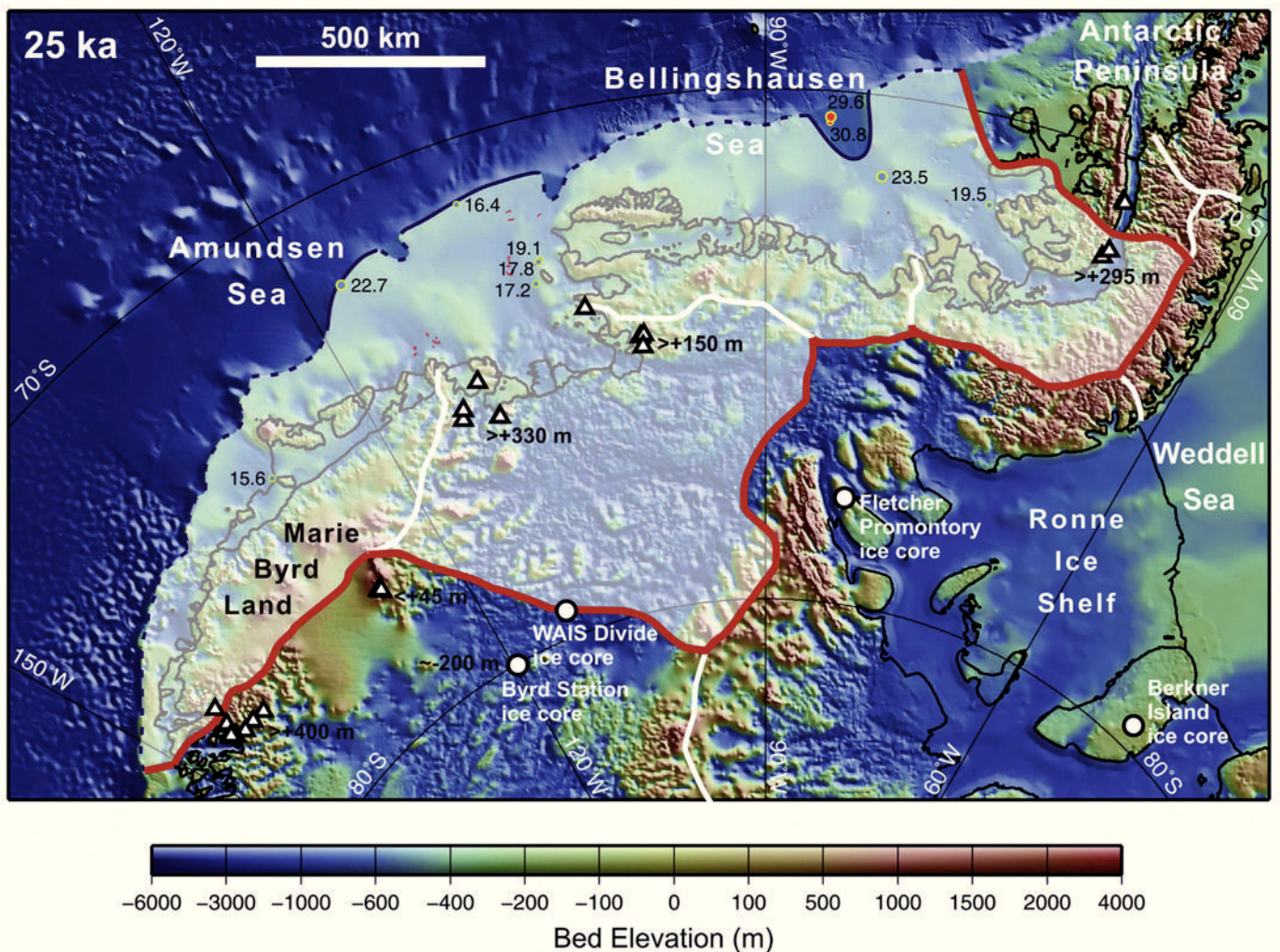


**Fig. 10.** Reconstruction for 25 ka overlaid on Bedmap2 ice sheet bed and bathymetry, which is displayed with shaded-relief illumination from the upper right. Extent of ice sheet indicated by semi-transparent white fill (only shown within Amundsen–Bellingshausen sector). Ice margin marked by dark blue line (dashed where less certain). Thick red line is the sector boundary, which follows the main ice drainage divides. Thick white lines mark other major ice divides. Core sites constraining reconstruction marked by yellow circles, with minimum ages of glaciation annotated (in cal ka BP) and indicated by size and fill colour (red fill – ages older than time of reconstruction; blue fill – younger ages; large circles – ages within  $\pm 5$  ka of time of reconstruction; small circles – ages within 5–10 ka). Cosmogenic surface exposure age sample locations marked by white-filled triangles, and deep ice core sites by white-filled circles, with surface elevation constraints they provide for time of reconstruction annotated. Thin red lines mark the crests of grounding zone wedge and moraines that represent past grounding line positions.

#### 4.1. 25 ka

Well-preserved subglacial bedforms in the outer part of several cross-shelf troughs (e.g. Figs. 4 and 9), in some cases supported by AMS  $^{14}\text{C}$  dates from thin glaciomarine sediments overlying the diamictons they are formed in, indicate that the grounding line advanced to, or at least close to, the continental shelf edge during the last glacial period (Fig. 10; Ó Cofaigh et al., 2005b; Evans et al., 2006; Graham et al., 2010; Smith et al., 2011; Kirshner et al., 2012). AMS  $^{14}\text{C}$  dates on AIOM samples from deglacial sediments in the outermost part of the Belgica Trough, however, suggest that the grounding line had already retreated from the shelf edge before 29 cal ka BP (ages  $30,758 \pm 2262$  and  $29,585 \pm 1780$  cal yr BP, Supplementary Table 2; Hillenbrand et al., 2010a).

Other AMS  $^{14}\text{C}$  dates on AIOM samples from soft tills in the outer and middle parts of Belgica Trough were interpreted by Hillenbrand et al. (2010a) as maximum ages for ice-sheet advance across the shelf. The ages we obtain from calibration of these dates are

$42,748 \pm 7165$  and  $39,481 \pm 7980$  cal yr BP (Supplementary Table 2).

Both in Belgica Trough and elsewhere, evidence of geomorphic features that might represent limits of LGM grounding line advance on the outer shelf is generally lacking. The only exceptions are the pair of asymmetric mounds in PITE that Graham et al. (2010) interpreted as GZWs (Fig. 3), but as yet there are no direct age constraints on these features. The simplest explanation of the fact that such features are generally lacking is that the grounding line advanced all the way to the shelf edge, that the grounded ice eroded features formed during advance, and that there were no significant pauses during subsequent grounding line retreat (e.g. Larter et al., 2009).

Ice surface elevations during the LGM were probably more than 150 m above the modern level in the Hudson Mountains (Bentley et al., 2011; Johnson et al., 2012), more than 400 m above the modern level in the landward parts of the Ford Ranges (Stone et al., 2003), but similar to, or even a little lower than, the modern level in the interior of WAIS (Raynaud and Whillans, 1982; Ackert et al., 1999).

xxxix



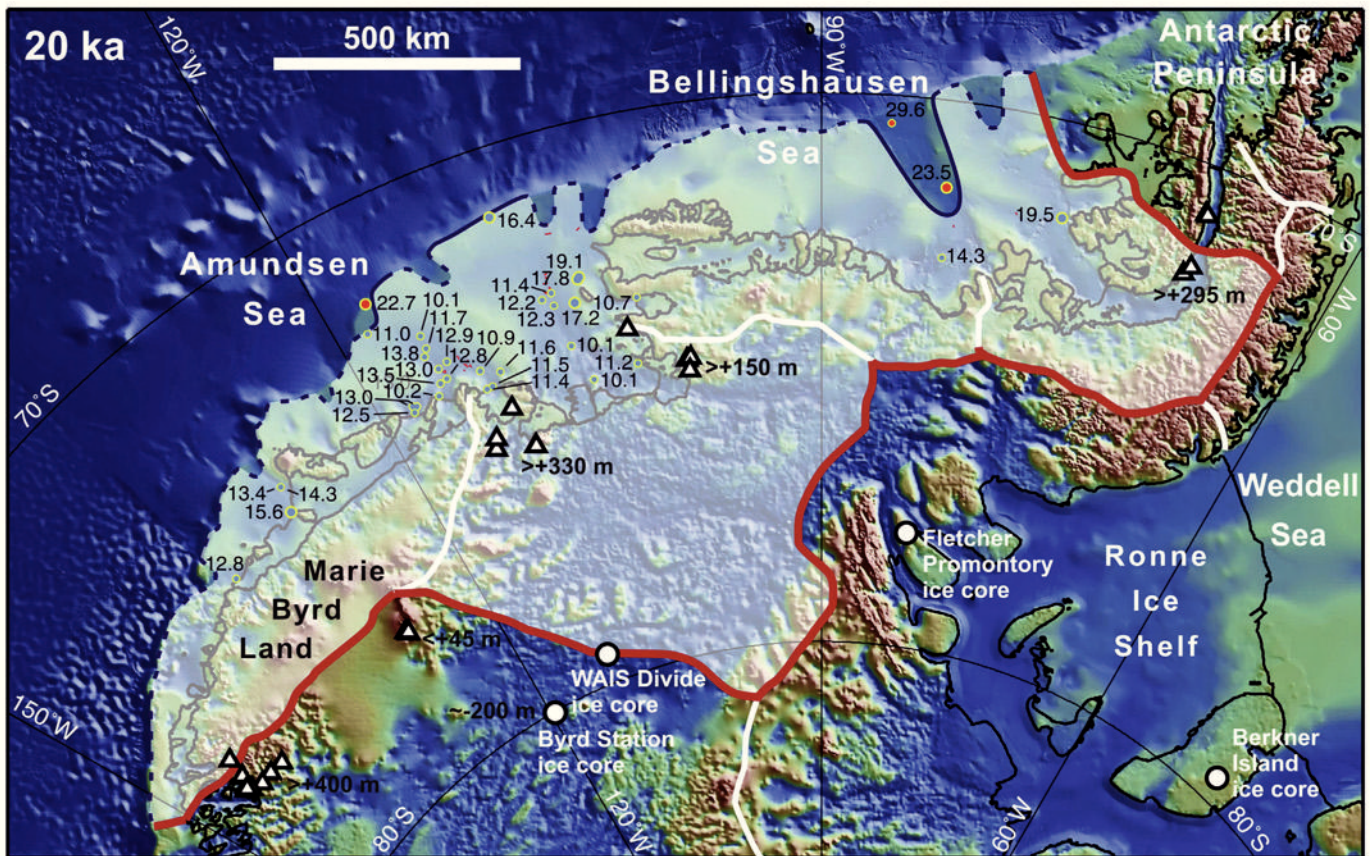


Fig. 11. Reconstruction for 20 ka. See Fig. 10 caption for explanation of symbols and annotations.

#### 4.2. 20 ka

Diamicton in an outer shelf sediment core (VC436; Fig. 7) collected from a site to the east of the DGT mouth contained enough planktonic and/or benthic foraminifera at six different depths for AMS  $^{14}\text{C}$  dates to be obtained (Smith et al., 2011). The diamicton was interpreted by Smith et al. (2011) as a sequence consisting of iceberg-rafted deposits and iceberg turbates, because (i) the diamicton exhibits highly variable shear strengths down-core (ii) multibeam bathymetry data show that the area around the core site has been scoured by icebergs, and (iii) the AMS  $^{14}\text{C}$  dates exhibit a significant down-core age reversal. The relatively high abundance of foraminifera in distinct layers implies that the grounding line was landward of the site at the time of their deposition. The oldest dates obtained on foraminifera from this core yielded ages of  $22,679 \pm 545$  and  $19,909 \pm 335$  cal yr BP (Supplementary Table 2), and Smith et al. (2011) interpreted grounding line retreat as having started before the older of these two ages. An alternative possibility is that its position fluctuated across the outer shelf during the LGM.

As the sea floor on the outer shelf across most of the sector has a slight landward dip (Nitsche et al., 2007; Graham et al., 2011), the inherent instability of ice sheet grounding lines on open, reverse gradient slopes (Weertmann 1974; Schoof, 2007) could have made LGM grounding lines sensitive to small forcing perturbations, leading to fluctuations in their position. While recognising the possibility that there may have been dynamic variations on the fringes of the ice sheet at this time, we show a grounding line position in Fig. 11 landward of the shelf edge in several troughs but at the shelf edge in most other places. By analogy with the pattern of retreat observed at the margins of modern ice sheets (e.g. Joughin et al., 2010; Tinto and Bell, 2011), retreat in cross-shelf

troughs probably led retreat on the intervening banks. AMS  $^{14}\text{C}$  dates from cores recovered on an outer shelf bank, however, have been interpreted as indicating that the grounding line had retreated by 19.1–17.8 cal ka BP, which suggests that any lag between retreat in the troughs and on intervening banks was short (Klages et al., 2013).

In Belgica Trough, a constraint on the extent of grounding line retreat by this time is provided by an AMS  $^{14}\text{C}$  date on AIOM from gravely sandy mud overlying soft till in a core from the mid-shelf (GC368; Fig. 8). The date was interpreted by Hillenbrand et al. (2010a) as a reliable minimum age for deglaciation and the age we obtain from calibration of this date is  $23,527 \pm 1984$  cal yr BP (Supplementary Table 2), implying that the grounding line had already retreated more than 190 km landward of the shelf edge along Belgica Trough before 20 cal ka BP (Fig. 11). Hillenbrand et al. (2010a) also obtained an AMS  $^{14}\text{C}$  date from the base of season open-marine facies in a core (GC358) near Beethoven Peninsula, Alexander Island (Fig. 8) of  $19,456 \pm 577$  cal yr BP (Supplementary Table 2). However, another core (GC359) less than 2 km from this site yielded a minimum age of deglaciation of only  $7503 \pm 323$  cal yr BP. The old age from GC358 is also difficult to reconcile with the general pattern of deglaciation inferred from other core sites on the Bellingshausen Sea continental shelf, and has therefore not been used as a constraint on the position of the ice sheet limit in Figs. 11–13.

#### 4.3. 15 ka

Across most of the sector the detailed pattern and rate of ice retreat across the outer shelf is poorly constrained, as widespread ploughing of sea-floor sediments by iceberg keels makes undisturbed sedimentary records difficult to find (Lowe and Anderson,



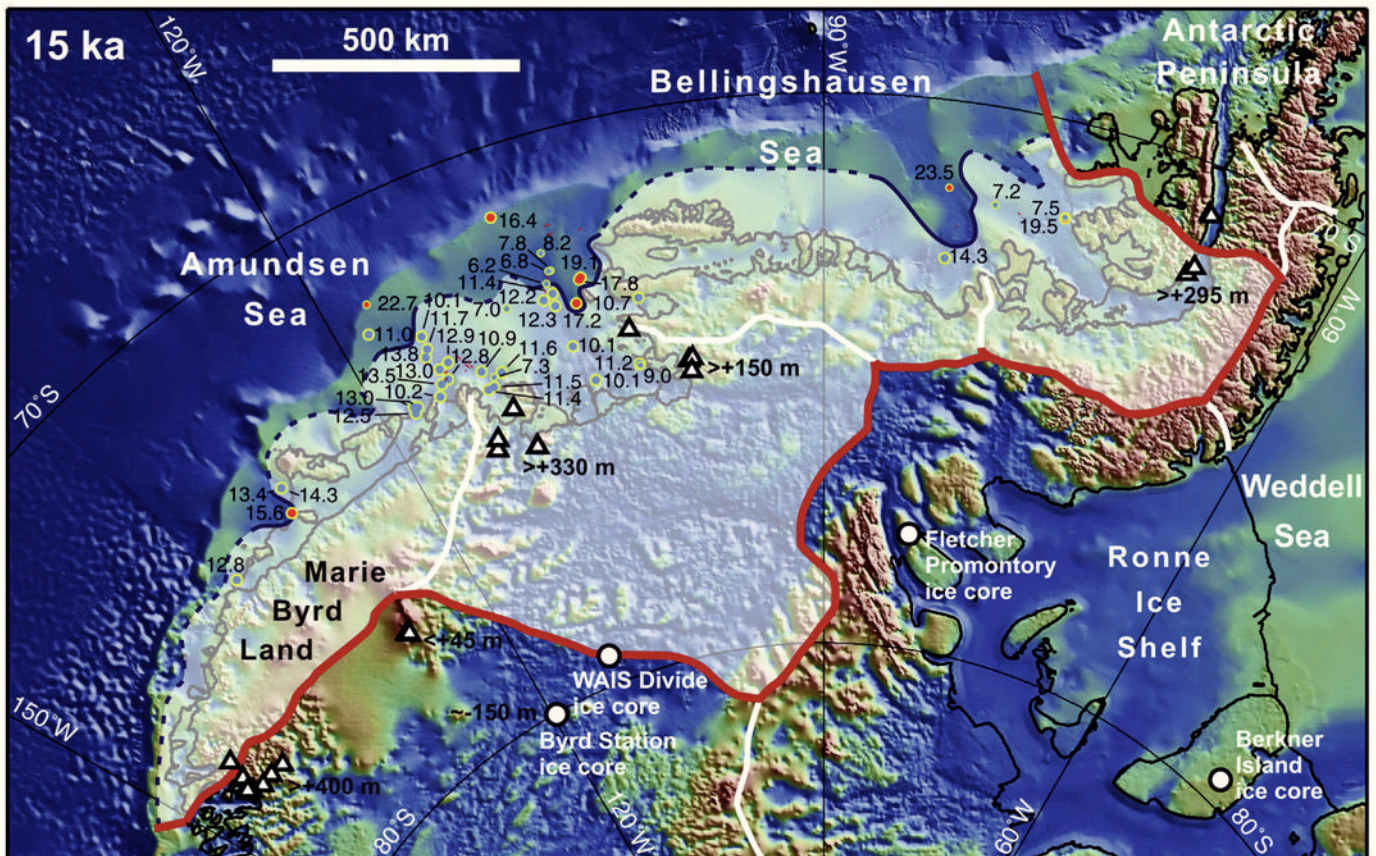


Fig. 12. Reconstruction for 15 ka. See Fig. 10 caption for explanation of symbols and annotations.

2002; Ó Cofaigh et al., 2005b; Dowdeswell and Bamber, 2007; Graham et al., 2010). At 15 cal ka BP, grounded ice still extended across the mid-shelf part of the ASE (Fig. 12; Smith et al., 2011; Kirshner et al., 2012), but it is not clear whether the grounding line retreated across the outer shelf gradually or in a stepwise manner. Graham et al. (2010) interpreted features observed in multibeam swath bathymetry and acoustic sub-bottom profiler data from the axis of PITE as GZWs, which suggests a stepwise retreat along this outer shelf trough.

Hillenbrand et al. (2010a) reported an AMS  $^{14}\text{C}$  date on AIOM from the base of seasonal open-marine muds in a core from Eltanin Bay (GC366; Fig. 8) of  $14,346 \pm 847$  cal yr BP (Supplementary Table 2). This indicates that grounding line retreat had reached the inner shelf along this tributary to Belgica Trough by around 15 cal ka BP (Fig. 12). In contrast, AMS  $^{14}\text{C}$  dates on a core (GC357; Fig. 8) from the area where the trough originating from Ronne Entrance narrows and shallows westward before merging with Belgica Trough indicate very limited retreat along that tributary before 15 cal ka BP (Hillenbrand et al., 2010a). In particular, a date on AIOM in gravelly-sandy mud from just below the transition to seasonally open-marine muds of only  $7180 \pm 561$  cal yr BP (Supplementary Table 2) suggests that ice remained pinned on the relatively shallow "saddle" in this trough until long after 15 cal ka BP (Fig. 12).

#### 4.4. 10 ka

Numerous AMS  $^{14}\text{C}$  dates record rapid grounding line retreat from the middle shelf to near modern limits across the entire Amundsen Sea between 15 and 10 ka ago (Fig. 13; Anderson et al., 2002; Lowe and Anderson, 2002; Smith et al., 2011; Kirshner et al.,

2012; Hillenbrand et al., 2013), and an ice shelf has been interpreted as having been present over the mid-shelf part of PIT from 12.3 to 10.6 cal ka BP (Kirshner et al., 2012). If this interpretation is accepted, and a date interpreted as indicating that the grounding line had already retreated into inner PIB by 11.2 cal ka BP is also accepted (Hillenbrand et al., 2013), then the implication is that a very extensive ice shelf was present for >600 years in the earliest Holocene.

The few available cosmogenic surface exposure age results suggest that gradual ice thinning took place in the part of the WAIS to the south of the ASE since 14.5 ka ago (Johnson et al., 2008; Lindow et al., 2011), and similar gradual thinning has occurred in the Ford Ranges since 10 ka ago (Stone et al., 2003). Ice thinning had also started in southern Alexander Island by 13 ka ago (Hodgson et al., 2009; Bentley et al., 2011). However, cosmogenic surface exposure age data from Mount Waesche have been interpreted as indicating a highstand of the ice surface in the interior of the WAIS around 10 ka ago at up to 45 m above the modern level (Ackert et al., 1999, 2013). In the Hudson Mountains, ice surface elevations remained more than 150 m above the modern level until after 10 ka ago (Johnson et al., 2008; Bentley et al., 2011; Johnson et al., 2012).

In the Ronne Entrance tributary of Belgica Trough, the date of  $7180 \pm 561$  cal yr BP mentioned in the section above indicates that ice retreat continued to be very slow until after 8 cal ka BP. There are no age data from Eltanin Bay that constrain the Holocene ice retreat along that tributary, but as noted above, retreat had already reached the inner shelf in that area by around 15 cal ka BP. Therefore, subsequent retreat to modern ice limits was probably relatively slow (Fig. 13).



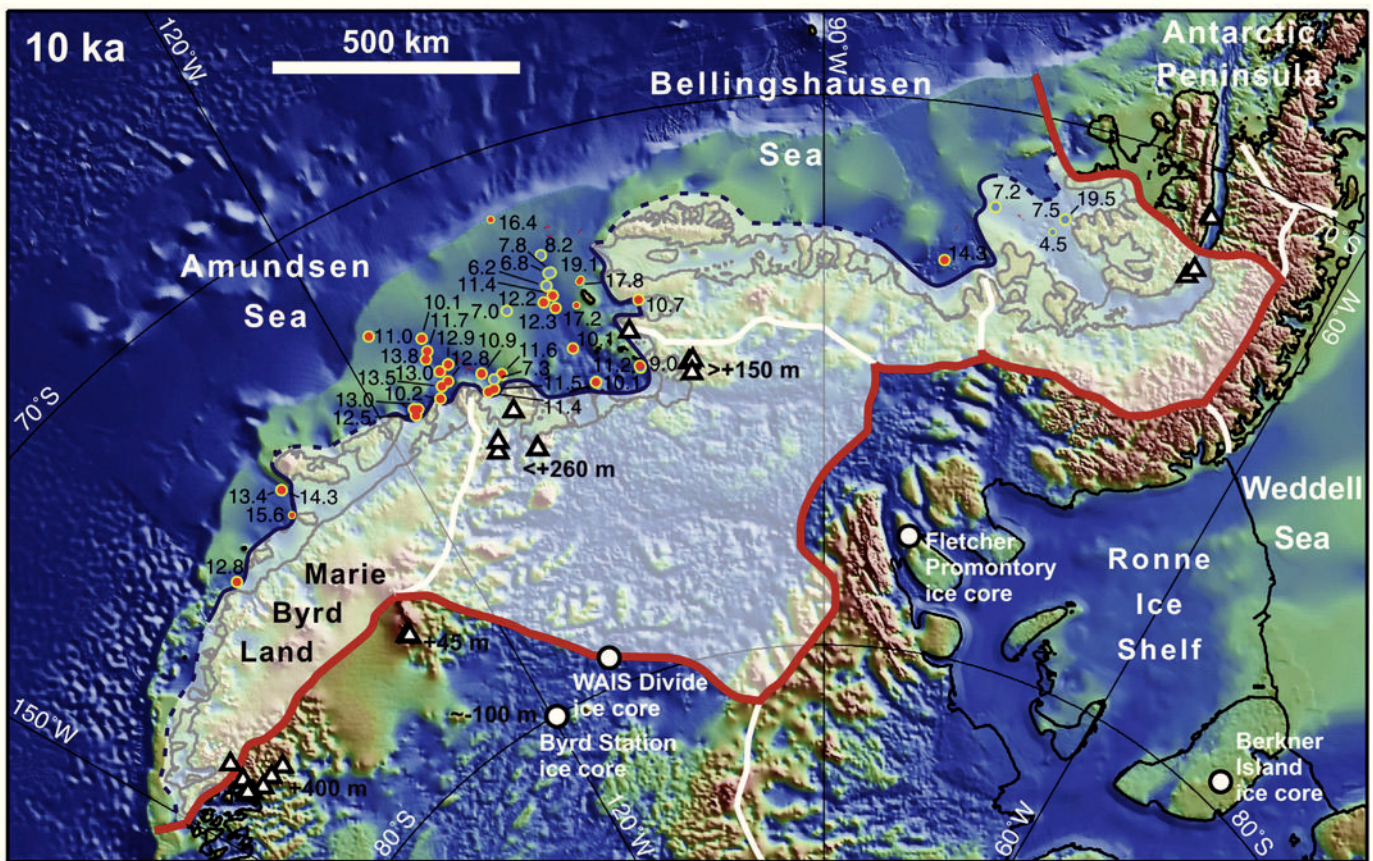


Fig. 13. Reconstruction for 10 ka. See Fig. 10 caption for explanation of symbols and annotations.

#### 4.5. 5 ka

In the Amundsen Sea and Eltanin Bay, the ice margin had already retreated close to modern limits before 10 cal ka BP (see above), and therefore there appears to have been little subsequent change in ice extent in these areas (Fig. 14), unless there was further retreat followed by readvance during the Holocene. So far, there is no evidence from this sector for such retreat and readvance, but neither can the possibility be dismissed. In the neighbouring Antarctic Peninsula sector, however, a rapid early Holocene ice retreat, accompanied by ice shelf collapse and followed by ice shelf reformation, has been documented in Marguerite Bay and George VI Sound (Bentley et al., 2005, 2011; Smith et al., 2007; Ó Cofaigh et al., in review).

The one part of the sector where the ice margin still appears to have been undergoing significant retreat 5 ka ago is in the Ronne Entrance (Fig. 14). This interpretation of continuing retreat is based on an AMS  $^{14}\text{C}$  date of  $4489 \pm 348$  cal yr BP (Supplementary Table 2) on AIOM from near the base of seasonally open-marine diatomaceous mud in a core (GC360; Fig. 8) located more than 170 km from the modern ice shelf front (Hillenbrand et al., 2010a). However, it is important to note that this date provides only a minimum age for grounding-line retreat.

In the interior of the WAIS, the cosmogenic surface exposure age results obtained by Ackert et al. (1999) from Mount Waesche (Fig. 2) imply ice thinning of no more than 45 m during the Holocene (i.e. an average rate of  $<0.5 \text{ cm yr}^{-1}$ ). Surface exposure age data from the Ford Ranges in western Marie Byrd Land (Fig. 2) indicate gradual ice thinning at a faster rate of  $2.5\text{--}9 \text{ cm yr}^{-1}$  through most of the Holocene (Stone et al., 2003). While an average

thinning rate within this range has also been estimated for the part of the WAIS to the south of the ASE, the sparse cosmogenic age data available from that area do not constrain the trajectory of thinning during the Holocene (Johnson et al., 2008; Lindow et al., 2011).

Palaeo-ice flow analysed using radio-echo sounding and global positioning system data acquired across the divide between the drainage basins of PIG and the Institute Ice Stream, which drains into the Weddell Sea, indicates that this ice divide has been stable for at least the last 7 ka, and possibly even the last 20 ka or longer (Ross et al., 2011). Neumann et al. (2008) tracked radar-detected layers from the Byrd ice core and a dated 105-m long ice core drilled near the western divide between the Amundsen Sea and the Ross Sea drainage basins in eastern Marie Byrd Land. The authors concluded from these data and modelling that the ice divide probably migrated within the last 8 ka. They infer that the divide is likely migrating toward the Ross Sea today but the direction of migration may have varied through the period studied.

#### 4.6. The modern ice sheet and observed recent changes

The modern configuration of the ice sheet in the sector is shown in Fig. 15. Over recent decades, the Amundsen–Bellingshausen sector of the WAIS has exhibited more rapid changes than any other part of Antarctica, with the possible exception of the Antarctic Peninsula (e.g. Cook et al., 2005). These changes have included thinning of ice shelves and thinning, flow velocity acceleration and grounding line retreat of ice streams feeding into them (Rignot, 1998; Rignot, 2008; Pritchard et al., 2009, 2012; Scott et al., 2009; Wingham et al., 2009; Joughin and Alley, 2011).



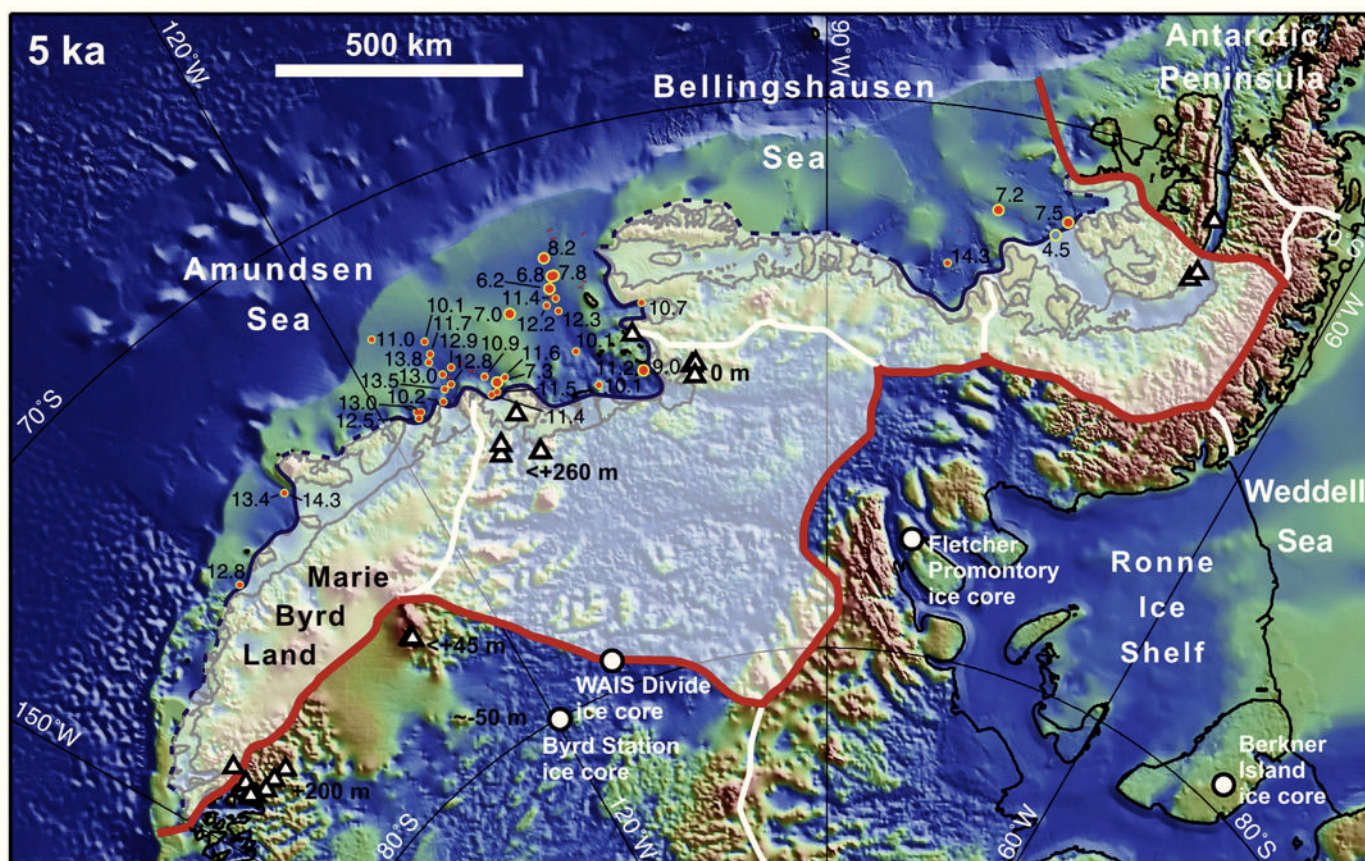


Fig. 14. Reconstruction for 5 ka. See Fig. 10 caption for explanation of symbols and annotations.

Analysis of ICESat laser altimetry data shows that ice shelves along the Amundsen and Bellingshausen Sea coasts thinned by up to  $6.8 \text{ m yr}^{-1}$  over the period 2003–2008 (Pritchard et al., 2012). Over approximately the same period (2003–2007), areas close to the grounding lines on Pine Island, Thwaites and Smith glaciers thinned by up to  $6 \text{ m yr}^{-1}$ ,  $\sim 4 \text{ m yr}^{-1}$ , and greater than  $9 \text{ m yr}^{-1}$ , respectively (Pritchard et al., 2009), and these rates are higher than those reported for the 2002–2004 period (Thomas et al., 2004). Similar recent thinning rates on PIG have been determined from ERS-2 and ENVISAT radar altimetry, and the longer time series of these data shows a progressive increase in thinning rate over the period 1995–2008 (Wingham et al., 2009). Ice flow velocities determined from interferometric Synthetic-Aperture Radar (InSAR) data collected with different satellites show that over the period 1996–2007 Pine Island and Smith glaciers sped up by 42% and 83%, respectively (Rignot, 2008). The flow velocity at the grounding line of PIG had accelerated to  $3500 \text{ m yr}^{-1}$  by 2006 and to  $4000 \text{ m yr}^{-1}$  by late 2008, with no further acceleration observed until early 2010 (Joughin et al., 2010). Whereas there was little or no acceleration along the centre line of Thwaites Glacier, the zone of fast flow widened over the same period (Rignot, 2008). An earlier increase in the flow velocity of Thwaites Glacier was calculated by tracking features in Landsat images, with average velocities 8% higher over 1984–1990 than over 1972–1984 (Ferrigno et al., 1993). Flow velocities on PIG determined from earlier InSAR data showed that the rate of acceleration increased with time, from  $0.8\% \text{ yr}^{-1}$  between 1974 and 1987 to  $3\% \text{ yr}^{-1}$  between 1996 and 2006 (Rignot, 2008). Ground based GPS measurements on PIG showed 6.4% acceleration 55 km upstream from the grounding line and 4.1% acceleration 116 km farther upstream over 2007 (Scott et al., 2009). PIG grounding line retreat of  $1.2 \pm 0.3 \text{ km yr}^{-1}$  between 1992 and 1996

was demonstrated using InSAR data by Rignot (1998). Further retreat by  $15 \pm 6 \text{ km}$  over the following 12 years has been estimated on the basis of changes in ice surface character observed in MODIS satellite images, and using the same approach up to 8 km retreat of the Smith Glacier grounding line has been depicted over the same 12-year period (Rignot, 2008). Joughin et al. (2010) inferred from Terra-SAR-X satellite data that sections of the PIG grounding-line had retreated by 20 km between 1996 and 2009.

Thwaites Glacier grounding line retreat of up to  $1 \text{ km yr}^{-1}$  between 1996 and 2009 was estimated by Tinto and Bell (2011) from comparing the 2009 grounding line position they calculated using airborne laser surface altimetry and radar ice thickness data with a 1996 position determined from a similar previous analysis by Rignot et al. (2004).

There is a growing consensus that these changes have resulted from increased inflow of relatively warm CDW across the continental shelf, which has increased basal melting of ice shelves (Jacobs et al., 1996, 2011; Shepherd et al., 2004; Arneborg et al., 2012; Pritchard et al., 2012). The CDW flows mainly along the bathymetric cross-shelf troughs (Walker et al., 2007; Wählin et al., 2010; Jacobs et al., 2011), and its upwelling is thought to be modulated by the westerly wind system over the Southern Ocean (Thoma et al., 2008). Siliceous microfossil assemblages from a sediment core on the Amundsen Sea continental rise have been interpreted as indicating that a climatic regime similar to the modern one, in which small perturbations in the westerly wind system may result in increased advection of CDW onto the continental shelf, became more common during interglacials after MIS 15 (621–563 ka ago; Konfirst et al., 2012). Over the past few decades, increased basal melting has caused thinning of ice shelves, reducing their buttressing effect and triggering a sequence of



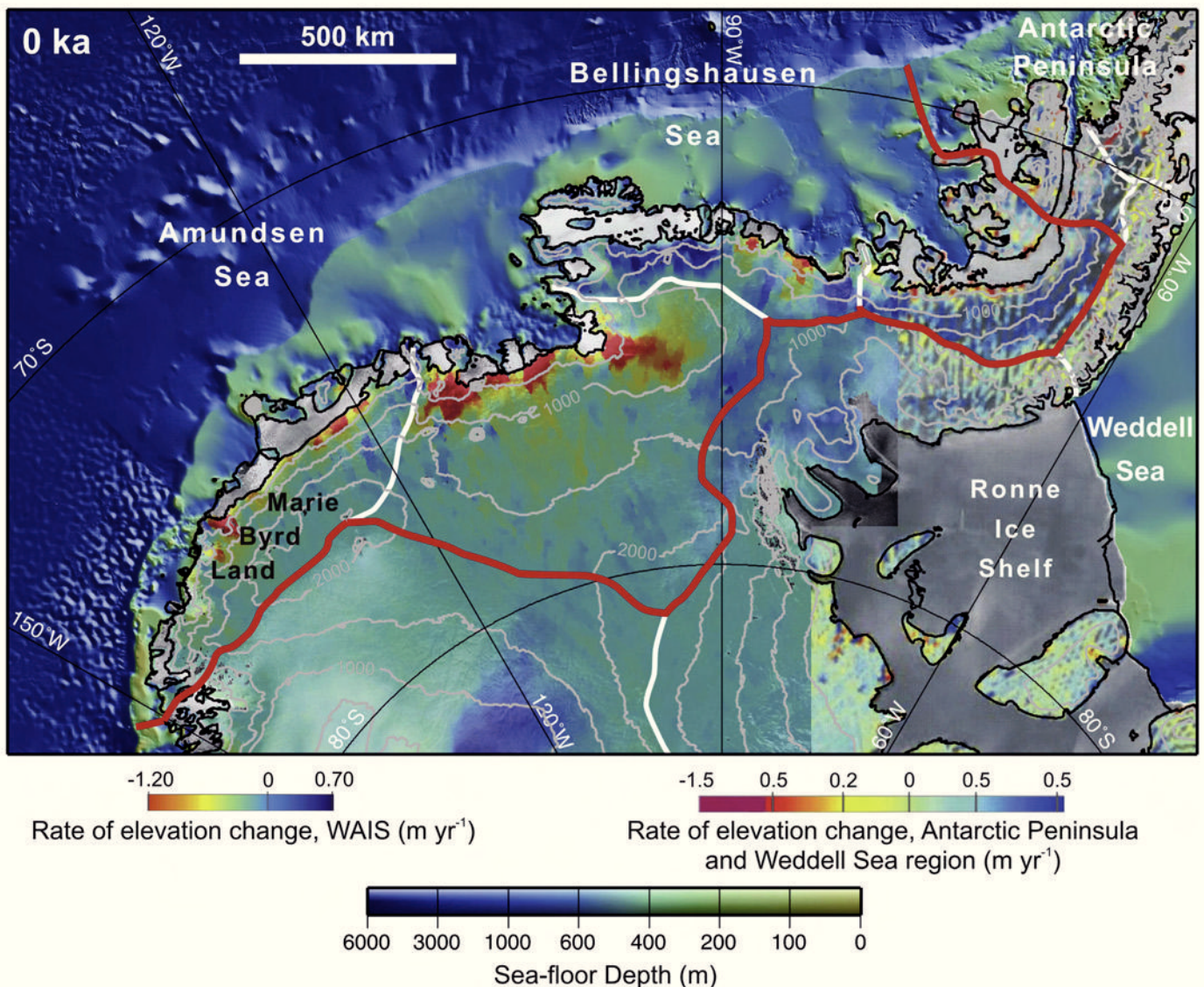


**Fig. 15.** Modern ice sheet configuration. Contours on the ice sheet (thin grey lines) show surface elevation at 500 m intervals from Bedmap2. Colours on ice sheet show rate of change of surface elevation over the period 2003–2007 from Pritchard et al. (2009); N.B. these data are displayed with slightly different colour scales over the WAIS compared to the Antarctic Peninsula and Weddell Sea region. Ice shelves and areas where elevation change data are lacking are shown with a grey or white fill. Colours offshore show bathymetry from Bedmap2, which is displayed with shaded-relief illumination from the upper right. Thick red line marks sector limit. Thick white lines mark other major ice divides.

changes in the ice streams commonly referred to as “dynamic thinning” (e.g. Pritchard et al., 2009). Through combined interpretation of sub-ice-shelf bathymetric data collected with an autonomous submersible vehicle and historical satellite imagery, Jenkins et al. (2010) showed that unpinning of the ice shelf from a submerged ridge about 30 years ago has probably been a major factor contributing to the observed dynamic thinning of PIG. On the basis of remote sensing data alone, Tinto and Bell (2011) suggested a similar scenario for Thwaites Glacier by arguing that about 55–150 years ago the ice stream may have uninned from the western part of a submarine ridge located 40 km seaward of its modern grounding line.

Most studies on recent and ongoing changes in the sector have focussed on the ASE, where the changes are conspicuous in a range of remote sensing datasets (Rignot, 1998, 2008; Chen et al., 2009; Pritchard et al., 2009, 2012; Wingham et al., 2009; Joughin et al., 2010; Lee et al., 2012). However, sub-ice shelf melting induced by upwelling of CDW has also been recorded in the Bellingshausen Sea

(Jenkins and Jacobs, 2008; Pritchard et al., 2012), while a negative mass balance has been calculated for drainage basins around it (Rignot et al., 2008; Pritchard et al., 2009). Furthermore, a recent study has shown that changes taking place in the Ferrigno Ice Stream, which flows into the Bellingshausen Sea, are comparable to those observed for the ASE ice streams (Bingham et al., 2012). A significant difference between the ASE and regions to its east and west is in the size of drainage basins. In contrast to the large drainage basins of Pine Island and Thwaites glaciers (combined area of 417,000 km<sup>2</sup>; Rignot et al., 2008), the drainage basin of Ferrigno Ice Stream, which is one of the largest around the Bellingshausen Sea, occupies an area of only 14,000 km<sup>2</sup> (Bingham et al., 2012).

Based on correlation of radar-layer data with the Byrd ice core and modelling, Neumann et al. (2008) showed that accumulation at the western divide between the Amundsen Sea and the Ross Sea drainage basins was approximately 30% higher than today from 5 ka BP to 3 ka BP. Conway and Rasmussen (2009) detected an



asymmetric pattern of thickness change across this ice divide and concluded that (i) the ice at the divide is currently thinning by  $0.08 \text{ m yr}^{-1}$ , and (ii) the divide is currently migrating towards the Ross Sea at a rate of  $10 \text{ m yr}^{-1}$ . The authors argued that the divide may have migrated towards the Siple Coast for at least the last 2000 years.

It has been argued that since the late 1950s atmospheric temperatures in the West Antarctic hinterland of the Amundsen-Bellinghousen Sea sector have risen faster than anywhere else in Antarctica (Steig et al., 2009), and that this area was even among the most rapidly warming regions on Earth (Bromwich et al., 2012). This warming, together with the increase of CDW upwelling onto the ASE shelf, has been linked to a teleconnection with atmospheric temperature increase in the tropical equatorial Pacific (Ding et al., 2011; Steig et al., 2012). Based on modelling results and climate data, Steig et al. (2012) concluded that a phase of significant warming in the central tropical Pacific around 1940 caused increased CDW upwelling onto the ASE shelf, which resulted in a partial ice-shelf collapse in inner PIB during that time. The authors argued that the ice-sheet changes observed in the ASE sector over the last two decades have their origin in this event and another episode of pronounced warming in the tropical Pacific that started around 1990 and intensified CDW advection onto the ASE shelf.

## 5. Discussion

### 5.1. Maximum ice extent and outer shelf ice dynamics

There is compelling evidence for the ice grounding line having advanced to, or at least close to, the continental shelf edge along several cross-shelf troughs during the last glacial period (Fig. 10). This evidence comes from a combination of streamlined bedforms observed in multibeam swath bathymetry images (e.g. Figs. 4 and 9), thin or absent acoustically-layered sediments overlying these bedforms, and radiocarbon dates from both the diamictos that host the bedforms and the overlying sediments (Lowe and Anderson, 2002; Ó Cofaigh et al., 2005b; Evans et al., 2006; Hillenbrand et al., 2010a; Graham et al., 2010; Smith et al., 2011; Kirshner et al., 2012).

Similar data from shallower parts of the outer shelf are more difficult to assess because most of these have been pervasively furrowed by iceberg keels, but it is unlikely that an advanced grounding line position could have been sustained in the troughs if ice was not also grounded on the intervening banks. As outlined in Section 4.2, AMS  $^{14}\text{C}$  dates on two foraminifera-bearing layers in a glaci-marine diamicton recovered from one of the outer shelf banks yielded LGM ages (Smith et al., 2011), which may hint at fluctuations of the LGM grounding line position. Such fluctuations might have occurred as a consequence of the inherent instability of ice sheet grounding lines on open, reverse gradient slopes (Weertmann, 1974; Schoof, 2007), which are typical on the outer shelf (Nitsche et al., 2007; Graham et al., 2011). Conversely, Alley et al. (2007) proposed that sensitivity to sea-level rise can be reduced by supply of sediment to the grounding line filling space beneath ice shelves. The presence of GZWs in the outer part of PITE suggests that sediment accumulation did temporarily retard grounding line retreat from the outer shelf during the last deglaciation, at least in that trough (Graham et al., 2010).

### 5.2. Ice dynamics and surface profile of the extended ice sheet

Although echo sounding data coverage over the continental shelf now accurately defines the positions of cross-shelf troughs across most of the sector, high-quality multibeam swath

bathymetry data still only covers a fraction of the area (Nitsche et al., 2007; Graham et al., 2011). Consequently, it is currently not possible to make a reliable assessment of how extensive streaming ice flow was on the continental shelf during the last glacial period, let alone the duration of such flow. This is important because the prevalence of streaming flow affects the average surface gradient near the margins of an ice sheet, and therefore such an assessment would be useful in estimating the volume of ice that covered the shelf during the LGM.

Margins of ice sheets where there are few ice streams have relatively steep surface gradients and the ice surface may rise by as much as 2 km within 150 km of the grounding line, e.g. in part of Wilkes Land in East Antarctica. In contrast, the average surface gradient is typically much lower on ice sheet margins with several closely-spaced ice streams, e.g. along the Siple Coast in the Ross Sea, where the average surface elevation 150 km upstream of the grounding line is  $< 300 \text{ m}$ . On this basis, the range of uncertainty in the thickness of ice over middle shelf areas in the Amundsen and Bellingshausen seas during the LGM is  $> 1700 \text{ m}$ , which also implies a large uncertainty in the mass of ice lost during deglaciation. However, the constraint that the maximum ice surface elevation at Mt Waesche, near the ice divide, during the last glacial cycle was only just above 2000 m implies lower elevations than this over the continental shelf. Moreover, as there were at least three major palaeo-ice streams in the ASE (in the DGT, PIT and Abbot Trough; Fig. 3; Nitsche et al., 2007), and two in the Bellingshausen Sea (in the Belgica and Latady Troughs; Fig. 8; Ó Cofaigh et al., 2005b; Graham et al., 2011) it seems likely that ice covering these broad shelf areas had a relatively low surface profile. As on the Siple Coast, extensive outcrop of sedimentary strata at the sea bed in the ASE and Bellingshausen Sea, which is documented in numerous seismic profiles (Nitsche et al., 1997, 2013; Wellner et al., 2001; Cunningham et al., 2002; Hillenbrand et al., 2009; Weigelt et al., 2009, 2012; Gohl et al., 2013b), probably facilitated development of a dilated basal sediment layer. Such a layer is widely considered to promote streaming flow (Alley et al., 1989; Tulaczyk et al., 1998; Kamb, 2001; Studinger et al., 2001; Wellner et al., 2001, 2006; Graham et al., 2009) and was recovered as a soft till in numerous cores from the study area (Lowe and Anderson, 2002; Hillenbrand et al., 2005, 2010a; Smith et al., 2011; Kirshner et al., 2012). In this context, it is also interesting to note that a diamicton with shear strength properties typical for soft till was recovered from the outer shelf to the west of Belgica Trough (site PS2543; Fig. 6; Hillenbrand et al., 2009, 2010a). This observation may suggest that at least at the end of the last glacial period ice streaming was not restricted to the trough, but occurred more widely on the outer shelf.

As noted in Section 3.2, cosmogenic surface exposure ages on a sample from 470 m above sea level on Bear Peninsula (on the southern coast of the ASE) could plausibly represent continuous exposure throughout the last glacial period (Johnson et al., 2008; Supplementary Table 3). As these are results from a single sample, we need to treat them with caution. However, if continuous exposure at this elevation on the southern coast of the ASE is confirmed by additional data, grounded ice on the shelf must have maintained a low surface profile throughout the LGM. This would suggest continuous, widespread streaming flow, rather than streaming starting at a late stage during the glacial period and triggering deglaciation (cf. Ó Cofaigh et al., 2005a; Mosola and Anderson, 2006). Moreover, confirmation of the result from Bear Peninsula by additional samples from high elevation coastal sites would provide an important constraint on the maximum ice volume on the ASE shelf and the dynamic behaviour of the LGM ice sheet. Therefore, collection of additional samples from such sites should be a priority for future research.



### 5.3. Spatially variable ice retreat histories

Perhaps the most surprising aspect of this reconstruction is the different ice retreat histories from the Amundsen and Bellingshausen Sea continental shelves (Figs. 10–15). In a wider context, the Amundsen Sea ice retreat to near present limits by early Holocene time, after relatively rapid retreat over the preceding few thousand years (Figs. 12 and 13; Smith et al., 2011; Kirshner et al., 2012; Hillenbrand et al., 2013), resembles the retreat history of the western Antarctic Peninsula (Heroy and Anderson, 2007; Bentley et al., 2011; Kilfeather et al., 2011). These retreat histories differ, however, from the progressive retreat in the western Ross Sea that had continued through most of the Holocene (e.g. Licht et al., 1996; Conway et al., 1999; Domack et al., 1999; Anderson et al. this volume). The gradual ice retreat along the outer and middle shelf parts of Belgica Trough and towards its Ronne Entrance tributary inferred by Hillenbrand et al. (2010a) is more similar to that recorded in the western Ross Sea, so available results suggest an alternation along the West Antarctic margin between zones in which gradual retreat continued during the Holocene with ones in which retreat close to modern limits was nearly complete by early Holocene time. Gradual Holocene ice retreat towards the Ronne Entrance (Figs. 13–15) is in marked contrast to the rapid early Holocene retreat and ice shelf collapse that occurred along the northern arm of George VI Sound (Bentley et al., 2005, 2011; Smith et al., 2007), but is consistent with an ice history model that reconstructs an ice dome to the south of the Ronne Entrance persisting into the Holocene (Ivins and James, 2005).

Although detailed records of oceanic, atmospheric and sea level forcing functions for the region remain sparse or lacking, there is presently no reason to suspect that they varied greatly across the sector. It is becoming increasingly clear that atmospheric warming and CDW inflow through cross-shelf troughs over the past few decades have affected the entire sector (Jenkins and Jacobs, 2008; Bromwich et al., 2012; Pritchard et al., 2012). If we presume that past forcings were similar across the sector and that the different retreat histories depicted in the reconstruction are correct, this implies that the differences are largely a consequence of how topographic and geological factors have affected ice flow, and of topographic influences on snow accumulation and warm water inflow. In this context, it may be significant that the mouth of the Belgica Trough is the deepest part of the shelf edge in this sector and, in contrast to the reverse gradient along most Antarctic palaeo-ice stream drainage paths, the sea floor dips slightly oceanward along the outer part of the trough (Fig. 8; Graham et al., 2011). Another factor that may have slowed retreat in Belgica Trough is the palaeo-ice drainage pattern, which is inferred to have been highly convergent on the inner and middle shelf (Ó Cofaigh et al., 2005b). In particular, available age data suggest that retreat paused for many thousands of years in the area where the trough originating from the Ronne Entrance narrows and shallows near its confluence with the main Belgica Trough (Hillenbrand et al., 2010a). Similarly, a “bottle neck” in PIT west of Burke Island may have been an important factor in causing the apparent pause in retreat and formation of GZWs in that area (Figs. 3 and 5; Lowe and Anderson, 2002; Graham et al., 2010; Jakobsson et al., 2012; Kirshner et al., 2012). The presence of GZWs in the DGT just to the north of where three tributary troughs merge (Larter et al., 2009; Gohl et al., 2013b) suggests a pause in retreat in that drainage system as well, although the timing of this pause is not well constrained by age data (Smith et al., 2011).

A priority for future ship-based work in the Bellingshausen Sea should be to search for additional core sites that are in shallower water but have escaped disturbance by iceberg keels, as such sites are more likely to preserve foraminifera of early deglacial age that

could be used to test the glacial retreat history proposed by Hillenbrand et al. (2010a).

### 5.4. Influence of reverse bed slopes on retreat

A long-standing and widely-held concern about ice-sheet grounding lines is that they are potentially unstable on submarine reverse slopes (bed slopes down towards continent) with the possibility of a runaway retreat (the “marine ice sheet instability hypothesis”; Weertman, 1974; Schoof, 2007; Katz and Worster, 2010). Although some recent modelling studies have simulated pauses in grounding line retreat (Jamieson et al., 2012) and even stable states (Gudmundsson et al., 2012) on such slopes in settings where there is convergent ice flow, ice grounded on reverse slopes is still thought to be vulnerable in most circumstances. This is a particular concern in relation to future retreat of the WAIS, as reverse slopes extend back from near the modern grounding line to deep basins beneath the centre of the ice sheet (Fig. 2). It has been estimated that loss of ice from the WAIS by unstable retreat along reverse bed slopes could contribute up to 3.4 m to global sea-level rise (Bamber et al., 2009b; Fretwell et al., 2013). The steepest reverse gradients on the broad ASE continental shelf occur on the seaward flanks of inner shelf basins that are up to 1600 m deep (Figs. 3, 6 and 7). In DGT, Smith et al. (2011) estimated that an average retreat rate of 18 m yr<sup>-1</sup> across the outer shelf accelerated to > 40 m yr<sup>-1</sup> as the grounding line approached the deep basins. The deglacial age data presented by Smith et al. (2011) allow the possibility that retreat across the deep basins and back into the tributary troughs was much faster, but the short distances between cores sites and uncertainties associated with the ages mean the level of confidence in such rates is low. In PIT, the grounding line retreated from the middle shelf by 12.3 cal ka BP (Kirshner et al. 2012) and had already retreated across the deepest inner shelf basins to reach inner PIB by 11.2 cal ka BP (Hillenbrand et al., 2013; recalibrated age from Supplementary Table 2). These dates imply a retreat by about 200 km in ~1100 years, which equates to a retreat rate of c. 180 m yr<sup>-1</sup> (between 110 and 370 m yr<sup>-1</sup>, allowing for the uncertainty ranges of the calibrated ages). Therefore, available deglacial ages from shelf sediment cores suggest relatively rapid retreat across these deep basins, which is consistent with the marine ice sheet instability hypothesis. However, in both cases the inner shelf basins also lie landward of the point where the narrowest “bottle neck” in the trough occurs, so these observations are also consistent with the hypothesis that flow convergence may have contributed to a previous pause or slowdown in retreat. Our calculated grounding-line retreat rate for the PIT palaeo-ice stream around the start of the Holocene is almost an order of magnitude lower than fast retreat recorded for PIG over the last 30 years (Joughin et al., 2010), but it should be noted that the palaeo-retreat rate is averaged over more than a millennium.

A range of factors could have contributed to the slow-down in retreat rates when the PIG grounding line approached its modern position, e.g. high basal shear stress over the rugged bedrock that characterises the inner shelf (Wellner et al., 2001, 2006; Lowe and Anderson, 2002; Nitsche et al., 2013), the transverse ridge under the modern Pine Island ice shelf acting as a pinning point (Jenkins et al., 2010), and the fact that inner PIB is another “bottle neck” constricting the flow of the trunk of PIG.

Slow grounding-line retreat from the outer to middle shelf in Belgica Trough (Hillenbrand et al., 2010a) may be explained by the seaward sloping bed of the outer continental shelf in the trough (Fig. 8; Graham et al., 2011). The slow-down and subsequent acceleration of palaeo-ice stream retreat from the middle to the inner shelf along the Ronne Entrance tributary of Belgica



Trough was attributed to bed-slope control associated with the existence of a bathymetric saddle in this area (Hillenbrand et al., 2010a).

Modelling studies may provide further insight into how shelf topography and drainage pattern have affected ice retreat rates (e.g. Gudmundsson et al., 2012; Jamieson et al., 2012). The lack/scarcity of LGM to recent records of oceanic, atmospheric and relative sea-level forcing from within the sector, however, presents a substantial obstacle to realistic modelling of long-term ice sheet changes. The most relevant records of atmospheric change come from the Byrd Station ice core (Blunier and Brook, 2001), which was drilled in the neighbouring Ross Sea sector, and the WAIS Divide ice core (Fig. 2; WAIS Divide Project Members, 2013). A record from a deep ice core drilled on Fletcher Promontory in the Weddell Sea sector, which will be the nearest to the Bellingshausen Sea region, should also become available soon (Fig. 10; R. Mulvaney, pers. comm.). No records of relative sea-level change or changes in continental shelf water masses are available from the sector. Moreover, despite investigations of possible shelf water mass proxies (e.g. Carter et al., 2012; Majewski, 2013), a reliable and practical one has yet to be established. Obtaining LGM to recent records of forcing functions applicable to this critical sector of the WAIS should be a priority for future research.

##### 5.5. The role of subglacial meltwater

There is evidence of extensive bedrock erosion by subglacial meltwater in PIB and in front of the eastern Getz Ice Shelf, but the timing of meltwater discharges is poorly constrained and therefore it remains unclear whether or not they played a significant role in deglaciation (Lowe and Anderson, 2002, 2003; Larter et al., 2009; Smith et al., 2009; Nitsche et al., 2013). Comparison of the size of some of the channels with modelled melt production rates suggests that water must have been stored subglacially and released episodically in order to achieve the flow velocities that would be required to erode bedrock (Nitsche et al., 2013). Furthermore, in view of the dimensions of some of the channels and the fact that they have been carved into bedrock, it seems likely that they formed incrementally over many glacial cycles (Smith et al., 2009; Nitsche et al., 2013). Well-sorted sands and gravels recovered at shallow depth below the seabed in a sediment core from one channel in PIB suggest that this channel was active during deglaciation, although there are no direct age constraints (Lowe and Anderson, 2003). Furthermore, in PIT a mud drape has been interpreted as a meltwater outflow deposit (Kirshner et al., 2012). In contrast, the sequence of facies recovered in three sediment cores from subglacial meltwater-eroded channels in the western ASE is very different, with that recovered from a site north of the eastern Getz Ice Shelf giving evidence that the channel there was overridden by grounded ice since it was last active (Smith et al., 2009).

##### 5.6. Ice surface elevation changes

The few available palaeo-ice surface elevation constraints from the sector suggest that interior elevations have changed little since the LGM (Raynaud and Whillans, 1982; Lorius et al., 1984; Ackert et al., 1999) whereas, in general, a gradual decrease in surface elevations has been detected near the ice sheet margins by 2.5–9 cm yr<sup>-1</sup> since up to 14.5 ka ago (Stone et al., 2003; Bentley et al., 2006, 2011; Johnson et al., 2008; Hodgson et al., 2009; Lindow et al., 2011). Such thinning may have started earlier, but if so ice either covered all nunataks in coastal areas or ones that record the earliest stages of thinning have not yet been sampled. Greater thinning rates that have occurred over short intervals in some coastal areas

may be associated with retreat of steeper ice surface gradients near the grounding line (e.g. Stone et al., 2003).

##### 5.7. Long-term context of recent changes

The rates of thinning and grounding line retreat observed on ice shelves and glaciers around the ASE over the past two decades are significantly faster than any that can be reliably established in deglacial records from the sector. With the available data, however, we cannot insist that such rapid changes are unprecedented since the LGM. Taking into account the evidence for highly episodic grounding-line retreat from the outer and middle shelf parts of PIT during the early stages of the last deglaciation (e.g. Graham et al., 2010; Jakobsson et al., 2012), the grounding line may well have retreated from one GZW position to the next landward GZW position at a rate comparable to that of modern retreat. Although the net retreat of the PIG grounding line has been no more than 112 km over the past 11.2 ka (an average rate of 10 m yr<sup>-1</sup>), we cannot presently discount the possibility that this could have been achieved by up to four periods of retreat lasting no more than 30 years, each at rates similar to those observed over recent decades, with the grounding line remaining steady between those periods (Hillenbrand et al., 2013). Neither can we dismiss the possibility that the grounding line may have retreated beyond its present position at some stage during the Holocene and subsequently re-advanced prior to the period of historical observations. Although there is presently no clear evidence for such a scenario, it is one possible interpretation of recently-reported observations from beneath the PIG ice shelf (Graham et al., 2013). Similarly, if there were past, short-lived phases of ice thinning at rates similar to those observed in the recent past (i.e. several m yr<sup>-1</sup>), the sparse cosmogenic surface exposure age sample sets presently available from the sector are not yet adequate to resolve such abrupt changes.

## 6. Summary and conclusions

Over the past decade airborne and marine surveys in this sector have greatly improved knowledge of bed topography beneath the ice sheet (Fretwell et al., 2013) and of continental shelf bathymetry (Nitsche et al., 2007, 2013; Graham et al., 2011), providing a much more accurate basal boundary for ice sheet and palaeo-ice sheet models. Further airborne geophysical surveys are needed, however, to improve knowledge of ice bed topography around the Bellingshausen Sea and coastal areas of Marie Byrd Land, and further multibeam swath bathymetry surveys are needed to constrain the dynamics of ice that covered continental shelf areas.

Over the same period there has been a several-fold increase in the number of radiocarbon and cosmogenic surface exposure dates constraining the progress of the last deglaciation. Despite this increase, data points remain sparse and unevenly distributed, and in many cases the uncertainty range of ages is too large to determine reliable rates of change. Cosmogenic surface exposure age data remain particularly sparse, and are completely lacking for the region to the south of the Bellingshausen Sea. Although there are few nunataks in this region, collecting samples from them for cosmogenic isotope dating should be a priority for future research. Radiocarbon dates constraining ice retreat are almost exclusively from cross-shelf troughs because, in general, shallower parts of the continental shelf have been pervasively furrowed by icebergs, making it difficult to find undisturbed records extending back to the time of grounding line retreat. However, renewed efforts need to be made to locate sites between cross-shelf troughs that have been protected from iceberg furrowing (e.g. small depressions surrounded by closed contours), particularly as carbonate material



is more likely to be preserved at shallower water sites (Hillenbrand et al., 2003, 2013; Hauck et al., 2012). The radiocarbon dates presently constraining ice retreat in the Bellingshausen Sea are all on AIOM, so it is particularly important to search for carbonate material of early deglacial age from that region in order to refine the history of retreat.

Although there are several shortcomings and large gaps in the available data, we are able to draw the following conclusions:

1. The ice grounding line advanced to, or close to, the continental shelf edge across most of the Amundsen-Bellingshausen sector during the last glacial period, although in at least one area (Belgica Trough) the maximum advance seems to have occurred before the global LGM (23–19 cal ka BP).
2. In the extended ice sheet at least three major ice streams flowed across the continental shelf in the ASE and at least two flowed across the Bellingshausen Sea shelf. We cannot be certain that these were all active throughout the last glacial period, but if they were, then it is likely that ice covering these broad shelf areas had a relatively low surface profile.
3. The middle and outer continental shelf in the ASE and at least the outer shelf in the Bellingshausen Sea are underlain by thick sedimentary strata, which would have made widespread streaming flow more likely by facilitating the formation of a dilated sediment layer at the bed of overriding ice.
4. The few cosmogenic surface exposure ages and ice core data available from the interior of West Antarctica indicate that ice surface elevations there have changed little since the LGM.
5. Ice in the Amundsen Sea had retreated close to its modern limits by early Holocene time, after relatively rapid retreat from the middle shelf during the preceding few thousand years. In contrast, gradual ice retreat occurred from the outer to middle-shelf along Belgica Trough in the Bellingshausen Sea. The inner shelf of its Etlanin Bay tributary had also become free of grounded ice by the early Holocene, but retreat into its Ronne Entrance tributary continued through most of the Holocene. The retreat trajectory in the ASE resembles that on the continental shelf west of the Antarctic Peninsula, whereas the trajectory along the Ronne Entrance tributary of Belgica Trough resembles the progressive retreat recorded in the Ross Sea. Therefore, there seems to be an alternation along the West Antarctic margin between zones in which gradual retreat continued during the Holocene and ones in which retreat close to modern limits was nearly complete by early Holocene time.
6. Grounding line retreat paused for several thousand years and GZWs formed in an area where there is a “bottle neck” in Pine Island Trough, west of Burke Island. Available age data from the Bellingshausen Sea suggest a similar pause in retreat where the trough originating from the Ronne Entrance narrows and shallows near its confluence with the main Belgica Trough.
7. The highest ice retreat rates are found where the grounding line retreated across deep basins on the inner shelf parts of the Pine Island and Dotson-Getz troughs, which is consistent with the marine ice sheet instability hypothesis.
8. Although there is evidence of extensive bedrock erosion by subglacial meltwater on parts of the inner continental shelf in the ASE, the timing of meltwater discharges is poorly constrained and therefore it remains unclear whether or not they played a significant role in deglaciation.
9. In most areas near the margin of the ice sheet from which cosmogenic surface exposure data are available there appears to have been a gradual decrease in surface elevations by 2.5–9 cm yr<sup>-1</sup> since up to 14.5 ka ago. However, in most areas average rates have been derived from small sample sets that would not resolve short periods of more rapid change.
10. The rates of thinning and grounding line retreat observed on ice shelves and glaciers around the ASE over the past two decades are significantly faster than any that can be reliably established in deglacial records from the sector. With existing data, however, we cannot insist that they are unprecedented during the Holocene.

### Acknowledgements

This paper draws on results obtained from many research cruises and field parties. We thank all of the captains, officers, crews, pilots, field support staff, technicians and fellow scientists who contributed to collection of the data used. The Scientific Committee for Antarctic Research Past Antarctic Ice Sheet Dynamics Programme (SCAR-PAIS) and the earlier Antarctic Climate Evolution Programme (SCAR-ACE) have supported the Community Antarctic Ice Sheet Reconstruction Project to which this work contributes. The paper was improved by constructive comments from two anonymous referees.

### Appendix A. Supplementary data

Supplementary data related to this article can be found at <http://dx.doi.org/10.1016/j.quascirev.2013.10.016>.

### References

- Ackert, R.P., Barclay, D.J., Borns, H.W., Calkin, P.E., Kurz, M.D., Fastook, J.L., Steig, E.J., 1999. Measurements of past ice sheet elevations in interior West Antarctica. *Science* 286, 276–280.
- Ackert, R.P., Putnam, A.E., Mukhopadhyay, S., Pollard, D., DeConto, R.M., Kurz, M.D., Borns, H.W., 2013. Controls on interior West Antarctic Ice Sheet elevations: inferences from geologic constraints and ice sheet modelling. *Quat. Sci. Rev.* 65, 26–38.
- Alley, R.B., Blankenship, D.D., Bentley, C.R., Rooney, S.T., 1987. Till beneath Ice Stream B. 3. Till deformation: evidence and implications. *J. Geophys. Res.* 92, 8921–8929.
- Alley, R.B., Blankenship, D.D., Rooney, S.T., Bentley, C.R., 1989. Sedimentation beneath ice shelves: the view from Ice Stream B. *Mar. Geol.* 85, 101–120.
- Alley, R.B., Anandakrishnan, S., Dupont, T.K., Parizek, B.R., Pollard, D., 2007. Effect of sedimentation on ice-sheet grounding-line stability. *Science* 315, 1838–1841.
- Anderson, J.B., Myers, N.C., 1981. USCGC *Glacier* Deep Freeze 81 expedition to the Amundsen sea and Bransfield Strait. *Antarct. J. U. S.* 16 (5), 118–119.
- Anderson, J.B., Wellner, J.S., Lowe, A.L., Mosola, A.B., Shipp, S.S., 2001. Footprint of the expanded West Antarctic Ice Sheet: ice stream history and behavior. *GSA Today* 11 (10), 4–9.
- Anderson, J.B., Shipp, S.S., Lowe, A.L., Wellner, J.S., Mosola, A.B., 2002. The Antarctic Ice Sheet during the Last Glacial Maximum and its subsequent retreat history: a review. *Quat. Sci. Rev.* 21, 49–70.
- Anderson, J.B., Conway, H., Bart, P.J., Witus, A.E., Greenwood, S.L., McKay, R.M., Hall, B.L., Ackert, R.P., Licht, K., Jakobsson, M., Stone, J.O., 2013. Ross Sea paleo-ice sheet drainage and deglacial history during and since the LGM. *Quat. Sci. Rev.* <http://dx.doi.org/10.1016/j.quascirev.2013.08.020>.
- Andrews, J.T., Domack, E.W., Cunningham, W.L., Leverett, A., Licht, K.J., Jull, A.J.T., DeMaster, D.J., Jennings, A.E., 1999. Problems and possible solutions concerning radiocarbon dating of surface marine sediments, Ross Sea, Antarctica. *Quat. Res.* 52, 206–216.
- Arneborg, L., Wåhlin, A.K., Björk, G., Liljebladh, B., Orsi, A.H., 2012. Persistent inflow of warm water onto the central Amundsen shelf. *Nat. Geosci.* 5, 876–880.
- Arthern, R.J., Winebrenner, D.P., Vaughan, D.G., 2006. Antarctic snow accumulation mapped using polarization of 4.3-cm wavelength microwave emission. *J. Geophys. Res.* 111, D06107. <http://dx.doi.org/10.1029/2004JD005667>.
- Balco, G., Stone, J.O., Lifton, N.A., Dunai, T.J., 2008. A complete and easily accessible means of calculating surface exposure ages or erosion rates from <sup>10</sup>Be and <sup>26</sup>Al measurements. *Quat. Geochronol.* 3, 174–195.
- Bamber, J.L., Alley, R.B., Joughin, I., 2007. Rapid response of modern day ice sheets to external forcing. *Earth Planet. Sci. Lett.* 257, 1–13.



- Bamber, J.L., Gomez-Dans, J.L., Griggs, J.A., 2009a. A new 1 km digital elevation model of the Antarctic derived from combined satellite radar and laser data – Part 1: data and methods. *The Cryosphere* 3, 101–111. <http://dx.doi.org/10.5194/tc-3-113-2009>.
- Bamber, J.L., Riva, R.E.M., Vermeersen, B.L.A., LeBrocq, A.M., 2009b. Reassessment of the potential sea-level rise from a collapse of the West Antarctic Ice Sheet. *Science* 324, 901–903.
- Bentley, M.J., 2010. The Antarctic palaeo record and its role in improving predictions of future Antarctic ice sheet change. *J. Quat. Sci.* 25, 5–18.
- Bentley, M.J., Hodgson, D.A., Sugden, D.E., Roberts, S.J., Smith, J.A., Leng, M.J., Bryant, C., 2005. Early Holocene retreat of the George VI ice shelf, Antarctic Peninsula. *Geology* 33, 173–176.
- Bentley, M.J., Fogwill, C.J., Kubik, P.W., Sugden, D.E., 2006. Geomorphological evidence and cosmogenic  $^{10}\text{Be}/^{26}\text{Al}$  exposure ages for the Last Glacial Maximum and deglaciation of the Antarctic Peninsula Ice Sheet. *Geol. Soc. America* 118, 1149–1159.
- Bentley, M.J., Johnson, J.S., Hodgson, D.A., Dunai, T., Freeman, S.P.H.T., Ó Cofaigh, C., 2011. Rapid deglaciation of Marguerite Bay, western Antarctic Peninsula in the early Holocene. *Quat. Sci. Rev.* 30, 3338–3349.
- Bentley, M.J., Johnson, J.S., Fogwill, C.J., 2011. Deglacial history of Hudson Mountains, Amundsen Sea embayment. In: 11th International Symposium on Antarctic Earth Sciences, p. 245. Program and Abstracts (John McIntyre Conference Centre, Edinburgh, Scotland, 11–15 July 2011), Abstract PS19.10.
- Berkman, P.A., Forman, S.L., 1996. Pre-bomb radiocarbon and the reservoir correction for calcareous marine species in the Southern Ocean. *Geophys. Res. Lett.* 23, 363–366.
- Bindschadler, R., 1998. Future of the west Antarctic ice sheet. *Science* 282, 428–429.
- Bingham, R.G., Ferraccioli, F., King, E.C., Larter, R.D., Pritchard, H.D., Smith, A.M., Vaughan, D.G., 2012. Inland thinning of West Antarctic Ice Sheet steered along subglacial rifts. *Nature* 487, 468–471.
- Blunier, T., Brook, E.J., 2001. Timing of millennial-scale climate change in Antarctica and Greenland during the last glacial period. *Science* 291, 109–112.
- Bromwich, D.H., Nicolas, J.P., Monaghan, A.J., Lazzara, M.A., Keller, L.M., Weidner, G.A., Wilson, A.B., 2012. Central west Antarctica among the most rapidly warming regions on Earth. *Nat. Geosci.* 6, 139–145.
- Cande, S.C., Stock, J.M., Müller, R.D., Ishihara, T., 2000. Cenozoic motion between East and West Antarctica. *Nature* 404, 145–150.
- Carter, P., Vance, D., Hillenbrand, C.-D., Smith, J.A., Shoosmith, D.R., 2012. The neodymium isotopic composition of waters masses in the eastern Pacific sector of the Southern Ocean. *Geochim. Cosmochim. Acta* 79, 41–59.
- Chen, J.L., Wilson, C.R., Blankenship, D., Tapley, B.D., 2009. Accelerated Antarctic ice loss from satellite gravity measurements. *Nat. Geosci.* 2, 859–862.
- Convey, P., Gibson, J.A.E., Hillenbrand, C.-D., Hodgson, D.A., Pugh, P.J.A., Smellie, J.L., Stevens, M.I., 2008. Antarctic terrestrial life – challenging the history of the frozen continent? *Biol. Rev.* 83, 103–117.
- Convey, P., Stevens, M.I., Gibson, J.A.E., Hodgson, D.A., Smellie, J.L., Hillenbrand, C.-D., Barnes, D.K.A., Clarke, A., Pugh, P.J.A., Linse, K., Cary, S.C., 2009. Exploring biological constraints on the glacial history of Antarctica. *Quat. Sci. Rev.* 28, 3035–3048.
- Conway, H., Rasmussen, L.A., 2009. Recent thinning and migration of the western divide, central West Antarctica. *Geophys. Res. Lett.* 36, L12502. <http://dx.doi.org/10.1029/2009GL038072>.
- Conway, H., Hall, B.L., Denton, G.H., Gades, A.M., Waddington, E.D., 1999. Past and future grounding-line retreat of the West Antarctic Ice Sheet. *Science* 286, 280–283.
- Cook, F.A., 1909. Through the First Antarctic Night 1898–1899: a Narrative of the Voyage of the “Belgica” Among Newly Discovered Lands and over an Unknown Sea about the South Pole. Doubleday, Page and Co, New York, p. 478. <http://archive.org/details/throughfirstanta00cookrich>.
- Cook, A.J., Fox, A.J., Vaughan, D.G., Ferrigno, J.G., 2005. Retreating glacier fronts on the Antarctic Peninsula over the past half-century. *Science* 308, 541–544.
- Corr, H.F.J., Vaughan, D.G., 2008. A recent volcanic eruption beneath the West Antarctic ice sheet. *Nat. Geosci.* 1, 122–125.
- Cunningham, A.P., Larter, R.D., Barker, P.F., 1994. Glacially prograded sequences on the Bellingshausen Sea continental margin near 90°W. *Terra Antarctica* 1, 267–268.
- Cunningham, A.P., Larter, R.D., Barker, P.F., Gohl, K., Nitsche, F.O., 2002. Tectonic evolution of the Pacific margin of Antarctica 2. Structure of Late Cretaceous–early Tertiary plate boundaries in the Bellingshausen Sea from seismic reflection and gravity data. *J. Geophys. Res.* 107, 2346. <http://dx.doi.org/10.1029/2002JB001897>.
- Danesi, S., Morelli, A., 2000. Group velocity of Rayleigh waves in the Antarctic region. *Phys. Earth Planet. Interiors* 122, 55–66.
- Declair, H. (Ed.), 1999. Roald Amundsen’s *Belgica* Diary: the First Scientific Expedition to the Antarctic, p. 208. Bluntisham, Huntingdon (U.K.).
- Desilets, D., Zreda, M., Prabu, T., 2006. Extended scaling factors for in situ cosmogenic nuclides: new measurements at low latitude. *Earth Planet. Sci. Lett.* 246, 265–276.
- Ding, Q., Steig, E.J., Battisti, D.S., Küttel, M., 2011. Winter warming in West Antarctica caused by central tropical Pacific warming. *Nat. Geosci.* 4, 398–403.
- Domack, E.W., Jacobson, E.A., Shipp, S., Anderson, J.B., 1999. Late Pleistocene–Holocene retreat of the west Antarctic ice-sheet system in the Ross sea: Part 2. Sedimentologic and stratigraphic signature. *Geol. Soc. America Bull.* 111, 1517–1536.
- Domack, E.W., Leventer, A., Dunbar, R., Taylor, F., Brachfeld, S., Sjunneskog, C., ODP Leg 178 Scientific Party, 2001. Chronology of the Palmer Deep site, Antarctic Peninsula: a Holocene paleoenvironmental reference for the circum-Antarctic. *Holocene* 11, 1–9.
- Domack, E., Duran, D., Leventer, A., Ishman, S., Doane, S., McCallum, S., Ambias, D., Ring, J., Gilbert, R., Prentice, M., 2005. Stability of the Larsen B ice shelf on the Antarctic Peninsula during the Holocene epoch. *Nature* 436, 681–685.
- Dowdeswell, J.A., Bamber, J., 2007. Keel depths of modern Antarctic icebergs and implications for sea-floor scouring in the geological record. *Mar. Geol.* 243, 120–131.
- Dowdeswell, J.A., Ó Cofaigh, C., Pudsey, C.J., 2004. Thickness and extent of the subglacial till layer beneath an Antarctic paleo-ice stream. *Geology* 32, 13–16.
- Dowdeswell, J.A., Evans, J., Ó Cofaigh, C., Anderson, J.B., 2006. Morphology and sedimentary processes on the continental slope off Pine Island Bay, Amundsen Sea, West Antarctica. *Geol. Soc. America Bull.* 118, 606–619.
- Dowdeswell, J.A., Ó Cofaigh, C., Noormets, R., Larter, R.D., Hillenbrand, C.-D., Benetti, S., Evans, J., Pudsey, C.J., 2008. A major trough-mouth fan on the continental margin of the Bellingshausen Sea, West Antarctica: the Belgica Fan. *Mar. Geol.* 252, 129–140.
- Dunai, T., 2001. Influence of secular variation of the magnetic field on production rates of in situ produced cosmogenic nuclides. *Earth Planet. Sci. Lett.* 193, 197–212.
- Eagles, G., Larter, R.D., Gohl, K., Vaughan, A.P.M., 2009. West Antarctic rift system in the Antarctic Peninsula. *Geophys. Res. Lett.* 36, L21305. <http://dx.doi.org/10.1029/2009GL040721>.
- Ehrmann, W., Hillenbrand, C.-D., Smith, J.A., Graham, A.G.C., Kuhn, G., Larter, R.D., 2011. Provenance changes between recent and glacial-time sediments in the Amundsen Sea embayment, West Antarctica: clay mineral assemblage evidence. *Antarc. Sci.* 23, 471–486.
- Esper, O., Gersonde, R., Kadagies, N., 2010. Diatom distribution in southeastern Pacific surface sediments and their relationship to modern environmental variables. *Palaeogeogr. Palaeoclimatol. Palaeoecol.* 287, 1–27.
- Evans, J., Dowdeswell, J.A., Ó Cofaigh, C., Benham, T.J., Anderson, J.B., 2006. Extent and dynamics of the West Antarctic Ice Sheet on the outer continental shelf of Pine Island Bay during the last glaciation. *Mar. Geol.* 230, 53–72.
- Ferrigno, J.G., Lucchitta, B.K., Mullins, K.F., Allison, A.L., Allen, R.J., Gould, W.G., 1993. Velocity measurements and changes in position of Thwaites glacier/iceberg tongue from aerial photography, Landsat images and NOAA AVHRR data. *Ann. Glaciol.* 17, 239–244.
- Finn, C.A., Müller, R.D., Panter, K.S., 2005. A Cenozoic diffuse alkaline magmatic province (DAMP) in the southwest Pacific without rift or plume origin. *Geochim. Geophys. Geosyst.* 6, Q02005. <http://dx.doi.org/10.1029/2004GC000723>.
- Fretwell, P., Pritchard, H.D., Vaughan, D.G., 57 others, 2013. Bedmap2: improved ice bed, surface and thickness datasets for Antarctica. *Cryosphere* 7, 375–393. <http://dx.doi.org/10.5194/tc-7-375-2013>.
- Gales, J.A., Larter, R.D., Mitchell, N.C., Dowdeswell, J.A., 2013. Geomorphic signature of Antarctic submarine gullies: implications for continental slope processes. *Mar. Geol.* 337, 112–124.
- Gohl, K. (Ed.), 2007. The Expedition ANTARKTIS-XXIII/4 of the Research Vessel “Polarstern” in 2006. *Meeresforschung*, vol. 557. Alfred-Wegener-Institut für Polar- und Meeresforschung, Bremerhaven (Germany), p. 166. <http://hdl.handle.net/10013/epic.27102>.
- Gohl, K. (Ed.), 2010. The Expedition of the Research Vessel “Polarstern” to the Amundsen Sea, Antarctica, in 2010 (ANT-xxvi/3). *Berichte zur Polar- und Meeresforschung*, vol. 617. Alfred-Wegener-Institut für Polar- und Meeresforschung, Bremerhaven (Germany), p. 168. <http://hdl.handle.net/10013/epic.35668>.
- Gohl, K., 2012. Basement control on past ice sheet dynamics in the Amundsen Sea Embayment, West Antarctica. *Palaeogeogr. Palaeoclimatol. Palaeoecol.* 335–336, 35–41.
- Gohl, K., Teterin, D., Eagles, G., Netzeband, G., Grobys, J.W.G., Parsiegl, N., Schlüter, P., Leinweber, V., Larter, R.D., Uenzelmann-Neben, G., Udintsev, G.B., 2007. Geophysical Survey Reveals Tectonic Structures in the Amundsen Sea Embayment, West Antarctica. U.S. Geological Survey and The National Academies. USGS OF-2007-1047, Short Research Paper 047 <http://dx.doi.org/10.3133/of2007-1047.srp047>.
- Gohl, K., Denk, A., Wobbe, F., Eagles, G., 2013a. Deciphering tectonic phases of the Amundsen Sea Embayment shelf, West Antarctica, from a magnetic anomaly grid. *Tectonophysics* 585, 113–123.
- Gohl, K., Uenzelmann-Neben, G., Larter, R.D., Hillenbrand, C.-D., Hochmuth, K., Kalberg, T., Weigelt, E., Davy, B., Kuhn, G., Nitsche, F.O., 2013b. Seismic stratigraphic record of the Amundsen Sea Embayment shelf from pre-glacial to recent times: evidence for a dynamic West Antarctic ice sheet. *Mar. Geol.* 344, 115–131.
- Graham, A.G.C., Larter, R.D., Gohl, K., Hillenbrand, C.-D., Smith, J.A., Kuhn, G., 2009. Bedform signature of a West Antarctic palaeo-ice stream reveals a multi-temporal record of flow and substrate control. *Quat. Sci. Rev.* 28, 2774–2793.
- Graham, A.G.C., Larter, R.D., Gohl, K., Dowdeswell, J.A., Hillenbrand, C.-D., Smith, J.A., Evans, J., Kuhn, G., 2010. Flow and retreat of the Late Quaternary Pine Island–Thwaites palaeo-ice stream, West Antarctica. *J. Geophys. Res.* 115, F03025. <http://dx.doi.org/10.1029/2009JF001482>.
- Graham, A.G.C., Nitsche, F.O., Larter, R.D., 2011. An improved bathymetry compilation for the Bellingshausen Sea, Antarctica, to inform ice-sheet and ocean models. *Cryosphere* 5, 95–106. <http://dx.doi.org/10.5194/tc-5-95-2011>.



- Graham, A.G.C., Dutrieux, P., Vaughan, D.G., Nitsche, F.O., Gyllencreutz, R., Greenwood, S.L., Larter, R.D., Jenkins, A., 2013. Sea-bed corrugations beneath an Antarctic ice shelf revealed by autonomous underwater vehicle survey: origin and implications for the history of Pine Island Glacier. *J. Geophys. Res.* 118. <http://dx.doi.org/10.1002/jgrf.20087>.
- Granot, R., Cande, S.C., Stock, J.M., Davey, F.J., Clayton, R.W., 2010. Postspreading rifting in the Adare Basin, Antarctica: regional tectonic consequences. *Geochim. Geophys. Geosyst.* 11, Q08005. <http://dx.doi.org/10.1029/2010GC003105>.
- Gudmundsson, G.H., Krug, J., Durand, G., Favier, L., Gagliardini, O., 2012. The stability of grounding lines on retrograde slopes. *Cryosphere* 6, 1497–1505. <http://dx.doi.org/10.5194/tc-6-1497-2012>.
- Harden, S.L., DeMaster, D.J., Nittrouer, C.A., 1992. Developing sediment geochronologies for high-latitude continental shelf deposits: a radiochemical approach. *Mar. Geol.* 103, 69–97.
- Hauck, J., Gerdes, D., Hillenbrand, C.-D., Hoppema, M., Kuhn, G., Nehrke, G., Völker, C., Wolf-Gladrow, D.A., 2012. Distribution and mineralogy of carbonate sediments on Antarctic shelves. *J. Mar. Syst.* 90, 77–87.
- Heroy, D.C., Anderson, J.B., 2007. Radiocarbon constraints on Antarctic Peninsula ice sheet retreat following the last glacial maximum (LGM). *Quat. Sci. Rev.* 26, 3286–3297.
- Hillenbrand, C.-D., Grobe, H., Diekmann, B., Kuhn, G., Fütterer, D.K., 2003. Distribution of clay minerals and proxies for productivity in surface sediments of the Bellingshausen and Amundsen seas (West Antarctica) – relation to modern environmental conditions. *Mar. Geol.* 193, 253–271.
- Hillenbrand, C.-D., Baesler, A., Grobe, H., 2005. The sedimentary record of the last glaciation in the western Bellingshausen Sea (West Antarctica): implications for the interpretation of diamictites in a polar-marine setting. *Mar. Geol.* 216, 191–204.
- Hillenbrand, C.-D., Ehrmann, W., Larter, R.D., Benetti, S., Dowdeswell, J.A., Ó Cofaigh, C., Graham, A.G.C., Grobe, H., 2009. Clay mineral provenance of sediments in the southern Bellingshausen Sea reveals drainage changes of the West Antarctic Ice Sheet during the Late Quaternary. *Mar. Geol.* 265, 1–18.
- Hillenbrand, C.-D., Larter, R.D., Dowdeswell, J.A., Ehrmann, W., Ó Cofaigh, C., Benetti, S., Graham, A.G.C., Grobe, H., 2010a. The sedimentary legacy of a palaeo-ice stream on the shelf of the southern Bellingshausen Sea: clues to West Antarctic glacial history during the Late Quaternary. *Quat. Sci. Rev.* 29, 2741–2763.
- Hillenbrand, C.-D., Smith, J.A., Kuhn, G., Esper, O., Gersonde, R., Larter, R.D., Maher, B., Moreton, S.G., Schimmield, T.M., Korte, M., 2010b. Age assignment of diatomaceous ooze deposited in the western Amundsen Sea Embayment after the Last Glacial Maximum. *J. Quat. Sci.* 25, 280–295. <http://dx.doi.org/10.1002/jqs.1308>.
- Hillenbrand, C.-D., Kuhn, G., Smith, J.A., Gohl, K., Graham, A.G.C., Larter, R.D., Klages, J.P., Downey, R., Moreton, S.G., Forwick, M., Vaughan, D.G., 2013. Grounding-line retreat of the west Antarctic ice sheet from inner Pine Island Bay. *Geology* 41, 35–38.
- Hillenbrand, C.-D., Bentley, M.J., Stollendorff, T.D., Hein, A.S., Kuhn, G., Graham, A.G.C., Fogwill, C.J., Kristoffersen, Y., Smith, J.A., Anderson, J.A., Larter, R.D., Melles, M., Hodgson, D.A., Mulvaney, R., Sugden, D.E., 2013. Reconstruction of changes in the Weddell Sea sector of the Antarctic Ice Sheet since the Last Glacial Maximum. *Quat. Sci. Rev.* <http://dx.doi.org/10.1016/j.quascirev.2013.07.020>.
- Hochmuth, K., Gohl, K., 2013. Glacio-marine sedimentation dynamics of the Abbot glacial trough of the Amundsen Sea Embayment shelf, West Antarctica. In: Hambrey Barker, M., P.F., Barrett, P.J., Bowman, V., Davies, B., Smellie, J.L., Tranter, M. (Eds.), *Antarctic Palaeoenvironments and Earth-surface Processes*, Geological Society Special Publications, vol. 381. Geological Society, London (U.K.). <http://dx.doi.org/10.1144/SP381.21>.
- Hodgson, D.A., Roberts, S.J., Bentley, M.J., Smith, J.A., Johnson, J.S., Verleyen, E., Vyverman, W., Hodson, A.J., Leng, M.J., Czfiferszky, A., Fox, A.J., Sanderson, D.C.W., 2009. Exploring former subglacial Hodgson lake, Antarctica Paper I: site description, geomorphology and limnology. *Quat. Sci. Rev.* 28, 2295–2309.
- Hole, M.J., LeMasurier, W., 1994. Tectonic controls on the geochemical composition of Cenozoic, mafic alkaline volcanic rocks from West Antarctica. *Contrib. Mineral. Petrol.* 117, 187–202.
- Holt, J.W., Blankenship, D.D., Morse, D.L., Young, D.W., Peters, M.E., Kempf, S.D., Richter, T.G., Vaughan, D.G., Corr, H.F.J., 2006. New boundary conditions for the West Antarctic Ice Sheet: subglacial topography of the Thwaites and Smith glacier catchments. *Geophys. Res. Lett.* 33, L09502. <http://dx.doi.org/10.1029/2005GL025561>.
- Hughes, T.J., 1981. The weak underbelly of the West Antarctic ice sheet. *J. Glaciol.* 27, 518–525.
- IOC, IHO and BODC, 2003. Centenary Edition of the GEBCO Digital Atlas. Published on CD-ROM on behalf of the Intergovernmental Oceanographic Commission and the International Hydrographic Organization as part of the General Bathymetric Chart of the Oceans. British Oceanographic Data Centre, Liverpool (U.K.).
- Ivins, E.R., James, T.S., 2005. Antarctic glacial isostatic adjustment: a new assessment. *Antarct. Sci.* 17, 541–553.
- Jacobs, S.S., Hellmer, H.H., Jenkins, A., 1996. Antarctic ice sheet melting in the Southeast Pacific. *Geophys. Res. Lett.* 23, 957–960.
- Jacobs, S.S., Jenkins, A., Giulivi, C.F., Dutrieux, P., 2011. Stronger ocean circulation and increased melting under Pine Island Glacier ice shelf. *Nat. Geosci.* 4, 519–523.
- Jakobsson, M., Anderson, J.B., Nitsche, F., Dowdeswell, J.A., Gyllencreutz, R., Kirchner, N., Mohammad, R., O'Regan, M., Alley, R.B., Anandakrishnan, S., Eriksson, B., Kirchner, A., Fernandez, R., Stollendorff, T., Minzoni, R., Majewski, W., 2011. Geological record of ice shelf break-up and grounding line retreat, Pine Island Bay, West Antarctica. *Geology* 39, 691–694.
- Jakobsson, M., Anderson, J.B., Nitsche, F., Gyllencreutz, R., Kirchner, A., Kirchner, N., O'Regan, M., Mohammad, R., Eriksson, B., 2012. Ice sheet retreat dynamics inferred from glacial morphology of the central Pine Island Bay Trough, West Antarctica. *Quat. Sci. Rev.* 38, 1–10.
- Jamieson, S.S.R., Vieli, A., Livingstone, S.J., Ó Cofaigh, C., Stokes, C., Hillenbrand, C.-D., Dowdeswell, J.A., 2012. Ice-stream stability on a reverse bed slope. *Nat. Geosci.* 5, 799–802.
- Jenkins, A., Jacobs, S., 2008. Circulation and melting beneath George VI ice shelf, Antarctica. *J. Geophys. Res.* 113, C04013. <http://dx.doi.org/10.1029/2007JC004449>.
- Jenkins, A., Dutrieux, P., Jacobs, S.S., McPhail, S.D., Perrett, J.R., Webb, A.T., White, D., 2010. Observations beneath Pine Island glacier in west Antarctica and implications for its retreat. *Nat. Geosci.* 3, 468–472.
- Jenssen, D., 1983. Elevation and climatic changes from total gas content and stable isotopic measurements. In: Robin de, G.Q. (Ed.), *The Climatic Record in Polar Ice Sheets*. Cambridge University Press, London (U.K.), pp. 138–144.
- Johnson, J.S., Bentley, M.J., Gohl, K., 2008. First exposure ages from the Amundsen sea embayment, west Antarctica: the Late Quaternary context for recent thinning of Pine Island, Smith, and Pope Glaciers. *Geology* 36, 223–226.
- Johnson, J.S., Schaefer, J.M., Bentley, M.J., Fogwill, C.J., Smith, J.A., Schimmelfennig, I., Gohl, K., 2012. Rapid early- to mid-Holocene thinning of Pine Island Glacier detected using cosmogenic exposure dating (abstract). *Mineraol. Mag* 76 (6), 1903.
- Jordan, T.A., Ferraccioli, F., Vaughan, D.G., Holt, J.W., Corr, H., Blankenship, D.D., Diehl, T.M., 2010. Aerogravity evidence for major crustal thinning under the Pine Island Glacier region (West Antarctica). *Geol. Soc. America Bull.* 122, 714–726.
- Joughin, I., Alley, R.B., 2011. Stability of the West Antarctic ice sheet in a warming world. *Nat. Geosci.* 4, 506–513.
- Joughin, I., Smith, B.E., Holland, D.M., 2010. Sensitivity of 21st century sea level to ocean-induced thinning of Pine Island Glacier, Antarctica. *Geophys. Res. Lett.* 37, L20502. <http://dx.doi.org/10.1029/2010GL044819>.
- Kamb, B., 2001. Basal zone of the West Antarctic ice streams and its role in lubrication of their rapid motion. In: Alley, R.B., Bindschadler, R.A. (Eds.), *The West Antarctic Ice Sheet: Behavior and Environment*, Antarctic Research Series, vol. 77. AGU, Washington, D. C., pp. 157–199.
- Katz, R.F., Worster, M.G., 2010. Stability of ice-sheet grounding lines. *Proc. R. Soc. A* 466, 1597–1620.
- Kellogg, T.B., Kellogg, D.E., 1987a. Late Quaternary deglaciation of the Amundsen Sea: implications for ice sheet modelling. In: Waddington, E.D., Walder, J.S. (Eds.), *The Physical Basis of Ice Sheet Modelling*. International Association of Hydrological Sciences Publication No. 170. IAHS Press, Wallingford (U.K.), pp. 349–357.
- Kellogg, T.B., Kellogg, D.E., 1987b. Recent glacial history and rapid ice retreat in the Amundsen Sea. *J. Geophys. Res.* 92, 8859–8864.
- Kilfeather, A.A., Ó Cofaigh, C., Lloyd, J.M., Dowdeswell, J.A., Xu, S., Moreton, S.G., 2011. Ice-stream retreat and ice-shelf history in Marguerite Trough, Antarctic Peninsula: sedimentological and foraminiferal signatures. *Geol. Soc. America Bull.* 123, 997–1015.
- King, M.A., Bingham, R.J., Moore, P., Whitehouse, P.L., Bentley, M.J., Milne, G.A., 2012. Lower satellite-gravimetry estimates of Antarctic sea-level contribution. *Nature* 491, 586–589.
- Kirchner, A., Anderson, J.B., Jakobsson, M., O'Regan, M., Majewski, W., Nitsche, F., 2012. Post-LGM deglaciation in Pine Island Bay, west Antarctica. *Quat. Sci. Rev.* 38, 11–26.
- Klages, J.P., Kuhn, G., Hillenbrand, C.-D., Graham, A.G.C., Smith, J.A., Larter, R.D., Gohl, K., 2013. First geomorphological record and glacial history of an inter-ice stream ridge on the West Antarctic continental shelf. *Quat. Sci. Rev.* 61, 47–61.
- Konfirst, M.A., Scherer, R.P., Hillenbrand, C.-D., Kuhn, G., 2012. A marine diatom record from the Amundsen Sea – Insights into oceanographic and climatic response to the Mid-Pleistocene Transition in the West Antarctic sector of the Southern Ocean. *Mar. Micropaleontol.* 92–93, 40–51.
- Lal, D., 1991. Cosmic ray labeling of erosion surfaces: in situ nuclide production rates and erosion models. *Earth Planet. Sci. Lett.* 104, 424–439.
- Larter, R.D., Gohl, K., Hillenbrand, C.-D., Kuhn, G., Deen, T.J., Dietrich, R., Eagles, G., Johnson, J.S., Livermore, R.A., Nitsche, F.O., Pudsey, C.J., Schenke, H.-W., Smith, J.A., Udintsev, G., Uenzelmann-Neben, G., 2007. West Antarctic ice sheet change since the last glacial period. *Eos, Transactions. Am. Geophys. Union* 88, 189–190. <http://dx.doi.org/10.1029/2007EO170001>.
- Larter, R.D., Graham, A.G.C., Gohl, K., Kuhn, G., Hillenbrand, C.-D., Smith, J.A., Deen, T.J., Livermore, R.A., Schenke, H.-W., 2009. Subglacial bedforms reveal complex basal regime in a zone of paleo-ice stream convergence, Amundsen Sea Embayment, West Antarctica. *Geology* 37, 411–414.
- Lawley, B., Ripley, S., Bridge, P., Convey, P., 2004. Molecular analysis of geographic patterns of eukaryotic diversity in Antarctic soils. *Appl. Environ. Microbiol.* 70, 5963–5972.
- Le Brocq, A.M., Payne, A.J., Vieli, A., 2010. An improved Antarctic dataset for high resolution numerical ice sheet models (ALBMAP v1). *Earth Syst. Sci. Data* 2, 247–260. <http://dx.doi.org/10.5194/essd-2-247-2010>.
- Lee, H., Shum, C.K., Howat, I.M., Monaghan, A., Ahn, Y., Duan, J., Guo, J.-Y., Kuo, C.-Y., Wang, L., 2012. Continuously accelerating ice loss over Amundsen Sea catchment, West Antarctica, revealed by integrating altimetry and GRACE data. *Earth Planet. Sci. Lett.* 321–322, 74–80.



- LeMasurier, W., Kawachi, Y., Rex, D., Wade, F., 1990. Marie Byrd Land. In: LeMasurier, W., Thomson, J., Baker, P., Kyle, P., Rowley, P., Smellie, J., Verwoerd, W. (Eds.), 1990. Volcanoes of the Antarctic Plate and Southern Oceans, Antarctic Research Series, vol. 48. AGU, Washington, D. C., p. 487.
- Licht, K.J., Andrews, J.T., 2002. The  $^{14}\text{C}$  record of Late Pleistocene ice advance and retreat in the central Ross Sea, Antarctica. *Arctic, Antarct. Alpine Res.* 34, 324–333.
- Licht, K.J., Jennings, A.E., Andrews, J.T., Williams, K.M., 1996. Chronology of late Wisconsin ice retreat from the western Ross Sea, Antarctica. *Geology* 24, 223–226.
- Licht, K.J., Cunningham, W.L., Andrews, J.T., Domack, E.W., Jennings, A.E., 1998. Establishing chronologies from acid-insoluble organic  $^{14}\text{C}$  dates on Antarctic (Ross Sea) and Arctic (North Atlantic) marine sediments. *Polar Res.* 17, 203–216.
- Lifton, N.A., Bieber, J.W., Clem, J.M., Duldig, M.L., Evenson, P., Humber, J.E., Pyle, R., 2005. Addressing solar modulation and long-term uncertainties in scaling secondary cosmic rays for in situ cosmogenic nuclide applications. *Earth Planet. Sci. Lett.* 239, 140–161.
- Lindow, J., Spiegel, C., Johnson, J., Castex, M., Lisker, F., Gohl, K., 2011. Glacial retreat since the Last Glacial Maximum – New constraints from the Walgreen Coast, West Antarctica. In: 11th International Symposium on Antarctic Earth Sciences, p. 513. Program and Abstracts (John McIntyre Conference Centre, Edinburgh, Scotland, 11–15 July 2011), Abstract PO19.4.
- Livingstone, S.J., Ó Cofaigh, C., Stokes, C.R., Hillenbrand, C.-D., Vieli, A., Jamieson, S.S.R., 2012. Antarctic palaeo-ice streams. *Earth-Science Rev.* 111, 90–128.
- Lorius, C., Raynaud, D., Petit, J.-R., Jouzel, J., Merlivat, L., 1984. Late-glacial maximum–Holocene atmospheric and ice-thickness changes from Antarctic ice-core studies. *Ann. Glaciol.* 5, 88–94.
- Lowe, A.L., Anderson, J.B., 2002. Reconstruction of the West Antarctic ice sheet in Pine Island Bay during the Last Glacial maximum and its subsequent retreat history. *Quat. Sci. Rev.* 21, 1879–1897.
- Lowe, A.L., Anderson, J.B., 2003. Evidence for abundant subglacial meltwater beneath the paleo-ice sheet in Pine Island Bay, Antarctica. *J. Glaciol.* 49, 125–138.
- Lythe, M., Vaughan, D.G., the BEDMAP Consortium, 2001. BEDMAP: a new ice thickness and subglacial topographic model of Antarctica. *J. Geophys. Res.* 106, 11,335–11,352.
- Mackensen, A., 2012. Strong thermodynamic imprint on recent bottom-water and epibenthic  $\delta^{13}\text{C}$  in the Weddell Sea revealed: Implications for glacial Southern Ocean ventilation. *Earth Planet. Sci. Lett.* 317–318, 20–26.
- Majewski, W., 2013. Benthic foraminifera from Pine Island and Ferrero bays, Amundsen sea. *Polish Polar Res.* 34, 169–200.
- Martinerie, P., Raynaud, D., Etheridge, D.M., Barnola, J.-M., Mazaudier, D., 1992. Physical and climatic parameters which influence the air content in polar ice. *Earth Planet. Sci. Lett.* 112, 1–13.
- Maslen, N.R., Convey, P., 2006. Nematode diversity and distribution in the southern maritime Antarctic – clues to history? *Soil Biol. Biochem.* 38, 3141–3151.
- Mercer, J.H., 1978. West Antarctic ice sheet and  $\text{CO}_2$  greenhouse effect: a threat of disaster. *Nature* 271, 321–325.
- Miller, H., Grobe, H. (Eds.), 1996. The Expedition ANTARKTIS-XI/3 with RV Polarstern in 1994. Reports on Polar Research, 188. Alfred-Wegener-Institut für Polar- und Meeresforschung, Bremerhaven (Germany), p. 115. <http://hdl.handle.net/10013/epic.10189>.
- Mosola, A.B., Anderson, J.B., 2006. Expansion and rapid retreat of the West Antarctic ice sheet in eastern Ross Sea: possible consequence of over-extended ice streams? *Quat. Sci. Rev.* 25, 2177–2196.
- Muto, A., Anandakrishnan, S., Alley, R.B., 2013. Subglacial bathymetry and sediment layer distribution beneath the Pine Island Glacier ice shelf, West Antarctica, modelled using aerogravity and autonomous underwater vehicle data. *Ann. Glaciol.* 54. <http://dx.doi.org/10.3189/2013AoG64A110>.
- Neumann, T.A., Conway, H., Price, S.F., Waddington, E.D., Catania, G.A., Morse, D.L., 2008. Holocene accumulation and ice sheet dynamics in central West Antarctica. *J. Geophys. Res.* 113, F02018. <http://dx.doi.org/10.1029/2007JF000764>.
- Nishiizumi, K., Kohl, C.P., Arnold, J.R., Winterer, E.L., Lal, D., Klein, J., Middleton, R., 1989. Cosmic ray production rates of  $^{26}\text{Al}$  and  $^{10}\text{Be}$  in quartz from glacially polished rocks. *J. Geophys. Res.* 94, 17907–17915.
- Nitsche, F.-O., 1998. Bellingshausen Sea and Amundsen Sea: Development of a Sedimentation Model. *Berichte zur Polarforschung*, vol. 258. Alfred-Wegener-Institut für Polar- und Meeresforschung, Bremerhaven (Germany), p. 144. <http://hdl.handle.net/10013/epic.10261>.
- Nitsche, F.O., Gohl, K., Vanneste, K., Miller, H., 1997. Seismic expression of glacially deposited sequences in the Bellingshausen and Amundsen Seas, West Antarctica. In: Barker, P.F., Cooper, A.K. (Eds.), *Geology and Seismic Stratigraphy of the Antarctic Margin, Part 2*. Antarctic Research Series vol. 71. AGU, Washington, D.C., pp. 95–108.
- Nitsche, F.O., Cunningham, A.P., Larter, R.D., Gohl, K., 2000. Geometry and development of glacial continental margin depositional systems in the Bellingshausen Sea. *Mar. Geol.* 162, 277–302.
- Nitsche, F.O., Jacobs, S.S., Larter, R.D., Gohl, K., 2007. Bathymetry of the Amundsen Sea continental shelf: implications for geology, oceanography, and glaciology. *Geochem. Geophys. Geosyst.* 8, Q10009. <http://dx.doi.org/10.1029/2007GC001694>.
- Nitsche, F.O., Gohl, K., Larter, R.D., Hillenbrand, C.-D., Kuhn, G., Smith, J.A., Jacobs, S., Anderson, J.B., Jakobsson, M., 2013. Paleo ice flow and subglacial meltwater dynamics in Pine Island Bay, West Antarctica. *Cryosphere* 7, 249–262. <http://dx.doi.org/10.5194/tc-7-249-2013>.
- Noormets, R., Dowdeswell, J.A., Larter, R.D., Ó Cofaigh, C., Evans, J., 2009. Morphology of the upper continental slope in the Bellingshausen and Amundsen Seas – implications for sedimentary processes at the shelf edge of West Antarctica. *Mar. Geol.* 258, 100–114.
- Ó Cofaigh, C., Dowdeswell, J.A., Allen, C.S., Hiemstra, J.F., Pudsey, C.J., Evans, J., Evans, D.J.A., 2005a. Flow dynamics and till genesis associated with a marine-based Antarctic palaeo-ice stream. *Quat. Sci. Rev.* 24, 709–740.
- Ó Cofaigh, C., Larter, R.D., Dowdeswell, J.A., Hillenbrand, C.-D., Pudsey, C.J., Evans, J., Morris, P., 2005b. Flow of the West Antarctic Ice Sheet on the continental margin of the Bellingshausen Sea at the Last Glacial Maximum. *J. Geophys. Res.* 110, B11103. <http://dx.doi.org/10.1029/2005JB003619>.
- Ó Cofaigh, C., Evans, J., Dowdeswell, J.A., Larter, R.D., 2007. Till characteristics, genesis and transport beneath Antarctic paleo-ice streams. *J. Geophys. Res.* 112, F03006. <http://dx.doi.org/10.1029/2006JF000606>.
- Ó Cofaigh, C., Davies, B.J., Livingstone, S.J., Smith, J.A., Johnson, J.S., Hocking, E.P., Hodgson, D.A., Anderson, J.B., Bentley, M.J., Canals, M., Domack, E., Dowdeswell, J.A., Evans, J., Glasser, N.F., Hillenbrand, C.-D., Larter, R.D., Roberts, S.J., Simms, A.R., Reconstruction of ice-sheet changes in the Antarctic Peninsula since the Last Glacial Maximum. *Quat. Sci. Rev.* (in review).
- Oppenheimer, M., 1998. Global warming and the stability of the West Antarctic Ice Sheet. *Nature* 393, 325–332.
- Powell, R.D., 1984. Glacimarine processes and inductive lithofacies modelling of ice shelf and tidewater glacier sediments based on Quaternary examples. *Mar. Geology* 57, 1–52.
- Pritchard, H.D., Arthern, R.J., Vaughan, D.G., Edwards, L.A., 2009. Extensive dynamic thinning on the margins of the Greenland and Antarctic ice sheets. *Nature* 461, 971–975.
- Pritchard, H.D., Ligtenberg, S.R.M., Fricker, H.A., Vaughan, D.G., van den Broeke, M.R., Padman, L., 2012. Antarctic ice-sheet loss driven by basal melting of ice shelves. *Nature* 484, 502–505.
- Pudsey, C.J., Murray, J.W., Appleby, P., Evans, J., 2006. Ice shelf history from petrographic and foraminiferal evidence, Northeast Antarctic Peninsula. *Quat. Sci. Rev.* 25, 2357–2379.
- Rabus, B.T., Lang, O., Adolphs, U., 2003. Interannual velocity variations and recent calving of Thwaites Glacier Tongue, West Antarctica. *Ann. Glaciol.* 36, 215–224.
- Raynaud, D., Lebel, B., 1979. Total gas content and surface elevation of polar ice sheets. *Nature* 281, 289–291.
- Raynaud, D., Whillans, I.M., 1982. Air content of the Byrd core and past changes in the West Antarctic Ice Sheet. *Ann. Glaciol.* 3, 269–273.
- Reimer, P.J., et al., 2009. IntCal09 and Marine09 radiocarbon age calibration curves, 0–50,000 years cal BP. *Radiocarbon* 51, 1111–1150.
- Rignot, E.J., 1998. Fast recession of a west Antarctic glacier. *Science* 281, 549–551.
- Rignot, E., 2008. Changes in West Antarctic ice stream dynamics observed with ALOS PALSAR data. *Geophys. Res. Lett.* 35, L12505. <http://dx.doi.org/10.1029/2008GL033365>.
- Rignot, E., Vaughan, D.G., Schmeltz, M., Dupont, T., MacAyeal, D., 2002. Acceleration of Pine Island and Thwaites glaciers, west Antarctica. *Ann. Glaciol.* 34, 189–194.
- Rignot, E., Thomas, R.H., Kanagaratnam, P., Casassa, G., Frederick, E., Gogineni, S., Krabill, W., Rivera, A., Russell, R., Sonntag, J., Swift, R., Yungel, J., 2004. Improved estimation of the mass balance of glaciers draining into the Amundsen Sea sector of West Antarctica from the CECS/NASA 2002 campaign. *Ann. Glaciol.* 39, 231–237.
- Rignot, E., Bamber, J.L., van den Broeke, M.R., Davis, C., Li, Y., van de Berg, W.J., van Meijgaard, E., 2008. Recent Antarctic ice mass loss from radar interferometry and regional climate modelling. *Nat. Geosci.* 1, 106–110.
- Rignot, E., Mouginot, J., Scheuchl, B., 2011. Ice flow of the Antarctic ice sheet. *Science* 333, 1427–1430.
- Rosenheim, B.E., Day, M.B., Domack, E., Schrum, H., Benthien, A., Hays, J.M., 2008. Antarctic sediment chronology by programmed-temperature pyrolysis: methodology and data treatment. *Geochem. Geophys. Geosyst.* 9, Q04005. <http://dx.doi.org/10.1029/2007GC001816>.
- Ross, N., Siegert, M.J., Woodward, J., Smith, A.M., Corr, H.F.J., Bentley, M.J., Hindmarsh, R.C.A., King, E.C., Rivera, A., 2011. Holocene stability of the Amundsen–Weddell ice divide, West Antarctica. *Geology* 39, 935–938.
- Schoof, C., 2007. Ice sheet grounding line dynamics: steady states, stability, and hysteresis. *J. Geophys. Res.* 112, F03S28. <http://dx.doi.org/10.1029/2006JF000664>.
- Scott, J.B.T., Gudmundsson, G.H., Smith, A.M., Bingham, R.G., Pritchard, H.D., Vaughan, D.G., 2009. Increased rate of acceleration on Pine Island Glacier strongly coupled to changes in gravitational driving stress. *Cryosphere* 3, 125–131. <http://www.the-cryosphere.net/3/125/2009/>.
- Shapiro, N.M., Ritzwoller, M.H., 2004. Inferring surface heat flux distributions guided by a global seismic model: particular application to Antarctica. *Earth Planet. Sci. Lett.* 223, 213–224.
- Shepherd, A., Wingham, D., Rignot, E., 2004. Warm ocean is eroding west Antarctic ice sheet. *Geophys. Res. Lett.* 31, L23402. <http://dx.doi.org/10.1029/2004GL021106>.
- Shepherd, A., Ivins, E.R., 45 others, 2012. A reconciled estimate of ice-sheet mass balance. *Science* 338, 1183–1189.
- Siddoway, C.S., Sass, L.C., Esser, R.P., 2005. Kinematic history of western Marie Byrd Land, west Antarctica: direct evidence from Cretaceous mafic dykes. In: Vaughan, A.P.M., Leat, P.T., Pankhurst, R.J. (Eds.), *Terrane Processes at the*



- Margins of Gondwana, Geological Society Special Publications, vol. 246. Geological Society, London (U.K.), pp. 417–438.
- Smith, A.M., Murray, T., 2009. Bedform topography and basal conditions beneath a fast-flowing West Antarctic ice stream. *Quat. Sci. Rev.* 28, 584–596.
- Smith, J.A., Bentley, M.J., Hodgson, D.A., Roberts, S.J., Leng, M.J., Lloyd, J.M., Barrett, M.S., Bryant, C., Sugden, D.E., 2007. Oceanic and atmospheric forcing of early Holocene ice shelf retreat, George VI Ice Shelf, Antarctica Peninsula. *Quat. Sci. Rev.* 26, 500–516.
- Smith, J.A., Hillenbrand, C.-D., Larter, R.D., Graham, A.G.C., Kuhn, G., 2009. The sediment infill of subglacial meltwater channels on the West Antarctic continental shelf. *Quat. Res.* 71, 190–200.
- Smith, J.A., Hillenbrand, C.-D., Kuhn, G., Larter, R.D., Graham, A.G.C., Ehrmann, W., Moreton, S.G., Forwick, M., 2011. Deglacial history of the west Antarctic ice sheet in the western Amundsen sea embayment. *Quat. Sci. Rev.* 30, 488–505.
- Smith, A.M., Jordan, T.A., Ferraccioli, F., Bingham, R.G., 2013. Influence of subglacial conditions on ice stream dynamics: seismic and potential field data from Pine Island Glacier, West Antarctica. *J. Geophys. Res.* 118, 1471–1482. <http://dx.doi.org/10.1029/2012JB009582>.
- Solomon, S., Qin, D., Manning, M., Chen, Z., Marquis, M., Averyt, K.B., Tignor, M., Miller, H.L. (Eds.), 2007. Contribution of Working Group I to the Fourth Assessment Report of the Intergovernmental Panel on Climate Change, 2007. Cambridge University Press, Cambridge, UK and New York, NY, USA, p. 1056. [http://www.ipcc.ch/publications\\_and\\_data/ar4/wg1/en/contents.html](http://www.ipcc.ch/publications_and_data/ar4/wg1/en/contents.html).
- S.P.R.I.T.E., Group, Boyer, C.G., 1992. The southern rim of the Pacific ocean: preliminary geologic report of the Amundsen Sea–Bellingshausen sea cruise of the *Polar Sea*, 12 February–21 March 1992. *Antarc. J. U. S.* 27 (1), 11–14.
- Steig, E.J., Schneider, D.P., Rutherford, S.D., Mann, M.E., Comiso, J.C., Shindell, D.T., 2009. Warming of the Antarctic ice-sheet surface since the 1957 International Geophysical Year. *Nature* 457, 459–462.
- Steig, E.J., Ding, Q., Battisti, D.S., Jenkins, A., 2012. Tropical forcing of Circumpolar deep water inflow and outlet glacier thinning in the Amundsen sea embayment, west Antarctica. *Ann. Glaciol.* 53 (60), 19–28.
- Stone, J.O., 2000. Air pressure and cosmogenic isotope productions. *J. Geophys. Res.* 105, 23753–23759.
- Stone, J.O., Balco, G.A., Sugden, D.E., Caffee, M.W., Sass, L.C., Cowdery, S.G., Siddoway, C., 2003. Holocene deglaciation of Marie Byrd Land, west Antarctica. *Science* 299, 99–102.
- Studinger, M., Bell, R.E., Blankenship, D.D., Finn, C.A., Arko, R.A., Morse, D.L., Joughin, I., 2001. Subglacial sediments: a regional geological template for ice flow in West Antarctica. *Geophys. Res. Lett.* 28, 3493–3496.
- Studinger, M., Allen, C., Blake, W., Shi, L., Elieff, S., Krabill, W.B., Sonntag, J.G., Martin, S., Dutrieux, P., Jenkins, A., Bell, R.E., 2010. Mapping Pine Island Glacier's Sub-ice Cavity with Airborne Gravimetry. Abstract C11A-0528, Fall Meeting. AGU.
- Thoma, M., Jenkins, A., Holland, D., Jacobs, S., 2008. Modelling circumpolar deep water intrusions on the Amundsen sea continental shelf, Antarctica. *Geophys. Res. Lett.* 35, L18602. <http://dx.doi.org/10.1029/2008GL034939>.
- Thomas, R., Rignot, E., Casassa, G., Kanagaratnam, P., Acuña, C., Akins, T., Brecher, H., Frederick, E., Gogineni, P., Krabill, W., Manizade, S., Ramamoorthy, H., Rivera, A., Russell, R., Sonntag, J., Swift, R., Yungel, J., Zwally, J., 2004. Accelerated sea-level rise from West Antarctica. *Science* 306, 255–258.
- Tinto, K.J., Bell, R.E., 2011. Progressive unpinning of Thwaites glacier from newly identified offshore ridge: constraints from aerogravity. *Geophys. Res. Lett.* 38, L20503. <http://dx.doi.org/10.1029/2011GL049026>.
- Tucholke, B.E., Houtz, R.E., 1976. Sedimentary framework of the Bellingshausen Basin from seismic profiler data. In: Hollister, C.D., Craddock, C., et al. (Eds.), Initial Reports of the Deep Sea Drilling Project, vol. 35. U.S. Government Printing Office, Washington, D.C., pp. 197–228.
- Tulaczyk, S., Kamb, B., Scherer, R.P., Engelhardt, H.F., 1998. Sedimentary processes at the base of a West Antarctic ice stream; constraints from textural and compositional properties of subglacial debris. *J. Sediment. Res.* 68, 487–496.
- Uenzelmann-Neben, G., Gohl, K., Larter, R.D., Schlüter, P., 2007. Differences in Ice Retreat across Pine Island Bay, West Antarctica, since the Last Glacial Maximum: Indications from Multichannel Seismic Reflection Data. U.S. Geological Survey and The National Academies. USGS OF-2007-1047, Short Research Paper 084 <http://dx.doi.org/10.3133/of2007-1047.srp084>.
- Vaughan, D.G., 2008. West Antarctic Ice Sheet collapse – the fall and rise of a paradigm. *Clim. Change* 91, 65–79.
- Vaughan, D.G., Corr, H.F.J., Ferraccioli, F., Frearson, N., O'Hare, A., Mach, D., Holt, J.W., Blankenship, D.D., Morse, D.L., Young, D.A., 2006. New boundary conditions for the West Antarctic ice sheet: subglacial topography beneath Pine Island Glacier. *Geophys. Res. Lett.* 33, L09501. <http://dx.doi.org/10.1029/2005GL025588>.
- Wählin, A.K., Yuan, X., Björk, G., Nohr, C., 2010. Inflow of warm Circumpolar Deep Water in the central Amundsen shelf. *J. Phys. Oceanogr.* 40, 1427–1434.
- WAIS Divide Project Members, 2013. Onset of deglacial warming in West Antarctica driven by local orbital forcing. *Nature*. <http://dx.doi.org/10.1038/nature12376>.
- Walker, D.P., Brandon, M.A., Jenkins, A., Allen, J.T., Dowdeswell, J.A., Evans, J., 2007. Oceanic heat transport onto the Amundsen Sea shelf through a submarine glacial trough. *Geophys. Res. Lett.* 34, L02602. <http://dx.doi.org/10.1029/2006GL028154>.
- Weertman, J., 1974. Stability of the junction of an ice sheet and an ice shelf. *J. Glaciol.* 13, 3–11.
- Weigelt, E., Gohl, K., Uenzelmann-Neben, G., Larter, R.D., 2009. Late Cenozoic ice sheet cyclicity in the western Amundsen Sea Embayment – evidence from seismic records. *Glob. Planet. Change* 69, 162–169.
- Weigelt, E., Uenzelmann-Neben, G., Gohl, K., Larter, R.D., 2012. Did massive glacial dewatering modify sedimentary structures on the Amundsen Sea Embayment shelf, West Antarctica? *Global Planet. Change* 92–93, 8–16.
- Wellner, J.S., Lowe, A.L., Shipp, S.S., Anderson, J.B., 2001. Distribution of glacial geomorphic features on the Antarctic continental shelf and correlation with substrate: implications for ice behavior. *J. Glaciol.* 47, 397–411.
- Wellner, J.S., Heroy, D.C., Anderson, J.B., 2006. The death mask of the Antarctic ice sheet: comparison of glacial geomorphic features across the continental shelf. *Geomorphology* 75, 157–171.
- Whitehouse, P.L., Bentley, M.J., Milne, G.A., King, M.A., Thomas, I.D., 2012. A new glacial isostatic adjustment model for Antarctica: calibrated and tested using observations of relative sea-level change and present-day uplift rates. *Geophys. J. Int.* 190, 1464–1482.
- Wilch, T.I., McIntosh, W.C., Dunbar, N.W., 1999. Late Quaternary volcanic activity in Marie Byrd Land: potential <sup>40</sup>Ar/<sup>39</sup>Ar-dated time horizons in West Antarctic ice and marine cores. *Geol. Soc. America Bull.* 111, 1563–1580.
- Wingham, D.J., Wallis, D.W., Shepherd, A., 2009. Spatial and temporal evolution of Pine Island Glacier thinning, 1995–2006. *Geophys. Res. Lett.* 36, L17501. <http://dx.doi.org/10.1029/2009GL039126>.
- Zheng, Y., Anderson, R.F., Froelich, P.N., Beck, W., McNichol, A.P., Guilderson, T., 2002. Challenges in radiocarbon dating organic carbon in opal rich marine sediments. *Radiocarbon* 44, 123–136.



**Co-author publications (submitted / under review)**

Bentley, M.J., Ó Cofaigh, C., Anderson, J.B., Conway, H., Davies, B., Graham, A.G.C., Hillenbrand, C.-D., Hodgson, D.A., Jamieson, S.S.R., Larter, R.D., Mackintosh, A., Smith, J.A., Verleyen, E., Ackert, R.P., Bart, P.J., Berg, S., Brunstein, D., Canals, M., Colhoun, E.A., Crosta, X., Dickens, W.A., Domack, E., Dowdeswell, J.A., Dunbar, R., Ehrmann, W., Evans, J., Favier, V., Fink, D., Fogwill, C.J., Glasser, N.F., Gohl, K., Golledge, N.R., Goodwin, I., Gore, D.B., Greenwood, S.L., Hall, B.L., Hall, K., Hedding, D.W., Hein, A.S., Hocking, E.P., Jakobsson, M., Johnson, J.S., Jomelli, V., Jones, R.S., **Klages, J.P.**, Kristoffersen, Y., Kuhn, G., Leventer, A., Licht, K., Lilly, K., Lindow, J., Livingstone, S.J., Massé, G., McGlone, M.S., McKay, R.M., Melles, M., Miura, H., Mulvaney, R., Nel, W., Nitsche, F.O., O'Brien, P.E., Post, A.L., Roberts, S.J., Saunders, K.M., Selkirk, P.M., Simms, A.R., Spiegel, C., Stollendorf, T.D., Stone, J.O., Sugden, D.E., van der Putten, N., van Ommen, T., Verfaillie, D., Vyverman, W., Wagner, B., White, D.A., Witus, A.E., Zwartz, D., submitted. A community-based reconstruction of Antarctic Ice Sheet deglaciation since the Last Glacial Maximum. *Quaternary Science Reviews*.

Smith, J.A., Hillenbrand, C.-D., Kuhn, G., **Klages, J.P.**, Graham, A.G.C., Larter, R.D., Ehrmann, W., Moreton, S.G., Wiers, S., submitted. New constraints on the timing of West Antarctic Ice Sheet retreat in the eastern Amundsen Sea since the Last Glacial Maximum. *Quaternary Science Reviews*.